

ABSTRACTS

(94-261)

BREAST PATHOLOGY

32
24
20
21



94 Paget Disease of the Nipple is Limited to Ductal Breast Tumors and Has No association with Lobular Carcinoma: A Retrospective Review of 808 Mastectomy Specimens at an Academic Tertiary Center

Evi Abada¹, M. Ruhul Quddus¹, C. James Sung¹, Kamaljeet Singh²

¹Women & Infants Hospital/Alpert Medical School of Brown University, Providence, RI, ²Women and Infants Hospital, Providence, RI

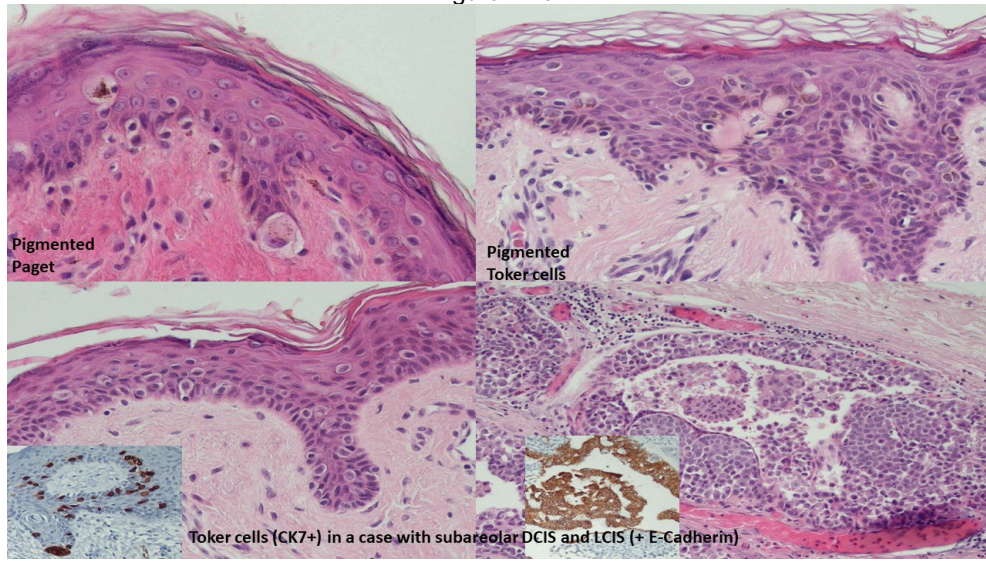
Disclosures: Evi Abada: None; M. Ruhul Quddus: None; C. James Sung: None; Kamaljeet Singh: None

Background: Paget disease of the nipple-areolar complex is an uncommon type of intraepithelial adenocarcinoma, characterized histologically by glandular differentiation, intracellular mucin, and immunoreactivity for cytokeratins, epithelial membrane antigen and carcinoembryonic antigen. Although the cell of origin in Paget disease remains controversial, the prevailing view is that most cases arise from in situ or invasive ductal carcinoma. Associations of Paget disease of the nipple with lobular breast neoplasia is largely unknown. We, therefore, aimed to investigate whether Paget disease has any association with lobular breast tumors or is strictly limited to ductal breast malignancies.

Design: We reviewed mastectomy specimens done for carcinoma at our institution from 2007 to 2016. We retrieved H&E sections containing only the nipple to identify characteristic pathologic findings. Paget disease was defined as single cells to nests of intraepithelial adenocarcinoma-like cells with intracellular mucin and confirmed by immunohistochemistry with cytokeratin and/or epithelial membrane antigen.

Results: A total of 808 H&E-stained nipple sections were reviewed from 432 unilateral and 188 bilateral mastectomies of 620 female patients. Paget disease was identified in 28/808 (3.5%) cases; all Paget were unilateral, and one (3.5%) Paget was pigmented (Fig 1). All Paget diseases were of ductal phenotype. Five (18%) Paget cases that contained invasive or in-situ lobular neoplasia in the nipple or breast tissue confirmed ductal phenotype of Paget disease by E-cadherin and p120 immunohistochemistry (Fig 1). Seven (25%) Paget cases also contained concomitant Toker cells (Fig 1). Toker cells were identified in 124 (15%) nipples from 115 (18.5%) patients, of which 9 (1.4%) patients had bilateral Toker cells. Toker cells contained melanin pigment in 4 cases and showed duct formation in 2 cases. Invasive carcinoma was present in the nipple section in 66 (8%) cases: ductal 41(5%), lobular 14(2%), and others 11(1.4%). In-situ carcinoma was present in the nipple sections in 73 (9%) cases: ductal 50(6%) and lobular 23(3%). Other histological findings included: squamous metaplasia (31), papilloma (9), lactational-like changes (4), adenomyoma (1), osteoid (1), and granuloma (1).

Figure 1 - 94



Conclusions: This is the first comprehensive study of histological and pathological findings of the female nipple. Our findings indicate that Paget disease is purely associated with ductal-type neoplasia and absent with lobular breast lesions.

95 Pure Intralymphatic Breast Carcinoma Following Neoadjuvant Treatment: Clinicopathologic Features and Outcome of a Rare Pattern of Residual Disease

Rodrigo Abreu¹, Cynthia Osorio¹, Tábata Alves Domingos², Warley Nunes¹, Cristiano Oliveira¹, Monique Tavares¹, Almir Bitencourt¹, Fabiana Makdissi¹, Solange Sanches¹, Marina De Brot¹

¹A.C.Camargo Cancer Center, São Paulo, Brazil, ²Brigham and Women's Hospital, Boston, MA

Disclosures: Rodrigo Abreu: None; Cynthia Osorio: None; Tábata Alves Domingos: None; Warley Nunes: None; Cristiano Oliveira: None; Monique Tavares: None; Almir Bitencourt: None; Fabiana Makdissi: None; Solange Sanches: None; Marina De Brot: None

Background: Pure intralymphatic breast carcinoma (PIC) after neoadjuvant systemic therapy (NAST) represents an unusual pattern of residual disease and data in the literature are limited. Here, we sought to assess clinicopathologic features and outcome of residual PIC/predominantly PIC.

Design: Electronic medical records were searched to identify patients with PIC/predominantly PIC post-NAST between 2007-2022 at a Cancer Center and clinicopathologic data were retrieved. Slides from surgical specimens were reviewed. Survival analysis was performed using Kaplan-Meier curves and the log-rank test.

Results: Amongst a cohort of 1113 breast cancer patients submitted to NAST, we detected 7 (0.6%) cases of PIC. All were female, being 6 pre-menopausal. Average age at diagnosis was 42.4 years old (range 24-51 yo). Clinically, 4 women presented with a palpable breast mass, 2 with inflammatory carcinoma, and 1 with a non-palpable lesion. Mean tumor size was 4.3 cm (range 0.8-13 cm) and 1 patient was metastatic. Regarding nodal status, 5 patients had axillary LN metastasis before treatment. Histologic evaluation demonstrated 3 no-special type invasive breast carcinomas, 2 invasive carcinomas with apocrine differentiation, 1 pleomorphic invasive lobular carcinoma, and 1 micropapillary. Interestingly, 2 cases exhibited LVI pre-NAST. When stratified by molecular subtype, 4(57.1%) were HER2+; 1(14.3%) triple-negative; 1 luminal B-HER2; and 1 luminal B. Following treatment, most cases (5/7; 71.4%) were categorized as RCB I, size of residual intralymphatic carcinoma ranged from 0.2-40 mm (mean 7.4 mm) and residual DCIS was present in 2 cases. While 5 patients showed no LN metastasis, 2 had micrometastasis. At a mean follow-up time of 16.14 months (2-56 mos), all patients were alive without evidence of disease. Compared to the whole NAST population, PIC patients demonstrated a distinct survival ($p<0.005$), with better outcome. However, there was no statistical difference when taking each RCB group into consideration, due to the small number of PIC cases and short follow-up time.

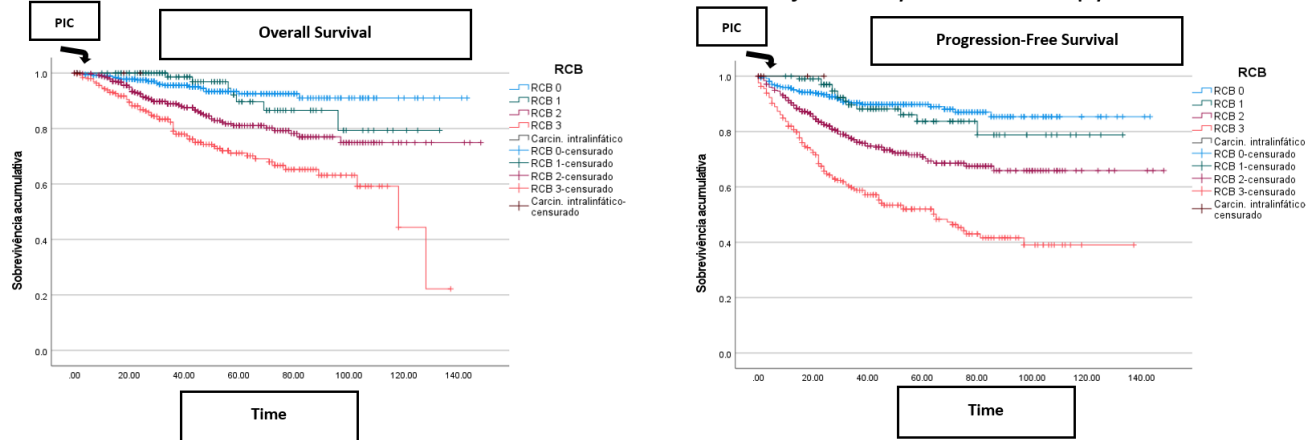
Age at diagnosis (years old)	42	47	24	51	38	45	50
Imaging Pattern	Non-mass enhancement; nipple thickening	PET-scan SUV max up to 13.4	Irregular nodule with heterogeneous enhancement	Non-mass enhancement	Non-mass enhancement; skin thickening	Irregular nodule with heterogeneous enhancement	Irregular nodule with peripheral enhancement
Clinical Tumor Size (cm)	13.0	1.3	5.4	0.8	1.6	3.5	4.5
Core Needle Biopsy (CNB) Diagnosis	PILC Nottingham grade II	Invasive carcinoma with apocrine differentiation Nottingham grade II	Invasive carcinoma with apocrine differentiation Nottingham grade III	Invasive micropapillary carcinoma Nottingham grade II	Invasive breast carcinoma of no-special type Nottingham grade II	Invasive breast carcinoma of no-special type Nottingham grade III	Invasive breast carcinoma of no-special type Nottingham grade II
Lymphovascular Invasion on CNB	No	Yes	No	Yes	No	No	No
Pre-NAST Axillary LN Status	Positive FNA	Positive FNA	Positive FNA	Suspicious lymph node on the ultrasound	Positive FNA	Negative FNA	Positive FNA
Clinical Stage	cT4d cN2	cT2 cN2	cT3 cN2	cT2 cN1	cT4d cN1	cT2 cN0	cT3 cN+ M1
Immunophenotype	ER- PR- HER2+ Ki67 20%	ER- PR+ HER2+ Ki67 30%	ER- PR- HER2+ Ki67 80%	ER- PR- HER2+ Ki67 30%	ER+ PR+ HER2- Ki67 25%	ER- PR- HER2- Ki67 60%	ER- PR- HER2+ Ki67 35%
Neoadjuvant Therapy Scheme	ACdd+ lipegfilgrastim	TCHP	AC-TH	TCHP	ACdT	DdAC-T(C)	DTP
AFTER NAST							
Clinical response	Partial response	Partial response	Complete response	Complete response	Partial response	Complete response	**
Post-NAST Imaging Pattern	Non-mass enhancement	Mild parenchymal enhancement	Architectural distortion without enhancement	Absence of mass or areas of suspicious enhancement	Architectural distortion	Architectural distortion without contrast enhancement	Architectural distortion without contrast enhancement
Surgical Modality	Mastectomy	Adenomastectomy	Adenomastectomy	Conservative surgical excision	Conservative surgical excision	Mastectomy	Mastectomy
#Paraffin Blocks (Residual Macroscopic Tumor Bed)	28	11	14	10	9	15	36
Residual LVI Size (mm) in the Breast	0.82 x 0.35	0.2 x 0.1	1.6 x 0.2	1.0	0.2	1.3 x 0.8	40.0 x 4.6
Residual Axillary LN Metastases	0/11	0/14	0/25	0/5	1/13 (1.0 mm)	0/2	1/34 (0.5 mm)
RCB ^a Class and Index Pathologic stage	I (0.481) ypT0ypN0	I (0.978) ypT0ypN0	I (0.533) ypTisypN0	I (0.698) ypT0ypN0	II (1.408) pT0yN1mi	I (0.642) ypT0ypN0(sn)	II (2.199) ypT0yN1mi
Adjuvant Treatment	RT + anti-HER2	RT + anti-HER2	RT + anti-HER2	RT + anti-HER2	None	RT	RT + anti-HER2
Follow-Up (Months)	56	22	4	8	19	2	2
Outcome	NED	NED	NED	NED	NED	NED	NED

^aResidual cancer burden was calculated by estimating the size and area of the neoplastic emboli occupying the tumor bed. NAST, neoadjuvant systemic therapy; PILC, pleomorphic invasive lobular carcinoma; FNA, fine needle aspirate; RCB, residual cancer

burden; RT, radiation therapy; Acdd, dose dense doxorubicin and cyclophosphamide; TCHP, docetaxel, carboplatin, trastuzumab, and pertuzumab; AC-TH, doxorubicin and cyclophosphamide, followed by paclitaxel and trastuzumab; ACdT, doxorubicin, dose dense cyclophosphamide, paclitaxel; ddAC-(T), doxorubicin and dose dense cyclophosphamide followed by paclitaxel; DTP, docetaxel, trastuzumab, pertuzumab; NED, no evidence of disease; ** missing

Figure 1 - 95

Survival Curves of Breast Cancer Patients Submitted to Neoadjuvant Systemic Therapy



Conclusions: PIC is an extremely rare pattern of residual disease after NAST. The majority of breast cancers were HER2+ with an advanced clinical stage at diagnosis. In contrast to previous reports, we did not find a poor outcome associated with intralymphatic carcinoma, although a longer follow-up time is required to determine and better understand the prognosis of this cohort.

96 Investigation of Clinical, Pathological, and Molecular Characteristics of Triple Negative Invasive Lobular Carcinoma

Daniel Ahmadi¹, Horacio Maluf², Reza Setoodeh², Souzan Sanati²

¹Washington University in St. Louis, St Louis, MO, ²Cedars-Sinai Medical Center, Los Angeles, CA

Disclosures: Daniel Ahmadi: None; Horacio Maluf: None; Reza Setoodeh: None; Souzan Sanati: None

Background: Invasive lobular carcinoma (ILC) is a subtype of breast cancer (BC) that is characterized by the loss of E-cadherin, a surface molecule that constitutes cell cohesion. The growth of majority of ILCs is propagated through stimulation by ER, hence hormonal therapy is the main line of therapy. A minority of ILCs (<1%) are negative for ER, PgR, and Her2, so called triple negative (TN), which while rare, is an important and understudied group of ILC with limited treatment options. We aimed to study clinical, pathologic, and molecular characteristics of TN-ILC.

Design: A retrospective search between 2006 and August 2022 for TN-ILC was performed. Demographic and clinical data including age, laterality, biomarker status (ER, PgR, Her2, Ki-67), focality, size, grade, LVI, DCIS, LCIS [classic vs. pleomorphic (P)], LN status, TNM stage, neoadjuvant therapy (NT), and sequencing results were collected. 24 consecutive ER+ ILCs were randomly selected as control. Androgen receptor (AR) IHC was performed using standard protocol (SP107).

Results: 28 TN-ILCs were identified: mean age was 67.7 (Range: 48-98) years; tumor size 2.5 (Range: 0.1-9.5) cm; 1 tumor was grade 1, 13 grade 2, and 11 grade 3; 10 tumors had LN metastasis, 4 in >3 LNs; 6 patients received NT, 1 achieved complete response and 1 partial response. ER+ ILCs did not show significant differences in age, tumor size, LN status, and LVI, but they showed less grade 3 tumors (2 grade 1, 19 grade 2, 2 grade 3). Mean Ki-67 expression was higher in TN ILCs 18% (3%-74%) vs. ER+ ILCs 8% (1-21%). 100% of TN-ILCs were ILC-P compared to 32% of ER+ ILCs. Except 2 TN-ILCs which didn't show AR expression, all tumors were AR positive. One AR+ TN-ILC showed good response to anti-AR therapy. 10 TN-ILCs and 8 ER+ ILCs were sequenced. In TN-ILCs a range of pathogenic [PALB2 (1), MUTYH (1)], and potentially actionable [AKT1 (1), CDH-1 (1), and PIK3CA (1)] mutations, and VUS [ATM (1), POLE (2), BARD1 (1), SDHB (1), APC (1), BLM (1), FANCM (1), CDH-1 (1), MSH3 (1) and PIK3CA (1)] were seen in 8 of 10 tumors. In ER+ ILC only 1 tumor showed VUS in BRCA2 and CFTR; 7 tumors showed no mutations or alterations.

Conclusions: All TN-ILC in our series were P-ILCs. Actionable and pathogenic mutations and VUS were seen more commonly in TN-ILC cases in our series. Anti-AR therapy can be a potential treatment option in TN-ILCs with limited treatment options.

97 Reassessing Histopathology of Breast Cancer Cases with Pathologic Complete Response after Neoadjuvant Therapy

Di (Andy) Ai¹, Lauren Postlewait¹, Yuan Gao¹, Xiaoxian Li¹

¹Emory University, Atlanta, GA

Disclosures: Di (Andy) Ai: None; Lauren Postlewait: None; Yuan Gao: None; Xiaoxian Li: None

Background: Pathologic complete response (pCR) is defined as no residual invasive carcinoma (RIC) in the breast and no lymph node metastasis (LNM) on evaluation of surgical specimens post neoadjuvant therapy (NAT). Patients who do not achieve pCR have worse outcomes and thus may receive additional chemotherapy. Evaluation of pCR is usually based on one level of H&E section. The aim of this study is to assess whether occult RIC or LNM can be identified in deeper level recuts of tumor bed and lymph nodes in cases originally reported as pCR and whether occult RIC or LNM is associated with worse outcomes.

Design: We collected 40 triple negative breast cancer (TNBC) cases with pCR from 2010 to 2017 at our institution. Three deeper level recuts were performed on the tumor bed and all lymph nodes. First and third level recuts were stained with H&E and the second was stained with pancytokeratin (AE1/3) by immunohistochemistry. The slides were reviewed by two pathologists. This study was approved by the Institutional Research Board.

Results: Occult disease was identified in 7 (17.5%) of the 40 cases, including 6 (15%) RIC and 2 (5.0%) LNM (1 case had both RIC and LNM) (See Table for details). The MD Anderson residual cancer burden was class I in all 7 cases. Median follow up time was 47.9 months for the entire group. In all patients, there was 1 local recurrence and 4 distant metastases. All recurrence events occurred in the group with pCR without residual occult disease, with no recurrence or distant metastatic events in the group with occult RIC or LNM. There was no statistical difference in median disease-free survival (DFS 42.8 mo vs 38.0 mo, p=0.97) or overall survival (OS 47.9 mo vs 38.0 mo, p=0.79) between these two groups.

Table 1. Pathologic diagnosis and DFS/OS for groups without and with occult carcinoma.

	Case #	Diagnosis before surgery	ALN Metastases case # before surgery	Local Recurrence #	Distant Metastasis	DFS ** (Median ± 95% CI)	OS ** (Median ± 95% CI)
Group without occult carcinoma	33	IDC (31); IMC (1); DCIS with LNM (1)	9	1	4 *	42.8 ± 9.0	47.9 ± 8.8
Group with occult RIC and/or LNM	7	IDC (6); IDC with lobular differentiation (1)	3	0	0	38.0 ± 18.8	38.0 ± 32.6
T-Test (P value)						0.97	0.79

* Metastatic sites: liver (2), pleural fluid (1), abdominal wall (1).

** DFS and OS in months.

IDC: Invasive ductal carcinoma; IMC: Invasive mammary carcinoma; ALN: Axillary lymph node; DFS: Disease free survival; OS: Overall survival.

Conclusions: In patients with TNBC undergoing NAT who appeared to have a pCR by standard pathologic assessment, 17.5% had occult residual disease in deeper sections of the tumor and/or lymph nodes. This occult disease was not associated with poorer DFS or OS. Our results suggest evaluation with one H&E slide of the tumor bed and lymph nodes as currently standard practice is sufficient to identify clinically meaningful residual disease. Patients with occult minimal residual tumor burden after neoadjuvant therapy have similar prognosis as patients who achieved true pCR, and additional chemotherapy may not be needed.

98 Identification of Glandular (Acinar)/Tubule Formation in Invasive Breast Cancer: A Pilot Study to Investigate if an Expanded Definition Can Improve Concordance

Rana Aldrees¹, Marie-Hélène Ngo¹, Susan Fineberg², Ian Ellis³, Stuart Schnitt⁴, Susan Lester¹

¹Brigham and Women's Hospital, Boston, MA, ²Montefiore Medical Center, Bronx, NY, ³University of Nottingham, Nottingham, United Kingdom, ⁴Brigham and Women's Hospital, Dana-Farber Cancer Institute, Harvard Medical School, Boston, MA

Disclosures: Rana Aldrees: None; Marie-Hélène Ngo: None; Susan Fineberg: None; Ian Ellis: None; Stuart Schnitt: None; Susan Lester: None

Background: The Nottingham Grading System (NGS) is used to determine prognosis and AJCC stage, as well as to guide treatment for invasive breast carcinoma (IBC). In WHO, the glandular/tubular formation (G/TF) component of NGS is specified to include "only structures exhibiting clear central lumina surrounded by polarized neoplastic cells". A recent study showed poor concordance when 35 breast pathologists used this definition to classify 58 structures (with each structure circled) as determined

ABSTRACTS | BREAST PATHOLOGY

by Dr. Ian Ellis (manuscript in preparation). Based on these results, this pilot study was undertaken to determine if an expanded definition of G/TF could improve concordance.

Design: The expanded definition addressed areas of difficulty identified in the initial study, included more information about structures that should be considered G/TF, and provided a definition of polarization. In addition, there was guidance about classifying complex/cribriform, mucinous, and micropapillary patterns. The same 58 images used for the original study were used for the pilot study. These images were sent in PowerPoint format along with the expanded definition to 10 experienced breast pathologists who did not participate in the original study.

Results: The 10 invited pathologists completed the survey. The overall concordance increased from a mean of 66% (range 40-97%; kappa statistic 0.324) in the original study (Figure 1) to a mean of 94% (range 86-100%; kappa statistic 0.868) in the pilot study (Figure 2). The concordance for the 41 structures that should be considered G/TF increased from a mean of 57% (range 15-100%) to a mean of 99% (93-100%). However, the concordance for the 17 structures that should not be considered G/TF decreased from a mean of 91% (range 18-100%) to a mean of 81% (range 53-100%). Of the 32 misclassifications in this latter group, 10 involved a micropapillary pattern (a solid nest with inverted polarity) and 9 involved solid nests with a possible artifactual space.

Figure 1 - 98

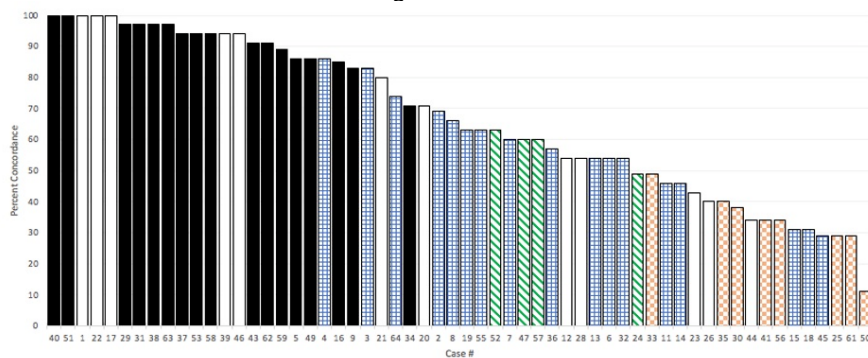
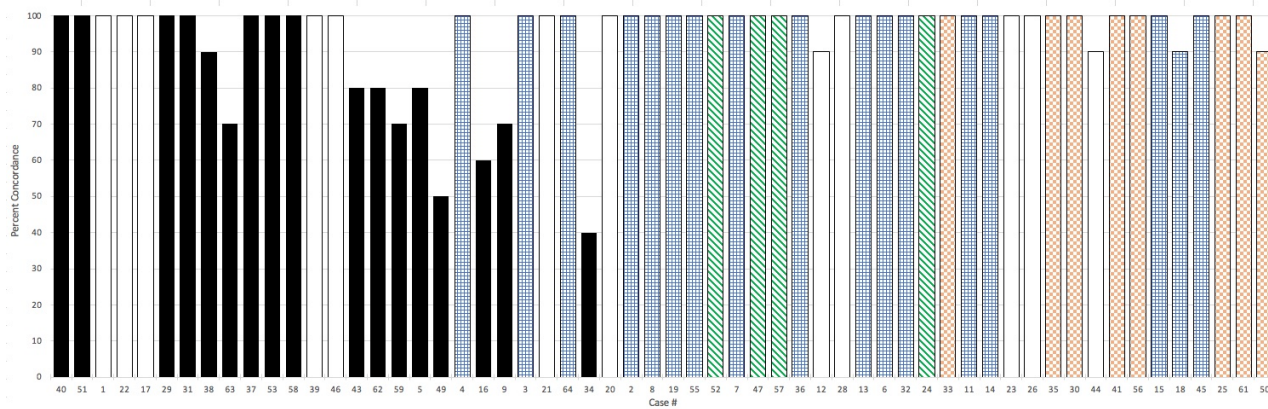


Figure 1: Prior Study: For the 35 pathologists using the WHO definition, concordance for the individual cases ranged from 11% to 100%. The highest concordance was for non-G/TF cases (black) (mean 91%; range 71-100%). Overall concordance for G/TF cases was lower (mean 57%). The highest was for G/TF cases showing simple tubules (white)(mean 72%; range 34%-100%), and lower for cases with complex/cribriform patterns (grid/blue)(mean 57%; range 29-86%), micropapillary architecture with "inverted tubules" (cell nests with inverted polarity surrounding a hollow center)(diagonal/green)(mean 58%; range 49%-63%), and mucinous carcinoma (checkerboard/orange)(mean 33%; range 11%-49%).

Figure 2 - 98



Conclusions: In this pilot study, an expanded definition of G/TF markedly improved overall concordance and concordance for the recognition of structures that should be included as G/TF. However, concordance for structures that should not be classified as G/TF decreased, suggesting that the definition could be improved further, especially for the micropapillary pattern. Additional validation studies using a revised definition on a new larger set of challenging cases to determine if concordance can be further improved would be of value.

99 The Dynamic of HER2-low Expression during Breast Cancer Progression

Sarah Anderson¹, Brooke Bartow¹, Xiao Huang¹, Shi Wei²

¹The University of Alabama at Birmingham, Birmingham, AL, ²The University of Kansas School of Medicine, Kansas City, KS

Disclosures: Sarah Anderson: None; Brooke Bartow: None; Xiao Huang: None; Shi Wei: None

Background: Low HER2 expression is emerging as an actionable target for the treatment of breast cancer (BC) with the antibody drug conjugate Trastuzumab deruxtecan (T-DXd). However, the evolution of HER2-low expression during BC progression remains poorly characterized. The aim of this study is to evaluate the evolution of HER2 expression in primary and metastatic BCs (pBCs/mBCs) by including the HER2-low category.

Design: The HER2 statuses of pBCs and their paired mBCs available at the authors' institution between 01/2000 and 08/2020 were retrospectively collected. Those from regional lymph nodes were excluded. The HER2 status, evaluated by immunohistochemistry (IHC) and/or in situ hybridization (ISH), was categorized as HER2-0, HER2-low (IHC 1+ or 2+/non-amplified) and HER2-positive (HER2+). The cases with non-amplified HER2 but no IHC performed and those with a negative IHC result from referring institutions but without an IHC score were not included. A total of 171 paired pBC/mBC cases were available in the study period.

Results: The proportions of HER2-low cases were 25.7% in pBCs and 23.4% in mBCs, respectively, while those of HER2-0 cases were 35.1% and 42.7%, respectively. The overall conversion rate between HER2-0 and HER2-low was 31.7%. HER2-low switching to HER2-0 (19/44, 54.2%) was more frequent than the vice versa (14/60, 24.1%; $p=0.03$). No significant difference was found when comparing the conversion rates among the common organs of relapses, including bone, liver, lung and brain ($p=0.8$). Two (3.3%) and 9 (20.5%) cases of pBCs with a HER2-0 and a HER2-low status, respectively, were converted to HER2+ mBCs. In contrast, 10 (14.9%) and 10 cases of the 67 HER2+ pBCs were converted to HER2-0 and HER2-low mBCs, respectively, significantly higher when compared to the HER2-0 to HER2+ ($p=0.03$), but not HER2-low to HER2+ ($p=0.45$) conversions. Of the 17 patients with multiorgan metastases, 7 (41.2%) had discordance among the different sites of relapse, including 3 with HER2-0/HER2-low, 3 with HER2-0/HER2+ and 1 with HER2-low/HER2+, respectively. Overall, about 25% of cases (43/171) had a switch from or to a HER2-low status.

Conclusions: HER2-low expression is highly unstable during BC evolution. Furthermore, discordance of HER2 status is frequent among the distant sites of relapse. Thus, repeat testing is warranted in patients with accessible metastases, and to preferentially use the HER2 status of the metastasis to direct therapy in the pursuit of precision medicine.

100 HER2-Low Luminal Breast Carcinoma Is Not a Homogenous Clinicopathological and Molecular Entity

Céline Andre¹, Aurélie Bertaut¹, Sylvain Ladoire², Isabelle Desmoulins¹, Clémentine Jankowski¹, Céline Charon Barra¹, Françoise Beltjens¹, Anthony Bergeron³, Corentin Richard¹, Romain Boidot¹, Laurent Arnould¹

¹Centre Georges-François Leclerc, Dijon, France, ²Dijon, France, ³Unit of Pathology, Department of Biology and Pathology of the Tumor, Centre Georges-François Leclerc, Dijon, France

Disclosures: Céline Andre: None; Aurélie Bertaut: None; Sylvain Ladoire: None; Isabelle Desmoulins: None; Clémentine Jankowski: None; Céline Charon Barra: None; Françoise Beltjens: None; Anthony Bergeron: None; Corentin Richard: None; Romain Boidot: None; Laurent Arnould: None

Background: Given therapeutic opportunities brought about by new antibody-drug conjugates, the HER2 classification of breast cancer has been refined to include the new HER2-low (H2L) category comprising HER2 1+ by IHC, 2+ and non-amplified by ISH, and double-equivocal tumors. We analyzed three downstream HER2 effector pathways: PI3K-AKT, MAPK, and JAK-STAT, in H2L tumors in association with clinical and pathologic features, compared to those of HER2-positive and HER2-negative tumors.

Design: The study comprised 62 luminal H2L carcinomas matched by hormone-positive status to 20 HER2-negative (0+) and 43 HER2-positive tumors (20 2+weakly-amplified and 23 3+). The transcriptomic activity of the three signaling pathways was analyzed by RNA sequencing and the mutational status of key breast cancer-related genes by DNA sequencing.

Results: H2L tumors had lower histoprognostic grades ($p=0.0017$), and lower mitotic and Ki67 proliferation indexes than HER2-positive tumors ($p=0.0042$ and 0.0003). Their PIK3CA mutation rates were close to those of HER2-negative and significantly higher than in HER2-positive tumors ($p=0.0048$), which was opposite to TP53 mutations ($p=0.0028$). We found no differences between H2L and HER2-negative tumors (Table 1). At the transcriptomic level, we identified three groups with distinct profiles which did not reflect the new HER2 classification and did not single out a H2L tumor-specific profile (Fig. 1). Double-equivocal and weakly-amplified tumors had similar mutation rates and transcriptomic profiles. Furthermore, we observed that the presence of a mutation in a signaling pathway had a strong pathway activation effect regardless of the HER2 tumor status (Fig. 2). Consequently, H2L tumors had similar PIK3CA mutation prevalence and similar transcriptomic profiles to HER2-negative tumors.

ABSTRACTS | BREAST PATHOLOGY

	H2L (n=62)	HER2-negative (n=20)	HER2-positive (n=43)	P-values	All	0+ vs. H2L	HER2-positive vs. H2L
	n (%)	n (%)	n (%)				
Age				0.9054			
Mean ± SD	65.0 ± 12.6	65.3 ± 12.8	64.0 ± 13.5				
Median [min - max]	67.0 [34.0 - 93.0]	68.5 [36.0 - 91.0]	64.0 [37.0 - 89.0]				
Menopausal status				0.4422			
Peri/premenopausal	10 (16.1)	5 (25.0)	11 (25.6)				
Postmenopausal	52 (83.9)	15 (75.0)	32 (74.4)				
Tumor size (US, mm)				0.126			
Mean ± SD	18.9 ± 14.1	14.9 ± 12.3	18.7 ± 11.4				
Median [min - max]	15.0 [5.0 - 70.0]	11.3 [3.5 - 50.0]	15.0 [4.0 - 58.0]				
N (US)				0.5397			
N0	59 (95.2)	18 (90.0)	38 (88.4)				
N1	3 (4.8)	2 (10.0)	4 (9.3)				
N3	0 (0)	0 (0)	1 (2.3)				
Multifocality				0.5519			
Unifocal	50 (80.6)	18 (90.0)	37 (86.0)				
Bifocal	12 (19.4)	2 (10.0)	6 (14.0)				
Tumor size (mm)				0.8995			
Mean ± SD	18.1 ± 11.9	18.1 ± 11.7	18.9 ± 11.6				
Median [min - max]	15.0 [4.5 - 70.0]	15.5 [6.0 - 55.0]	15.0 [5.8 - 58.0]				
N stage				0.0146	0.0531	0.6476	
pN0	41 (66.1)	9 (45.0)	34 (79.1)				
pN1	19 (30.6)	6 (30.0)	7 (16.3)				
pN2	2 (3.2)	4 (20.0)	2 (4.7)				
pN3	0 (0)	1 (5.0)	0 (0)				
Grade				0.0005	0.9656	0.0017	
I	25 (40.3)	10 (50.0)	3 (7.0)				
II	31 (50.0)	10 (50.0)	31 (72.1)				
III	6 (9.7)	0 (0)	9 (20.9)				
Glandular differentiation				0.1734			
1	3 (4.8)	1 (5.0)	0 (0)				
2	30 (48.4)	9 (45.0)	14 (32.6)				
2	29 (46.8)	10 (50.0)	29 (67.4)				
Nuclear grade				0.0348	1	0.0756	
1	2 (3.2)	0 (0)	0 (0)				
2	54 (87.1)	19 (95.0)	31 (72.1)				
3	6 (9.7)	1 (5.0)	12 (27.9)				
Mitosis score				0.0003	0.0651	0.0537	
1	39 (62.9)	19 (95.0)	15 (34.9)				
2	14 (22.6)	1 (5.0)	18 (41.9)				
3	9 (14.5)	0 (0)	10 (23.3)				
Mitotic index (/mm²)				0.0002	0.4007	0.0042	
Mean ± SD	2.9 ± 2.6	1.8 ± 1.6	4.8 ± 3.2				
Median [min - max]	1.8 [0.4 - 10.5]	0.9 [0.4 - 6.6]	4.4 [0.4 - 15.1]				
Histologic subtype				0.5616			
Micropapillary	2 (3.2)	0 (0)	1 (2.3)				
Mucinous	0 (0)	1 (5.0)	0 (0)				
NST	57 (91.9)	18 (90.0)	41 (95.3)				
NST + micropapillary	3 (4.8)	1 (5.0)	1 (2.3)				
Lymphovascular emboli				0.9027			
No	41 (66.1)	13 (65.0)	30 (69.8)				
Yes	21 (33.9)	7 (3.0)	13 (30.2)				
sTIL (%)				0.1407			
Mean ± SD	7.0 ± 7.6	8.2 ± 9.3	10.6 ± 9.6				
Median [min - max]	5.0 [1.0 - 50.0]	4.0 [1.0 - 30.0]	5.0 [1.0 - 40.0]				
sTIL (≤ 10%)				0.0507			
No	8 (12.9)	4 (20.0)	14 (32.6)				
Yes	54 (87.1)	16 (80.0)	29 (67.4)				
ER (I x %)				0.5524			
Mean ± SD	285.2 ± 34.0	280.0 ± 41.9	277.3 ± 43.2				
Median [min - max]	300.0 [180.0 - 300.0]	300.0 [160.0 - 300.0]	300.0 [140.0 - 300.0]				
PR (I x %)				0.0281	0.7856	0.0567	
Mean ± SD	198.4 ± 99.4	212.3 ± 100.2	151.0 ± 110.4				
Median [min - max]	210.0 [0.0 - 300.0]	247.5 [20.0 - 300.0]	140.0 [0.0 - 300.0]				
Ki67 (%)				<.0001	0.3919	0.0003	
Mean ± SD	15.7 ± 10.2	14.4 ± 13.5	23.8 ± 11.4 *				
Median [min - max]	14.5 [2.0 - 60.0]	11.0 [2.0 - 60.0]	21.5 [5.0 - 60.0] *				
PIK3CA mutations				0.0063	1	0.0048	
Yes (Gain of function)	28 (45.2)	8 (40.0)	6 (15.0) *				
TP53 mutations				0.0003	1	0.0028	
Yes (Loss of function)	3 (4.8)	0 (0)	12 (30.0) *				
AKT1 mutations				0.1104			
Yes (Gain of function)	5 (8.1)	0 (0)	0 (0) *				
PTEN mutations				1			
Yes (Loss of function)	1 (1.6)	0 (0)	1 (2.5) *				
BRCA2 mutations				0.854			
Yes (Loss of function)	3 (4.8)	0 (0)	2 (5.0) *				
ARID1A mutations				0.4918			
Yes (Loss of function)	0 (0)	0 (0)	1 (2.5) *				
KRAS, NRAS, BRAF, PALB2 mutations				-			

Figure 1 - 100

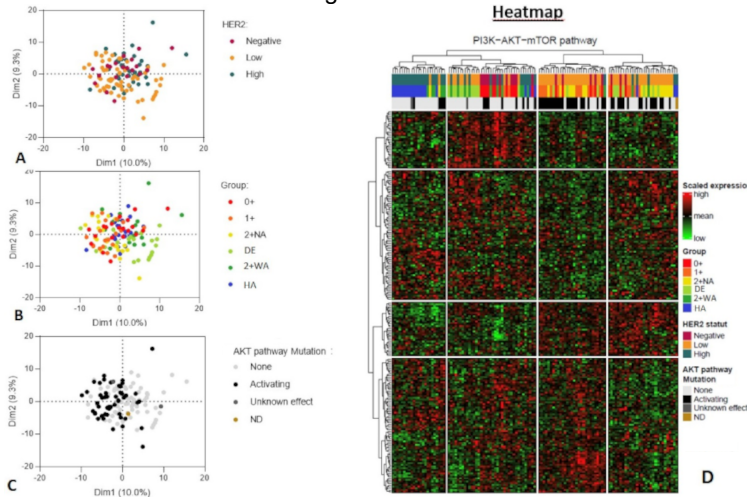
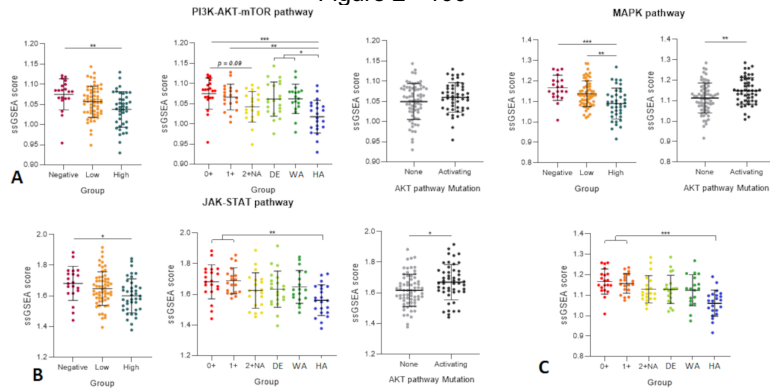


Figure 2 - 100



Conclusions: We found that luminal H2L and HER2-negative carcinomas shared most of clinicopathological, molecular and transcriptomic characteristics, except for HER2 membrane expression and mRNA levels. Transcriptomic clustering did not overlap with tumor groups in the new HER2 classification. Furthermore, *PIK3CA* mutations were more prevalent in these tumors, leading to a strong activation of the PI3K-AKT signaling pathway even in the absence of HER2 overexpression/amplification. From a therapeutic point of view, *PIK3CA* mutations may explain the failure of conventional anti-HER2 treatments, suggesting that targeted anti-PI3K therapies and – possibly - new antibody-drug conjugates may be more effective.

101 Adenomyoepithelioma: A Clinicopathological Study of 18 Cases of a Rare Breast Neoplasm with Literature Review

Saba Anjum¹, Nasir Ud Din¹, Muhammad Usman Tariq¹, Naila Kayani¹

¹Aga Khan University Hospital, Karachi, Pakistan

Disclosures: Saba Anjum: None; Nasir Ud Din: None; Muhammad Usman Tariq: None; Naila Kayani: None

Background: Adenomyoepithelioma (AME) is an uncommon breast tumor, accounting <0.5% of breast tumors. AME is typically benign; however, atypical and malignant categories are also recognized, and few cases may be associated with carcinoma. Classical AMEs pursue benign course and complete surgical excision is curative. We aimed to describe the clinicopathological features of this rare entity along with follow up.

Design: H&E and IHC slides of AME cases diagnosed between 2012 and 2021(n=18) were retrieved and reviewed. Demographic data was collected from surgical pathology reports. Follow up was obtained.

Results: Patient's age ranged from 26-73 (Median 48) years. All presented with a palpable lump, associated with nipple discharge in 8 cases. Tumor was multifocal in 1 case. Tumor size ranged from 1.1 to 16 (Median 4.8) cm. Benign AME had circumscribed borders while cases with malignant features showed infiltrative borders. Architecturally Tubular pattern was seen in 10, Spindle pattern in 3 and Mixed pattern in 5 cases. Hyaline degeneration (15), calcification (11), cystic degeneration (4), apocrine metaplasia

(5), squamous and mucinous metaplasia (2) was noted. No significant mitotic activity was noted in benign tumors. Histologically, 13 tumors showed morphological features of benign AME, 1 was diagnosed as atypical AME, 1 as malignant AME, 2 as Metaplastic carcinoma arising in AME and 1 as Epithelial-myoepithelial carcinoma in AME. Mitotic count ranged from 9-15/ mm² in malignant tumors. All tumors demonstrated heterogenous expression for keratins. ASMA and P63 were positive in myoepithelial cells in all cases. S100, CK5/6 and ER were positive with variable frequency. Available follow up of 16 patients ranged from 12-124 (Median 39.5) months. All benign including 1 atypical AME cases were treated with surgery alone (n=14). Adjuvant chemo and/or radiotherapy was administered in 2 malignant cases; remaining 2 cases (Metaplastic carcinoma and Epithelial-myoepithelial carcinoma in AME) lost to follow up. Rest of the patients were alive and disease free.

Conclusions: AME exhibits distinct morphological and IHC features. Atypical, malignant forms and associated carcinoma are not uncommon. Typical cases show indolent behavior. Limited follow-up in our cohort of patients showed recurrence in 1 patient with atypical AME. Thus, long term follow up will accurately determine its clinical behavior.

102 Genomic Testing on Core Needle Biopsy Samples from Newly Diagnosed ER+/HER2- Breast Cancer Patients Decreases Use of Neoadjuvant Chemotherapy

Amna Anzar¹, Joy Knight¹, Philip Bomeisl², Alberto Montero³, Hannah Gilmore⁴

¹University Hospitals Cleveland Medical Center, Case Western Reserve University, Cleveland, OH, ²University Hospitals Cleveland Medical Center, Cleveland, OH, ³Case Western Reserve University/University Hospitals Cleveland Medical Center, Cleveland, OH, ⁴University Hospitals Case Medical Center, Case Western Reserve University, Cleveland, OH

Disclosures: Amna Anzar: None; Joy Knight: None; Philip Bomeisl: None; Alberto Montero: None; Hannah Gilmore: None

Background: Genomic profiling assays for invasive breast cancer (BC) are performed most commonly on surgical resection specimens in patients with ER+/HER2- disease to help determine the need for chemotherapy. However, obtaining this genomic information earlier in the course of treatment from core needle biopsy (CNB) material has numerous advantages including identifying patients who would benefit from neoadjuvant chemotherapy (NAC). In 2020, our breast program began a pilot study where all newly diagnosed breast cancers were sent for genomic analysis using the Agendia MammaPrint (MPT) and BluePrint (BPT) assays on CNB material to assess overall clinical utility and impact.

Design: After obtaining IRB approval, the system tumor registry was queried for all patients diagnosed with BC from 8/2019-12/2021. We then compared the population of ER+/HER2- patients who had genomic testing by MPT/BPT on the initial CNB sample to those who did not to determine rate of NAC usage. Pearson χ^2 test was used to analyze the data using SPSS software.

Results: 952 patients with newly diagnosed ER+/HER2- BC were identified. There were 585 patients with reflex genomic testing on CNB and 367 who were treated based upon traditional clinicopathologic features alone. When the two groups were compared, NAC was used significantly more often in patients who had not undergone genomic testing on the initial CNB. While 20.1% (74/367) of ER+/HER2- patients underwent NAC in the time before the pilot reflex testing program, only 9.74% (57/585) received NAC when the genomic result was available on the CNB material (odds ratio (OR), 2.339, P<0.0001). Genomic testing on the initial CNB identified many patients for whom NAC would have been offered based upon traditional clinicopathologic features but who would not have benefited significantly.

Conclusions: Patients with newly diagnosed ER+/HER2- breast cancer were significantly more likely to undergo NAC when genomic testing was not performed on the initial CNB. Genomic testing identified patients with high risk clinicopathologic features but low risk genomic features who were unlikely to benefit from NAC, allowing the both the clinician and patient to better understand the tumor biology and make treatment decisions earlier in the course of care. Furthermore, despite the cost of genomic testing, reflex testing of ER+/HER2- BC on CNB may be cost effective because of the significant reduction in NAC.

103 Histologic Correlates of Molecular Subtypes of Triple Negative Breast Cancer

Alexandre Archambault-Marsan¹, Jahg Wong², Ayman Al Shoukari³, Leonardo Lando⁴, Maëlle Batardière⁵, Vincent Quoc-Huy Trinh⁶, Philippe Echelard⁷

¹Université de Montréal, Montreal, QC, ²Centre Hospitalier de l'Université de Montréal (CHUM), Montreal, QC, ³American University of Beirut, Beirut, Lebanon, ⁴University of Toronto, Toronto, ON, ⁵Institute for Research in Immunology and Cancer, Montréal, QC, ⁶Institute for Research in Immunology and Cancer, Montréal, QC, ⁷Université de Sherbrooke, Sherbrooke, QC

Disclosures: Alexandre Archambault-Marsan: None; Jahg Wong: None; Ayman Al Shoukari: None; Leonardo Lando: None; Maëlle Batardière: None; Vincent Quoc-Huy Trinh: None; Philippe Echelard: None

Background: Molecular studies have reclassified triple-negative breast cancer (TNBC) into basal-like 1 (BL1), basal-like 2 (BL2), mesenchymal (MSL), and luminal androgen-receptor (LAR). Studies have noted differences in inflammatory infiltrates and

differences in stromal signatures, but no study has focused on the histologic findings specific to each of these molecular subtypes. We aim to identify histological findings that are associated to TNBC molecular subtypes.

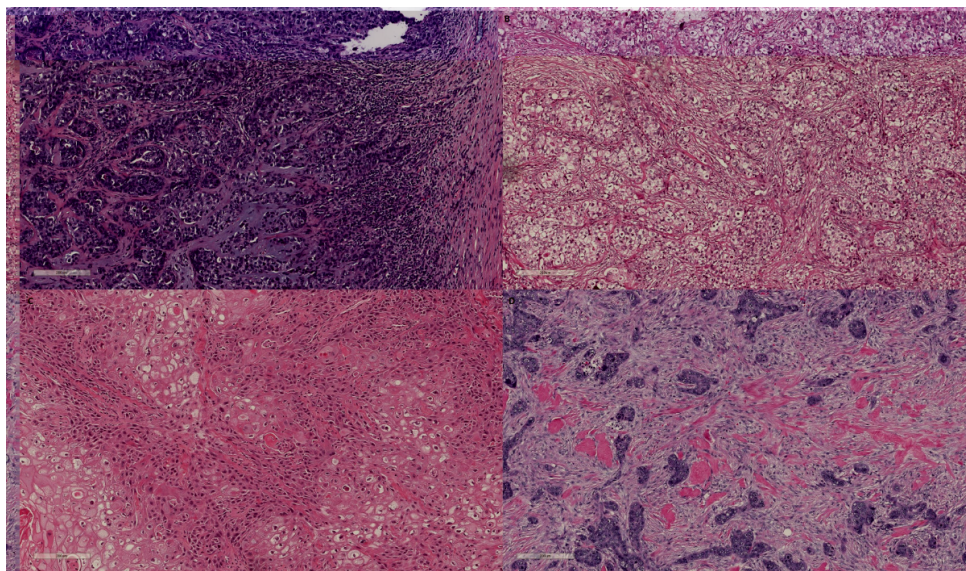
Design: Molecular subtypes were extracted from classifications generated by Jiang et al. Cancer Cell 2019, based on data from the Cancer Genome Atlas and validated in an external cohort. We downloaded corresponding slides from the TCGA using the GDC Data Transfer Tool. We created a list based on a review of the literature of prior histological classifications of TNBC and for classical histological findings : squamoid morphology intercellular bridges, keratin whorls, keratinization, matrix production, spindle cells, sarcomatoid, tubular, nuclear pleomorphism, color of cytoplasm, abundance of cytoplasm, syncytial growth, heterologous elements, NC ratio, presence of DCIS, invasive tumor necrosis, tumoral tumor-infiltrating lymphocytes (TILs), peritumoral TILs, necrosis, cribriform features, lymphovascular invasion, perineural invasion, SBR grade. The slides were reviewed by two observers including a pathologist. The presence of these findings was then correlated to molecular subtypes.

Results: There were 122 patients with molecular subclassification, adequate for histology review, and confirmed TNBC. An example of different histological patterns is presented in figure 1. As described in previous studies, TILs were significantly associated to molecular subtypes. The only features that two pathologists could reliably replicate with molecular subtypes were squamoid morphology, intercellular bridges, keratin whorls, keratinization, cytoplasmic abundance, and NC ratio (table1). The presence of DCIS was present in all 4 molecular subtypes, although it was significantly more prevalent in the MSL subtype. Also, the color of the cytoplasm, the SBR grade, spindle cells, and matrix production were not specific to a molecular subtype (table 1).

Table 1. Histological correlations with molecular subtypes.

	Basal-like 1	Basal-like 2	Mesenchymal	Luminal androgen receptor	P
Squamoid morphology	0 (0%)	6 (21%)	1 (3%)	1 (5%)	0.004
Intercellular bridges	0 (0%)	5 (17%)	1 (3%)	0 (0%)	0.005
Keratin whorls	0 (0%)	6 (21%)	1 (3%)	0 (0%)	0.001
Keratinization	0 (0%)	6 (21%)	1 (3%)	1 (5%)	0.004
Matrix production	4 (10%)	3 (11%)	5 (15%)	2 (10%)	0.9
Spindle cells	4 (10%)	3 (11%)	6 (18%)	4 (19%)	0.634
Sarcomatoid	3 (8%)	3 (11%)	5 (15%)	3 (14%)	0.763
Tubular differentiation	3 (8%)	2 (7.1%)	4 (12%)	4 (19%)	0.492
Nuclear pleomorphism	11 (28%)	7 (25%)	11 (33%)	7 (33%)	0.749
Low	14 (36%)	7 (25%)	12 (36%)	8 (38%)	
Intermediate	14 (36%)	14 (50%)	10 (30%)	6 (29%)	
High					
Nucleoli prominence	13 (33%)	12 (42%)	21 (64%)	13 (62%)	0.117
Low	24 (62%)	14 (50%)	10 (30%)	6 (29%)	
Intermediate	2 (5%)	2 (7%)	2 (6%)	2 (10%)	
High					
Cytoplasmic abundance	28 (72%)	10 (36%)	23 (70%)	6 (29%)	0.003
Low	9 (23%)	12 (43%)	9 (27%)	12 (57%)	
Moderate	2 (5%)	6 (21%)	1 (3%)	3 (14%)	
Abundant					
Cytoplasmic color	13 (32%)	14 (36%)	9 (27%)	10 (48%)	0.092
eosinophilic	21 (53%)	12 (43%)	14 (42%)	10 (48%)	
amphophilic	6 (15%)	2 (7%)	10 (30%)	1 (5%)	
basophilic					
Syncytial growth	10 (26%)	5 (18%)	6 (18%)	5 (24%)	0.826
Heterologous elements	5 (13%)	3 (11%)	5 (27%)	9 (29%)	0.235
N:C ratio	0 (0%)	1 (4%)	0 (0%)	2 (10%)	0.002
Low	5 (13%)	12 (43%)	4 (12%)	9 (38%)	
Intermediate	34 (87%)	15 (54%)	29 (88%)	11 (52%)	
High					
Presence of DCIS on slide	8 (20%)	5 (18%)	6 (18%)	10 (48%)	0.046
Tumor infiltrating lymphocytes	24 (57%)	16 (55%)	8 (22%)	8 (36%)	0.050
Peritumoral lymphocytes	0 (0%)	1 (3%)	6 (17%)	2 (9%)	0.003
None	2 (5%)	5 (17%)	9 (25%)	3 (14%)	
Low	8 (19%)	3 (10%)	8 (22%)	4 (18%)	
Moderate	26 (62%)	14 (48%)	5 (14%)	12 (55%)	
Dense	6 (14%)	6 (21%)	8 (22%)	1 (5%)	
Adjacent N/A					
Invasive tumor necrosis	8 (19%)	11 (38%)	13 (36%)	15 (68%)	0.057
None	1 (2%)	2 (7%)	2 (6%)	0 (0%)	
Focal	5 (12%)	3 (10%)	4 (11%)	3 (14%)	
Non-focal	25 (60%)	11 (38%)	13 (36%)	3 (14%)	
Confluent					
Tumor border	8 (19%)	10 (35%)	11 (31%)	9 (40%)	0.365
Infiltrative	11 (26%)	5 (17%)	10 (28%)	7 (32%)	
Mixed	17 (40%)	8 (28%)	7 (19%)	4 (18%)	
Pushing					
Cribriform features	33 (78%)	25 (86%)	23 (64%)	19 (86%)	0.763
None	1 (2%)	0 (0%)	3 (8%)	1 (5%)	
Focal	3 (7%)	1 (3%)	4 (11%)	1 (5%)	
Non-focal	2 (5%)	1 (3%)	2 (6%)	0 (0%)	
Diffuse					

Figure 1 – 103



Conclusions: Overall, our findings show some histological findings are significantly associated with molecular subtypes. However, if molecular subtyping of TNBC is clinically warranted, molecular ancillary testing will likely be required.

104 Evaluating Low HER2 Status in Breast Cancer Cases with Absent and Low HER2 Protein Expression

Gokce Ardor¹, Miglena Komforti², Helena Hanna², Aziza Nassar²

¹Mayo Clinic College of Medicine and Science, Mayo Clinic Florida, Jacksonville, FL, ²Mayo Clinic, Jacksonville, FL

Disclosures: Gokce Ardor: None; Miglena Komforti: None; Helena Hanna: None; Aziza Nassar: None

Background: HER2-low expression in breast cancer is defined as HER2 immunohistochemistry (IHC) score of 1+ or 2+ with a negative in-situ hybridization (ISH) assay, according to current scoring criteria. Recent studies have demonstrated clinical benefits to patients with primary and metastatic breast cancers showing HER2-low expression using novel anti-HER2 antibody-drug conjugates. More HER2-low tumors are recognized by careful exam under 200× and high power (400×) magnification, according to a recent article. Herein, we further evaluated HER2-low status in invasive breast tumors with absent and low (1+) protein expression.

Design: We identified 112 invasive breast cancer cases in our pathology database (n=114, including two patients with two tumors each), from 2019-2022 that were interpreted as either HER-0 or HER2-1+ on the final pathology report. Two blinded breast pathologists independently reviewed the slides using 200× and 400× magnification, categorized into three groups: HER2(0) - complete lack of expression; HER2(very low), >0% but <10% tumor cells with faint incomplete membranous staining; and HER2(low, 1+), >10% faint incomplete membranous staining. Discordant cases between the two pathologists were rescored together. Cohen's kappa test was used to analyze differences between original report interpretations and rescored HER2 IHC results and between the two breast pathologists (BP).

Results: The original report HER2 interpretation, and the first and second round of re-scoring is shown in the Table 1. Comparison of first round of re-scoring between BP1 and BP2 showed moderate agreement with Cohen's kappa value of 0.62. Whereas the comparison of original report interpretation and the second re-scoring showed no agreement with Cohen's kappa value of 0.16.

Table 1: Re-categorization of invasive breast cancer with absent and low (1+) HER2 protein expression into HER2 0, HER2 very low, and HER2 1+ in 112 patients

HER2 IHC scores	Original report interpretation, n and %	First rescored BP1, n and %	First rescored BP2, n and %	Second Rescoring (BP1 and BP2), n and %
HER2(0)	38 (33.3%)	17 (14.9%)	20 (17.6%)	15 (13.1%)
HER2(very low)	NA	31 (27.2%)	33 (28.9%)	35 (30.7%)
HER2(1+)	76 (66.7%)	64 (56.2%)	61 (53.5%)	63 (55.3%)
HER2(2+)	NA	2 (1.8%)	NA	1 (0.9%)

Conclusions: Given the significant treatment implications and prognosis of HER2-low breast cancers, its recognition as a new reporting category in HER2 IHC scoring algorithms is paramount. Our data supports that HER2 IHC results can be reliably classified into the following updated categories: HER2(0), HER2(very low), and HER2(low,1+). Analysis should be performed by skilled breast pathologists utilizing the 200x and 400x methods. Interpretations with close cut-off values may require consensus review by a second pathologist. The significance to patient management in regards to biological significance and tumor behavior between the new categories remains to be investigated.

105 Validation and Clinical Deployment of an Artificial Intelligence Solution for Diagnosis Support in Breast Biopsies

Margaret Assaad¹, Ira Krasnitsky², Jonathan Harel², Stephanie Cowles¹, Laurie Jacobsen¹, Judith Sandbank³, Manuela Vecsler², Srinivasa Mandavilli⁴

¹Hartford Hospital, Hartford, CT, ²Ibex Medical Analytics, Tel Aviv, Israel, ³Maccabi Health Services, Kiriat Ono, Israel, ⁴Hartford Hospital, CT

Disclosures: Margaret Assaad: None; Ira Krasnitsky: None; Jonathan Harel: None; Stephanie Cowles: None; Laurie Jacobsen: None; Judith Sandbank: None; Manuela Vecsler: None; Srinivasa Mandavilli: None

Background: This study aimed to validate the performance and clinical utility of an artificial intelligence (AI) solution in the detection of invasive and in situ breast carcinoma in real world clinical routine use in a hospital pathology laboratory setting.

Design: The study included an enriched cohort of 475 retrospective breast core needle biopsies, comprising 5081 H&E slides, enriched with invasive carcinoma (180 biopsies; 38%), DCIS (112; 23%) and ADH (45; 9%). All the slides were digitized and blindly processed by the AI solution. Alerts were triggered in case of discrepancies between the AI results and the ground truth (GT) that was based on the original sign-out reports, prompting a second review by two independent breast pathologists. After the completion of the validation, the solution will be deployed as a quality control system prospectively, on all new breast biopsies.

Results: The AI solution demonstrated high performance for the detection of invasive carcinoma with an AUC of 0.98 (sensitivity and specificity of 95.6% and 91.5%, respectively) and AUC of 0.99 for the detection of DCIS (sensitivity and specificity of 95.5% and 95.7%, respectively) when compared with the GT. The AI differentiated well between subtypes/grades of invasive and in-situ cancers with an AUC of 0.97 for IDC vs. ILC and AUC of 0.92 for DCIS high grade vs. low grade/ADH, respectively.

	# Positive /Negative	AUC	AUC 95% Confidence Interval	Sensitivity	Specificity	PPV	NPV
Carcinoma	292 / 183	0.975	[0.96,0.99]	94.20%	90. 2%	0.95	0.9
Invasive carcinoma	180 / 295	0.98	[0.97,0.99]	95.60%	91.50%	0.87	0.97
DCIS	112 / 138	0.99	[0.98, 0.99]	95.50%	95.70%	0.95	0.96

Conclusions: We report the successful validation, deployment and prospective usage of an AI diagnostic support solution, in routine clinical practice. The AI solution enabled 100% quality control on breast biopsies. Such technology has the potential to support and complement the traditional microscopic evaluation done by pathologists, potentially increasing both diagnostic accuracy and patient safety.

106 Intraoperative Assessment of Axillary Sentinel Lymph Nodes by Telepathology

Sunil Badve¹, Sandra Gjorgova Gjeorgjievski¹, Qun Wang¹, Abdulwahab Ewaz¹, Di (Andy) Ai¹, Xiaoxian Li¹, Gulisa Turashvili¹

¹Emory University, Atlanta, GA

Disclosures: Sunil Badve: None; Sandra Gjorgova Gjeorgjievski: None; Qun Wang: None; Abdulwahab Ewaz: None; Di (Andy) Ai: None; Xiaoxian Li: None; Gulisa Turashvili: None

Background: Although axillary dissection is no longer indicated for many breast cancer patients with positive axillary sentinel lymph nodes (ASLN), intraoperative ASLN assessment is still necessary for some patients. With recent advancements in digital pathology, pathologists are increasingly expected to evaluate ASLN via telepathology.

Design: We aimed to compare the performance characteristics of remote telepathology and conventional on-site intraoperative ASLN assessment. Data from ASLN evaluation for breast cancer patients performed by the same group of pathologists at two sites between April 2021 and August 2022 was collated. Remote telepathology consultation was conducted via the Aperio eSlideManager system.

Results: Intraoperative ASLN assessment was performed in a total of 308 patients during the study period (67 telepathology, 241 on-site evaluations). The overall discrepancy rate between intraoperative and final diagnoses was 10.4% (7/67) for telepathology and 6.6% (16/241) for on-site assessment ($p=0.0035$). The rate of interpretive errors was 1.5% (1/67) for telepathology and 2.5% (6/241) for on-site assessment. Of 7 discrepant cases assessed via telepathology, all were false negative, including 1 macrometastasis (MaMet), 4 micrometastases (MiMet), and 2 isolated tumor cells (ITCs). These included 1 interpretive (invasive lobular carcinoma [ILC]) and 6 sampling errors (3 ILCs, 3 invasive carcinomas of no special type [IC-NST]), all in treatment-naïve patients. Of 16 discrepant cases assessed on-site, there were 10 sampling and 6 interpretive errors, the latter including 2 false positive results in treatment-naïve patients with invasive carcinoma with ductal and lobular features and 4 false negative results in patients with IC-NSTs (1 post-neoadjuvant chemotherapy [PNACT], 3 treatment-naïve). The 14 false negative cases included 4 MaMets, 5 MiMets and 5 ITCs, of which 7 were PNACT. The deferral rate was 3% (2/67) for telepathology and 3.7% (9/241) for on-site ASLN assessment. All deferrals were atypical cells interpreted as benign on permanent sections, except for 2 cases reported as atypical cells on-site but showing MaMets on permanent sections.

Conclusions: ASLN assessment via telepathology appears to have a higher discrepancy rate compared with on-site evaluation (10.4% vs. 6.6%; $p=0.0035$), while the rates of interpretive errors (1.5% vs. 2.5%) and deferrals (3% vs. 3.7%) are comparable. Further studies are warranted to ensure accuracy of ASLN assessment via telepathology.

107 Diagnostic Accuracy of Image Guided Breast Biopsies: Comparison of Traditional Stereotactic Biopsy and the Brevera Biopsy System

Spencer Barnes¹, Valarie McMurtry², Eric Goold², Rachel Factor³, Jonathon Mahlow¹

¹The University of Utah/ARUP Laboratories, Salt Lake City, UT, ²The University of Utah, Salt Lake City, UT, ³Duke University, Durham, NC

Disclosures: Spencer Barnes: None; Valarie McMurtry: None; Eric Goold: None; Rachel Factor: None; Jonathon Mahlow: None

Background: Different methods are employed by radiologists to biopsy imaging detected lesions in the breast. At our institution, the Brevera Biopsy System (Hologic, Inc.) (BBS) is now preferred over the traditional stereotactic guided biopsy (SB) for calcifications. From a radiology standpoint, there are benefits, including improved time and efficiency of work flow, as well as the real-time confirmation of calcifications in the sample. Multiple biopsies can be taken at the same time, which also improves sampling. However, there is an increase in slide number per biopsy compared SB, with an increase in case review time for the pathologist. The aim of this study is to compare the diagnoses and attributes of biopsies take by SB and BBS in terms of both pathologist workload and sampling efficacy.

Design: Pathology reports and slides were collected from stereotactic breast biopsies performed during the entire 2012 calendar year and compared to breast biopsies performed utilizing the Brevera system during the 2019 calendar year. The slides were retrospectively reviewed for diagnostic findings. Diagnosis, age at biopsy, BIRADS score, identification of calcifications, number of blocks per case, and additional levels ordered were compared.

Results: 85 cases utilizing SB were compared against 78 cases utilizing BBS. BBS detected significantly more disease and showed a broader range of diagnoses including benign (n=33), atypia of any type (n=9) and carcinoma in situ (n=27) categorized together as “pre-cancer”, and invasive carcinoma (n=9). Fewer cases of atypia or malignancy were detected by SB. The difference between diagnostic categories between the two methods was statistically significant (table 1). On average, the number of blocks per case was 2.4 for BBS and 1.1 for SB ($p=<0.001$). Patient age, BIRADS score, presence of calcifications, and whether additional levels were needed to find calcifications did not significantly differ between sampling methods.

	Brevera Biopsy System	Stereotactic Biopsy	Significance
Cases examined (n=)	78	85	
Mean age (years)	57.2	55.2	$p = 0.33$
BIRADS score (Mode)	4	4	$p = 0.078$
Benign diagnosis (n=)	33	69	$p = <0.001$
Atypia (of any type) (n=) (pre-cancer)	9	2	$p = <0.001$
Carcinoma in situ (n=) (pre-cancer)	27	14	
Invasive Cancer (n=)	9	0	$p = 0.001$
Average number of blocks per case (n=)	2.4	1.1	$p = <0.001$

Conclusions: In a uniform sample population matched by radiologic risk stratification (BIRADS score) and age, BBS increased pathology work-load but resulted in a significant increase in detection of atypia/malignancy compared to SB. The data suggests that BBS is a superior sampling method for the detection of atypia, DCIS, and malignancy associated with calcifications.

108 Mutations in Homologous Recombination Genes and Loss of Heterozygosity Status in Advanced Stage Breast Carcinoma

Brooke Bartow¹, Gene Siegal¹, Lei Huo², Qingqing Ding², Aysegul Sahin², Shuko Harada¹, Xiao Huang¹

¹The University of Alabama at Birmingham, Birmingham, AL, ²The University of Texas MD Anderson Cancer Center, Houston, TX

Disclosures: Brooke Bartow: None; Gene Siegal: None; Lei Huo: None; Qingqing Ding: None; Aysegul Sahin: None; Shuko Harada: None; Xiao Huang: None

Background: Poly (adenosine diphosphate-ribose) polymerase inhibitors (PARPi) recently have been approved by the FDA for the treatment of germline *BRCA1/2* associated breast cancer. PARPi have also been found to be efficacious in *BRCA* wild-type (*BRCAwt*) carcinomas with high genomic loss of heterozygosity (LOH-high) or other identifiable mutations in homologous recombination repair (HR) genes in ovarian carcinomas. The goal of this study was to retrospectively investigate tumor mutations in HR genes and LOH status in advanced stage breast carcinomas (BC).

Design: Patients diagnosed with invasive breast carcinoma between 2019 and 2022 whose tumors underwent whole exome sequencing were identified. LOH was determined by analyzing single nucleotide polymorphisms throughout the genome. Tumor pathologic genomic alterations and LOH score were collected. Patients' medical records were also reviewed to obtain data on demographic and pathologic characteristics. The cohort was divided into three groups: *BRCA1/2* mutated (*BRCAmt*), *BRCA* wild-type HR-mutated (*BRCAwt-HRmt*), and HR wild-type (*HRwt*).

Results: We identified 36 patients with locally advanced or metastatic breast carcinoma; their clinicopathological characteristics and the associations with HRD are given in the table. Of the 36 cases, 12 (33%) had HR mutations, including 3 (8%) *BRCA1*, 3 (8%) *BRCA2*, and 6 (17%) *BRCAwt-HR* (Figure 1). There was no association between HR mutations and Nottingham grade (NG) or triple negativity (TN). LOH data was available for 23 cases. Seven (7/23, 30%) had HR mutations, including 3 (43%) in *BRCA1/2* and 4 (57%) in *BRCAwt-HR* (figure 2A). Eight (35%) and 16 (70%) of the 23 were LOH-high using 16% and 10% cutoffs respectively. LOH-high ($\geq 10\%$) had a positive association with *BRCAmt* ($p < 0.0001$). *BRCA1/2* mutations were only identified in LOH-high ($\geq 10\%$) cases. There was no association between LOH-high ($\geq 16\%$) and *BRCAmt*. Five of 15 (33%), and 2 of 7 (29%) LOH-low cases had HR mutations with 16% and 10% cutoffs respectively (figure 2B and 2C). LOH-high was positively associated with TN, but not NG.

Clinicopathological features of patients with advanced stage breast carcinoma

Characteristic	All patients (N=36)	
	Number	%
Clinical stage		
1	0	0
2	2	6
3	2	6
4	32	89
Nottingham grade		
1	0	0
2	11	31
3	25	69
ER status		
Positive	16	44
Low positive	2	6
Negative	18	50
PR status		
Positive	16	44
Negative	20	56
HER2 status		
Positive	6	17
Negative	30	83
Neoadjuvant therapy		
Yes	13	36
No	23	64

Association between HRR and pathologic features

	Nottingham grade		P value	Triple negativity		P value
	2	3		Yes	No	
HRmt (N=12)	4 (33%)	8 (67%)	0.5408	5(42%)	7(58%)	1.0
HRwt (N=24)	7 (29%)	17(71%)		10(42%)	14(58%)	
LOH ($\geq 10\%$) (N=16)	4 (25%)	12(75%)	0.5241	6(38%)	10(63%)	P<0.00001
LOH (<10%) (N=7)	2(29%)	5(71%)		0(0%)	7(100%)	
LOH ($\geq 16\%$) (N=8)	2(25%)	6(75%)	0.5241	4(50%)	4(50%)	P<0.00001
LOH (<16%) (N=15)	4(29%)	11(71%)		2(13%)	13(87%)	

Figure 1 – 108

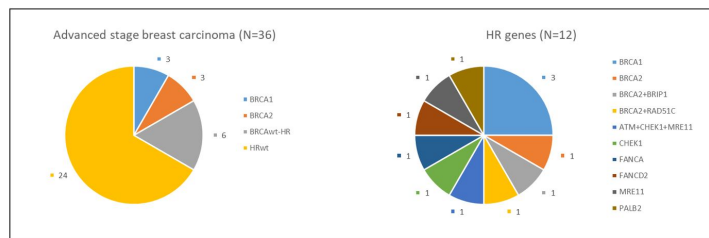
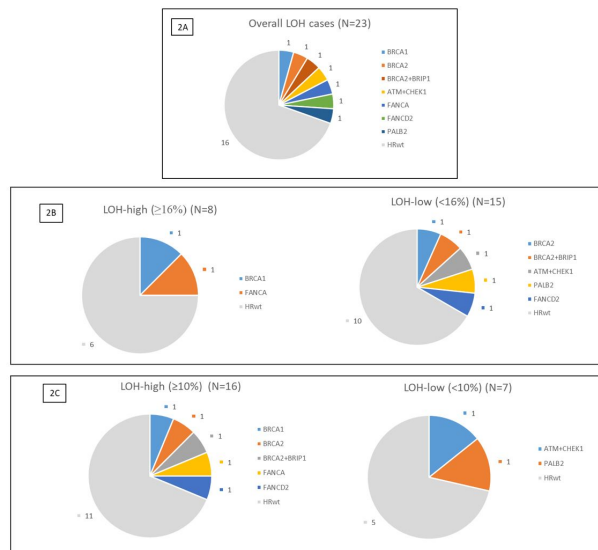


Figure 2 - 108



Conclusions: 17% of 36 cases showed HR gene mutations other than *BRCA 1/2*. Although LOH-high showed positive association with *BRCAm*t only, a subset of LOH-low cases showed mutations in *BRCAw*t-HR and/or *BRCA* genes. The necessity of next generation sequencing with homologous recombination deficiency gene analysis requires further investigation in large clinical trials.

109 PD-L1 Expression by Immunohistochemistry: Comparison Between Tissue Microarrays and Whole Slide Sections in Breast Carcinoma

Harsh Batra¹, Elizve Barrientos¹, Hua Guo², Xiao Huang³, Maria Gabriela Raso¹, Qingqing Ding¹, Lei Huo¹

¹The University of Texas MD Anderson Cancer Center, Houston, TX, ²Columbia University Irving Medical Center, New York, NY, ³The University of Alabama at Birmingham, Birmingham, AL

Disclosures: Harsh Batra: None; Elizve Barrientos: None; Hua Guo: None; Xiao Huang: None; Maria Gabriela Raso: None; Qingqing Ding: None; Lei Huo: None

Background: Anti-PD1/PD-L1 clinical trials in breast cancer have allowed both small biopsies and large surgical specimens for PD-L1 immunohistochemistry (IHC) testing. Many research studies on PD-L1 expression used tissue microarrays (TMA) in order to test a large number of tumors in a cost-effective manner. However, the concordance between small tumor samples and large tumor sections for PD-L1 expression has not been well studied. Here, we compared PD-L1 IHC staining between TMAs and whole slide sections (WSS) using two FDA-approved assays and three scores.

Design: The study cohort consisted of 24 patients (14 with triple-negative breast cancer (TNBC) and 10 with non-TNBC) diagnosed between 2004 and 2016. WSSs of surgically resected tumors and the corresponding TMAs (1.0 mm puncher, duplicate punches) were stained for PD-L1 using the Dako 22C3 and 28-8 assays. The tumor cell (TC) score was calculated as the percent of invasive carcinoma cells showing membranous staining for PD-L1. The tumor-infiltrating immune cells (IC) score was assessed as the proportion of tumor area occupied by PD-L1-positive immune cells. The combined positive score (CPS) was calculated as the number of PD-L1 stained immune cells and invasive carcinoma cells divided by the number of invasive carcinoma cells, multiplied by 100. For TC and IC, 1% or greater was considered positive. For CPS, two cutoffs of 1 and 10 were applied. Concordance was evaluated based on positive versus negative categories.

Results: The numbers of PD-L1 positive tumors and the concordance rates in each scoring method are shown in Table 1. The concordance rates ranged from 71% to 100%. There were 30 discordant events in all comparisons: 22 had positive staining only in WSSs, and 8 had positive staining only in TMAs. Among the tumors that showed discordance in any of the comparisons, only one tumor, which was a TNBC, had discordance in all scoring methods and with both 22C3 and 28-8.

Table 1. Comparison of PD-L1 expression between whole slide sections and tissue microarrays in 24 breast carcinomas

Concordance No. (%)	22C3 WSS vs. TMA				28-8 WSS vs. TMA			
	TNBC (n=14)		non-TNBC (n=10)		TNBC (n=14)		non-TNBC (n=10)	
TC 1%	11 (79)		9 (90)		11 (79)		10 (100)	
IC 1%	11 (79)		8 (80)		12 (86)		8 (80)	
CPS 1	11 (79)		9 (90)		10 (71)		9 (90)	
CPS 10	13 (93)		9 (90)		13 (93)		8 (80)	
22C3 IHC								
Positive No. of cases	TNBC (n=14)		non-TNBC (n=10)		TNBC (n=14)		non-TNBC (n=10)	
	WSS	TMA	WSS	TMA	WSS	TMA	WSS	TMA
TC 1%	6	3	2	3	6	3	3	3
IC 1%	6	3	3	3	6	4	4	4
CPS 1	6	5	3	4	7	5	4	5
CPS 10	5	4	3	4	5	4	3	3

Conclusions: In a minor proportion of tested tumors, TMA underestimated or overestimated PD-L1 staining compared with WSS. CPS with a cutoff of 10 improved the concordance rate in TNBC over CPS with a cutoff of 1. Our findings suggest that in clinical settings using CPS 10 as the cutoff, small tumor samples are comparable to large tumor sections in the vast majority of breast tumors.

110 Molecular Apocrine Breast Carcinoma: Histomolecular and Prognosis Characterization – A Multicentric Retrospective Study

Anthony Bergeron¹, Gaetan Macgrogan², Aurélie Bertaut³, Romain Boidot³, Françoise Beltjens³, Céline Charon Barra³, Isabelle Desmoulins³, Sylvain Ladoire⁴, Anne Vincent-Salomon⁵, Laurent Arnould³

¹Unit of Pathology, Department of Biology and Pathology of the Tumor, Centre Georges-François Leclerc, Dijon, France,

²Institut Bergonié, Lyon, France, ³Centre Georges-François Leclerc, Dijon, France, ⁴Dijon, France, ⁵Institut Curie, Paris, France

Disclosures: Anthony Bergeron: None; Gaetan Macgrogan: None; Aurélie Bertaut: None; Romain Boidot: None; Françoise Beltjens: None; Céline Charon Barra: None; Isabelle Desmoulins: None; Sylvain Ladoire: None; Anne Vincent-Salomon: None; Laurent Arnould: None

Background: Molecular apocrine breast carcinoma (MABC), defined as estrogen and progesterone receptor negative breast cancer with androgen receptor (AR) expression, is rare. It encompasses different morphologic entities with or without apocrine differentiation. Histopathological, molecular and prognostic characteristics of these tumors are not fully understood. The aim of this work is to better characterize the subgroup of MABC.

Design: We analyzed clinicopathological and genomic characteristics of 92 MABCs, retrieved from the files of three Cancer Centers between 2004 and 2020. Clinicopathological, immunohistochemical characteristics and follow-up information, were collected. Molecular profiles were obtained by Exome and RNA sequencing by NGS and analysis of overall (OS) and progression-free survival was done according to Kaplan-Meier method.

Results: Among the 92 MABCs, 24 were HER2-amplified (HER2+) and 68 triple-negative (Luminal androgen receptor tumors (LAR)). These two groups shared some histomolecular characteristics, but some features were significantly different. Basal marker expression (CK5/6 ($p=0.040$) and EGFR ($p=0.006$)) was more frequently observed in LAR while ERBB2 mutations ($p=0.027$) were more frequent in HER2+ tumors. When focusing on the LAR subgroup, tumors with apocrine morphology had lower grade ($p=0.024$) and proliferation index ($p<0.001$) than those without apocrine features. The former lesions displayed higher expression levels of AR ($p<0.001$), FOXA1, GGT1, BCL2 ($p<0.001$) and GCDFP15 ($p=0.002$), and lower expression levels of FOXC1 and SOX10 ($p<0.001$). PIK3CA mutations were more frequent in tumors with apocrine features ($p=0.043$). Morphological, immunohistochemical and molecular characteristics of these tumors are compared in the Table. OS was significantly better for

HER2+ tumors compared to LAR ($p=0.029$) and for LAR tumors with apocrine morphology compared to those without apocrine features ($p=0.020$) (Fig. 1). Multivariate analyses determined only TILs as parameter associated with survival in LAR tumors ($p=0.017$) (Fig. 2).

Table. Clinicopathologic, immunohistochemical and genomic characteristics of molecular apocrine breast carcinomas according to the HER2 status and apocrine differentiation (only for LAR (HER2-negative) tumors)				
	HER2 status (n=92)		LAR tumors (n=68)	
	HER2+ (n=24)	HER2- (n=68)	with apocrine differentiation(n=52)	without apocrine differentiation (n=16)
Age at diagnosis (years)				
Mean ± SD	62.2 ± 14.5	66.6 ± 14.8	64.6 ± 15.0	67.3 ± 14.8
Median [min-max]	60.0 [40.0-87.0]	66.5 [34.0-100.0]	66.0 [34.0-100.0]	67.5 [35.0-86.0]
P-values	0.206		0.528	
Tumor size (cm)				
Mean ± SD	2.4 ± 1.2	2.3 ± 1.8	2.4 ± 2.0	1.9 ± 1.3
Median [min-max]	2.3 [1.2-5.8]	1.7 [0.7-10.0]	1.8 [0.7-10.0]	1.6 [0.7-6.0]
P-values	0.056		0.381	
SBR grade				
I	0 (0.0%)	1 (1.5%)	1 (1.9%)	0 (0.0%)
II	7 (29.2%)	31 (45.6%)	28 (53.8%)	3 (18.8%)
III	17 (70.8%)	36 (52.9%)	23 (44.3%)	13 (81.2%)
P-values	0.378		0.024	
Glandular differentiation				
I	0 (0.0%)	0 (0.0%)	0 (0.0%)	0 (0.0%)
II	7 (29.2%)	15 (22.1%)	13 (25.0%)	2 (12.5%)
III	17 (70.8%)	53 (77.9%)	39 (75.0%)	14 (87.5%)
P-values	0.483		0.492	
Nuclear grade				
I	0 (0.0%)	0 (0.0%)	0 (0.0%)	0 (0.0%)
II	3 (12.5%)	17 (25.0%)	15 (28.8%)	2 (12.5%)
III	21 (87.5%)	51 (75.0%)	37 (71.2%)	14 (87.5%)
P-values	0.202		0.322	
Mitosis score				
I	7 (29.2%)	27 (39.7%)	25 (48.0%)	2 (12.5%)
II	3 (12.5%)	18 (26.5%)	16 (30.8%)	2 (12.5%)
III	14 (58.3%)	23 (33.8%)	11 (21.2%)	12 (75.0%)
P-values	0.095		<0.001	
Mitosis index (/mm²)				
Mean ± SD	7.4 ± 5.2	6.4 ± 7.0	4.4 ± 3.9	13.0 ± 10.1
Median [min-max]	6.6 [1.0-20.5]	4.2 [0.0-35.3]	3.4 [0.0-19.3]	10.9 [0.9-35.3]
P-values	0.105		<0.001	
Apocrine differentiation	19 (79.2%)	52 (76.5%)	52 (100%)	0 (0.0%)
P-values	0.787		<0.001	
TILs (%)				
Mean ± SD	19.0 ± 9.0	18.0 ± 18.1	17.9 ± 17.1	18.3 ± 21.7
Median [min-max]	10.0 [2.0-70.0]	10.0 [1.0-80.0]	10.0 [1.0-80.0]	10.0 [1.0-70.0]
P-values	0.903		0.661	
AR (≥10%)				
Mean ± SD	82.7 ± 18.3	83.5 ± 23.6	89.6 ± 17.6	63.8 ± 29.7
Median [min-max]	87.5 [30.0-100]	95.0 [10.0-100]	95.0 [20.0-100]	65.0 [10.0-100]
P-values	0.214		<0.001	
FOXA1	23 (95.2%)	60 (88.2%)	49 (94.2%)	11 (68.8%)
P-values	0.437		0.015	
GGT1	17 (70.8%)	53 (77.9%)	47 (90.4%)	6 (37.5%)
P-values	0.483		<0.001	
GCDFP15	19 (79.2%)	54 (79.4%)	46 (88.5%)	8 (50.0%)
P-values	1		0.002	
BCL2	5 (20.8%)	19 (27.9%)	8 (15.4%)	11 (68.8%)
P-values	0.495		<0.001	
FOXC1	3 (12.5%)	22 (32.4%)	11 (21.2%)	11 (68.8%)
P-values	0.060		<0.001	
CK5/6	9 (37.5%)	42 (61.8%)	30 (57.7%)	12 (75.0%)
P-values	0.040		0.213	
EGFR	13 (54.2%)	56 (82.4%)	45 (86.5%)	11 (68.8%)
P-values	0.006		0.136	
SOX10	0 (0.0%)	7 (10.3%)	1 (1.9%)	6 (37.5%)
P-values	0.184		<0.001	
Ki67 (%)				
Mean ± SD	34.3 ± 18.9	31.8 ± 25.0	24.8 ± 19.1	54.5 ± 28.8
Median [min-max]	30.0 [5.0-70.0]	25.0 [2.0-90.0]	20.0 [2.0-90.0]	60.0 [5.0-90.0]
P-values	0.248		<0.001	
PIK3CA mutation	12 (50.0%)	32 (47.1%)	28 (53.8%)	4 (25.0%)
P-values	0.804		0.043	
PTEN mutation	3 (12.5%)	11 (16.2%)	10 (19.2%)	1 (6.2%)
P-values	1		0.437	
AKT mutation	2 (8.3%)	6 (8.8%)	6 (11.5%)	0 (0.0%)
P-values	1		0.323	
TP53 mutation	17 (70.8%)	43 (63.2%)	33 (63.5%)	10 (62.5%)
P-values	0.502		0.944	
ERBB2 mutation	8 (33.3%)	8 (11.8%)	7 (13.5%)	1 (6.2%)
P-values	0.027		0.670	
BRCA1 mutation	5 (20.8%)	5 (7.4%)	4 (7.7%)	1 (6.2%)
P-values	0.200		1	

LAR: luminal androgen receptor, SD: standard deviation

Figure 1 - 110

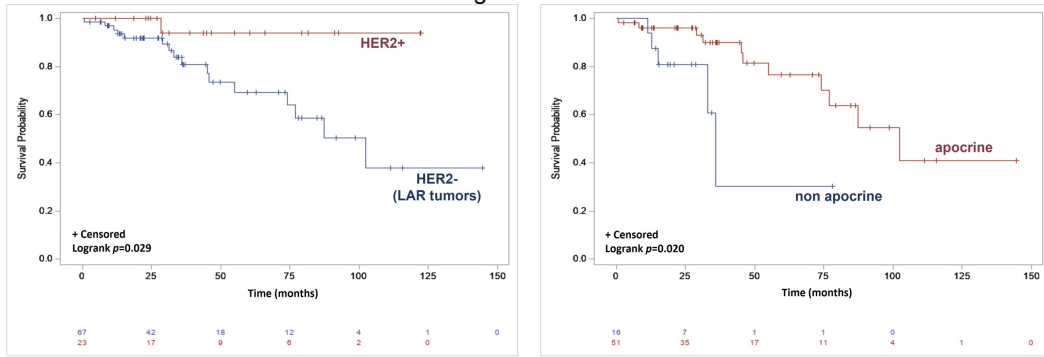


Figure 1. Clinical outcome of molecular apocrine breast carcinomas according to the HER2 status and morphologic apocrine differentiation for the LAR subgroup. Kaplan-Meier curves of overall survival for HER2-amplified compared to HER2-negative tumors (A) and LAR (HER2-negative) tumors with apocrine features compared to LAR tumors without apocrine differentiation (B). The tables below the curves indicate the numbers of patients at risk. HER2+: HER2-amplified, HER2-: HER2-negative, LAR: luminal androgen receptor.

Figure 2 - 110

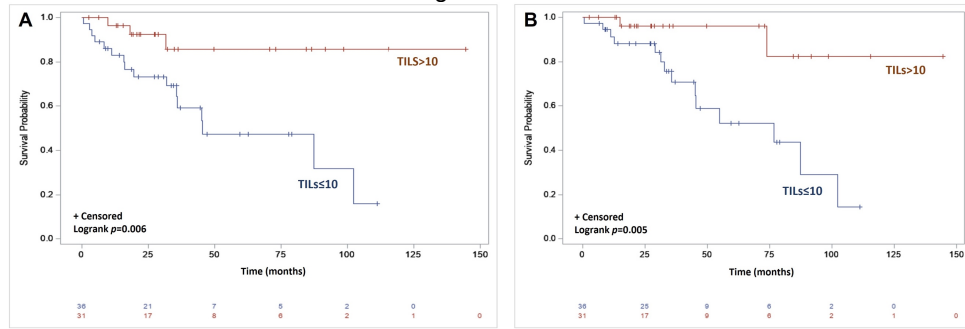


Figure 2. Clinical outcome of luminal androgen receptor (LAR) tumors according to the level of tumor-infiltrating lymphocytes (TILs). Kaplan-Meier curves of overall (A) and progression-free survival (B) for LAR tumors (A) according to the level of TILs (>10 vs ≤10). The tables below the curves indicate the numbers of patients at risk.

Conclusions: MABC is a peculiar tumor subgroup which encompasses distinct entities with specific histomolecular and prognostic characteristics. Excluding HER2+ tumors which harbor a good prognosis due to targeted therapy, LAR tumors seems to be a heterogeneous subgroup with a worse prognosis, including more than only one entity. RNA sequencing will be presented during the USCAP 2023 meeting, and will attempt to shed light on this complex tumor subgroup.

111 Consistency of Scoring HER-2 Low Tested by IHC in Breast Cancer: Academic Institutional Study Including Experts and In-training Pathologists

Boulos Beshai¹, Mohamed Desouki¹, Agnieszka Witkiewicz¹, Sayeeda Yasmeen¹, Maha Khedr¹, Haiyan Li¹, Muhammad Ali¹, Thaer Khoury¹

¹Roswell Park Comprehensive Cancer Center, Buffalo, NY

Disclosures: Boulos Beshai: None; Mohamed Desouki: None; Agnieszka Witkiewicz: None; Sayeeda Yasmeen: None; Maha Khedr: None; Haiyan Li: None; Muhammad Ali: None; Thaer Khoury: None

Background: HER2-low is a newly described entity due to the benefit from target therapy of Trastuzumab/Deruxtecan. Consistency in evaluating HER2-low is a new challenge for the practicing pathologists. The aims of the study are to: 1) evaluate the inter-observer and intra-observer variability in interpreting HER2 based on the new definition, and 2) examine the benefit from educational online HER2-know material.

Design: Tissue Microarray (TMA) slides from the College of American Pathologists (CAP) stained with HER-2 as part of the laboratory proficiency test for four years (2018-2021) were retrieved. The TMAs were stained with HercepTest Antibody. Total of 156 readable TMA cores were evaluated by 5 practicing breast pathologists (experience range of 2-15 years; including 3 full time breast pathologists) and 3 surgical pathology fellows. ASCO-CAP 2018 scoring guidelines were followed. A precise percentage of scoring (0+, 1+, and 2+) was recorded. After reviewing an educational online material of HER-2 know “experts-reviewed challenging cases”, the TMAs’ order was shuffled, and the cores were re-scored. Cases scored 3+ were removed if majority of each group agreed on the scoring. Results were compared to assess consistency among the entire group, intra-observer, pre- and post-online preview, and between practicing and in-training pathologists. Fleiss' kappa test is used to assess the agreement among the participants with K= 0.81-1.00 almost perfect agreement, and K= 0.61-0.80 a substantial agreement.

Results: The kappa was calculated based on the majority agreement among three categories; practicing pathologists (at least 4), trainees (at least 2), and combined (at least 6 participants). Overall consistency of scoring HER-2 0+ versus 1+ or 2+ was higher than scoring them individually. Overall scoring 1+ was the lowest in agreement compared to scoring 0 and 2+, and it was further decreased after reviewing the online material. The agreement improved after the online review for trainees but worsened for the practicing pathologists (Table 1).

*Total number of cases is variable based on the eliminated 3+ scored cases in the three evaluating groups.

	Scores 0 vs. 1+ vs. 2+	Scores 0 vs. 1+/2+	Agreement on score 0 n (%), kappa	Agreement on score 1+ n (%), kappa	Agreement on score 2+ n (%), kappa	Disagreement n (%)	Total cases*
Pre- HER2-Know educational review							
Faculty	0.671	0.725	99 (83.2), 0.797	9 (7.6), 0.620	4 (3.3), 0.609	7 (5.9)	119
Fellows	0.709	0.764	103 (84.4), 0.764	11 (9), 0.538	7 (5.7), 0.828	1 (0.8)	122
Combined	0.666	0.765	99 (83.2), 0.774	5 (4.2), 0.508	5 (4.2), 0.698	10 (8.4)	119
Post- HER2-Know educational review							
Faculty	0.642	0.736	101 (84.9), 0.736	4 (3.3), 0.423	5 (4.2), 0.727	9 (7.6)	119
Fellows	0.721	0.769	104 (78.2), 0.769	8 (6), 0.232	20 (15), 0.903	1 (0.7)	133
Combined	0.651	0.722	99 (81.8), 0.722	2 (1.6), 0.384	7 (5.8), 0.797	13 (10.7)	121

Conclusions: HER-2 score 1+ on IHC remains a challenge, and it is recommended to review such cases in a consensus conference. Online review has more benefit to trainees, which indicates that it is of value to the new in practice and community pathologists.

112 Whole-genome Sequencing Analysis of Metaplastic Breast Cancers Shows Infrequent Homologous Recombination Deficiency

Shirin Bhaloo¹, Andrea Gazzo¹, Arnaud Da Cruz Paula¹, Edaise M. da Silva¹, Pier Selenica¹, Yingjie Zhu¹, Juan Blanco-Heredia¹, Xin Pei¹, Juber Patel¹, Hannah Wen¹, Nadeem Riaz¹, Simon Powell¹, Sarat Chandarlapaty¹, Larry Norton¹, David Brown¹, Britta Weigelt¹, Fresia Pareja¹, Jorge Reis-Filho¹

¹Memorial Sloan Kettering Cancer Center, New York, NY

Disclosures: Shirin Bhaloo: None; Andrea Gazzo: None; Arnaud Da Cruz Paula: None; Edaise M. da Silva: None; Pier Selenica: None; Yingjie Zhu: None; Juan Blanco-Heredia: None; Xin Pei: None; Juber Patel: None; Hannah Wen: None; Nadeem Riaz: None; Simon Powell: None; Sarat Chandarlapaty: None; Larry Norton: None; David Brown: None; Britta Weigelt: None; Fresia Pareja: None; Jorge Reis-Filho: None

Background: Metaplastic breast cancer (MBC) is an aggressive type of triple-negative breast cancer characterized by complex genomes. Based on whole-exome and targeted sequencing, it has been suggested that ~40% of MBCs display homologous recombination (HR) DNA repair deficiency (HRD), however only a minority of MBCs benefit from platinum-based chemotherapy. We performed an HRD assessment of MBCs utilizing the 'gold standard' of whole genome sequencing (WGS) to define whether these cancers harbor only partial genomic features of HRD or are classified as true HRD, and if so, whether HRD is underpinned by bi-allelic alterations affecting HR-related genes.

Design: Twenty-one MBC were reviewed according to the WHO criteria. Estrogen receptor (ER) and HER2 status were evaluated according to clinical guidelines. Tumor and normal samples were subjected to WGS at a median of 94x (range 75x-107x) and 49x (range 42x-62x), respectively. Single nucleotide substitution (SBS) mutational signatures were inferred using Signal. Large-scale state transitions (LSTs) were defined using state-of-the-art methods. HRD was predicted using the Homologous Recombination Deficiency Detect (HRDetect) classifier. The presence of mutations, copy number alterations and rearrangements targeting HRD genes was interrogated.

Results: Of the 21 MBCs, 9 were chondroid, 5 spindle cell, 5 squamous, 1 osseous, and 1 myoepithelial. All MBCs were of histologic grade 3 and most (95%) were ER-/HER2-; 1 case was ER-/HER2+. SBS analysis revealed a dominant HRD mutational signature (i.e. COSMIC SBS3 and/or SBS8) in 8/21 (38%) MBCs, and 10/21 (48%) MBCs had LST-high scores. Five MBCs (24%) displayed both dominant HRD SBS mutational signatures and high LST scores. HRDetect, the "gold standard" for WGS, however, demonstrated that only three (14%) MBCs harbored a complete HRD genomic profile, characterized by a marked enrichment in deletions with microhomology, HRD SBS mutational signatures, LST-high scores and HRD rearrangement signatures. Analysis of the repertoire of somatic genetic alterations of the three bona fide HRD MBCs demonstrated the presence of bi-allelic BRCA1 mutations in two cases.

Conclusions: Our findings reconcile the clinical observations of relative chemo-resistance of MBCs and their genomic profiles, given that only a minority of MBCs (14%) harbor a complete HRD, despite the high prevalence of a dominant HRD SBS mutational signature and LST-high scores. *Bona fide* HRD MBCs often harbor bi-allelic inactivation of *BRCA1*.

113 A Comparative Analysis of the Value of Her2 Immunohistochemistry Scoring in Primary and Metastatic Breast Cancer, in the Era of Her2 "LOW" Breast Cancers

Swati Bhardwaj¹, Avi Kandel¹, Victoria Collins¹, Nebras Zeizafoun², Jennifer Zeng³, Shabnam Jaffer⁴

¹Icahn School of Medicine at Mount Sinai, New York, NY, ²Mount Sinai Health System, New York, NY, ³Mount Sinai Hospital Icahn School of Medicine, New York, NY, ⁴Northwell Health Lenox Hill Hospital, New York, NY

Disclosures: Swati Bhardwaj: None; Avi Kandel: None; Victoria Collins: None; Nebras Zeizafoun: None; Jennifer Zeng: None; Shabnam Jaffer: None

Background: In the recent DESTINY-Breast04 trial, patients with previously treated Her2 low metastatic (met) breast cancer treated with Trastuzumab had significant improvement in survival compared to those treated with chemotherapy. This provides a new targeted therapeutic option for patients with met Her2 low breast cancer, defined as Her2 immunohistochemistry (ihc) score of 1+ or 2+ and negative FISH result. This has created an impetus for detailed Her2 ihc scoring (Negative=0&1+; Equivocal=2+, Positive= 3+). The goal of our study was to compare the Her2 ihc scores of paired primary breast cancers (PBC) and mets, with particular emphasis on Her2 low criteria and its implications for detailed ihc interpretation.

Design: Using the institution pathology database from 2002, we identified 276 cases of PBC and paired mets. We reviewed and scored all Her2 ihc slides using detailed CAP Her2 ihc (0,1+,2+,3+) criteria and FISH scores, checked for concordance, and calculated the incidence of Her2 low (see Table below).

Results: The met sites included: bone(84), liver(60), lung(44), brain(36), soft tissue(24), lymph nodes(20), gyn(5), and GI(3) and had no effect on ihc score. Compared to the primary, Her2 ihc score in the mets changed in 113/276 (41%) cases; increased in 71/276 (26%) and decreased in 42 (15%). In the context of Her2 low criteria, these results were only meaningful in 76/276 (28%) cases that were upgraded from ihc score 0 to 1+/2+ (49/71=69%) or that were downgraded to 0 (27/42=64%). The remaining cases were already scored either 1+ or 2+ and thus qualified as Her2 low by criteria. The few discordances of 0 to 3+ were due to the primary being tested in the 1990s and not meeting the ischemic and fixation times and the mets being tested 10 years later. The few discordances of 3+ to lower were due to heterogeneity.

Comparison of primary to metastatic Her2 values															
0 to 0	0 to 1+	0 to 2+	0 to 3+	1+ to 0	1+ to 1+	1+ to 2+	1+ to 3+	2+ to 0	2+ to 1+	2+ to 2+	2+ to 3+	3+ to 0	3+ to 1+	3+ to 2+	3+ to 3+
77	29	20	4	10	21	16	1	17	11	27	1	1	0	3	38
CONCORDANCE															
PRIMARY					METASTASES					73%					
0					130					105					60%
1					48					61					44%
2					56					66					48%
3					42					44					90%
Her2 low					104					127					59%

Conclusions: The concordance rate of Her2 ihc scores in matched PBC and mets decreased from 73% to 59% with detailed analysis. While concordance was highest in 3+ cases (90%), it was lowest in PBC that changed from 0 to 1+/2+ in mets. The incidence of Her2 low was higher in the mets by 8% compared to primary. We agree that Her2 should be tested in mets and recommend comparing the results with the primary, due to meaningful differences in Her2 low scores as seen in 28% of our cases, which will have clinical implications in the new Her2 low era of treatment.

114 Genetic and Immunohistochemical Characterization of Mammary Hidradenoma and Comparison to Mucoepidermoid Carcinoma

Margaret Black¹, Saleh Najjar², Aihui Wang³, Megan Troxell⁴, Poonam Vohra⁵, Cynthia Gasper⁶, Gregor Krings⁵, Yunn-Yi Chen⁵, Gregory Bean³

¹University of Colorado Anschutz Medical Campus, Aurora, CO, ²King Faisal Specialist Hospital & Research Centre, Riyadh, Saudi Arabia, ³Stanford Medicine/Stanford University, Stanford, CA, ⁴Stanford University Medical Center, Stanford, CA, ⁵University of California, San Francisco, San Francisco, CA, ⁶UCSF Pathology, San Francisco, CA

Disclosures: Margaret Black: None; Saleh Najjar: None; Aihui Wang: None; Megan Troxell: None; Poonam Vohra: None; Cynthia Gasper: None; Gregor Krings: None; Yunn-Yi Chen: None; Gregory Bean: None

ABSTRACTS | BREAST PATHOLOGY

Background: Mucoepidermoid carcinoma (MEC) is exceedingly rare in the breast, with <50 cases reported. While ER/PR/HER2 triple-negative, MEC is characterized as a special subtype of breast carcinoma with significantly better prognosis than conventional basal-type tumors. Hidradenoma (HA) is considered a benign cutaneous adnexal neoplasm showing histomorphologic overlap with MEC. Rare cases of HA have been reported in the breast. Molecularly, both salivary gland MEC and cutaneous HA harbor recurrent *CRTC1-MAML2* or less common *CRTC3-MAML2* rearrangements. We previously described 2 cases of breast MEC and confirmed that they also harbor *CRTC1-MAML2* fusions. We now report the largest series to date of breast/axillary HA, with clinicopathologic, immunohistochemical (IHC) and molecular comparison to 3 breast MEC.

Design: Ten cases are included in this study: 3 were diagnosed as MEC and 7 cases as HA. Nine arose in the breast and 1 was axillary. IHC for high- and low-molecular weight keratins, p63, GATA3, SOX10, mammaglobin, GCDFP15, AR and MUC4, as well as breakapart *MAML2* fluorescence in situ hybridization (FISH), were performed. All cases were subjected to next-generation sequencing (NGS) for mutation testing using a 648-gene panel and fusion testing using a 137-gene panel.

Results: Patients included 9 females and 1 male, with a mean age of 48 years. Cases presented as a palpable mass (n=5), mass on imaging (n=4) or asymmetry (n=1). MEC cases were low-intermediate grade, and no cases showed highly atypical or pleiomorphic features. MEC demonstrated a more infiltrative growth pattern than HA, with myosin and calponin immunostains highlighting an *in situ* component in all 3 cases. Distinguishing immunostains included SOX10 ($\geq 90\%$ positive cells staining in MEC, $\leq 10\%$ in HA), mammaglobin ($\geq 40\%$ in MEC, $\leq 10\%$ in HA) and MUC4 ($\geq 20\%$ in MEC, $\leq 5\%$ in HA); other markers were similar. All cases were positive for *MAML2* FISH. Nine cases demonstrated a *CRTC1-MAML2* rearrangement by NGS, and 1 MEC harbored a *CRTC3-MAML2* fusion. Mutational burden was low, with only 1 HA exhibiting a *MAP3K1* pathogenic alteration.

	Age/Sex	Location	Size (cm)	Architecture	Lesional Contour	In Situ Carcinoma?	Benign Breast Present	MAML2 FISH	Fusion	Pathogenic Mutations
MEC1 ^a	53/F	L breast, upper	1.6	cystic/solid	infiltrative	focal <i>in situ</i> MEC	+	+	<i>CRTC1-MAML2</i>	none
MEC2 ^a	49/F	R breast, upper	≥ 5	cystic/solid	infiltrative	extensive <i>in situ</i> MEC	+	+	<i>CRTC1-MAML2</i>	<i>SETD2 p.S543*</i>
MEC3	65/F	L breast, lower	1.3	cystic/solid	infiltrative	extensive <i>in situ</i> MEC	+	+	<i>CRTC3-MAML2</i>	none
HA1	49/M	R breast, subareolar	1.8	unifocal, solid/papillary nodular mass filling cystic cavity	circumscribed	none	+	+	<i>CRTC1-MAML2</i>	none
HA2	41/F	L breast, outer	0.5	unifocal, glandular/tubular, hyalinized background	circumscribed	none	+	+	<i>CRTC1-MAML2</i>	<i>MAP3K1 p.W57*</i>
HA3	36/F	L breast, upper outer	2.7	unifocal, solid/papillary nodular mass filling cystic cavity	circumscribed	none	+	+	<i>CRTC1-MAML2</i>	none
HA4	38/F	L breast, lower	1.5	multifocal, cystic/solid	circumscribed	none	-	+	<i>CRTC1-MAML2</i>	none ^b
HA5	64/F	L axilla	2	unifocal, solid/papillary nodular mass	irregular but circumscribed	none	-	+	<i>CRTC1-MAML2</i>	none
HA6	51/F	L breast, upper inner	1.4	unifocal, solid/papillary nodular mass	circumscribed	ER+ DCIS	+	+	<i>CRTC1-MAML2</i>	none
HA7	36/F	L breast, inner	0.5	unifocal, solid nodular mass, hyalinized background	circumscribed	none	-	+	<i>CRTC1-MAML2</i>	none

^aPreviously reported

^bKnown germline *BRCA2 p.S2670L* mutation identified; no evidence of somatic alteration

Conclusions: Breast MEC and HA show considerable histologic overlap and *MAML2* gene fusions. Their immunophenotypes are also similar, with apparent differences in SOX10, mammaglobin and MUC4 stains. As in salivary gland, breast MEC cases harbor infrequent *CRTC3-MAML2* rearrangements, a novel finding. More work is needed to elucidate this spectrum of *MAML2*-positive neoplasms and distinguish benign from malignant tumors.

115 Ki-67 Expression in Invasive carcinomas of the Breast: Does Specimen Type and Manual vs Automated Counting Impact Abemaciclib Eligibility?

Therese Bocklage¹, Virgilius Cornea¹, Jessica Moss², Derek Allison¹, Robert McDonald¹, Sara Bachert¹

¹University of Kentucky College of Medicine, Lexington, KY, ²University of Kentucky, Lexington, KY

Disclosures: Therese Bocklage: None; Virgilius Cornea: None; Jessica Moss: None; Derek Allison: None; Robert McDonald: None; Sara Bachert: None

Background: Abemaciclib is FDA-approved for adjuvant treatment of hormone receptor-positive, HER2-negative, node-positive breast carcinomas with Ki67 expression (Ki67%) $\geq 20\%$. There are no guidelines regarding specimen type to use for scoring Ki67%.

Since prior studies have shown inconsistent variation in Ki67% between biopsies and resections, we set out to evaluate Ki67% variability between sample type and possible impact on drug eligibility by performing manual counts and quantitative image analysis (QIA).

Design: We found 51 consecutive breast cancer patients with ER positive, HER2 negative, and at least N1 stage disease. Per patient, we stained a block from 1) the core needle biopsy (CNB), 2) resection (RES), and 3) largest lymph node metastasis (LN) for MIB-1 using the Dako Omnis assay. Two to three pathologists independently manually counted Ki67% using the weighted Ki67 scoring protocol recommended by the Ki67 IWG. QIA was also used to score Ki67%.

Results: Specimens comprised 64 CNB (13 patients with multiple CNB), 53 RES and 51 LN (total = 168). The highest Ki67% was in CNB in 20 patients, 20 in LN, and 11 in RES. The lowest Ki67% was in LN in 18 patients, 17 in RES and 16 in CNB. The average Ki67% difference between the highest specimen and lowest/patient was 8.89 (range: 0.44 to 38.2). There was an impact on treatment choice in 9 patients with the highest Ki67% in CNB in 4 patients, LN in 3 patients, and RES in 2 patients. Overall, the average Ki67% difference between CNB vs RES was 4.65, 6.89 for CNB vs LN, and 5.43 RES vs LN; however, these were not statistically significant differences ($p = 0.90, 0.88, 0.97$). For 13 patients with two CNB, the average difference between the 2 CNB was 7.47, and 4 patients would have had changes in treatment eligibility. The average difference between automatic scoring with QIA versus manual counting was 3.86 (range: 0.03 to 21.76), with near statistical significance ($p=0.051$). A total of 17 specimens would have had clinically significant differences between automatic vs manual scoring (< vs $\geq 20\%$ Ki67), which would have impacted 13 patients.

Conclusions: There was no statistical difference in mean Ki67% between CNB, RES, and LN specimens using the weighted Ki67 scoring protocol; however, 9 patients in our cohort (18%) would have treatment changes based on which specimen was chosen for analysis and 13 (25%) whether manual or automated counting was performed. To ensure reproducible eligibility assessment, further refinement in scoring Ki67% is needed.

116 Ki-67 Expression in Invasive Carcinomas of the Breast: Does Scoring Method Impact Abemaciclib Eligibility?

Therese Bocklage¹, Virgilius Cornea¹, Mara Chambers², Jessica Moss², Sara Bachert¹

¹University of Kentucky College of Medicine, Lexington, KY, ²University of Kentucky, Lexington, KY

Disclosures: Therese Bocklage: None; Virgilius Cornea: None; Mara Chambers: None; Jessica Moss: None; Sara Bachert: None

Background: Abemaciclib is FDA-approved for adjuvant treatment of hormone receptor-positive, HER2-negative, axillary node-positive breast carcinoma with Ki67 expression $\geq 20\%$. As there are no required Ki67 scoring methods, we chose to evaluate variability in Ki67 expression (Ki67%) among proposed scoring methods to assess possible impact on patient eligibility for abemaciclib.

Design: We identified 51, treatment-naive patients meeting eligibility criteria for abemaciclib. Per patient, we stained a representative block from 1) the core needle biopsy (CNB), 2) resection (RES), and 3) largest lymph node (LN) metastasis for MIB-1 using the Dako Omnis assay, the recommended companion diagnostic assay. Two breast pathologists manually counted Ki67% by three methods: 1) overall estimation (EST), 2) weighted Ki67 score (per the Ki67 international working group (IKWG) protocol) (WT), and 3) unweighted Ki67 score (per IKWG protocol) (UNWT).

Results: Specimens included 64 CNB (13 patients had multiple CNB), 53 resections (2 patients with multifocal disease), and 51 LN (168 specimens in toto). Average range of Ki67% between pathologists was 5.5 for EST method, 3.59 for UNWT, and 3.60 for WT. When sorted by specimen type, there was a statistically significant difference in range between EST vs UNWT in CNB and LN ($p=0.059, p=0.014$) and EST vs WT in RES and LNs ($p=0.034, p=0.015$). There was no significant difference in UNW vs WT. Using EST, there were 28 cases with interobserver variability resulting in treatment eligibility discordancy (Ki67 score < vs $\geq 20\%$), to include 10 CNB, 9 RES, and 9 LN (19 patients). However, this discordance was seen in only 13 patients for WT, and 14 patients for UNWT (Table 1). For all specimens, there was a significant difference between EST vs WT ($p=0.02$), but not for EST vs UNWT ($p=0.078$). However, when sorted by specimen type, there was no significant difference between the three scoring methods. (EST vs WT for: CNB $p=0.285$, RES $p=0.139$, LN $p=0.148$). The averaged UNWT count was the highest count in 63 specimens, followed by EST in 53, and WT in 37.

Specimen Type	Overall Estimation (EST)	Unweighted score (UNW)	Weighted score (WT)
CNB (n=64)	5.2 (10)	3.3 (6)	4.4 (5)
RES (n=53)	6.2 (9)	4.2 (4)	3.5 (7)
LN (n=51)	5.2 (9)	3.1 (4)	3.2 (5)

Table 1. Average range between the pathologists for each scoring method and specimen type. Number of cases with discordances < vs $\geq 20\%$ which could lead to treatment eligibility differences listed in parentheses.

Conclusions: UNWT and WT trend toward better interobserver variability compared to the EST. Count differences between pathologists that would have led to treatment difference were minimized using the WT protocol; however, this was not statistically significant when sorted by specimen type. Overall, our study suggests that further refinement in Ki67% scoring is advisable to reduce clinically significant manual score variation.

117 Histology and Differential Gene Expression in Basal-like Immune-Activated and Immune-Suppressed Subtypes of Triple Negative Breast Cancer (TNBC)

Roberto Bonfim Pimenta Peixoto¹, Tábata Alves Domingos¹, Ashka Patel¹, Krishan Taneja¹, Oliver Pigeon¹, Vikas Prabhakar¹, Wendy Chen², Elizabeth Mittendorf³, Elizabeth Cespedes Feliciano⁴, Deborah Dillon⁵

¹Brigham and Women's Hospital, Boston, MA, ²Dana-Farber Cancer Institute, Boston, MA, ³Dana-Farber Cancer Institute, Brigham and Women's Cancer Center, Boston, MA, ⁴Kaiser Permanente, Oakland, CA, ⁵Harvard Medical School, Boston, MA

Disclosures: Roberto Bonfim Pimenta Peixoto: None; Tábata Alves Domingos: None; Ashka Patel: None; Krishan Taneja: None; Oliver Pigeon: None; Vikas Prabhakar: None; Wendy Chen: None; Elizabeth Mittendorf: None; Elizabeth Cespedes Feliciano: None; Deborah Dillon: None

Background: Molecular subtypes of TNBC show distinct clinical outcomes and suggest new therapies. However, therapeutic options are still limited for the immune-suppressed subtype. Here, we compare histologic features and gene expression patterns of basal-like immune-activated (BLIA) and basal-like immune-suppressed (BLIS) TNBCs.

Design: Stage II and III breast cancers were identified in the pathology archives (2005-2015) and triple negative status was determined from Cancer Registry data. Histologic subtype, presence of apocrine, metaplastic, syncytial or micropapillary features, nuclear grade, mitotic score, and Tumor Infiltrating Lymphocytes (TILs) were recorded. Cases were macrodissected and evaluated using the NanoString BC360 gene expression assay. Histologic and molecular features were then compared between BLIA (characterized by upregulation of B, T and NK cells) and BLIS (characterized by the downregulation of these pathways).

Results: Of 72 TNBCs, 41 cases were classified as BLIA (56.9%) and 14 as BLIS (19.4%), with the remainder as luminal androgen receptor or mesenchymal types. BLIA and BLIS tumors differed significantly in TILs, with BLIA average TILs of 32% vs BLIS average TILs of 9% (p- value<0.001) and differed significantly in survival (BLIA average 9.17 vs BLIS average 5.54 years; (p- value <0.001). Both BLIA and BLIS tumors were predominantly high nuclear grade and had high mitotic scores. Syncytial architecture was seen only in the BLIA group (2/41 cases) with no significant difference between the groups in lobular, metaplastic, apocrine, micropapillary or other features. Using a p-value of 0.01, 99 genes were differentially expressed between BLIA and BLIS tumors. The majority of the genes overexpressed in the BLIA tumors were immune cell-associated. Four genes were found to be overexpressed in the BLIS group, including FOXC2, MAPT, BAMBI and HES1. Overexpression of these genes in tumor cells has been associated with poor survival and chemotherapy resistance in preclinical models and in other malignancies.

Conclusions: BLIA and BLIS subtypes are distinguished histologically by the level of TILs but otherwise show similar morphologic features. In gene expression analysis, BLIS tumors showed higher expression of four genes (FOXC2, MAPT, BAMBI and HES1). Overexpression of these genes may be useful as clinical markers of the BLIS phenotype, especially in tumors with intermediate TILs, and may also serve as potential targets in this therapeutically challenging subtype of TNBC.

118 HER2-low Breast Cancer: Retrospective Study to Evaluate Prevalence and Clinicopathologic Features in a Referral Center

Leticia Bornstein-Quevedo¹, Claudia Bautista-Wong², Katia Hop-Garcia³, Pamela Mendoza², Christian Lopez², German Lizarraga-Villarreal

¹INMUNOQ, Mexico City, Mexico, ²Mexico City, Mexico, ³Instituto Mexicano del Seguro Social, IMSS, Mexico City, Mexico

Disclosures: Leticia Bornstein-Quevedo: None; Claudia Bautista-Wong: None; Katia Hop-Garcia: None; Pamela Mendoza: None; Christian Lopez: None; German Lizarraga-Villarreal: None

Background: HER2-targeted therapies for HER2-low metastatic BC (mBC) are under investigation, but HER2 assays currently used to select patients for approved anti-HER2 therapies are optimized for high HER2 expression and are not validated for HER2-low detection. Approximately 50-60% of BCs traditionally categorized as HER2 negative (HER2-neg) express low levels of HER2 (IHC 1+ or IHC 2+/ISH- and the interobserver agreement in evaluation of IHC scores of 0 and 1+ using current HER2 assays ranges from <70%. Our objectives were to assess the prevalence of HER2-low among HER2-neg cases based on rescored HER2 IHC slides and describe patients characteristics of HER2-low vs HER2 IHC 0 mBC.

Design: The retrospective study included patients with mBC with available HER2 slides diagnosed between January 2021 and May 2022. Observers were blinded to historical HER2 scores. HER2 was assessed using Ventana 4B5 clone in a Benchmark ULTRA instrument. BCs were categorized as HER2-low or HER2 IHC 0. The prevalence of HER2-low BC among patients originally scored

as HER2-neg was measured. Demographics and clinicopathological characteristics were retrieved from medical records. Concordance between historical HER2 scores and rescores was assessed.

Results: HER2 rescores were obtained for 7230 patients (mean age, 59 y). HER2-low prevalence was 58.4%. The majority of these HER2-low cases were clinical stage II, with 7.8% being stage III. Most of the HER2-low cancers had a invasive ductal phenotype (87%), histologic grades 2 (94%) were ER positive (96%), PR positive (80%), and were luminal molecular subtypes (96%). Compared to HER2-negative cancers, HER2-low BC showed a higher ER positivity ($p<0.05$), higher pathologic stage ($p<0.05$), and were more likely to be of the luminal A subtype ($p<0.05$). There was no significant difference in age, tumor size, histologic type, histologic grade, presence of lymphovascular invasion or PR score. Concordance rate between historical and rescored slides for HER2-status classification was 84.8%.

Conclusions: HER-2 low breast cancers represent a heterogeneous group, and the majority are lower grade, early-stage, hormonal receptor positive with luminal molecular phenotype. Since data on HER2-low prevalence in BC is limited, this study provides a baseline clinicopathologic and molecular features of HER2-low BCs and support development of best practices for identifying patients with HER2-low expression who may benefit from HER2-targeted therapies.

119 Impact of Shave Margins in Breast Conserving Surgery on Pathology Workload

Ankica Braun¹, Andrea Madrigrano¹, Vijaya Reddy¹, Paolo Gattuso¹

¹Rush University Medical Center, Chicago, IL

Disclosures: Ankica Braun: None; Andrea Madrigrano: None; Vijaya Reddy: None; Paolo Gattuso: None

Background: Breast conserving surgery is a common approach for women with early-stage breast cancer. Nearly 1/3 women undergoing lumpectomy will have a positive margin on final pathology and surgeons have adopted performing shave margins at the time of index surgery to reduce the need for additional surgery. This practice has led to increased workload in pathology. We performed a retrospective study to assess how the findings in additional shave margins impact final margin status and need for additional surgery to assess if it justifies the increased workload.

Design: A retrospective chart review from 2019 to 2021 evaluating breast conserving specimens with the pre-operative diagnosis of ductal carcinoma in situ (DCIS) or invasive cancer for which additional shave margins were taken.

Results: A total of 97 DCIS cases were identified, 17 were grade 1, 48 grade 2, and 32 grade 3. All patients were female with age range of 36-87 years (mean 62 years). 33/97 (34%) cases contained DCIS in the additional shaving margins, in 20/33 (60%) the DCIS was <2 mm from the margin of resection, of which 3/20 (15%) were grade 1, 11/20 (55%) grade 2, and 6/20 (30%) grade 3. 18/20 (90%) of these cases underwent re-excision, 11/18 had residual tumor, 5 cases were <2 mm and 6 cases ??2 mm from the margins of resection. The number of shaved margins taken ranged from 1 to 9, mean 3.5. The number of glass slides examined ranged from 1-52, mean 12.1. There were a total of 88 invasive ductal carcinoma. All patients were female with age range 31-96 years, mean 63 years. 18/88 (20%) contained tumor in the shaved margins (12 DCIS and 6 invasive tumors). In 3 cases the tumor was ??2 mm and in 15 was <2 mm from the margin of resection, with positive margin for invasive tumor in 1 case. 6/15 cases underwent re-excision, residual tumor was found in 5 (4 DCIS, 1 invasive). The number of shaved margins ranged from 1- 7, mean 3.6. The number of glass slides examined ranged from 1-38, mean 8.8.

Conclusions: Our data demonstrate that additional shave margins performed at the index operation did reduce the need for re-excision in 13% of patients with DCIS. In palpable lesions and those with invasive carcinoma, this approach is of greatest benefit. Patients with large spans of DCIS that are associated with non-calcified disease are at greatest risk for continued positive margins despite shave margins, although reduced. Although re-excision rates are reduced it comes at the expense of increased burden on pathology.

120 HER2-Low Breast Cancer: Evolution of HER2 expression from Primary Tumor to Distant Metastases

Mengyuan Cai¹, Ming Li¹, Hong Lv¹, Shuling Zhou¹, Xiaoli Xu¹, Ruohong Shui¹, Wentao Yang¹

¹Fudan University Shanghai Cancer Center, Shanghai, China

Disclosures: Mengyuan Cai: None; Ming Li: None; Hong Lv: None; Shuling Zhou: None; Xiaoli Xu: None; Ruohong Shui: None; Wentao Yang: None

Background: Breast cancer (BC) with low human epidermal growth factor receptor 2 (HER2) expression is attracting much attention due to the breakthrough progress of novel anti-HER2 antibody-drug conjugates. In this study we aim to investigate the changes of HER2 expression in patients with HER2-low BC and their distant metastases, so as to further clarify the dynamic characteristics of HER2 low expression in the process of disease progression.

Design: This study included patients with confirmed HER2 low breast cancer (defined as IHC1+ or IHC2+/ISH-) diagnosed from 2012 to 2021. HER2 expression was tested by Ventana 4B5, and was rescored by pathologists blinded to historical HER2 scores. We evaluated HER2 status of primary and metastatic sites, compared the impact of different clinicopathological parameters on HER2 status of metastases and compared the disease-free survival and overall survival of patients with different HER2 status in metastases.

Results: 98 patients were included. All HER2 IHC scores were confirmed and the consistent rate with the original pathological report was 81.1%. 27.6% of the patients showed different HER2 status in metastases (Fig. 1). The HER2 discordance rate differed among different metastatic sites (lung/pleura vs liver vs bone vs skin and soft tissue vs others = 14.3% vs 24.4% 53.8% vs 27.3% vs 60.0%, p=0.040) (Figure 2A). The higher the T stage of the primary BC, the higher the rate of HER2 discordance was observed (T1 vs T2 vs T3=9.1% vs 27.3% vs 66.7%, p=0.042) (Fig. 2B). For the specimen type of metastasis, the rate of HER2 discordance was higher in surgical specimen than biopsy (45.0% vs 23.1%, p=0.050) (Fig. 2C). No difference of HER2 discordance rate was found between HER2-1+ and HER2-2+ patients. But comparing HER2 IHC score, HER2-2+ patients were less likely to have consistent metastatic HER2 levels than HER2-1+ patients (56.4% vs 39.6%, p=0.006) (Fig. 2D). No difference in survival outcomes was observed between patients with different HER2 status in metastases.

Figure 1 - 120

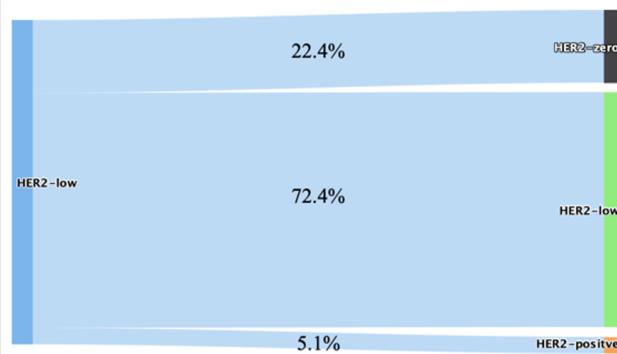


Figure 1: The evolution of the HER2 status between primary tumors and metastases

Figure 2 - 120

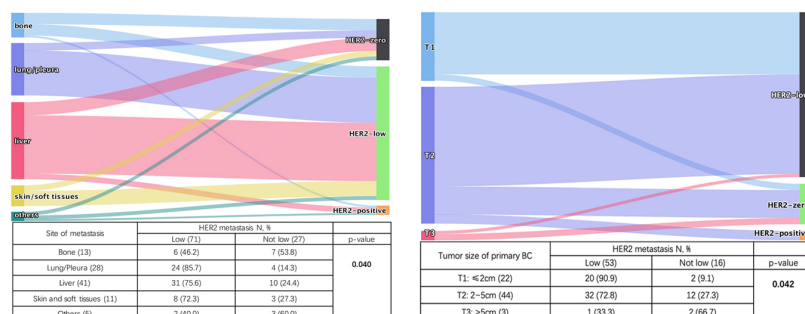


Figure 2A. The evolution of the HER2 status between primary tumors and metastases stratified by site of metastasis.

Tumor size of primary BC

Figure 2B. The evolution of the HER2 status between primary tumors and metastases stratified by T stages of primary BC.

Metastatic specimen collection

Figure 2C. The evolution of the HER2 status between primary tumors and metastases stratified by the specimen type of distant metastasis.

HER2 primary BC N, %

Figure 2D. The evolution of the HER2 IHC score between primary tumors and metastases.

Conclusions: There is a possibility of HER2 expression alteration in the metastases of HER2-low BC. The rate of altered HER2 low expression was different among different metastatic sites, and the discordant rate of bone metastasis was the highest. The discordant rates of HER2 were also different among different T stages of primary BC and different specimen type of metastasis. No

difference of HER2 discordance rate was found between HER2-1+ and HER2-2+ patients. No prognostic significance was observed.

121 Aberrant E-cadherin Expression in Lobular Carcinoma in Situ: A Comprehensive Immunohistochemical Evaluation of N-terminal, Extracellular, and C-terminal E-cadherin Domains

Rita Canas-Marques¹, David Pinto¹, Maria Antónia Vasconcelos¹

¹Champalimaud Foundation, Lisboa, Portugal

Disclosures: Rita Canas-Marques: None; David Pinto: None; Maria Antónia Vasconcelos: None

Background: Approximately 15% of invasive lobular carcinomas show aberrant expression of E-cadherin (E-cad), but the frequency of aberrant E-cad expression in lobular carcinoma in situ (LCIS) is less well characterized. Further, among LCIS cases with aberrant E-cad expression, the domains of the E-cad molecule that are aberrantly expressed and the relationship to expression of other components of the cadherin-catenin complex and to LCIS subtype have not been previously analyzed.

Design: To address this, we identified 50 cases of LCIS without concurrent invasive carcinoma diagnosed in core needle biopsies and categorized each case as classic (type A or B), florid, or pleomorphic using the WHO 5th edition criteria. In addition, for each case immunohistochemical staining was performed to identify the frequency and patterns of expression of components of the cadherin-catenin complex including the E-cad N-terminal (N; 36B5, Leica), extracellular (ECD; EP700Y, Abcam), and C-terminal (C; M168, Abcam) domains, p120 catenin (EP66, Leica), and beta-catenin (17C2, Leica).

Results: Mean patient age at diagnosis was 55 yrs (range: 38-74 yrs). The most common radiologic presentation was microcalcifications (36/50; 72%). The majority of LCIS were of classic type (32/50, 64%; 22 type A; 10 type B), and 9 cases each were florid (18%) or pleomorphic (18%). Loss of membrane expression of all 3 E-cad domains was seen in 34 cases (68%) whereas aberrant expression of one or more E-cad domains was seen in 16(32%) including 3/22 classic type A, 3/10 classic type B, 5/9 florid and 5/9 pleomorphic LCIS. The frequency of aberrant expression of E-cad domains was N+ECD+C=5(Fig1);N+ECD=5;C+ECD=2(Fig2);C only=2;ECD only=1;N only=1(see Table). Aberrant E-cad expression was most often partial, fragmented membrane staining; complete, circumferential membrane staining and cytoplasmic staining were less frequently seen. Among the cases with aberrant E-cad expression, aberrant expression of p120 catenin, beta-catenin, or both was seen in 4 cases, 3 cases and 5 cases, respectively.

Aberrant E-cadherin	LCIS Subtype			
	Classic A	Classic B	Florid	Pleomorphic
N+ECD+C (n=5)	0	1	2	2
N+ECD (n=5)	2	0	1	2
C+ECD (n=2)	0	1	1	0
C only (n=2)	0	1	0	1
ECD only (n=1)	0	0	1	0
N only (n=1)	1	0	0	0

Table. Aberrant E-cadherin expression patterns in 16 of 50 cases of LCIS.

Abbreviations: N, N-terminal domain; ECD, extracellular domain; C, C-terminal domain

Figure 1 - 121

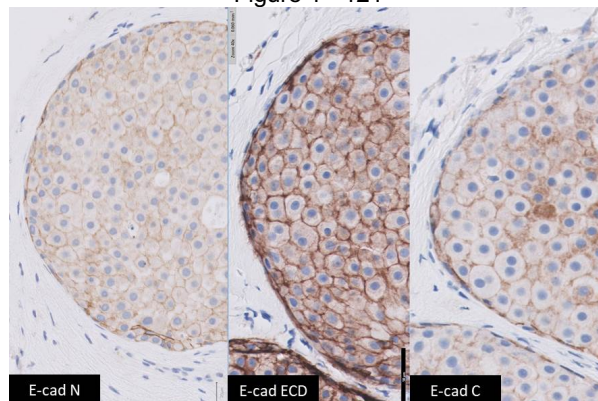
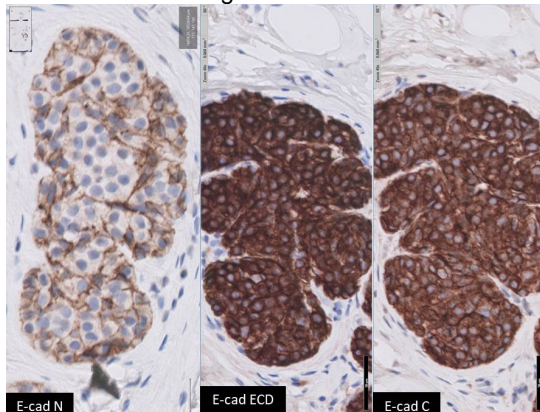


Figure 2 - 121



Conclusions: To our knowledge this is the first study to evaluate aberrant E-cad expression in LCIS by examining expression of distinct domains of E-cad. Our results demonstrate that aberrant E-cad expression is seen in all LCIS subtypes and may be due to expression of various E-cad domains, singly and in combination. This, in turn, likely reflects different mechanisms of E-cad alterations in LCIS, the underlying nature of which merits further study.

122 Clinicopathological Findings in Patients with a Genetic Predisposition to Breast Cancer by Variable Penetrance Genes

McKinley Carey¹, Heather Rocha², Nicole Ortiz², Chelsea Mehr³

¹Geisinger Commonwealth School of Medicine, Scranton, PA, ²Geisinger Medical Center, Danville, PA, ³Geisinger Health, Wilkes-Barre, PA

Disclosures: McKinley Carey: None; Heather Rocha: None; Nicole Ortiz: None; Chelsea Mehr: None

Background: Variable penetrance genes, including *ATM*, *BARD1*, *BRIP1*, *PALB2*, *PTEN*, *RAD51C*, *RAD51D*, and *TP53*, are linked to genetic predisposition to breast cancer and have become increasingly prevalent in screening panels as a result of improvements in technology. The understanding of the clinical significance of these mutations is currently limited. Early identification of mutation carriers and understanding their clinicopathological features will assist in understanding the screening tests and surveillance needed for patients with the goal of mortality reduction. Our study aimed to analyze the clinicopathological presentation of patients within our healthcare system who carry mutations in variable penetrance genes.

Design: This study analyzed 103 patients within our healthcare system who tested positive for mutations in variable penetrance genes. The study team collected data on clinical characteristics, including age at diagnosis and personal and family history of cancer, as well as pathologic characteristics, including hormone receptor status, cancer type, tumor size, stage, and grade, then quantified the data and observed various trends to understand how these mutations impact prevalence and progression of disease.

Results: In the cohort, 31% (12/39) of *ATM* patients were diagnosed with breast cancer, 0% (0/6) for *BARD1*, 20% (2/10) for *BRIP1*, 21% (4/19) for *PALB2*, 75% (3/4) for *PTEN*, 22% (2/9) for *RAD51C*, 25% (2/8) for *RAD51D*, and 38% (3/8) for *TP53*. Notable trends include the presence of only grade 2 and 3 invasive carcinomas, 100% of *ATM* cancers being estrogen receptor positive, and 80% (4/5) of *PTEN* cancers being classified as ductal carcinoma in situ (Table 1).

Table 1: Pathologic Data of Breast Cancers

Gene	ATM	BARD1	BRIP1	PALB2	PTEN	RAD51C	RAD51D	TP53
Hormone Receptor status								
ER+	100% (19/19)	N/A	0% (0/3)	57% (4/7)	75% (3/4)	0% (0/1)	No data	100% (2/2)
PR+	72% (13/18)	N/A	50% (1/2)	43% (3/7)	75% (3/4)	0% (0/1)	No data	50% (1/2)
HER2+	0% (0/15)	N/A	50% (1/2)	43% (3/7)	No data	0% (0/1)	No data	0% (0/2)
Average Tumor Size (mm)								
	19.8	N/A	40.3	24	51.8	22	No data	20
Grade								
1	0% (0/17)	N/A	0% (0/3)	0% (0/6)	0% (0/4)	0% (0/1)	No data	0% (0/2)
2	59% (10/17)	N/A	0% (0/3)	50% (3/6)	100% (4/4)	0% (0/1)	No data	0% (0/2)
3	41% (7/17)	N/A	100% (3/3)	50% (3/6)	0% (0/4)	100% (1/1)	No data	100% (2/2)
Cancer Type								
DCIS	15% (3/20)	N/A	0% (0/3)	0% (0/6)	80% (4/5)	0% (0/2)	No data	0% (0/2)
Ductal	75% (15/20)	N/A	100% (3/3)	83% (5/6)	0% (0/5)	100% (2/2)	No data	100% (2/2)
Lobular	10% (2/20)	N/A	0% (0/3)	17% (1/6)	0% (0/5)	0% (0/2)	No data	0% (0/2)
Stage								
Tis	19% (3/16)	N/A	0% (0/2)	0% (0/3)	100% (4/4)	0% (0/1)	No data	0% (0/1)
T1	44% (7/16)	N/A	50% (1/2)	33% (1/3)	0% (0/4)	0% (0/1)	No data	100% (1/1)
T2	31% (5/16)	N/A	50% (1/2)	67% (2/3)	0% (0/4)	100% (1/1)	No data	0% (0/1)
T3	6% (1/16)	N/A	0% (0/2)	0% (0/3)	0% (0/4)	0% (0/1)	No data	0% (0/1)
T4	0% (0/16)	N/A	0% (0/2)	0% (0/3)	0% (0/4)	0% (0/1)	No data	0% (0/1)

Conclusions: Evaluation of the prevalence of variable penetrance genes in our healthcare system will aid in early identification of breast cancer susceptibility in patients and their relatives. The data show that patients with *PTEN* and *TP53* mutations had higher prevalence's of breast cancer than the other genes studied. Many of the tumors are of higher grade, which is helpful to clinicians and patients in understanding the significance of these mutations. Knowing the clinicopathological features of these patients will enable physicians to expedite screening, improve preventive medicine and target treatment protocols.

123 Validating Artificial Intelligence Algorithm to Screen Sentinel Lymph Node Metastasis in a Digital Pathology Workflow

Bindu Challa¹, David Kellough², Giovanni Lujan³, Shaoli Sun¹, Anil Parwani¹, Zaibo Li¹

¹The Ohio State University Wexner Medical Center, Columbus, OH, ²The Ohio State University Wexner Medical Center/James Cancer Hospital, Columbus, OH, ³The Ohio State University, Columbus, OH

Disclosures: Bindu Challa: None; David Kellough: None; Giovanni Lujan: Consultant: Leica; Shaoli Sun: None; Anil Parwani: None; Zaibo Li: None

Background: Many institutions use cytokeratin immunohistochemistry (IHC) to detect sentinel lymph node metastasis in breast cancer. We validated an artificial intelligence (AI) algorithm to screen sentinel lymph node metastasis with an aim to replace cytokeratin IHCs.

Design: We included 234 sentinel lymph nodes from 108 invasive breast carcinoma resections. All lymph nodes had two levels stained with H&E and one level stained with cytokeratin IHC. All slides had already been scanned into whole slide images (WSIs) and stored in clinical Imaging Managing System (IMS) during our routine digital workflow. The deepest H&E level WSIs were streamed directly from IMS into Visiopharm (VIS) platform without downloading/uploading. All WSIs were automatically batch analyzed using VIS tumor Detection algorithm without manual region of interest (ROI) selection. After the analysis, the results were exported into an Excel spreadsheet with the largest area of metastasis in mm² and length in mm.

Results: VIS AI algorithm detected all 46 metastases including 19 macro-metastases, 26 micro-metastases, 1 case with isolated tumor cells (ITC). There were no false negative cases, while false positive cases were 110 after comparing with cytokeratin-stained slides. The results showed a sensitivity of 100%, specificity of 41.5%, positive predictive value (PPV) of 29.5% and negative predictive value (NPV) of 100%. VIS AI annotated all potential metastasis on WSIs which was either confirmed as true metastasis or excluded as false metastasis very easily and quickly (average time 10 seconds). The false positivity was caused predominantly by histiocytes (52.7%), followed by crushed lymphocytes (18.2%), germinal centers (14.5%), blood vessels (6.4%), lymphocytes around adipocytes (6.4%) and others (1.8%, contaminated epithelium and nerve).

		GROUND TRUTH (CYTOKERATIN IHC)		
		POSITIVE	NEGATIVE	TOTAL
DIGITAL IMAGING ANALYSIS	POSITIVE	46	110	156
	NEGATIVE	0	78	78
		46	188	234

Figure 1 - 123

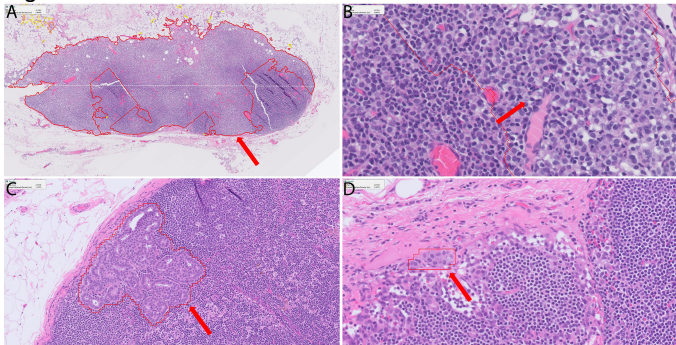
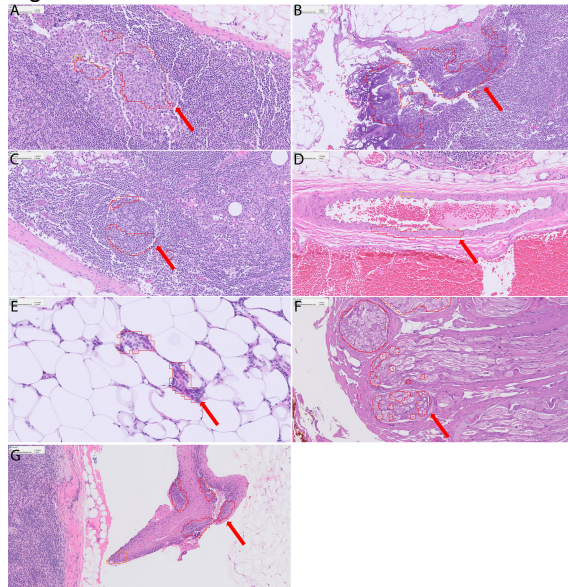


Figure 2 - 123



Conclusions: VIS AI algorithm showed perfect sensitivity and NPV in detecting sentinel lymph node metastasis, suggesting its potential utility as a screening modality in routine clinical digital pathology workflow to increase efficiency and decrease cost by eliminating cytokeratin IHCs.

124 Intraoperative Pathologic Assessment of Breast Lumpectomy Margins is an Accurate Method of Evaluation with Low Re-excision Rates

Ellen Chapel¹, Lakshmi Kunju², Liron Pantanowitz², Jane Brock³, David Chapel¹

¹Michigan Medicine, University of Michigan, Ann Arbor, MI, ²University of Michigan, Ann Arbor, MI, ³Brigham and Women's Hospital, Harvard Medical School, Boston, MA

Disclosures: Ellen Chapel: None; Lakshmi Kunju: None; Liron Pantanowitz: None; Jane Brock: None; David Chapel: None

Background: Re-excision rates following standard breast-conserving surgery (BCS) are approximately 20%. Intraoperative consultation (IOC), including frozen section (FS), on breast lumpectomy margins reduces subsequent re-excision rates. However, the efficacy of this practice following implementation of the 2014/2016 SSO-ASTRO margin guidelines remains unreported, and this practice has not been compared to cavity shave margins.

Design: We evaluated primary lumpectomy specimens sent for IOC between 2017 and 2022 from a single academic institution and compared concordance between IOC and final diagnosis. Surgical indications included invasive carcinoma, DCIS, and pleomorphic LCIS. Excisional biopsies and procedures with concurrent cavity shave margins were excluded from the IOC cohort. Subsequent re-excision rate for was compared to a cohort of lumpectomies with cavity shave margins from a separate academic institution during the same period (2017, 2019).

Results: IOC was performed for 1193 (91.8%) of 1300 lumpectomies. Tissue was submitted for FS in 1087 (91.4%) IOC lumpectomies, with the remainder evaluated by gross-only examination. 3620 blocks were submitted for FS, ranging from 1-29 blocks per case (including additional intraoperative margin re-excision specimens). FS and final diagnoses were concordant in 1030 (94.8%) cases. Among 57 discordant cases, 12 (21%) were due to interpretive error and 45 (79%) were due to sampling discrepancies. Among lumpectomies evaluated by gross-only examination ($n=130$), 9.2% had positive final margins that were not identified at IOC. The discordance rate trended higher for gross-only examinations, compared to cases for which FS was performed ($P=0.06$). Subsequent re-excision was performed for 137 (11.5%) of 1193 IOC cases, including 119 (10.9%) with FS and 18 (13.8%) with gross-only examination ($P=0.33$). There was no significant difference in re-excision rate from year to year. Among 386 lumpectomies with cavity shave margins, 49 (12.7%) required subsequent re-excision. There was no significant difference in subsequent re-excision rates for IOC lumpectomies compared to those with cavity shave margins ($P=0.52$).

Conclusions: IOC on breast lumpectomies results in subsequent re-excision rates that are comparable to cavity shave margins and lower than standard BCS. While gross-only examination is accurate in select cases, diagnostic concordance appears to be improved by FS.

125 Siglec-15 and Its Related Immune Phenotypes Can Predict the Efficacy of Breast Cancer with Neoadjuvant Chemotherapy

Honglei Chen¹, Sufang Tian²

¹Zhongnan Hospital of Wuhan University, Wuhan University Center for Pathology and Molecular Diagnostics, Wuhan, China, ²Wuhan University Zhongnan Hospital, Wuhan, China

Disclosures: Honglei Chen: None; Sufang Tian: None

Background: Breast cancer is an epithelial malignant tumor that occurs in the terminal ducts of the breast. Neoadjuvant chemotherapy (NACT) is an important part of breast cancer treatment. However, some patients who do not respond to NACT will lead deterioration in their condition. Therefore, prediction of NACT efficacy in breast cancer is vital for precision therapy. Sialic acid binding immunoglobulin like lectin 15 (Siglec-15) is an immunosuppressive factor equivalent to PD-L1 in the tumor microenvironment, which is a way of tumor immune escape. In this study, we aimed to explore whether Siglec-15 and related phenotypes can predict the NACT efficacy of breast cancer, combined with clinicopathological information and bioinformatics analysis.

Design: In this study, TCGA, GEO, WGCNA, TIMER and other public databases were used to analyze the bioinformatics functions of Siglec-15 in Pan cancer and breast cancer. Simultaneously, 32 patients with breast cancer who were treated by NACT were collected and divided into disease progression (PD) group and pathological complete response (pCR) group. The expression of Siglec-15 and related immunophenotypes were examined by immunohistochemistry, multiplex immunofluorescence histochemistry (mIHC) and multispectral quantitative analysis system. The relationship between the therapeutic effect of NACT and other clinicopathological parameters of breast cancer was evaluated.

Results: Bioinformatics analysis showed that Siglec-15 was up-regulated in breast cancer, which was related to stromal cells and immune cells in the tumor immune microenvironment (Fig.1). The expression of Siglec-15 in PD group was higher than that in pCR group before NACT ($p < 0.05$). High density of FoxP3 before treatment predicted a good response to NACT. mIHC confirmed that a novel immune phenotype of CD8 and FoxP3 co-expression in PD patients after NACT (Fig.2). Siglec-15 expression was also observed in the tumor-associated macrophages. The analysis of clinicopathological information showed that ER, PR, HER2, Ki-67 and molecular typing before treatment affected the efficacy of NACT. High expression of ER and PR before treatment indicated poor efficacy; on the contrary, overexpression of HER2 and Ki-67 had good therapeutic effect.

Figure 1 - 125

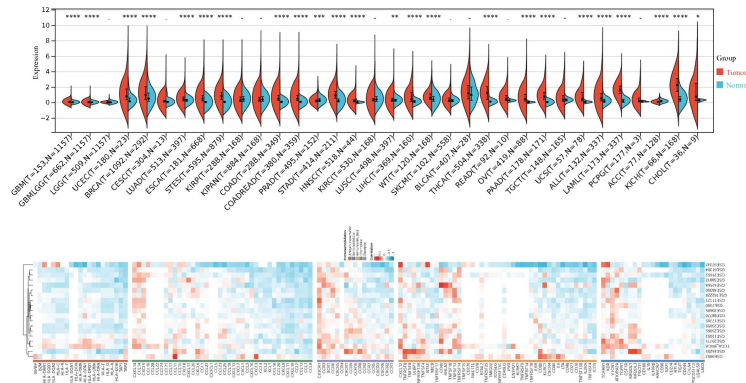


Figure 1 The different expression of Siglec-15 in the Pan cancer tissues and correlated with different immune cells

Figure 2 - 125

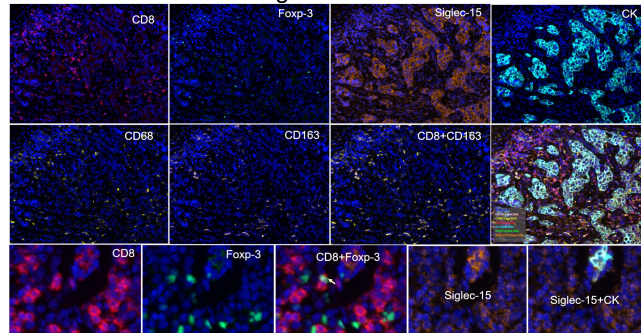


Figure 2 Siglec-15 expression and related phenotypes analysis after NACT

Conclusions: Siglec-15 up-regulates in breast cancer and affects the tumor immune microenvironment. High expression of Siglec-15 before NACT presaged poor efficacy. ER, PR, HER2, Ki-67 and molecular typing before NACT can predict the efficacy as well.

126 HER2-low Breast Cancers: Comparison of HER2 Scores by Immunohistochemistry and Oncotype DX

Hui Chen¹, Yun Wu¹, Qingqing Ding¹, Lei Huo¹, Laila Khazai¹, Aysegul Sahin¹, Constance Albarracin¹

¹The University of Texas MD Anderson Cancer Center, Houston, TX

Disclosures: Hui Chen: None; Yun Wu: None; Qingqing Ding: None; Lei Huo: None; Laila Khazai: None; Aysegul Sahin: None; Constance Albarracin: None

Background: Low HER2 expression, defined as immunohistochemical (IHC) score of 1+ or 2+, HER2 unamplified, is not considered as an indication for conventional anti-HER2 treatment in breast cancer. With the recently FDA-approved antibody-drug conjugate, trastuzumab-deruxtecan, HER2-low has emerged as a predictive marker to guide targeted therapy in advanced breast cancer in clinical trials. However, there is high interobserver variation in evaluating HER2 IHC scores of 0 and 1+. Here, we explored the value of Oncotype DX in distinguishing between HER2 IHC 0 and HER2-low tumors.

Design: We retrospectively reviewed 643 patients with ER-positive, HER2-negative and node-negative primary breast carcinomas with both HER2 IHC and Oncotype DX performed from 2010 to 2018. Medical records were reviewed for pathologic parameters and HER2 results by IHC and Oncotype DX. The correlation of HER2 results between the two assays was examined.

Results: Of the 643 cases, the HER2 IHC scores were as follows: 307 IHC 0, 266 IHC 1+, and 70 IHC 2+. All 70 IHC 2+ cases were HER2 non-amplified. The tumors were predominately ductal (533, 83%), grade 2 (374, 58%), ER-positive (643, 100%) with strong intensity (542, 84%), PR-positive (526, 82%), and of low Ki67 index (<17%) (342/524, 65%). The HER2 scores by Oncotype DX demonstrated a range from 6.8-10.9 (median 8.8 and mean 8.7) in the IHC 0 group, from 7.6-11.1 (median 8.9 and mean 8.9) in the IHC 1+ group, and from 7.6-10.6 (median 9.3 and mean 9.2) in the IHC 2+ group. There was a trend toward higher median and mean HER2 scores by Oncotype DX with higher IHC scores in the 3 different IHC groups ($p<0.05$). However, the wide range of HER2 scores by Oncotype DX was observed.

	HER2 IHC 0 N = 307	HER2 IHC 1+ N = 266	HER2 IHC 2+ N = 70	Total N = 643	P Value
Histology					0.58
Ductal	250 (81%)	221 (83%)	62 (89%)	533 (83%)	
Mixed	18 (6%)	16 (6%)	4 (6%)	38 (6%)	
Lobular	39 (13%)	29 (11%)	4 (6%)	72 (11%)	
Grade					<0.01
One	81 (26%)	69 (26%)	15 (21%)	165 (26%)	
Two	181 (59%)	159 (60%)	34 (49%)	374 (58%)	
Three	45 (15%)	38 (14%)	21 (30%)	104 (16%)	
ER					1
Positive (?10%)	307	266	70	643 (100%)	
ER					0.32
Strong	262 (85%)	219 (82%)	61 (87%)	542 (84%)	
Moderate	38 (12%)	32 (12%)	5 (7%)	75 (12%)	
Weak	6 (2%)	12 (5%)	3 (4%)	21 (3%)	
N/A	1	3	1	5	
PR					0.02
Positive	252 (82%)	223 (84%)	51 (73%)	526 (82%)	
Low Positive	17 (6%)	17 (6%)	2 (3%)	36 (13%)	
Negative	38 (12%)	26 (10%)	17 (24%)	81 (6%)	
Ki67					0.11
Low (<17%)	179 (69%)	134 (63%)	29 (55%)	342 (65%)	
Moderate (17-35%)	56 (22%)	58 (27%)	14 (26%)	128 (24%)	
High (>35%)	24 (9%)	20 (9%)	10 (19%)	54 (10%)	
N/A	48	54	17	119	
DX score					0.31
Low	160 (52%)	131 (49%)	31 (44%)	322 (50%)	
Intermediate	114 (37%)	102 (38%)	25 (36%)	241 (37%)	
High	33 (11%)	33 (12%)	14 (20%)	80 (12%)	

Conclusions: Our results demonstrated a trend of higher HER2 scores by Oncotype DX corresponding to IHC scores. However, Oncotype DX was not effective in further segregating HER2 IHC 0 from HER2-low tumors. Correlating with treatment response in large clinical trials is necessary to determine the best HER2 testing method to guide patient selection.

127 Validating Automated Digital Image Analysis Algorithm to Identify HER2-low Breast Carcinomas

Aaron Chow¹, Yan Hu¹, David Kellough², Anil Parwani¹, Zaibo Li¹

¹The Ohio State University Wexner Medical Center, Columbus, OH, ²The Ohio State University Wexner Medical Center/James Cancer Hospital, Columbus, OH

Disclosures: Aaron Chow: None; Yan Hu: None; David Kellough: None; Anil Parwani: None; Zaibo Li: None

Background: Human epidermal growth factor 2 (HER2) is an important biomarker for breast cancer prognosis and therapy. Recently, a novel HER2 antibody drug conjugate (ADC), trastuzumab deruxtecan (T-DXd), demonstrates benefit in breast carcinomas with low HER2 expression (IHC 1+ or 2+ with negative fluorescent in situ hybridization (FISH)). Therefore, the accurate and reproducible detection of HER2 IHC 1+ and 2+ levels is very important to identify candidate patients eligible for HER2 ADC therapy. As digital pathology and digital image analysis software (DIA) are becoming increasingly prevalent, we examine the capabilities of automated DIA on discriminating HER2-low cases from HER2 0 cases.

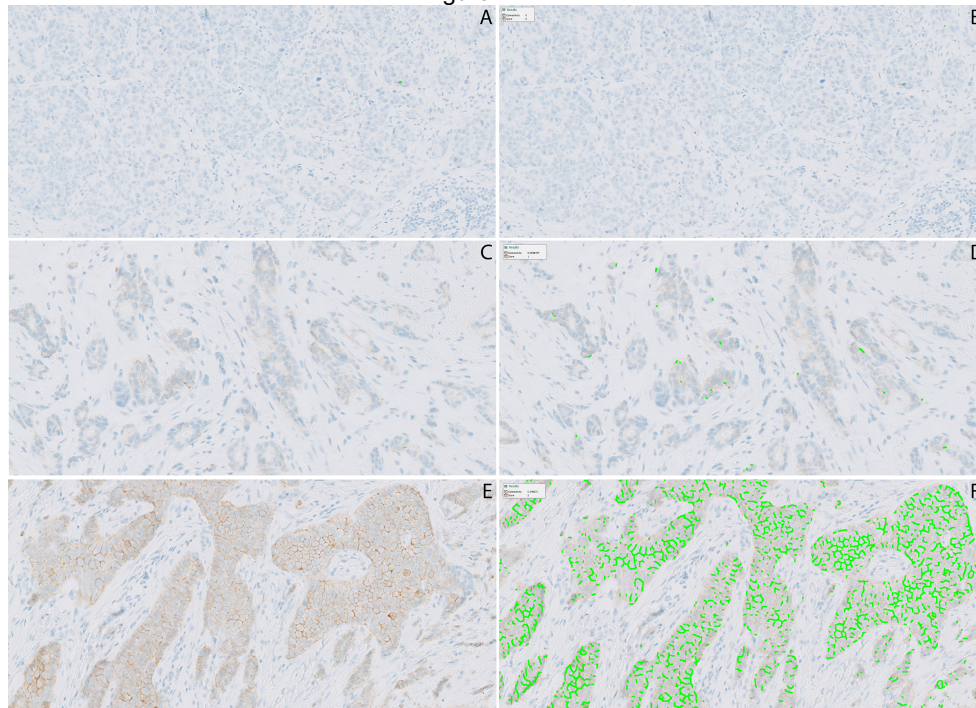
Design: A cohort of 376 cases consisting of HER2 IHC 0 (n=147), HER2-low (n=229; 1+: n=145; 2+/FISH negative: n=84) previously read by pathologists were re-read by Visiopharm DIA software. Representative images used for analysis are demonstrated in Figure 1 (Fig.1 A,B: one case with HER2 IHC 0. Fig.1 C,D: one case with HER2 IHC 1+. Fig.1 E,F: one case with HER2 IHC 2+). The DIA read for HER2-low (Fig.1 B,D,F) labeling was compared to pathologists' read, and both DIA and pathologist scorings were compared to HER2 copy number and HER2/CEP17 ratio by FISH.

Results: Eighty-nine percent of cases (334/376) were concordantly scored into either HER 0 or HER2-low category between pathologists and automated DIA, while eleven percent of cases (42/376) showed discordant scores (Table 1). By Cohen's weighted kappa, there was a substantial agreement between pathologist and automated DIA scores ($\kappa=0.638$; 95% CI: 0.581-0.696). HER2-low cases classified by pathologists had significantly higher mean HER2 copy number (3.22 vs 2.58, $p=1.96E-12$) and HER2/CEP17 ratio (1.26 vs 1.11, $p=1.25E-08$) compared to HER2 0 cases classified by pathologist. HER2-low cases classified by DIA also demonstrated significantly higher HER2 copy number (3.25 vs 2.57, $p=3.59E-14$) and HER2/CEP17 ratio (1.26 vs 1.11, $p=7.89E-09$) than HER2 0 cases classified by DIA with greater statistical significance.

Table 1: Correlation between pathologist read and DIA read of HER2 immunohistochemistry.

		DIA read		
		0	Low	Total
Path read	0	131	16	147
	Low	26	203	229
	Total	157	219	376

Figure 1 - 127



Conclusions: Automated DIA of low HER2 expression confers objective assessment and offers a substantial agreement with pathologist scoring, with the additional ability to more significantly discriminate HER2-low from HER2 0 based on correlation with HER2 copy numbers from FISH.

128 Low-Grade Fibromyxoid Sarcoma of the Breast: Evaluating the Utility of MUC4 Immunohistochemistry in Mammary Spindle Cell Lesions

Jeffrey Cloutier¹, Anthony Moreland², Christian Kunder³, Grace Allard⁴, Gregor Krings⁵, Greg Charville³, Gregory Bean³

¹Dartmouth-Hitchcock Medical Center, Geisel School of Medicine at Dartmouth, Lebanon, NH, ²Meharry Medical College, Nashville, TN, ³Stanford Medicine/Stanford University, Stanford, CA, ⁴Feinberg School of Medicine/Northwestern University, Chicago, IL, ⁵University of California, San Francisco, San Francisco, CA

Disclosures: Jeffrey Cloutier: None; Anthony Moreland: None; Christian Kunder: None; Grace Allard: None; Gregor Krings: None; Greg Charville: None; Gregory Bean: None

Background: Spindle cell lesions of the breast elicit a specific, relatively limited differential diagnosis, and accurate classification requires careful morphologic distinction between low- and high-grade lesions and assessment of a panel of immunohistochemical stains. Low-grade fibromyxoid sarcoma (LGFMS) is an uncommon malignancy with deceptively bland spindle cell morphology. Involvement of the breast is exceedingly rare. We examined the clinicopathologic and molecular characteristics of three cases of LGFMS involving the breast/axilla. In addition, we interrogated the immunoexpression of MUC4, a commonly used marker of LGFMS, in other breast spindle cell lesions.

Design: Three cases of mammary/axillary LGFMS were reviewed and subject to immunohistochemistry, fluorescence in situ hybridization (FISH) for *FUS* and *EWSR1*, and RNA-based next-generation (NGS) sequencing fusion testing. MUC4 immunostaining was performed on 144 cases of various breast spindle cell lesions using whole sections or tissue microarray.

Results: All LGFMS patients were female, with ages of 23, 33 and 59 years. Lesions were 1.1 to 3 cm in size. Two cases presented as palpable masses; one was incidentally noted on imaging. Microscopically, lesions were relatively well-circumscribed nodular masses of bland spindle cells with myxoid stroma. Immunohistochemically, all cases were diffusely positive for MUC4 and negative for keratin, CD34, desmin, S100 protein and nuclear beta-catenin. By comparison, MUC4 demonstrated only weak limited expression in a subset of cases of fibromatosis (10/20, ≤30%, 1-2+ staining), fibrous scar (5/9, ≤10%, 1+), spindle-cell metaplastic carcinoma (2/10, ≤5%, 1-2+), and phyllodes tumor (1/70, 10%, 1+). Pseudoangiomatous stromal hyperplasia (n=9), myofibroblastoma (n=5), periductal stromal tumor (n=3), and cellular/juvenile fibroadenoma (n=18) cases were entirely negative. FISH for *FUS* rearrangement was positive in two LGFMS cases and follow-up NGS on one confirmed an *FUS-CREB3L2* fusion. The third case was positive for *EWSR1* breakapart FISH and harbored an *EWSR1-CREB3L1* fusion by NGS. Outcome data were available for two patients; neither developed recurrence or metastasis.

Conclusions: LGFMS can rarely occur in the breast and should be considered in the differential diagnosis of breast spindle cell lesions, particularly those with myxoid stroma. Strong and diffuse MUC4 expression is highly specific for LGFMS in this context. Detection of an *FUS* or *EWSR1* rearrangement can confirm the diagnosis.

129 AI in Combination with the Global Counting Methodology Recommended by the International Ki67 in Breast Cancer Working Group Identifies More Patients Eligible for Treatment and Increases Diagnostic Speed by 8-fold

Eugenia Colon¹, Lorand Kis², Andrea Farkas³, Boel Linde⁴, Hanna Wessman⁵, Thomas Sollie⁶, Pehr Forsberg⁶

¹Unilabs, Sweden, Stockholm Sankt Görans Hospital, Sweden, ²Karolinska University Hospital, Stockholm, Sweden, ³Gävle, Sweden, ⁴Unilabs AB, Stockholm, Sweden, ⁵Sweden, ⁶Pathology Unilabs Sweden, Stockholm, Sweden

Disclosures: Eugenia Colon: None; Lorand Kis: None; Andrea Farkas: None; Boel Linde: None; Hanna Wessman: None; Thomas Sollie: None; Pehr Forsberg: None

Background: Ki-67 proliferation plays a role in prognosis and prediction of chemotherapy benefits and high and low values are helpful in the decision of oncology treatments in Sweden. In Sweden, the new national guidelines recommend the use of a global counting by the International Ki67 in Breast Cancer Working Group (IKWG). New cut-offs according to the data of IKWG were implemented in all pathology departments across Sweden (Global Score weighted score, Ki-67-low <6 %, Ki-67-medium 6-29 %, and Ki-67-high > 29 %)

Design: We used an algorithm from the AI-development company Mindpeak (Germany) to evaluate Ki-67 expression in invasive breast cancers on IHC stained whole slide images and compared the manual IHC scoring with the AI algorithm counting (Mindpeak). In a prospective study, 113 Ki-67-stained slides from breast cancer patients were analyzed, 102 from hospital Sankt Görans and 11 from Elskinstuna, using manual counting, and using AI algorithm for global counting including the following criteria: quality assurance in pre-analytical and analytical factors. The entire glass slide section was examined. The manual assessment

was performed (counting 400 cells, 4 areas) of the percentages of the invasive tumor in the glass slide that exhibit the following Ki-67 scores (excluding carcinoma in-situ and non-tumor tissue such as necrosis and fibrosis): Negative i.e. contains invasive cells but a very low (including zero), percentage of positive invasive cells with the following estimation: low, medium and high according to the protocol published by IKWG. The same methodology was chosen with the Mindpeak AI algorithm but here the software counted the cells automatically, did the mathematical calculations, and gave the Global Score weighted and Global Score unweighted as readout.

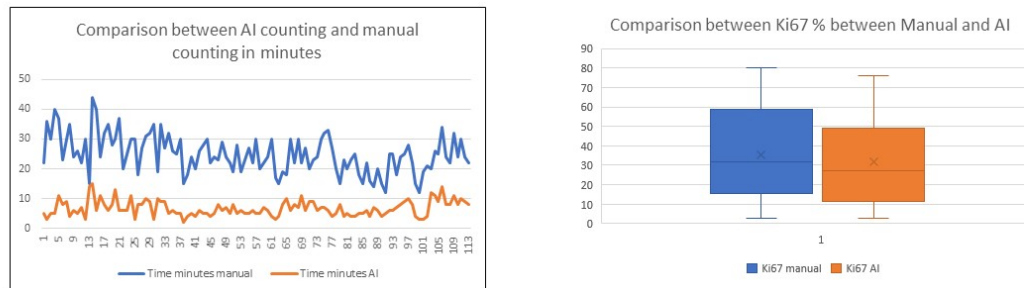
Results: The quantification of Ki-67 expression on tumor cells with the AI software identified more Ki-67 positive samples at cut-offs of $\geq 1\%$ and $\geq 5\%$ compared with manual scoring. Four additional patients were classified as low $> 5\%$ when more cells were considered by the AI software Figure 1. Similarly, two additional patients were recategorized into the medium range with 6%-29 %. In addition, the diagnostic time needed for quantification and calculation was 8 times shorter when using the AI software compared to the manual process as shown in figure 2. We found a correlation between manual counting and AI automatic counting.

Figure 1 - 129

Number of cells counting by AI or manual



Figure 2 - 129



Conclusions: Our study demonstrates the benefit of implementing digital pathology- AI in clinical practice.

130 Breast Cancers Harboring FANCA Genetic Alterations

Lorraine Colon Cartagena¹, Antonio Marra¹, David Brown¹, Andrea Gazzo¹, Pier Selenica¹, Higinio Dopeso¹, Edaise M. da Silva¹, Gagandeep Kaur¹, Dara Ross¹, Hong (Amy) Zhang¹, Sarat Chandarlapaty¹, Simon Powell¹, Diana Mandelker¹, Hannah Wen¹, Edi Brogi¹, Jorge Reis-Filho¹, Fresia Pareja¹

¹Memorial Sloan Kettering Cancer Center, New York, NY

Disclosures: Lorraine Colon Cartagena: None; Antonio Marra: None; David Brown: None; Andrea Gazzo: None; Pier Selenica: None; Higinio Dopeso: None; Edaise M. da Silva: None; Gagandeep Kaur: None; Dara Ross: None; Hong (Amy) Zhang: Consultant: Roche/Genentech; Roche/Genentech; Sarat Chandarlapaty: Consultant: AstraZeneca; Lilly; Novartis; Simon Powell: None; Diana Mandelker: None; Hannah Wen: None; Edi Brogi: None; Jorge Reis-Filho: Advisory Board Member: AstraZeneca; Merck; Fresia Pareja: None

Background: FANCA encodes for a pivotal component of the Fanconi anemia (FA) pathway which is central to the DNA damage response. FANCA alterations are associated to FA, a rare syndrome characterized by defective DNA repair and increased cancer risk. Little is known about the role of FANCA in breast cancer (BC). Here, we sought to characterize the clinicopathologic and genomic features of BCs harboring FANCA alterations.

Design: BCs with FANCA pathogenic alterations were identified among 8,477 BC patients, whose tumor and normal samples were previously subjected to targeted sequencing using an FDA-approved large multigene panel. We conducted the histologic review of

ABSTRACTS | BREAST PATHOLOGY

cases following the criteria put forward by the World Health Organization. The extent of tumor infiltrating lymphocytes (TILs) was assessed following the recommendations by the International TILs Working Group. ER and HER2 status were retrieved from medical records. Mutational signatures were evaluated using SigMA in cases with at least 5 SNVs,

Results: Our cohort included 61 BCs harboring pathogenic germline (n=17) or somatic (n=44) alterations targeting *FANCA*, including 24 primary (pBC) and 37 metastatic BCs (mBC). Bi-allelic *FANCA* inactivation was observed in most (75%; 46/61) cases, as homozygous deletions (n=25) or as loss-of-function mutations (n=15), intragenic deletions (n=4) or rearrangements (n=2) with loss-of heterozygosity of the wild-type allele (LOH). Most *FANCA*-altered pBCs and mBCs were invasive ductal carcinomas of no special type (IDC-NSTs; 83% and 95%), histologic grade 3/poorly differentiated (79% and 97%) and ER+ (67% and 81%) and displayed scarce TILs (median, 10% and 5%). Notably, most pBCs (70%) and mBCs (59%) lacked a homologous recombination deficiency (HRD) mutational signature, displaying dominant clock (50% and 18%) or APOBEC (20% and 41%) signatures, instead. Two *FANCA*-altered mBC, including an ER+/HER2- IDC-NST (*FANCA* E1420*) and an ER+/HER2+ IDC-NST (*FANCA* homozygous deletion), had a prior pBC sample subjected to targeted sequencing, which revealed wild-type *FANCA*.

Conclusions: *FANCA*-altered BCs are predominantly ER+ tumors of high histologic grade and minimal TIL infiltration, and lack a dominant HRD mutational signature, a hallmark genomic feature of BCs with inactivated canonical HRD genes (e.g., *BRCA1/2*). The presence of somatic *FANCA* alterations restricted to metastases in a subset of paired cases suggest that they might represent late events in evolution or progression.

131 Mucinous Carcinoma of the Breast After Neoadjuvant Therapy

Elizabeth C. Conner¹, Beth Harrison², Veerle Bossuyt¹

¹Massachusetts General Hospital, Boston, MA, ²Brigham and Women's Hospital, Boston, MA

Disclosures: Elizabeth C. Conner: None; Beth Harrison: None; Veerle Bossuyt: None

Background: Pure mucinous breast carcinoma usually has a good prognosis and often does not require chemotherapy. However, patients with breast carcinoma with mucinous differentiation (CMD) on initial core biopsy may be eligible for and receive neoadjuvant systemic treatment (NST). There is little information about the characteristics of the patients with CMD receiving NST or about the posttreatment pathology findings in these patients.

Design: We identified patients with breast carcinoma treated with NST with tumors showing mucinous differentiation before or after NST or mucin only (without residual invasive carcinoma cells) in the breast or the lymph nodes (LNs) from 2007 to 2022. We analysed patient characteristics, pre- and posttreatment pathology findings, and patient outcomes. We will identify additional patients from multiple institutions to evaluate the clinical significance of abundant mucin and mucin only in the breast and LNs.

Results: We identified 21 CMD (including 1 pure mucinous carcinoma) treated with NST. In 6 patients, the pretreatment core biopsy did not show a mucinous carcinoma component. Nine tumors were grade 3. Eleven tumors were HR+HER2-. Nine tumors were HER2+. One was triple negative (TN). Fifteen patients were clinically considered LN positive (13 with a positive LN biopsy) at diagnosis. Pathologic complete response (pCR) with mucin only was seen in only 1 patient (grade 3, TN, no mucinous component in the pretreatment core biopsy, biopsy proven positive LN). The posttreatment breast specimen in 6 patients showed abundant mucin (figure 1) with very few residual tumor cells. Acellular mucin only was present in a posttreatment LN of 3 patients (figure 2). All but 2 patients are alive without distant or local recurrence (follow-up 1 to 13 years, median 3 years). One patient died of disease (3 years after diagnosis), she developed bone metastases 1 year after diagnosis, followed by liver and brain metastases. However, she had contralateral grade 2 invasive carcinoma, NOS with 12 positive LNs in the posttreatment specimen. One patient was lost to follow-up.

Findings at diagnosis	
Age range (Median)	31-91 (51)
Mucinous differentiation only	1*
Mucinous carcinoma component	15
Invasive carcinoma NOS component	20
Micropapillary component	2**
Grade 1	1
Grade 2	11
Grade 3	9
ER+ PR+ HER2-	9
ER+ PR- HER2-	2
ER+ PR+ HER2+	3
ER+ PR- HER2+	6
ER- PR- HER2+	0
ER- PR- HER2-	1
Clinically LN + (with LN biopsy +)	15 (13)

*Patient presented with advanced disease
**The micropapillary component was not present in the post treatment specimen of 1 of the 2 patients

Figure 1 - 131

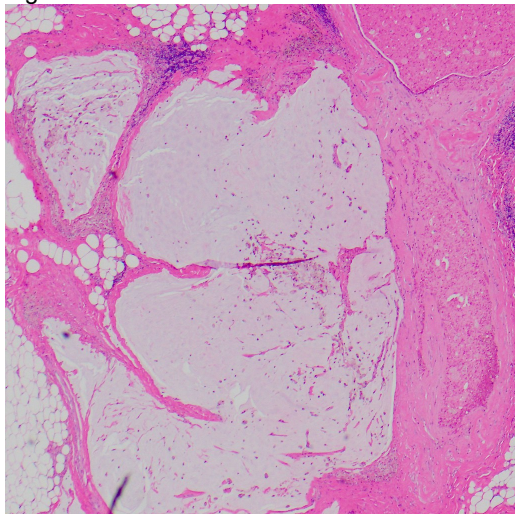
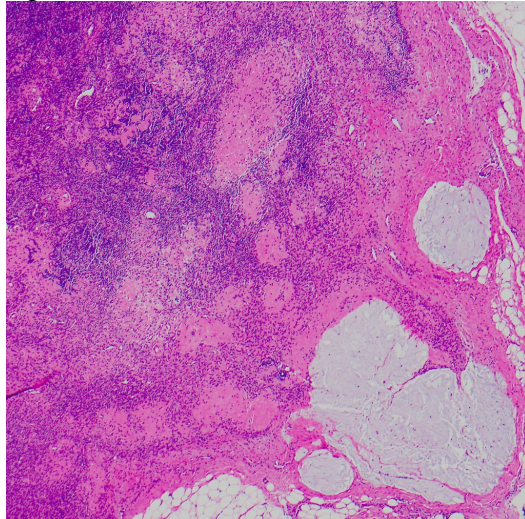


Figure 2 - 131



Conclusions: Patients with CMD treated with NST often present with high grade, HER2+, and LN+ disease. On occasion, a previously unknown mucinous carcinoma component is present in the posttreatment specimen. Large quantities of acellular mucin are often seen in the breast and LNs after treatment. Assessing the clinical implications of abundant mucin or mucin only in the breast and or LNs requires a multi-institutional study.

132 HER2-Low Breast Cancer Evaluation Using ASCO/CAP 2018 Guidelines: Retrospective Case Series Review of a Single Institution

Andreia Coutada¹, Maria Alzamora¹, Davy Fernandes², Jéssica Rodrigues¹, Maria Bento¹, Nuno Coimbra³, Conceição Leal¹
¹IPO Porto, Porto, Portugal, ²Resende, Portugal, ³Instituto Português de Oncologia do Porto FG, EPE, Portugal

Disclosures: Andreia Coutada: None; Maria Alzamora: None; Davy Fernandes: None; Jéssica Rodrigues: None; Maria Bento: None; Nuno Coimbra: None; Conceição Leal: None

Background: HER2 evaluation by IHC and/or ISH is performed in all primary and metastatic breast cancer (BC) to select patients for anti-HER2 therapies. Recent data demonstrated that novel HER2-targeted compounds can induce a response in the subgroup named HER2-low (IHC 1+ or IHC 2+/ISH-), formerly categorized as HER2-negative. Our study aims to describe how we identify HER2-low cases during daily practice using current ASCO/CAP guidelines, and to characterize its clinicopathologic features.

Design: Retrospective analysis of all primary BC diagnosed on core biopsy in our Institution, between May-2019 and November-2020. IHC status of Hormone Receptors and HER2, as well as FISH test results were assessed. Additional clinicopathologic features were included.

Results: A total of 877 cases of BC with HER2 evaluation were included and categorized as shown in Figure 1. Globally, HER2-low was the most prevalent group (43,3%) with distinctive clinicopathologic features (Table 1). Cases with borderline expression of HER2, 1+/2+ (4,8%) and 2+/3+ (0,8%), had a more detailed reporting. These cases were re-tested on surgical specimen or sent to FISH. There were no reported cases with 0/1+ expression. As shown in Figure 2, re-testing IHC on surgical specimen allowed for a more accurate HER2 classification. Most borderline and indeterminate cases directly sent to FISH on core biopsy were negative. Indeterminate cases without amplification (96,2%) weren't further characterized.

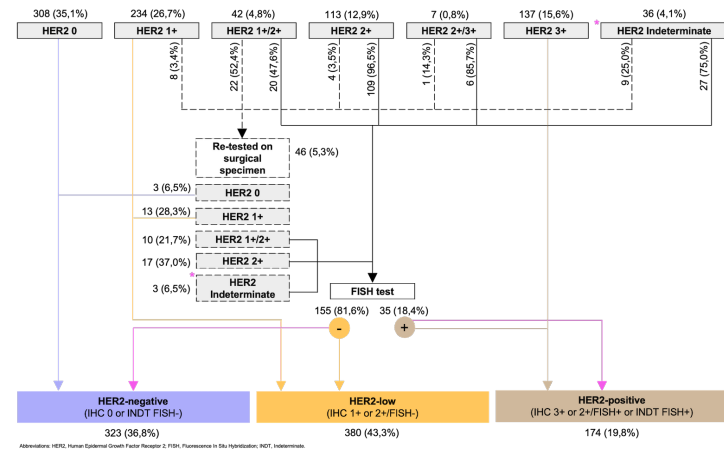
Table 1. Clinicopathologic features of HER2 groups

	HER2-negative	HER2-low	HER2-positive	Overall	p-value
Age, median (range)	61 (28-96)	61 (30-92)	55 (28-87)	59 (28-96)	<0,001
Histologic type					
Invasive BC NST	234 (72,4%)	283 (74,5%)	128 (74,9%)	645 (73,8%)	0,002
Lobular BC (including variants)	51 (15,8%)	40 (10,5%)	9 (5,3%)	100 (11,4%)	0,002
Invasive BC with special features	38 (11,8%)	57 (15,0%)	34 (19,9%)	129 (14,8%)	0,002
Histologic grade					
1	18 (5,6%)	11 (2,9%)	0 (0,0%)	29 (3,4%)	<0,001
½*	36 (11,3%)	38 (10,1%)	0 (0,0%)	74 (8,6%)	<0,001
2	151 (47,3%)	183 (48,8%)	39 (22,8%)	373 (43,1%)	<0,001
2/3*	61 (19,1%)	87 (23,2%)	62 (36,3%)	210 (24,3%)	<0,001
3	53 (16,6%)	56 (14,9%)	70 (40,9%)	179 (20,7%)	<0,001
Hormone receptors					
HR -	45 (13,9%)	24 (6,3%)	53 (30,6%)	122 (13,9%)	<0,001
HR +	278 (86,1%)	356 (93,7%)	120 (69,4%)	754 (86,1%)	<0,001

* Grade as reported on core biopsy

Figure 1 – 132

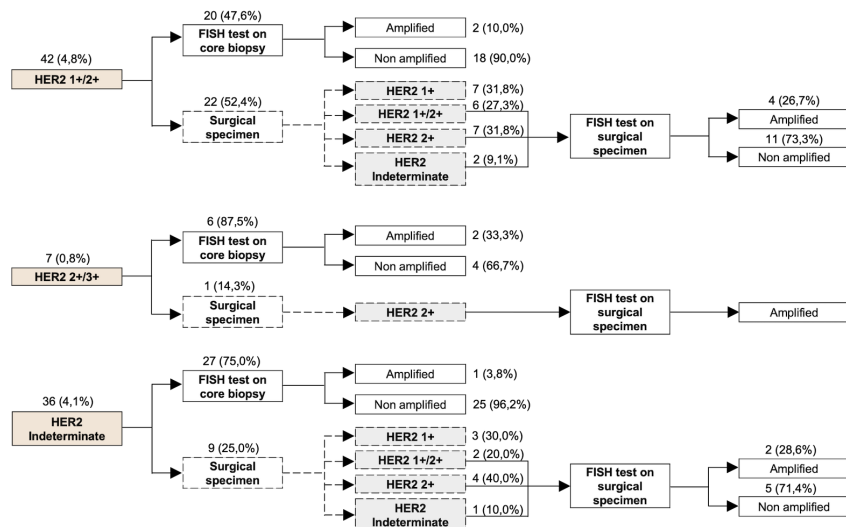
Figure 1. General results of HER2 status



Abbreviations: HER2: Human Epidermal Growth Factor Receptor 2; FISH: Fluorescence In Situ Hybridization; INDT: Indentation.

Figure 2 - 132

Figure 2. Results of HER2 status on surgical specimen



Conclusions: HER2-low concept is changing the traditional dichotomy of HER2 status. Although in the past wasn't clinically relevant to distinguish between negative (0) and negative (1+), ASCO/CAP 2018 guidelines allow this distinction which is fundamental for the HER2-low group identification. In recent literature, cases with heterogeneous/borderline staining on core biopsy should be additionally tested by FISH or on surgical specimen. We believe the second option should be favored since it grants better evaluation of tumour heterogeneity and reduces the number of cases sent to FISH. Moreover, it allows further characterization of non-amplified indeterminate cases and hypothetical FISH-Group 3 cases with borderline 1+/2+ expression. Although our case series showed similar results compared to those reported in literature, existence of borderline cases and increasing awareness of HER2-low group as a therapeutic target might require better discrimination and detailed reporting for each level of HER2 expression.

133 Histologic and Immunohistochemical Assessment of Early Stage, ER-Positive Breast Cancer Following Pre-Operative Endocrine Therapy

Michael Crawford¹, Max Meneveau², Trish Millard², Shayna Showalter², Kristen Atkins

¹University of Virginia, Charlottesville, VA, ²University of Virginia Health System, Charlottesville, VA

Disclosures: Michael Crawford: None; Max Meneveau: None; Trish Millard: None; Shayna Showalter: None; Kristen Atkins: None

Background: Early-stage, estrogen receptor (ER) positive breast cancer is traditionally treated breast conserving surgery (BCS) followed by adjuvant radiation therapy (RT) and 5-10 years of adjuvant endocrine therapy (AET). Long-term data from randomized controlled trials demonstrate that omission of RT in older women (≥ 65 years) with ER+, early-stage breast cancer who are treated with AET does not result in decreased survival. However, the majority of older women still received RT after BCS due to concerns about AET adherence. The POWER Trial (Pre-Operative Window of Endocrine Therapy to Inform Radiation Therapy Decisions; NCT 0427801) is an ongoing trial in which older women with early stage, ER+ breast cancer receive a 3-month course of pre-operative endocrine therapy (pre-ET) prior to subsequent adjuvant therapy decisions. The current study is an examination of the preliminary morphologic and immunohistochemistry (IHC) data of the first 20 patients enrolled in the POWER trial.

Design: For each participant, histologic and IHC evaluation was performed on the core biopsy and the lumpectomy specimen (after pre-ET). Estimation of tumor response was performed using a modified MD Anderson residual cancer burden scoring system, that consisted of tumor burden (scoring ten consecutive high-powered fields (hpf) and the percentage of tumor estimated and averaged), Ki67 (scored according to the International Ki67 Working Group using an unweighted global assessment of 100 cells in at least 4 hpf to derive a mean Ki67 score from the two highest proliferation hpf and 2 lowest proliferation hpf) and ER expression (assessed on a continuous level, ranging from <1% to 100%). A paired T-test was used to assess the differences between the core biopsy and lumpectomy resection specimens.

Results: Table 1 summarizes the histologic and IHC results. Two cases demonstrate a complete pathologic response with no residual tumor, while five cases show increased or unchanged tumor cellularity. The mean expression of ER showed a non-significant decrease of 3.78% ($P = 0.3894$). The mean expression of Ki-67 showed a significant decrease of 10.19% ($P = 0.0004$), and the mean tumor burden showed a significant decrease of 11.45% ($P = 0.0423$).

Case #	Core Biopsy				Lumpectomy			
	Nottingham Grade	ER (%)	Ki67 (%)	Tumor Burden (%)	Grade	ER (%)	Ki67 (%)	Tumor Burden (%)
1	1	100	10	36	2	100	1	38
2	2	100	26	50	2	100	0	10
3	2	90	7	23	1	100	2	14
4	1	90	15	24	-*	-*	-*	-*
5	2	100	22	38	-*	-*	-*	-*
6	1	95	1	27	1	100	1	23
7	3	90	-**	15	3	20	80	80
8	1	95	5	27	1	100	1	3
9	2	100	5	30	2	100	5	10
10	1	95	3	26	2	100	1	5
11	2	95	10	40	2	100	15	38
12	2	100	10	48	2	90	0	23
13	1	100	16	36	1	100	1	27
14	2	100	21	64	2	75	7	22
15	1	98	28	48	1	100	8	41
16	1	95	14	43	1	95	8	44
17	2	95	22	74	1	100	2	65
18	1	100	21	27	2	100	3	5
19	Micro***	100	24	40	2	100	5	58
20	2	100	-**	53	2	100	7	34

*Complete pathologic response with no residual tumor; **Insufficient tumor available for testing; ***Microinvasive only, not graded

Conclusions: For the evaluation of tumors treated with pre-operative endocrine therapy, we propose assessment of cellularity and Ki67 index. Expression of ER did not significantly decrease in this limited sampling.

134 MLPH (melanophilin), a Gene Involved with in Melanosome Transport and Skin Pigmentation Has Perhaps Unexpected Importance in Breast Cancer

Leslie Dalton, Dalton Pathology, West Lake Hills, TX

Disclosures: Leslie Dalton: None

Background: Nottingham score 9 (NS9) tumors encompass the most aggressive breast cancers. In a phenotype/genotype correlation it was not expected a gene involved with melanosome transport (MLPH) would best describe NS9 cancers.

Design: From TCGA cohort, and by examination of whole slide images, a Nottingham score was assigned to 773 cancers. With NS9 as label and mRNA expression of 16,864 genes as predictors, gradient boosting (R library xgboost) identified MLPH as best describing NS9 cancers. MLPH expression was also studied in the n= 3273 Sweden Cancerome Analysis Network (SCAN) patient cohort and n=1875 METABRIC cohort.

Results: In predicting NS9, MLPH had higher variable importance than the sum of all other coefficients. In TCGA, and by receiver operator curve analysis, AUC = 0.85 of MLPH expression with NS9 as response variable. This compared to ESR1 AUC=0.81. Spearman correlation of MLPH and ESR1 corresponded to rho: SCAN = 0.64; 0.62 in METABRIC; 0.60 in TCGA. MLPH had minimal to moderate correlation with vitamin D receptor gene (VDR) with rho: SCAN= -0.171; TCGA= -0.176; BRIC= -0.073. From examination of TCGA whole slide images, those tumors with concordant low ESR1 and MLPH expression often showed zonal necrosis and features typical of triple negative cancers (TNBC). Those cancers with low ESR1/high MLPH were often lobular cancers and tumors having complex glands with eosinophilic or overtly apocrine cytoplasm. In both SCAN and METABRIC, by plot inspection of MLPH expression with ESR1, three distinct clusters were evident corresponding to concordant high expression of ESR1 and MLPH; discordant low ESR1/high MLPH, and concordant low ESR1 & MLPH. In SCAN, 70% of those cancers in the low MLPH & low ESR1 were TNBC. In cluster of low ESR1/high MLPH; 25% were TNBC. 33% of low ESR1/high MLPH were HER2+, but only 1% in concordant low ESR1/MLPH. The low ESR1/high MLPH cluster trended toward intermediate survival probability but not statistically significant.

Conclusions: Literature trails involving MLPH expression extend in many directions. Intriguingly, in skin, melansome transport is under the influence of Vitamin D (VD). In breast cancer a disproportionate number of patients with VD deficiency have TNBC. Documented here is MLPH expression (lack thereof) also shows disproportionate low expression in TNBC. Perhaps level of MLPH expression can best provide a tissue based estimate of VD activity. The multiple roles of VD in cancer progression and prevention are increasingly becoming realized.

135 Quantifying the Number of “Significant” Genes in Predicting Breast Cancer Survival: More Than You Might Think

Leslie Dalton, Dalton Pathology, West Lake Hills, TX

Disclosures: Leslie Dalton: None

Background: From the n= 3247 Sweden Cancerome Analysis Network patient cohort (SCAN), mRNA expression of 7,465 genes showed p < 0.05 univariate significance in survival stratification (Cox Regression). This magnitude was surprising, if not astounding. Of interest, was to find the number of genes maintaining significance after, lowering p-values, multivariate analysis, and requiring significance in an independent patient cohort (n=1895 METABRIC).

Design: Evaluated were 16,914 genes common to SCAN and METABRIC. In SCAN, each gene was individually examined in multivariate Cox regression. The covariates were lymph node status (Inodes), tumour size, patient age, and mRNA expression of MKI67 and ESR1. In both cohorts, all of the just mentioned covariates were independently significant with each other (all p < 0.0005). While grade is important, cell-based biomarkers were limited to mRNA expression. A stepwise filtering approach counted number of genes remaining significant after increasing stringency. Those genes found significant in SCAN were then tested in METABRIC. Statistical analysis used functions and libraries from R.

Results: After covariates were added, 2,722 genes showed p <0.05 in SCAN, and 950 of these were then significant in METABRIC. At a more stringent p-value < 0.005, SCAN had 688 significant genes and 126 remained after METABRIC as test set. At a very stringent p-value < 0.0005, 101 genes were significant in SCAN. Of these, only 10 genes showed significance in METABRIC. The 10 were: HLA-DOB, IL7R, PIM2, PNOC, SLC2A8, SLC6A1, STAT4, TAB3, TNFAIP8, TNFRSF17. After literature review, the prevalent theme of function for the ten genes was immune response (although not exclusively so). For example, PIM2 is hypothesized to influence function of PD-L1 and has Spearman rho=0.58 (p<0.00001) with CD274.

Conclusions: Building yet another gene signature was not intended. This was planned as an illustrative exercise. Findings can be interpreted from many perspectives. Among the suggested: 1) given number of genes significant at $p < 0.05$, an essentially infinite number of gene signatures are possible to predict patient survival 2) given number of genes significant, the $p < 0.05$ threshold is too lenient; 3) independent test sets are essential; 4) Ten genes were identified deserving of greater attention.

136 Atypical Ductal Hyperplasia of the Breast: Morphologic Variables Have a Limited Value in Predicting Upgrade Rate in Subsequent Surgical Specimens

Edward Dent¹, Jessica Chen¹, Di (Andy) Ai¹, Ji-Hoon Lee², Thi Nguyen³, Gulisa Turashvili¹, Xiaoxian Li¹

¹Emory University, Atlanta, GA, ²Georgia Institute of Technology, Atlanta, GA, ³Emory University School of Medicine, Atlanta, GA

Disclosures: Edward Dent: None; Jessica Chen: None; Di (Andy) Ai: None; Ji-Hoon Lee: None; Thi Nguyen: None; Gulisa Turashvili: None; Xiaoxian Li: None

Background: Atypical ductal hyperplasia (ADH) of the breast is an atypical epithelial proliferation with low-grade cytologic atypia. ADH either partially involves multiple lobules/ducts or completely involves lobules/ducts but not exceeding 2 mm in maximum linear dimension. Few studies have examined whether complete involvement of lobules/ducts by ADH is associated with upgrade to breast cancer.

Design: This retrospective study included patients diagnosed with ADH in breast core needle biopsy (CNB) who underwent subsequent surgical excision between 2011 and 2018. Clinical data and microscopic slides were reviewed for the following variables: patient age, race, type of CNB, number of slides with ADH, number of atypical foci, extent of duct involvement (partial vs complete), size of each involved duct, nuclear grade, punctate necrosis, calcifications in ADH, lobular neoplasia, and background non-proliferative or proliferative lesions. Upgrade was defined as diagnosis of ductal carcinoma in situ (DCIS) or invasive carcinoma (any histologic type) in the surgical specimen. Statistical analysis included univariate and multivariate logistic regression models.

Results: A total of 123 CNBs with ADH were identified during the study period, including 97 (79%) stereotactic CNBs for calcifications, 19 (15%) ultrasound-guided CNBs for mass lesions, and 7 (6%) magnetic resonance imaging guided CNBs for non-mass enhancement. The median patient age was 55 years (31-82). Most patients (116, 94%) underwent excision, whereas mastectomy was performed in 7 (6%). The overall upgrade rate was 27% (33/123), with 23 cases diagnosed as DCIS and 10 as invasive carcinoma. Of the remaining cases, 41 (33%) had residual ADH, and 49 (40%) showed benign breast tissue. The 10 invasive carcinomas included invasive ductal carcinoma (4 cases), tubular carcinoma and invasive lobular carcinoma (3 cases each). None of the morphologic features was significantly associated with upgrade rate, including the extent of lobule/duct involvement by ADH ($p=0.19$). In the multivariate model, only the number of atypical foci was associated with upgrade rate ($p=0.03$), and the median and mean numbers of atypical foci were 1 and 1.7, respectively (range 1-6).

Conclusions: Morphologic features in breast CNBs have a limited value in predicting upgrade of ADH. The only feature associated with upgrade appears to be the number of ADH foci on CNB, whereas complete versus partial duct involvement is insignificant.

137 Integration of CDH1 Gene Mutations, E-cadherin Patterns of Expression and Clinico-Pathological Characteristics in a Series of Invasive Lobular Carcinomas of the Breast

Lounes Djerroudi¹, Camille Benoist¹, Amel Bendali¹, Victor Renault¹, Julien Masliah-Planchon¹, Gaëlle Pierron¹, Yann Kieffer, François Clément Bidard¹, Fatima Mechta-Grigoriou, Anne Vincent-Salomon¹

¹Institut Curie, Paris, France

Disclosures: Lounes Djerroudi: None; Camille Benoist: None; Amel Bendali: None; Victor Renault: None; Julien Masliah-Planchon: None; Gaëlle Pierron: None; Yann Kieffer: None; François Clément Bidard: None; Fatima Mechta-Grigoriou: None; Anne Vincent-Salomon: None

Background: Invasive lobular carcinomas (ILC) are characterized by a loss of E-cadherin expression and *CDH1* gene inactivation.

Design: We aimed to analyse the relationship between the type or position of *CDH1* mutations, E-cadherin expression and the clinical outcome in a retrospective series of 250 ILC patients treated by primary surgery between 2005 and 2008. The mutational status of E-cadherin was determined by RNA sequencing from frozen tumor samples. E-cadherin immunohistochemistry (clone 4A2C7 antibody) was performed on FFPE tumor blocks. Intensity (H-Score), localisation and distribution of staining (absent: 0%, focal 1-10%, heterogeneous 11-89%, or diffuse $\geq 90\%$ +ve cells respectively) were assessed. P120-catenin and beta-catenin expression were determined when E-cadherin was diffusely positive. The median follow-up was 106 months; 20 (8%) patients died of breast cancer.

Results: E-cadherin protein was detected in 52.4% of the cases (131/250), with a low or intermediate (≤ 200) H-score (128/131; 98%) and shown a focal (48%; 63/131), an heterogeneous (36.6%; 48/131), or a diffuse (15.26%; 20/131) pattern. Diffuse E-cadherin +ve cases had significantly lower p120-catenin and β -catenin H-scores compared to E-cadherin ($p < 0.05$), a lower tumor cellularity ($p=0.02$) and a lower estrogen receptor H-score ($p=0.024$) than E-cadherin-negative ILC. The *CDH1* gene mutation rate was 70.4% (176/250) and similar regardless of E-cadherin protein level of expression. Mutations were truncating, missense and in-frame in 91%, 7.3% and 1.7% of cases, respectively. Mutations were in the extracellular, the propeptide/signal peptide, the intramembranous and the intracytoplasmic domains in 60.2%, 26.1%, 3.4% and 10.2% of the cases respectively. There was no significant correlation between E-cadherin protein expression and the location of mutations in the *CDH1* gene. Diffuse E-cadherin staining was significantly associated with non-truncating mutations ($p<0.001$). In univariate analysis, truncating *CDH1* mutations were significantly associated with a poor Breast Cancer Specific Survival (BCSS) ($p=0.046$), and a shorter Metastatic-Free Survival (MFS) ($p=0.006$).

Conclusions: In this series, ILC with diffuse E-cadherin staining had similar rate of *CDH1* mutations than other ILC but were enriched in non-truncating mutations, a decreased expression of ER and β & p120 catenins. In univariate analysis, the presence of a truncating mutation was significantly associated with poorer BCSS and MFS.

138 Whole-genome Sequencing Analysis of Invasive Lobular Carcinomas Lacking *CDH1* Alterations

Higinio Dopeso¹, Pier Selenica¹, Fatemeh Derakhshan², Arnaud Da Cruz Paula¹, Antonio Marra¹, Edaise M. da Silva¹, Thais Basili¹, Andrea Gazzo¹, Shirin Bhaloo¹, Steffi Oesterreich³, Hannah Wen¹, Hong (Amy) Zhang¹, Edi Brogi¹, Britta Weigelt¹, Fresia Pareja¹, Jorge Reis-Filho¹

¹Memorial Sloan Kettering Cancer Center, New York, NY, ²Columbia University Irving Medical Center, New York, NY, ³University of Pittsburgh, Pittsburgh, PA

Disclosures: Higinio Dopeso: None; Pier Selenica: None; Fatemeh Derakhshan: None; Arnaud Da Cruz Paula: None; Antonio Marra: None; Edaise M. da Silva: None; Thais Basili: None; Andrea Gazzo: None; Shirin Bhaloo: None; Steffi Oesterreich: None; Hannah Wen: None; Hong (Amy) Zhang: None; Edi Brogi: None; Britta Weigelt: None; Fresia Pareja: None; Jorge Reis-Filho: None

Background: Invasive lobular carcinomas (ILCs) of the breast are characterized by their distinctive dis-cohesive growth pattern, largely due to *CDH1* genetic inactivation or promoter methylation. *CDH1* encodes for E-cadherin, a key component of the epithelial cell-cell adhesion complex. A small but substantial subset of ILCs, however, lack alterations in this gene, despite displaying a *bona fide* lobular phenotype. Here we sought to define the basis of the lobular phenotype in ILCs lacking *CDH1* genetic or epigenetic alterations.

Design: ILCs lacking genetic alterations or promoter methylation of *CDH1* were identified among 364 primary ILCs, previously subjected to clinical targeted massively parallel sequencing and/or to *CDH1* promoter methylation assessment. Tumor and normal samples of four cases were subjected to whole-genome sequencing (WGS) at a median of 71x (range 65x-73x) and 39x (range, 37x-39x), respectively. The presence of mutations, copy number alterations and rearrangements affecting genes involved in cell-cell adhesion was investigated. Confirmatory *CDH1* promoter methylation assessment was conducted using a digital droplet PCR assay (ddPCR). Homologous recombination deficiency (HRD) was assessed using HRDetect.

Results: Four primary ILCs lacking genetic alterations in *CDH1* were included in this study. None of the four cases displayed *CDH1* promoter methylation by ddPCR. WGS analysis revealed a median number of mutations of 15,049 (range, 2,771-47,139). In 3 of 4 cases, we identified inactivating genetic alterations in genes with key roles in cell-cell adhesion other than *CDH1*. One case harbored a truncating mutation in *PCDHGB2*, which encodes of a protocadherin that mediates cell-cell connections; a second case harbored a structural variant affecting *CDH1*; a third case had a truncating mutation in *AXIN2* which regulates the stability of catenins and orchestrates cell adhesion. Notably, this *AXIN2*-altered case also harbored a loss of function mutation affecting *BRCA2* and was predicted to be HR-deficient by HRDetect (score=0.99), while all other cases were predicted to be HR-proficient. No genetic alterations in cell-cell adhesion genes were found in the fourth *CDH1*-wild type ILC studied.

Conclusions: The lobular phenotype in ILCs lacking *CDH1* mutations or promoter methylation might be driven by *CDH1* structural rearrangements, or by the genetic inactivation of other genes playing key roles in epithelial cell-cell adhesion, such as *AXIN2* or genes encoding for protocadherins.

139 Adenomyoepitheliomas of the Breast: Histomorphologic Features, Estrogen Receptor Results, and Molecular Findings of 51 Cases

Lauren Duckworth¹, Andrew Sciallis², Raza Hoda², Maureen Jakubowski¹, John Van Arnam¹, Christine Booth², Xiaoyan Cui², Sherin Hashem², Gloria Lewis², J. Jordi Rowe², Gloria Zhang², Elizabeth Azzato¹, Patrick McIntire²

¹Cleveland Clinic Foundation, Cleveland, OH, ²Cleveland Clinic, Cleveland, OH

Disclosures: Lauren Duckworth: None; Andrew Sciallis: None; Raza Hoda: None; Maureen Jakubowski: None; John Van Arnam: None; Christine Booth: None; Xiaoyan Cui: None; Sherin Hashem: None; Gloria Lewis: None; J. Jordi Rowe: None; Gloria Zhang: None; Elizabeth Azzato: None; Patrick McIntire: None

Background: Adenomyoepitheliomas (AME) are rare biphasic neoplasms composed of both epithelial and myoepithelial cells. Estrogen receptor (ER) positive AME are more commonly associated with mutations in the PI3K pathway, while ER negative AME tend to harbor mutations in RAS/RAF pathway. Our study evaluates ER expression AME (including benign, atypical, and malignant) and next generation sequencing (NGS) hotspot panel testing on malignant AME.

Design: The anatomic pathology databases CoPath PlusTM and EPIC Beaker were searched from 2000-2022 for all cases of AME. Cases were re-reviewed with consensus of diagnosis, grading, and histologic features. Immunohistochemical stain for ER was performed using the Ventana Medical System Benchmark Special Stainer. Hotspot panel NGS assay including primary analysis performed by MiSeq Real Time analysis (RTA). Sequence alignment and variant calls are performed by NextGENe® software, Softgenetics®.

Results: 52 cases of AME from 41 patients were identified: 22 benign, 13 atypical, 2 malignant-in situ (MIS), and 13 malignant. See table 1 for histomorphologic findings. The majority of AME showed at least patchy ER expression (95% of benign, 83% of atypical, and 57% of malignant, see Figure 1). Of the malignant AME, 10 had a benign AME component in association with an in-situ and/or invasive component. Carcinoma subtypes included: 3 ductal carcinoma in situ, 2 invasive ductal carcinomas, 1 invasive mucinous carcinoma, 2 adenoid cystic carcinomas, 3 salivary analogue type tumors, 1 metaplastic carcinoma, and 2 epithelial-myoepithelial carcinomas (see Figure 2). Molecular hot spot panel testing on 12 of the malignant AME cases, including one case of MIS AME is actively ongoing.

Table 1. Pathologic Characteristics of Adenomyoepitheliomas

		Benign (n=22)	Atypical (n=13)	Malignant (n=15)
Architecture	Papillary	9 (41%)	5 (40%)	6 (40%)
	Tubular	19 (86%)	7 (54%)	11 (73%)
	Lobulated	9 (41%)	8 (62%)	7 (47%)
Tumor Border	Encapsulated	12 (55%)	3 (23%)	2 (13%)
	Multinodular	7 (32%)	6 (46%)	2 (13%)
	Infiltrative	0	3 (23%)	10 (67%)
	N/A (i.e. biopsy specimen)	3 (14%)	1 (8%)	1 (7%)
Myoepithelial Cell Morphology	Spindled	11 (50%)	8 (62%)	7 (7%)
	Epithelioid	14 (64%)	8 (62%)	10 (67%)
	Clear	5 (23%)	4 (31%)	4 (27%)
ER status	Positive	18 (82%)	8 (62%)	5 (33%)
	Patchy Positive	1 (5%)	2 (15%)	3 (20%)
	Negative	1 (5%)	2 (15%)	7 (47%)
	N/A	2 (9%)	1 (8%)	0
Presence of necrosis	0	0	5 (33%)	
Presence of a prominent malignant component	0	0	13 (87%)	
Mitotic Count/ 10 HPF (average, range)	0, 0-1	2, 0-10	5.5, 0-20	

Figure 1 - 139

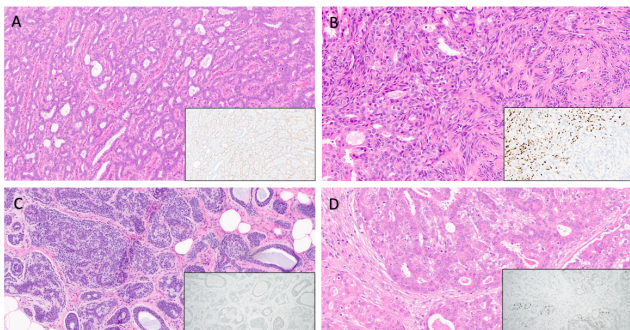


Figure 1. Benign AME with inset showing positive ER (moderate) in the epithelial cells (H&E, 10X) [A]. Atypical AME with inset showing positive ER (strong) in the epithelial cells (H&E, 10X) [B]. Malignant AME with inset showing negative ER (H&E, 20X) [C]. Malignant AME with inset showing positive ER (moderate) in the epithelial, myoepithelial, and invasive components (H&E, 10X) [D].

Figure 2 - 139

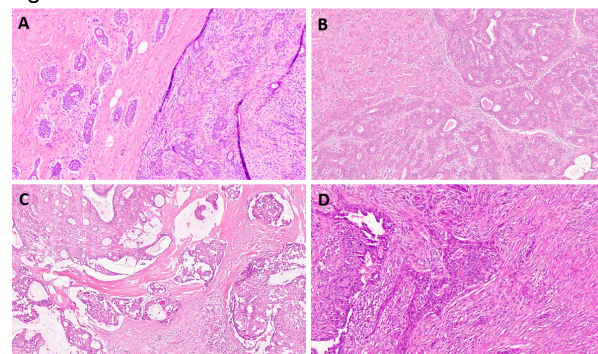


Figure 2. AME involved by adenoid cystic carcinoma (H&E, 10X) [A]. AME involved by invasive ductal carcinoma (H&E, 10X). AME involved by DCIS and invasive mucinous carcinoma (H&E, 8X) [C]. AME involved by epithelial-myoepithelial carcinoma (H&E, 10X) [D].

Conclusions: The majority of AME display at least patchy positivity for ER. Detailed molecular hot spot panel testing is forthcoming. Mutations in these tumors offer potential therapeutic targetable mutations.

140 Eight-Color Multispectral Immunofluorescence for Detection of PD-L1 Leads to Enhanced Prognostic Information in Triple Negative Breast Cancer

Andrew Dynka¹, Hanna Rosenheck², Proggya Paromita², Jianxin Wang², Erik Knudsen², Agnieszka Witkiewicz²

¹University at Buffalo, Roswell Park, Buffalo, NY, ²Roswell Park Comprehensive Cancer Center, Buffalo, NY

Disclosures: Andrew Dynka: None; Hanna Rosenheck: None; Proggya Paromita: None; Jianxin Wang: None; Erik Knudsen: None; Agnieszka Witkiewicz: None

Background: Immune checkpoint inhibitors (ICI) like anti-programmed death-1 (PD-1) and anti-PD-ligand 1 (PD-L1) have shown to be effective therapies in various cancers. However, the benefits of using ICIs in TNBC still remain unclear and can largely be attributed to the vague diagnostic indications and subpar detection methods. The current gold standard for assessing if a patient will benefit from ICIs is conventional immunohistochemistry (IHC) for PD-L1. IHC is limited as it only detects a single marker and doesn't convey the entire story of the TME. Here, we utilized multispectral immunofluorescence (mIF) to better characterize the TME and delineate which patients will respond best to ICI therapy.

Design: mIF was performed on two tumor micro arrays made up of 480 core biopsies taken from TNBC patients. The mIF panel consisted of 8 biomarkers that comprised CD3, CD8, PD-1, PD-L1, CD33, CD163, OX40 and AE1AE3. Slides were imaged on the Vectra Imaging System and cores were segmented into tumor and stroma regions. A phenotyping algorithm was then applied to all cores based on the abundance of each biomarker. The association of each phenotype and overall survival (OS) were analyzed using k-means clustering for PD-1 and PD-L1.

Results: Separation of patients into low, intermediate and high PD-L1 intensities revealed that high intensity on both tumor and immune cells is significantly associated with increased OS. Cluster 4 represents patients with the best overall survival and reveals a TME that is highly inflamed. Myeloid cells, macrophages and helper/cytotoxic T cells display high PD-L1 intensity. This cluster also has the highest level of tumor-infiltrating lymphocytes (TILs). Cluster 3 has the second-best OS, however the TME is slightly different. Here there are relatively low amounts of TILs and PD-L1 intensity is highest in the stroma. Cluster 2 consists of patients with lower overall survival and no lymphocytes are seen in the tumor or stroma. Macrophages dominate the TME and have high expression of PD-L1, suggesting a possible benefit from ICIs. Cluster 1 has the worst OS and lowest PD-L1 expression. This TME is characterized by an abundance of macrophages with no PD-L1.

Figure 1 - 140

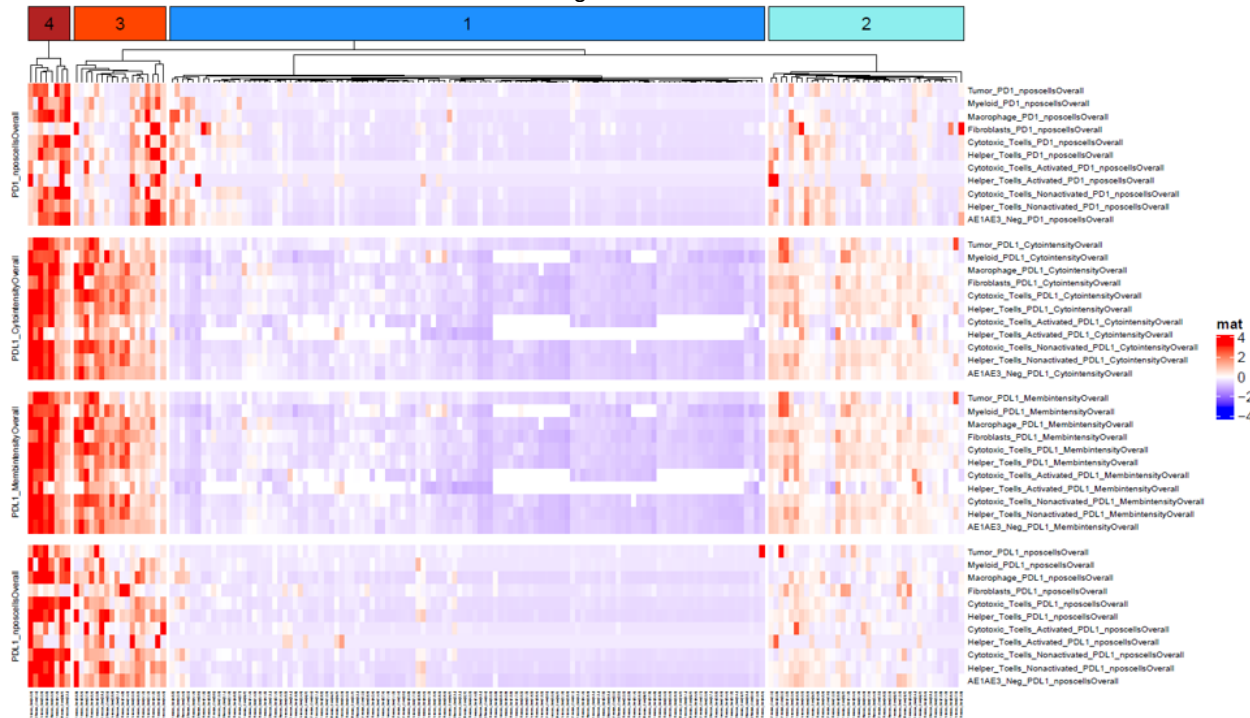
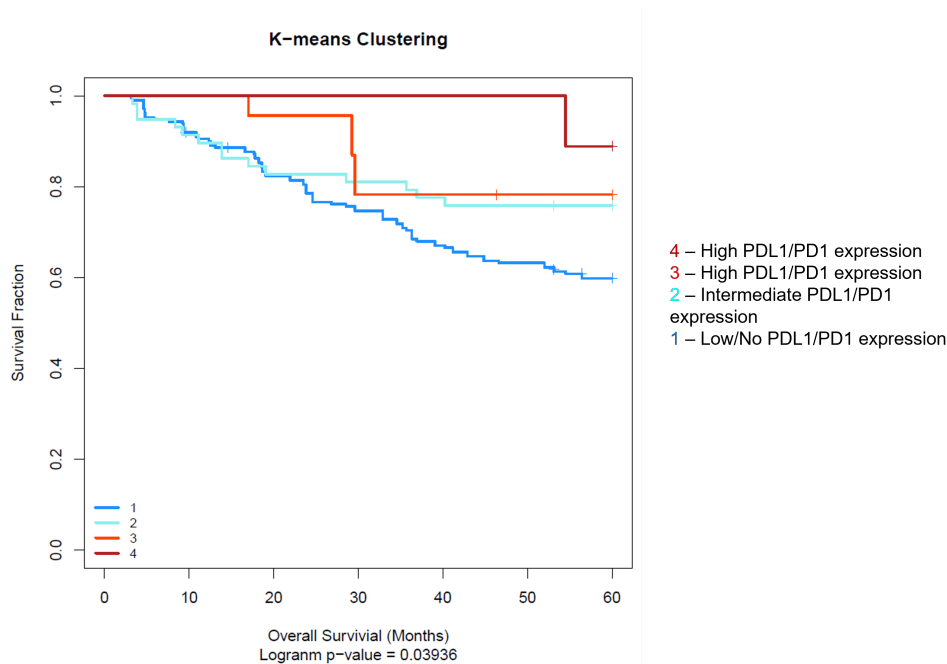


Figure 2 – 140



Conclusions: Determining which patients will benefit most from ICIs involves more than just looking at PD-L1 expression. Our mIF 8-biomarker assay allows for the TME to be considered as well. The greatest benefit may come to patients who have moderate PD-L1 expression, but an abundance of immunosuppressive cells.

141 A Comparison of the Biological Profiles of HER2-Low, HER2-Amplified and HER2-Zero Breast Cancers

Gelareh Farshid¹, Malcolm Pradhan²

¹Royal Adelaide Hospital, Adelaide, Australia, ²Alcidion Corporation, South Yarra, Australia

Disclosures: Gelareh Farshid: None; Malcolm Pradhan: None

Background: DESTINY-Breast04, a phase 3, open label RCT, recently demonstrated the efficacy and safety of Trastuzumab deruxtecan (T-DXd), compared with chemotherapy of physician's choice, in patients with HER2-Low unresectable or metastatic breast cancer. HER2-Low designation requires HER2 IHC 1+ or 2+ without amplification. HER2-Zero patients (IHC 0) were ineligible for this trial. Pathologists' concordance for distinguishing between HER2 IHC 0 and 1+ cancers is suboptimal. We sought to determine if HER2-Low cancers have distinctive biological features, compared to HER2-Amplified and HER2-Zero cancers.

Design: We performed statistical analysis of a consecutive series of breast cancers, evaluated in our laboratory during 2012-2017, when we routinely used both IHC and ISH for HER2 testing.

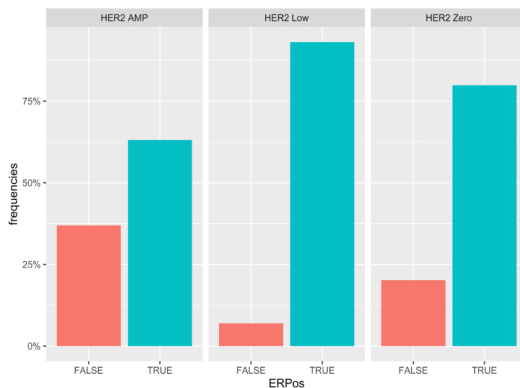
Results: 1744 invasive breast cancers (1735F, 9M) were evaluated. Of IHC 3+ cancers, 18 were non- amplified and are excluded. The remaining 1726 cases comprised HER2-Amplified: 16.9%, HER2-Low: 55.5% and HER2-Zero: 27.6% cancers. Significant differences were found for age, grade, subtype, ER and PR expression, Ki67 score, HER2 copy number and CEP 17 copy number, in all pairwise subgroup comparisons ($p < 0.0001$). The differences were greater between HER2-AMP and the other subgroups, but although smaller, remained statistically significant between HER2-Low and HER2-Zero cancers (Table). HER2-Zero cancers were significantly more likely to be triple negative (17.9%), compared to HER2-Low cancers (5.3%), less likely to express ER (79.8% versus 93.1% of HER2-Low cancers), with more grade 3 cancers and higher ki67 scores. Their HER2 copy number (1.95) was significantly lower than HER2-Low cancers (2.15), although these differences are presently not clinically meaningful.

Parameters	HER2-AMP	HER2-Low	HER2-Zero	AMP vs Low P value	AMP vs Zero P value	Low vs Zero P value
Mean age (years)	58.3	62.6	63.4	<0.0001	<0.0001	<0.0001
Grade 1	3 (1.2%)	164 (19.9%)	80 (18.6%)			
Grade 2	50 (19.3%)	376 (45.5%)	188 (43.6%)			
Grade 3	206 (79.5%)	286 (34.6%)	163 (37.8%)	<0.0001	<0.0001	<0.0001
Subtype						
NST	271 (93.1%)	733 (76.8%)	352 (73.8%)			
Lobular	10 (3.4%)	129 (13.5%)	76 (15.9%)			
Mucinous	1 (0.3%)	18 (1.9%)	19 (4.0%)			
Tubular	0 (0%)	25 (2.6%)	11 (2.3%)			
Basal-Like	1 (0.3%)	5 (0.5%)	8 (1.7%)			
Mixed D-L	1 (0.3%)	15 (1.6%)	4 (0.8%)	<0.0001	<0.0001	<0.0001
ER expression						
<1%	106 (37%)	66 (7.0%)	96 (20.2%)			
1-10%	16 (5.6%)	8 (0.8%)	6 (1.3%)			
11-33%	8 (2.8%)	3 (0.3%)	7 (1.5%)			
34-66%	13 (4.5%)	21 (2.2%)	12 (2.5%)			
>67%	144 (50.2%)	852 (89.7%)	355 (74.6%)	<0.0001	<0.0001	<0.0001
PR expression						
<1%	118 (41.3%)	124 (13.1%)	106 (22.4%)			
1-10%	35 (12.2%)	69 (7.3%)	35 (7.4%)			
11-33%	22 (7.7%)	67 (7.1%)	18 (3.8%)			
34-66%	43 (15.0%)	150 (15.8%)	52 (11.0%)			
>67%	68 (23.8%)	540 (56.8%)	262 (55.4%)	<0.0001	<0.0001	<0.0001
TNBC	0 (0%)	50 (5.3%)	85 (17.9%)	<0.0001	<0.0001	<0.0001
Mean Ki-67 score	48.5%	26.3%	31.1%	<0.0001	<0.0001	<0.0001
Mean HER2 copy number	8.95	2.15	1.95	<0.0001	<0.0001	<0.0001
Mean CEP 17 copy number	2.07	1.9	1.71	<0.0001	<0.0001	<0.0001
Mean HER2:CEP17 ratio	4.47	1.27	1.23	<0.0001	<0.0001	0.72

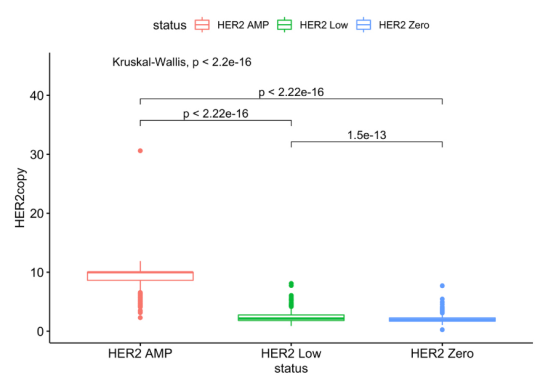
Figure 1 - 141

Figure 2 - 141

ER Positivity By HER2 Status



HER2 Copy Number by HER2 Status



Conclusions: In this large, consecutive series, we demonstrate significant biological differences between HER2-Amplified, HER2-Low and HER2-Zero cancers. While some of the differences are too small to be clinically meaningful, HER2-Low cancers are certainly enriched for ER expression, while TNBC are over-represented among HER2-Zero cancers.

Level 1 evidence supports the use of T-DXd for patients with HER2-Low cancers, but such evidence is presently lacking for HER2-Zero cancers and pathologists can legitimately be requested to make this distinction in the interest of patient care. In the absence of established reference standards distinguishing IHC 0 from 1+ cancers, for borderline cases, the differences we have found may assist in more consistent case assignment.

142 Development and Validation of an Artificial-Intelligent (AI) H&E Image Analysis Grading and Phenotyping Platform to Predict Risk of Early-Stage Breast Cancer Recurrence

Gerardo Fernandez¹, Marcel Prastawa², Richard Scott³, Bahram Marami³, Nina Shpalensky³, Abishek Sainath Madduri³, Krystal Cascetta³, Mary Sawyer⁴, Monica Chan, Giovanni Koll³, Rebecca DeAngel³, Douglas Malinowski³, Alexander Shtabsky⁵, Aaron Feliz¹, Thomas Hansen⁶, Brandon Veremis, Carlos Cordon-Cardo, Jack Zeineh, Michael Donovan⁵

¹PreciseDx, New York, NY, ²Mount Sinai Hospital, New York, NY, ³New York, NY, ⁴Icahn School of Medicine at Mount Sinai, New York, NY, ⁵Mount Sinai Hospital Icahn School of Medicine, New York, NY, ⁶Mount Sinai Health System, New York, NY

Disclosures: Gerardo Fernandez: None; Marcel Prastawa: None; Richard Scott: None; Bahram Marami: None; Nina Shpalensky: None; Abishek Sainath Madduri: None; Krystal Cascetta: None; Mary Sawyer: None; Monica Chan: None; Giovanni Koll: None; Rebecca DeAngel: None; Douglas Malinowski: None; Alexander Shtabsky: None; Aaron Feliz: None; Thomas Hansen: None; Brandon Veremis: None; Carlos Cordon-Cardo: None; Jack Zeineh: None; Michael Donovan: None

Background: Histopathological grade is the gold standard for cancer diagnosis, prognosis and treatment decision-making. The Nottingham grading system (NGS) is a well-established tool used to define the 'aggressive potential' for breast cancer (BC); however, a high percentage of patients are placed in an intermediate-risk group with indeterminate clinical value, highlighting the need for decision support tools to improve reproducibility and prognostic accuracy for histologic grade (HG) in clinical practice.

Design: We developed an AI-digital BC grade and phenotyping assay (AI-grade, AG) to predict low vs. high risk of early-stage BC recurrence within 6 years. We conducted a retrospective development and validation study utilizing samples from BC patients with infiltrating ductal carcinoma (IDC) in the Mount Sinai Health System. Participants were ≥ 23 years old, had H&E slides or paraffin blocks from the resected BC specimen and outcome data. H&E slides were digitized (40X) using a Philips Ultra-Fast scanner. 15,000 H&E slides and paired digital images were reviewed with a single WSI selected for model development. AUC/CI and Kaplan-Meier (KM) curves with HR were used to compare AG vs. HG.

Results: A total of 2075 eligible participants from 2004-2016 were subdivided (3:1) into training (Tr) (n=1559) and validation (Val) (n=516) cohorts. Samples were ER(+) (87%) and PR(+) (81%), with 13% Her2 amplified and 42% and 40% histologic grade 2 and 3, respectively. There were 289 (14%) total recurrence events (220 in Tr; 69 in Val) including metastases (n=85), loco-regional and nodal extension (n=72), and overall survival (n=126). In training, 7 AG features had a CI 0.72 (95%CI, 0.70-0.74) vs. HG 0.62 (95% CI, 0.59-0.64) and a test AG CI of 0.68 (95%CI, 0.63-0.71) vs HG CI 0.61 (95%CI, 0.57-0.64). KM curves comparing AG vs HG showed significant differences in both Tr (HR: 3.65, p-value <0.001) and Val models (HR: 2.1, p<0.001). Of the 868 Grade 2 cases in the total cohort (41% of 2075), 187 (22%) were reclassified as high-risk; 681 (78%) were reclassified as low risk by the AG model.

Conclusions: By applying image analysis tools, we extracted tissue architecture features and cell type characteristics, generating a novel BC grading and phenotyping method. The assay was more predictive of early-stage BC recurrence than histologic grade, identifying discrete biologically driven tumor elements not captured using the current BC NGS.

143 Identification of Glandular(acinar)/ Tubule Formation in Invasive Carcinoma: A Study to Determine Concordance Using the WHO Definition

Susan Fineberg¹, Ukuemi Edema², Fnu Sapna³, Javier Laurini³, Berrin Ustun³, Bryan Harmon⁴, Jennifer Zeng⁵, Yujun Gan⁶, Laleh Hakima⁷, Stuart Schnitt⁸, Ian Ellis⁹, Susan Lester¹⁰, Sonali Lanjewar¹¹, Yungtai Lo³

¹Montefiore Medical Center, Bronx, NY, ²Montefiore Medical Center - Moses Division, Bronx, NY, ³Albert Einstein College of Medicine, Montefiore Medical Center, Bronx, NY, ⁴Montefiore Medical Center, NY, ⁵Mount Sinai Hospital Icahn School of Medicine, New York, NY, ⁶Dartmouth-Hitchcock Medical Center, Lebanon, NH, ⁷The University of North Carolina at Chapel Hill, Chapel Hill, NC, ⁸Brigham and Women's Hospital, Dana-Farber Cancer Institute, Harvard Medical School, Boston, MA, ⁹University of Nottingham, Nottingham, United Kingdom, ¹⁰Brigham and Women's Hospital, Boston, MA, ¹¹Albert Einstein College of Medicine, Montefiore Medical Center, New York, NY

Disclosures: Susan Fineberg: None; Ukuemi Edema: None; Fnu Sapna: None; Javier Laurini: None; Berrin Ustun: None; Bryan Harmon: None; Jennifer Zeng: None; Yujun Gan: None; Laleh Hakima: None; Stuart Schnitt: None; Ian Ellis: None; Susan Lester: None; Sonali Lanjewar: None; Yungtai Lo: None

Background: The Nottingham Grading System (NGS) is used for prognosis, for AJCC stage, and to guide therapy for invasive breast cancer (IBC). Glandular (acinar)/tubular formation (G/TF) is one component of NGS and requires a pathologist to identify

and quantify G/TF structures. In this multi-institutional study, we investigated the ability of pathologists to identify individual structures that should be classified as G/TF.

Design: 58 unique H&E photographic images of IBC (NOS, mucinous, and micropapillary), with a single structure circled, were classified as showing G/TF (41 cases) or not showing G/TF (17 cases) by Dr. Ellis who helped develop the NGS. The images were sent in PowerPoint format to 35 breast pathologists who were provided with the WHO definition of tubule formation ("structures exhibiting clear central lumina surrounded by polarized neoplastic cells") and told to follow established guidelines to determine if a circled structure represented a tubule. If a structure was not considered a tubule, the participants could choose 6 possible reasons or write in a reason. Questions about practice and difficulties in tubule evaluation were included.

Results: Among the 35 pathologists who participated in the study the kappa statistic for overall agreement in evaluating the 58 images was 0.324 (95% C.I. 0.314-0.335), a kappa value considered poor agreement. The median (IQR) concordance rate between a participating pathologist and Dr. Ellis on evaluating the 17 non-tubule cases was 94.1% (88.2,100), but only 53.7% (34.2,85.4) for the 41 tubule cases. 41% of the tubule cases were classified correctly by <50% of the participants (Fig 1). Structures that resulted in frequent discordance with Dr. Ellis as G/TF present but misclassification by pathologists as not being a tubule included complex and cribriform patterns (especially when mucinous) and the "inverted tubule" pattern of micropapillary carcinoma (cell clusters with reverse polarity and a central space) (Fig 2). Eighty percent of participants reported they did not have clarity on what represented a tubule.

Figure 1 - 143

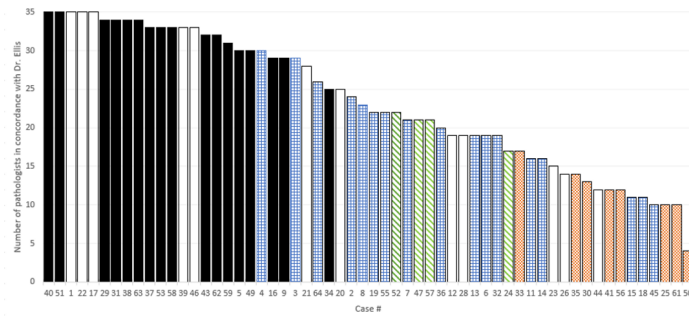


Figure 1. Number of pathologists with concordant/correct classification for the 58 cases ranged from 35 (100%) to 4 (11%). The highest concordance was for non-tubule cases (black) and for some cases showing single tubules (white). Lower concordance was seen for complex/cribriform patterns (hatch pattern/blue), micropapillary carcinoma with inverted tubules (diagonal lines/green), and mucinous carcinoma (checkerboard/orange).

Figure 2 - 143

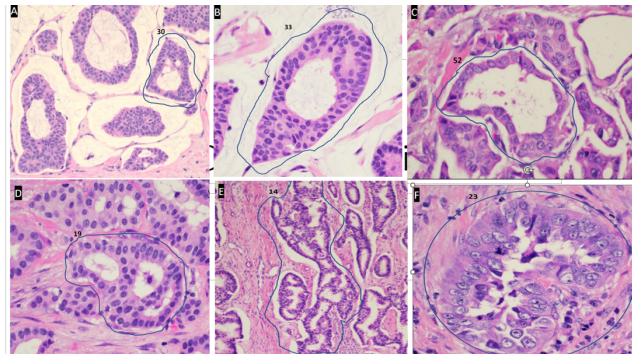


Fig 2. All images were classified as G/TF by NGS/Dr Ellis but were frequently misclassified by pathologists. A and B. These spaces in tumor cell clusters in mucinous carcinoma were not considered tubules by >50% of participants. C. This "inverted tubule" in a micropapillary carcinoma was not considered a tubule by 37% of participants. D. This cribriform pattern with multiple lumens was not classified as a tubule by 37% of participants. E. This duct with a complex luminal pattern was not classified as a tubule by 54% of participants. F. This structure with high grade nuclei was not considered a tubule by 57% of participants.

Conclusions: This study identified individual types of structures that should be included as G/TF, but that were not readily identified as such, even by pathologists experienced in breast pathology. Greater concordance for G/TF might be obtained by providing more detailed images and descriptions of the types of structures included in the NGS as G/TF. The study images can be used to illustrate difficult cases.

144 Concordance of HER2 IHC Scoring in HER2-Low Breast Biopsy and Subsequent Excision Specimens

Brian Finkelman¹, Huina Zhang¹, Haley Tyburski², Cansu Karakas¹, Linda Schiffhauer², Jack Chen², Xi Wang², Hani Katerji¹, David Hicks¹, Bradley Turner¹

¹University of Rochester Medical Center, Rochester, NY, ²University of Rochester, Rochester, NY

Disclosures: Brian Finkelman: None; Huina Zhang: None; Haley Tyburski: None; Cansu Karakas: None; Linda Schiffhauer: None; Jack Chen: None; Xi Wang: None; Hani Katerji: None; David Hicks: None; Bradley Turner: None

Background: Recent clinical trial evidence has demonstrated a benefit of novel anti-HER2 therapies in "HER2-low" breast cancer (BC), defined as BC with a score of 1+ on HER2 immunohistochemistry (IHC), or 2+ HER2 IHC with negative HER2 in-situ hybridization. The validity of the core needle biopsy (CNB) for detecting HER2-positive BC has been well established; however, the accuracy of the CNB for detecting HER2-low disease has not been studied.

Design: We identified 45 consecutive BC patients with HER2 IHC score 0 or HER2-low on CNB, with an available excision specimen, from the pathology database (2014-2015) at our institution. HER2 IHC was performed on the CNB and corresponding excision specimen by PATHWAY 4B5. All slides were reviewed individually by four subspecialty trained breast pathologists, and then separately by a collective group of subspecialty breast pathologists, all blinded to the original IHC interpretation diagnosis and each other's scores. Discordance rates for detecting HER2-low disease between CNB and excision specimens were calculated based on the "majority opinion" of individual raters. Sensitivity of CNB vs excision for detecting HER2-low disease was compared using the McNemar test. Inter-rater reliability for CNB and excision specimens was calculated using Krippendorff's alpha. All analyses were performed in R v4.1.1.

Results: On CNB, 32/45 (71%) patients were interpreted as HER2 0, 11/45 (24%) were interpreted as HER2 1+, and 2/45 (4%) were interpreted as HER2 2+. On excision, 32/45 (71%) patients were interpreted as HER2 0, 9/45 (20%) were interpreted as HER2 1+, and 4/45 (9%) were interpreted as HER2 2+. Comparison of CNB and excision HER2 scoring is shown in Table 1. Discordance between CNB and excision HER2 scoring was seen in 11/45 (24%) patients. 5/32 (16%) patients with an interpretation of HER2 0 on the CNB had an interpretation of HER2-low on the excision specimen. 5/13 (38%) patients with an interpretation of HER2-low on the CNB had an interpretation of HER2 0 on the excision specimen.

Table 1: Comparison of biopsy versus excision HER2 scores

	Excision Score		
Biopsy Score	0	1+	2+
0	27 (60%)	4 (9%)	1 (2%)
1+	5 (11%)	5 (11%)	1 (2%)
2+	0 (0%)	0 (0%)	2 (4%)

Biopsy and excision HER2 IHC scores are reported based on "majority opinion" of individual raters. No significant difference was seen in the sensitivity of biopsy (72%) and excision (72%) specimens for detection of HER2-low disease ($P>0.99$). Inter-rater reliability was similar for both biopsy ($\alpha=0.794$) and excision ($\alpha=0.792$) specimens.

Conclusions: When considering "HER2-low" status on CNB, our results demonstrate a potentially clinically significant subset of patients with discordant results between the CNB and excision specimen. Reasons for this likely include tumor volume and heterogeneity. As treatments for HER2-low disease are introduced into clinical practice, repeat testing on the excision specimen for patients that are HER2 0 or HER2 1+ on the CNB should be considered. Additional studies are warranted.

145 Discordant Breast Receptor Subtypes Associated with Worse Prognosis in Breast Cancer Brain Metastasis

Michelle Garlin Politis¹, Courtney Connelly¹, Diane Chen¹, Fatemeh Derakhshan², Tao Su², Hanina Hibshoosh³, Hua Guo²

¹Columbia University Irving Medical Center, New York Presbyterian Hospital, New York, NY, ²Columbia University Irving Medical Center, New York, NY, ³Columbia University Medical Center, New York, NY

Disclosures: Michelle Garlin Politis: None; Courtney Connelly: None; Diane Chen: None; Fatemeh Derakhshan: None; Tao Su: None; Hanina Hibshoosh: None; Hua Guo: None

Background: Tumor heterogeneity is a crucial pathologic feature, which may lead to subtype discordance between primary breast carcinoma (PBC) and brain metastasis (BCBM). Such discordance is indicative of a biological phenotype/therapy changes and has been described in limited studies. We aim to examine clinicopathologic features of BCBM with subtype discordance that may help define molecular mechanisms of brain metastasis.

Design: A retrospective query (7/6/2000~2/16/2021) identified 149 cases of PBC with subsequent BCBM. 89 BCBM cases had complete hormone and HER2 receptor data and were classified as HRonly (HR+/HER2-), triple negative (TNBC), and HER2pos

(HER2+/any HR). Additionally, we subclassified HER2pos to triple positive (TPBC, HER2+/HR+) and HER2only (HER2+/HR-). We compiled clinicopathologic data including subtype discordance between PBC and BCBM, microsatellite instability (MSI), mismatch repair (MMR) protein status, NTRK and PD-L1 expression in BCBM, and overall survival (OS) analysis since BCBM diagnosis.

Results: The median ages of PBC and BCBM diagnosis were 49.0 and 55.3 years respectively. The median time between BC and BCBM first diagnosis was 33.1 months. Most BCBM patients also had non-brain metastases (76.1%) and high nuclear grade (74.2%). Among BCBM, there were 36 (40.4%) HRonly, 31 (34.8%) HER2pos, and 22 (24.7%) TNBC. 56 (65.11%) cases showed receptor concordance between PBC and BCBM. PBC HRonly, TPBC, TNBC, and HER2only showed 65.9%, 47.4%, 77.8% and 75.0% concordance, respectively (Fig.1). HER2pos patients showed lower age at time of BCBM diagnosis (54.8% < 50y, p=0.035) and higher risk of LVI in BC (p=0.063). MMR deficiency was found in one BCBM HRpos case (n=21), but all 17 cases done for MSI were negative. Notably, 2 NTRK fusion positive cases were both TNBC. Two (20%) of TNBC showed PD-L1 positivity. The median follow-up time since BCBM diagnosis was 12 months (range 1~59.8 mos). Discordant breast receptor subtype cases showed significantly worse prognosis since brain metastasis when compared to concordant cases (p=0.004, Fig.2). HER2pos patients had the worst OS (p=0.05). Further subclassification showed similar OS between TPBC and TNBC, but better than HER2only (p=0.043).

Table 1. BCBM Patient's baseline characteristics based on subtypes

	Total (n=89)	HRonly (n=36, 40.4%)	HER2pos (n=31, 34.8%)	TNBC (n=22, 24.7%)	P value
Age at diagnosis of BCBM (mean)	54.81 ± 11.72	55.73 ± 10.52	55.47 ± 12.62	52.39 ± 12.46	0.53
Patients <50 y.o at the time of BCBM DX	33 (37.1%)	9 (25.0%)	17 (54.8%)	7 (31.8%)	0.035
OS Alive Deceased	41 (67.2%) 20 (32.8%)	24 (80.0%) 6 (20.0%)	9 (50.0%) 9 (50.0%)	8 (61.5%) 5 (38.5%)	0.08
Presence of other MT Present Absent	67 (76.1%) 21 (23.9%)	25 (69.4%) 11 (30.6%)	25 (83.3%) 5 (16.7%)	17 (77.3%) 5 (22.7%)	0.41
Histological subtype at initial diagnosis					0.36
IDC	69 (83.1%)	24 (75.0%)	26 (89.7%)	19 (86.4%)	
ILC	8 (9.6%)	6 (18.8%)	1 (3.4%)	1 (4.5%)	
Mixed	4 (4.8%)	1 (3.1%)	2 (6.9%)	1 (4.5%)	
Others	2 (2.4%)	1 (3.1%)	0 (0%)	1 (4.5%)	
Nuclear Grade					0.015
2	23 (25.8%)	14 (38.9%)	8 (25.8%)	1 (4.5%)	
3	66 (74.2%)	22 (61.1%)	23 (74.2%)	21 (95.5%)	
pT stage					0.87
1	18 (35.3%)	6 (37.5%)	8 (34.8%)	4 (33.3%)	
2	22 (43.1%)	6 (37.5%)	11 (47.8%)	5 (41.7%)	
3	7 (13.7%)	3 (18.8%)	3 (13.0%)	1 (8.3%)	
4	4 (7.8%)	1 (6.3%)	1 (4.3%)	2 (16.7%)	
pN stage					0.40
0	20 (36.4%)	6 (33.3%)	7 (26.9%)	7 (63.6%)	
1	17 (30.9%)	6 (33.3%)	8 (30.8%)	3 (27.3%)	
2	7 (12.7%)	2 (11.1%)	5 (19.2%)	0 (0%)	
3	11 (20.0%)	4 (22.2%)	6 (23.1%)	1 (9.1%)	
LVI in primary Positive Negative	24 (58.5%) 17 (41.5%)	7 (50.0%) 7 (50%)	14 (77.8%) 4 (22.2%)	3 (33.3%) 6 (66.7%)	0.063

Figure 1 - 145

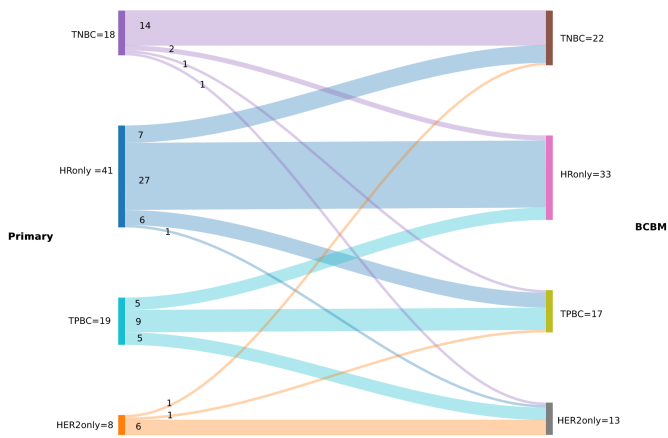
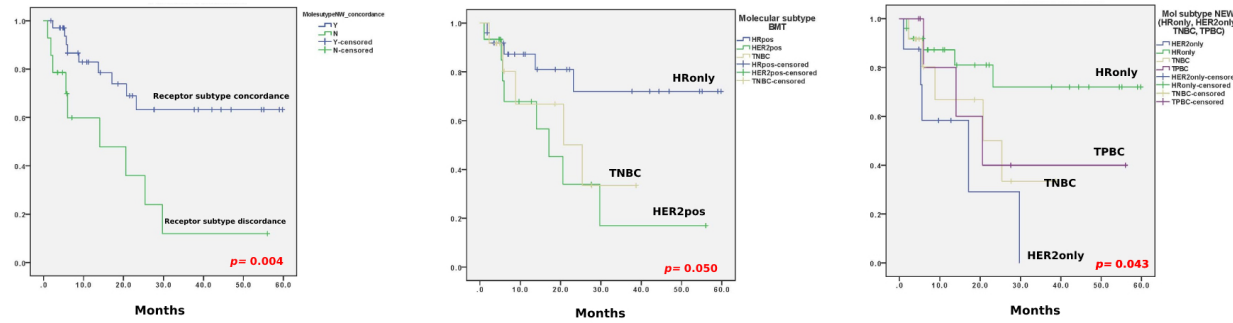


Figure 2 - 145

Kaplan-Meier plots of overall survival among BCBM carcinoma since brain metastasis diagnosis



Conclusions: Subtype discordance defines a poor prognosis phenotype that may aid in understanding the mechanisms of brain metastasis. TPBC group showed the lowest concordance rate with BCBM, which may be treatment related. HER2pos in brain metastases were the most aggressive tumor type in our cohort.

146 Clinicopathologic Characteristics and Outcomes of Breast Carcinoma Associated with Microglandular Adenosis

Iskender Genco¹, Melissa Krystel-Whittemore², Edi Brogi¹, Jorge Reis-Filho¹, Hannah Wen¹

¹Memorial Sloan Kettering Cancer Center, New York, NY, ²NYU Langone Health, New York, NY

Disclosures: Iskender Genco: None; Melissa Krystel-Whittemore: None; Edi Brogi: None; Jorge Reis-Filho: None; Hannah Wen: None

Background: Microglandular adenosis (MGA) is a rare benign yet infiltrative proliferation of small glands devoid of myoepithelium that morphologically mimics invasive carcinoma (IC). Molecular evidence has shown that MGA is a non-obligate precursor to triple-negative IC. Although the molecular alterations of MGA-associated carcinoma (MGA-CA) have been investigated, data regarding their clinical behavior are lacking.

Design: We searched the pathology database for patients with MGA, atypical MGA or MGA-CA diagnosed between 2000 to 2022. Kaplan-Meier method was used to estimate patient survival.

Results: A total of 115 patient were identified, including 42 with MGA, 8 with atypical MGA (AMGA), and 65 with MGA-CA. The clinicopathologic characteristic are summarized in Table 1. All MGA/AMGA were incidental findings in otherwise benign breast tissue or in specimens with separate focus of carcinoma. Among 65 patients with MGA-CA, 13 (20%) displayed carcinoma without definitive stromal invasion (MGA-CA *in situ*) and 52 (80%) had IC (MGA-CA IC). Of the 52 IC, approximately half were invasive carcinoma of no special type and the other half of a special histologic subtype, mostly matrix-producing metaplastic carcinoma (Table 1). Among 23 patients with MGA-CA who had BARCA germline testing, 13 (57%) had germline *BRCA1/2* mutation (*BRCA1*=11, 2 *BRCA2*=2). Five of six (83%) MGA-CA with molecular analysis available displayed

ABSTRACTS | BREAST PATHOLOGY

somatic mutation in *TP53*. Forty-three of 50 patients with MGA or AMGA who had follow-up information with a median follow-up time of 38 months (1-221 months) had no *locoregional recurrence (LRR)* or *distant metastasis (DM)*. Follow-up information was available for 49/65 (*in situ*=7/13, IC=42/52) patients with MGA-CA with a median follow-up time of 35 months (1-198 months). There was no *LRR* or *DM* among patients with MGA-CA *in situ*, whereas 11 (26%) patients with MGA-CA IC developed *DM*, 5 of which with *LRR* and *DM*. Overall, the 5-year recurrence-free survival and 5-year overall survival was 68% and 81%, respectively.

Characteristics	N	%
Age (years)		
Median (range)	50 (29-77)	
BRCA status		
Positive	13	57
Negative	10	43
Histologic subtype		
Non-invasive carcinoma	13	20
Invasive	52	80
Invasive carcinoma of no special type	29	56
Metaplastic	16	31
Acinic cell	5	10
Metaplastic + acinic cell	2	4
Nottingham grade		
1	2	4
2	12	25
3	34	71
Size (mm)		
Median (range)	14 (2-85)	
N stage		
N0	39	81
Nmi	2	4
N1	6	13
N2	1	2
Biomarkers		
Triple negative	48	94
Non-triple negative (ER-, PR+, HER2-)	3	6
Surgical Treatment		
Breast conserving surgery	34	55
Mastectomy	28	45
Radiotherapy		
Systemic therapy		
Neoadjuvant chemotherapy	15	32
Adjuvant chemotherapy	31	66

Conclusions: This is the largest cohort examining MGA-CA with follow-up information. MGA-CA was found to be associated with a high prevalence of *BRCA1/2* germline mutations and enriched for matrix-producing metaplastic carcinoma. Although *in situ* carcinoma associated with MGA is a controversial diagnosis, the outcome data in our cohort support the notion that MGA-CA without stromal invasion behaves like *in situ* carcinoma.

147 Changing Clinicopathologic Features of Malignant Phyllodes Tumors in the Setting of the COVID-19 Pandemic: Size Matters

Lianna Goetz¹, Sagar Dhamne², John Powell², Lucas McGowan²

¹Houston Methodist Hospital, Houston, TX, ²Baylor College of Medicine, Houston, TX

Disclosures: Lianna Goetz: None; Sagar Dhamne: None; John Powell: None; Lucas McGowan: None

Background: Malignant phyllodes tumors of the breast are a rare subset of fibroepithelial carcinomas with a recurrence rate of 23-30% per the World Health Organization. At our hospital, a tertiary care county center, there have been a number of malignant phyllodes cases with a high recurrence rate over the past few years. Additionally, in light of the recent COVID-19 pandemic with cancellation of elective procedures, patients have had delays in obtaining treatment and presented at advanced stages of disease. We present a case series of malignant phyllodes cases over the past five years at our hospital showing the clinicopathologic features in the setting of the Covid-19 pandemic.

Design: A retrospective review of the malignant phyllodes tumors from 2018-2022 was conducted at our institution. Data, including age at diagnosis, tumor size, margin status, free margin distance, histologic features including stromal overgrowth, mitotic count, necrosis percentage, infiltrative or pushing borders, heterologous components, lymphovascular invasion, local recurrence, distant metastasis and overall survival were analyzed.

Results: A total of 10 patients were identified as having malignant phyllodes tumors, 3 pre and 7 post-pandemic. The mean age at presentation was 53 years and the mean tumor size was 93 mm and 180 mm for pre- and post pandemic cases respectively. In all the cases, the surgical margins were negative with the closest margin most frequently being the deep margin, and average distance from the margin being 9 mm (range 1 -27 mm). Mitoses ranged from 15-40 mitoses per 10 high power fields and necrosis was present in 6 of 8 cases with an average of 29 %. 4 cases had malignant heterologous components; 2 were chondrosarcomatous, and 2 showed osteosarcomatous components. Local recurrence occurred in 4 cases at a mean interval of 29 months. All cases with local recurrence also had distant metastases. The follow-up range was from 8-60 months. 3 patients died of disease, all diagnosed after peak pandemic. The average interval from time of diagnosis to death was 12 months.

Figure 1 - 147

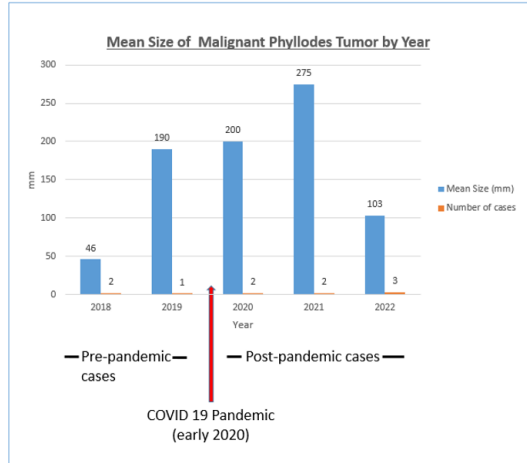


Figure 1. Mean Size of Malignant Phyllodes Tumor by Year

Figure 2 - 147

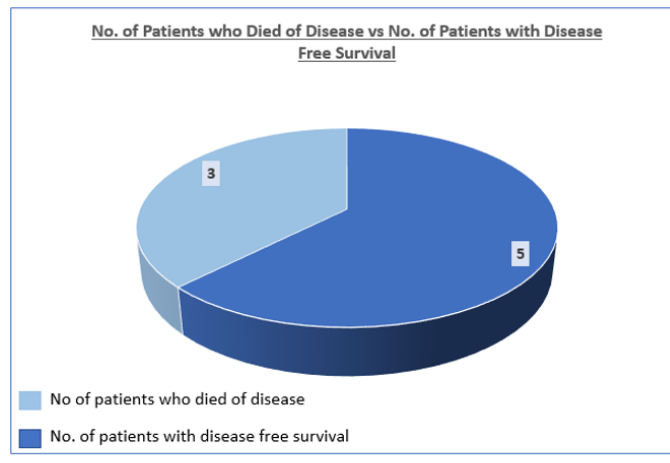


Figure 2. No. of Patients who Died of Disease vs No. of Patients with Disease Free Survival

Conclusions: We demonstrate that malignant phyllodes breast carcinoma can recur locally and with distant metastases in the absence of adequately negative margins. Patients presenting after the onset of the Covid-19 pandemic had larger tumors and poorer outcomes overall. This case series highlights the negative impact of the Covid-19 pandemic on delaying patient care and overall survival.

148 Radial Sclerosing Lesions (RSLs) found on Core Needle Biopsy (CNB): Can Surgery Be Avoided?

Anne Grabenstetter¹, Sandra Brennan¹, Timothy D'Alfonso¹, Lee Tan¹

¹Memorial Sloan Kettering Cancer Center, New York, NY

Disclosures: Anne Grabenstetter: None; Sandra Brennan: None; Timothy D'Alfonso: None; Lee Tan: None

Background: RSLs are benign breast lesions composed of glandular and epithelial proliferations radially arrayed around a fibro-elasticotic center, which mimic invasive carcinoma (IC) on imaging. Surgical management following a CNB diagnosis of RSL remains controversial with no standard guidelines as to whether excision (EXC) is necessary. This study evaluated the upgrade rate of RSLs.

Design: We retrospectively identified CNBs with RSL between 1/2015-1/2021. All CNB slides were reviewed to confirm the diagnosis. Cases were excluded if there was a co-existing lesion warranting EXC or if the patient had concurrent ipsilateral carcinoma without separate EXC for RSL. Imaging was reviewed by a dedicated breast radiologist to categorize each RSL as either the "target" lesion of the CNB or an "incidental" finding and determine radiologic-pathologic concordance. An upgrade was defined as IC or ductal carcinoma in situ (DCIS) in the EXC. The EXC slides of upgraded cases were reviewed.

Results: The final cohort consisted of 134 CNBs from 128 women (median age 52 years, range 27-76) that had EXC. Fifty-five (43%) patients had prior/concurrent history of carcinoma. The imaging modality was mammogram in 53 (40%) cases, MRI in 52 (39%) and ultrasound in 29 (21%). Most (109, 81%) CNBs were vacuum-assisted and 25 (19%) ultrasound-guided CNBs were not. The median size on imaging was 9 mm (range 2-41). The target was deemed by imaging to be completely removed by the CNB in 25 (19%) cases. The RSL was categorized as the target in 99 (74%) cases and incidental in 35 (26%). In 4 CNBs the pathology was assessed as being discordant with the imaging findings. Overall, 4 (3%) cases were upgraded at EXC (Table 1). Two of the RSLs upgraded on EXC were discordant with imaging, resulting in an upgrade rate of 1% (2/130) among cases with radiologic-pathologic concordance (Figs. 1, 2). Foci of IC/DCIS found in the EXC of upgraded cases were not closely associated with the RSL biopsy site. In cases without upgrade, 7 EXCs yielded atypical ductal hyperplasia. For 25 patients that did not undergo EXC of the RSL imaging follow up data was available and none developed carcinoma over a median of 31 months (range 9-74).

	Case 1	Case 2	Case 3	Case 4
Age (years)	43	69	58	47
Clinical history	Concurrent contralateral ILC	BRCA2 mutation, family hx breast cancer	Contralateral DCIS 7 years prior s/p excision and XRT	Concurrent ipsilateral DCIS
Imaging modality	MRI	MRI	Mammogram	Ultrasound
Imaging finding (lesion diameter)	NME (28 mm)	Mass (6 mm)	Asymmetry with Ca ²⁺ (17 mm)	Mass (7 mm)
Needle gauge	9 G vacuum assisted x 7 cores	9 G vacuum assisted x 6 cores	9 G vacuum assisted x 7 cores	14 G x 4 cores
Pathology on core biopsy	RSL, florid UDH, papillomatosis	RSL, fibrocystic changes	RSL, intraductal papilloma, LCIS; Ca ²⁺ associated with benign ducts	RSL, adenosis, UDH
RSL: incidental or target	Target	Incidental	Incidental	Incidental
Rad-path concordance	Concordant	Concordant	Discordant	Discordant
Imaging target removed by CNB	No	Yes	No	No
Pathology on excision	Microinvasive ILC, spanning <1 mm	IMC with lobular growth, grade 2, spanning 2 mm; DCIS, nuclear grade 2, spanning 2 mm*	DCIS, nuclear grade 2, with Ca ²⁺ , spanning ~3 mm; RSL	DCIS, nuclear grade 1, spanning 1 mm; RSL
Carcinoma associated with biopsy site	No	No	No	No

Table 1: Clinicopathologic findings in patients with radial sclerosing lesion on biopsy and malignancy on surgical excision

*Patient had subsequent mastectomy showing benign pathology only

hx – history, XRT – radiation, ILC – invasive lobular carcinoma, NME – non-mass enhancement, Ca²⁺ - calcifications, G – gauge, LCIS – lobular carcinoma in situ, UDH – usual ductal hyperplasia, rad-path – radiologic-pathologic, IMC – invasive mammary carcinoma with mixed ductal and lobular features

Figure 1 - 148

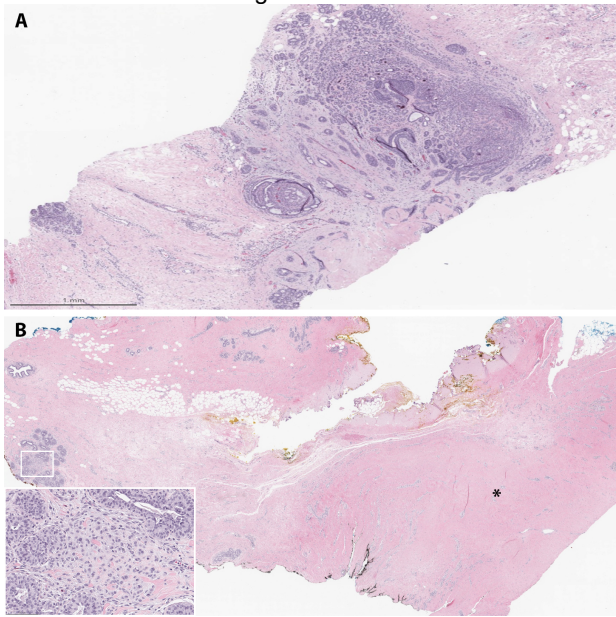
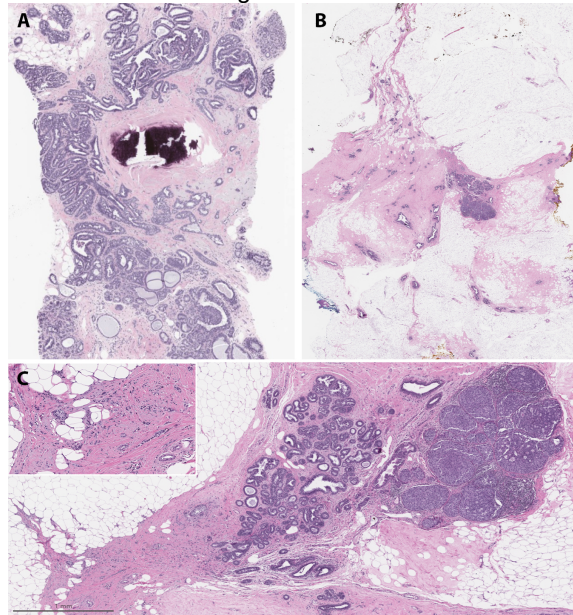


Figure 2 - 148



Conclusions: In this study, the upgrade rate of radiologic-pathologic concordant CNBs with RSL was 1%. Both upgrades are incidental, minute ICs not associated with the biopsy site. With careful radiologic and pathologic correlation, the upgrade rate of RSLs without atypia is very low and EXC can be safely avoided.

149 Rates of Atypia in Gender Affirming Mastectomies in Black Transgender Non-Binary Individuals

Ashleigh Graham¹, Katelynn Davis², Marissa White³, Qiqi Yu³, Pedram Argani⁴, Ashley Cimino-Mathews³

¹*Johns Hopkins University, Baltimore, MD*, ²*University of Pittsburgh Medical Center, PITTSBURGH, PA*, ³*Johns Hopkins University School of Medicine, Baltimore, MD*, ⁴*Johns Hopkins Hospital, Baltimore, MD*

Disclosures: Ashleigh Graham: None; Katelynn Davis: None; Marissa White: None; Qiqi Yu: None; Pedram Argani: None; Ashley Cimino-Mathews: None

Background: Numbers of gender affirming mastectomies have significantly increased within the last seven years as their access has increased. Population based statistics demonstrate that a higher percentage of Black individuals identify as transgendered and non-binary compared to White counterparts. Although Black individuals constitute 13.6% of the United States Census, young Black natal women have higher rates of aggressive, late stage breast cancers. However, to our knowledge, no study has specifically evaluated the rates of atypia in gender affirming mastectomies from Black transgendered individuals.

Design: A retrospective chart review was performed between January 1, 2000 and July 12, 2022 to chronologically curate a list of bilateral gender affirming mastectomies. Clinicopathologic data collected included patient age, family medical history, use and duration of gender affirming androgen-derived hormones, specimen weight, histopathological findings, and the total number of slides examined. GraphPad was utilized to calculate both Fisher's exact and t-tests.

Results: Gender affirming mastectomies were received from 151 patients, 21.8% (n=33) of which were from Black individuals. Two (6.1%) mastectomies from Black individuals contained atypical findings, consisting of atypical ductal hyperplasia in one and invasive and *in situ* ductal carcinoma in the other, with a carcinoma rate of 3.0%. In contrast, atypia was seen in 1 (0.85%) mastectomy from non-Black individuals [$p=0.12$], with no cases of carcinoma. Black individuals had a higher rate of breast cancer in a female relative (39%) and increased incidence of fibrocystic changes (42%) compared to non-Black individuals (30% and 34%, respectively). Black and non-Black individuals had similar rates of androgen therapy use (100% vs 93%), duration from initiating androgen therapy to surgery (2.1 vs 2.2 years), average specimen weight (1162 vs 1088g), number of slides submitted (11.9 vs 12.5), and average duration of follow-up (7.5 vs 8 days).

Conclusions: Black transgendered non-binary individuals had higher rates of atypia and carcinoma in gender affirming mastectomies than non-Black individuals. However, both groups had otherwise similar clinical parameters including management. Although the findings in this exploratory study were not statistically significant, they may be clinically noteworthy. Larger studies are warranted to evaluate whether increased breast cancer screening should be considered in this unique population.

150 Artificial Intelligence Assisted Assessment of HER2 IHC Using Semi- and Fully-Automated Workflows: Rapid Validation and Implementation as a Quality Assurance and Risk Mitigation Check Point

Ursula Green¹, Jenifer Caldara², Danielle Pirain³, Regan Baird³, Jochen Lennerz⁴

¹*Massachusetts General Hospital, Boston, MA*, ²*Visiopharm, Westminster, CO*, ³*Visiopharm A/S, Westminster, CO*, ⁴*Massachusetts General Hospital, Harvard Medical School, Boston, MA*

Disclosures: Ursula Green: None; Jenifer Caldara: None; Danielle Pirain: None; Regan Baird: None; Jochen Lennerz: None

Background: HER2 is a standard and critical biomarker in the staging, diagnosis, and management of breast cancer. Proper classification of HER2 in stained tissue sections is critical to precision pathology and personalized medicine for patients. Borderline cases require additional timely and costly tests, including reflex and ISH testing. Visiopharm's HER2Connect algorithm has a proven track-record of assisting pathologists by expediting review time during staging and reducing the number of borderline cases which are IHC positive, ISH negative. In this study, we show that the HER2Connect can be activated following manual sign-out as a checkpoint to mitigate risk on challenging cases by flagging non-concordant reads during this AI-based quality assurance step at the Center of Integrated Diagnosis (CID).

Design: 58 random patient samples were stained for HER2 IHC at one of 5 hospitals according to their standard staining methods. Samples were assessed by both IHC and FISH. Samples were digitized by a Motic Scanner at the MGH CID then tumor areas were analyzed by HER2Connect. Tumor areas were identified by either a Fully Automated workflow where the tumor was demarcated by AI prior to HER2Connect analysis; and a Semi-automated workflow where selection areas were guided by pathologist inking prior to imaging. Scores from both methods were then compared to manual pathology IHC and FISH interpretations.

Results: See Table 1.

		IHC			IHC 2+ Cases FISH	
		1+	2+	3+	Normal	FISH Abnormal
Fully Automated Workflow	1+	6	19	0	1+	17 2
	2+	2	8	0	2+	5 3
	3+	1	3	19	3+	3 0
Semi-Automated Workflow	1+	7	22	0	1+	21 1
	2+	2	6	0	2+	3 3
	3+	0	2	19	3+	1 1

Concordant

Positive Impact: Discordant IHC, Concordant FISH, Possible Impact on Treatment Strategy

Neural Impact: Discordant IHC, No Impact on Treatment Strategy (Minor discordance)

Negative Impact: Discordant IHC, Deleterious Impact on Treatment Strategy (Major discordance)

Conclusions: Both approaches yielded results which validated the HER2Connect for use in routine workflows. 19 (fully) and 22 (semi-automated) cases were appropriately reassigned by AI. The AI was not influenced by site specific clones and staining. Discordant cases demonstrate real examples of cases that would be flagged for re-examination by a pathologist. The AI also served as a QC checkpoint by confirming IHC(-) status on cases which displayed abnormal FISH. Alerting the laboratory of the inconsistency allows the pathologist to revisit samples for confirmation. The detection of excision and staining artifacts caused the major discordance cases and would easily be identified by an observer, confirming the power of AI paired with pathologist yields the highest level of precision medicine. Adding these artifacts in the AI training should negate all major discordant cases. HER2Connect can be validated and implemented within 2 days for QC and risk mitigation. Minimally positive specimens may qualify for new HER2-low treatment strategies and different from traditional HER2-therapy.

151 Whole Slide Imaging-Based Quantification of Ductal Carcinoma In-Situ in Needle Core Biopsies Predicts Margin Status in Breast-Conserving Surgery

Alexander Gross¹, Gerald Hobbs¹, Luis Samayoa², Stell Santiago¹

¹West Virginia University Health Sciences Center, Morgantown, WV, ²CPA Lab/Norton Healthcare, Louisville, KY

Disclosures: Alexander Gross: None; Gerald Hobbs: None; Luis Samayoa: None; Stell Santiago: None

Background: Dillon et al. found that the frequency of compromised margins after breast-conserving surgery (BCS) increases with the proportion of ductal carcinoma in-situ (DCIS) in needle core biopsy (NCB) specimens (*Mod Pathol* 2007;21:39-45). This is an attractive metric for risk stratification of BCS candidates; studies use estimated quantities. Our goal was to use a whole slide imaging platform for digital quantification of NCB DCIS and retrospectively analyze an association with BCS margin status.

Design: After institutional review board approval we retrieved BCS cases with DCIS alone or DCIS and admixed invasive ductal carcinoma (IDC) in the NCB treated at our institution from 2011-2021 (Table 1). We identified 180 cases and reviewed their clinical, radiologic, and pathologic data. We performed digital scans of a single slide in each case with the highest absolute quantity of DCIS. With whole slide imaging software we measured and outlined the areas of stroma, adipose tissue, DCIS, and invasive carcinoma (Figure 1). Positive margins were defined based on the 2019 American College of Breast Surgeons Consensus Guidelines on Lumpectomy Margins. Chi-square test was performed on categorical variables and either logistical regression or analysis of variance on continuous variables. *P*-value < .05 was considered statistically significant.

Results: Eighty-two cases were identified with positive margins and 97 cases with clear margins. By logistic regression of all cases an increasing percentage of DCIS was associated with a progressively higher probability of positive margins (Figure 2, *P* < .001). One positive case of extensive DCIS alone was excluded as an outlier. Additionally, a lumpectomy diagnosis of DCIS admixed with invasive ductal carcinoma was associated with an increase in positive margins compared to cases with DCIS alone (*P* < .001). Alternatively, in cases of NCB DCIS alone a mean of 9.5% DCIS (95% CI 6.4 to 12.51, *P* = .0149) was associated with the presence of IDC in the lumpectomy specimen. This is compared to cases of DCIS alone with a mean of 5.33% DCIS (95% CI 4.0 to 6.7, *P* = .0149).

		Positive margins	Negative margins	P
Total cases	180	83 (46%)	97 (54%)	0.9339
NCB - DCIS	103	48 (46%)	55 (54%)	0.31
NCB - IDC + DCIS	77	35 (45%)	55 (55%)	
Final - DCIS	91	21 (22%)	70 (88%)	<.00001
Final - IDC + DCIS	89	62 (70%)	27 (30%)	
Grade DCIS NCB				0.41
Low	32	12 (36%)	20 (64%)	
Intermediate	92	43 (47%)	49 (53%)	
High	56	28 (50%)	28 (50%)	
Grade IDC NCB				0.2
Low	36	12 (33%)	24 (67%)	
Intermediate	34	20 (59%)	14 (41%)	
High	7	3 (43%)	4 (57%)	
NCB DCIS Architecture				0.78
Solid	70	36 (52%)	34 (48%)	
Cribiform	111	49 (44%)	62 (56%)	
Papillary	10	2 (10%)	8 (80%)	
Comedo	77	42 (55%)	35 (45%)	
Clinging	9	5 (56%)	4 (44%)	
Apocrine	2	1 (50%)	1 (50%)	
Surgical Approach				0.63
Lumpectomy	40	17 (43%)	23 (57%)	
Lumpectomy with shave margins	140	66 (48%)	74 (52%)	

Figure 1 - 151

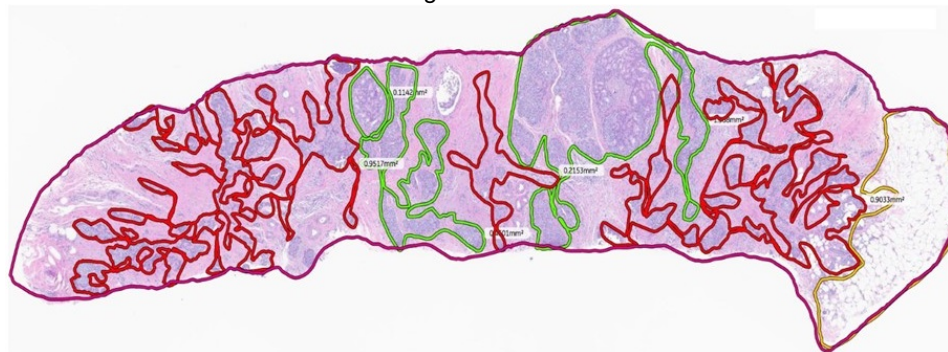
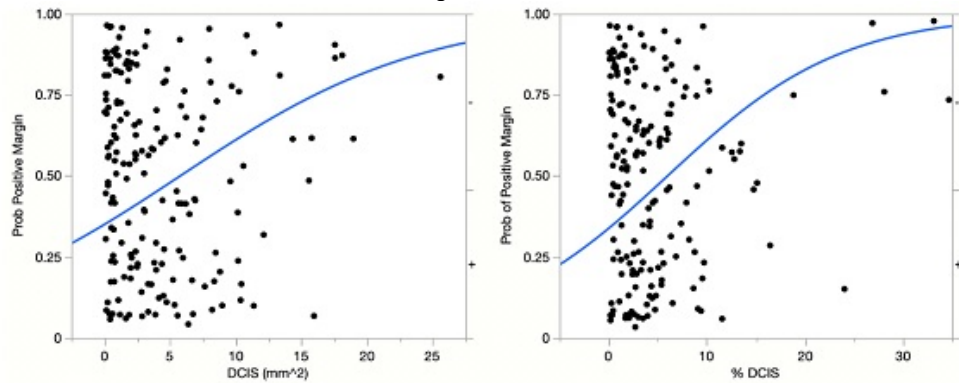


Figure 2 - 151



Conclusions: The selection of patients for BCS currently relies on imprecise criteria. The percentage of DCIS in a NCB predicts margin status at lumpectomy and the possibility of an unbiopsied IDC - % DCIS should appear in pathologic reporting. This combined with the clinical, radiologic, and pathologic presentation can provide an improved risk-stratification for patients considering BCS.

152 Prognostic Significance of Immunohistochemical Markers in Triple Negative Breast Cancer

Rachel Han¹, Sharon Nofech-Mozes², Ekaterina Olkhov-Mitsel³, Rania Chehade³, Katarzyna J. Jerzak⁴, Elzbieta Slodkowska⁵

¹University of Toronto, Toronto, ON, ²University of Toronto, Sunnybrook Health Sciences Centre, Toronto, ON, ³Sunnybrook Health Sciences Centre, Toronto, ON, ⁴Sunnybrook Health Sciences Centre, Odette Cancer Centre, Toronto, ON, ⁵Sunnybrook Health Sciences Centre, University of Toronto, Toronto, ON

Disclosures: Rachel Han: None; Sharon Nofech-Mozes: None; Ekaterina Olkhov-Mitsel: None; Rania Chehade: None; Katarzyna J. Jerzak: None; Elzbieta Slodkowska: None

Background: Triple negative breast cancers (TNBC) are a heterogeneous group of carcinomas with variable prognoses and limited treatment options. Though molecular profiling has allowed for better prognostication of TNBC, these techniques are not widely available for clinical use. We sought to determine the prognostic significance of several biomarkers by immunohistochemistry (IHC) in TNBC.

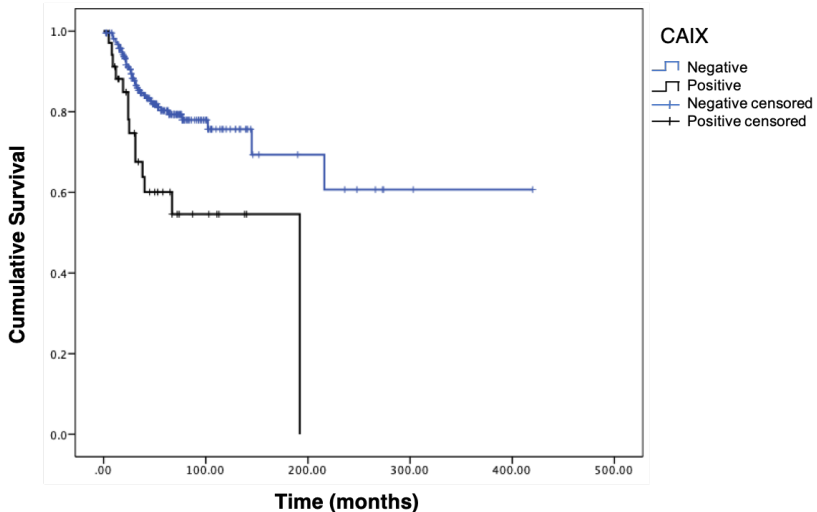
Design: TNBC cases diagnosed at our institution from 2009-2020 were retrieved through retrospective database review. Cases without adequate tumour including pathologic complete response and low cellularity post-neoadjuvant therapy were excluded. A total of 302 cases were identified. Tissue microarrays were immunostained and scored as follows: keratin 5 (K5) and androgen receptor (AR) (positive if >10% of tumour staining); CAIX and vimentin (positive if at least moderate staining in >50% or strong staining in >25% of tumour); RB1 (retained or lost); p16 (overexpressed or wildtype); p53 (mutant or wildtype); Ki67 (<20% or >=20%). Univariate and multivariate cox proportional-hazards regression methods were used to evaluate the impacts of clinicopathologic and IHC parameters on locoregional (LR) and distant recurrence (DR) and overall survival (OS). For statistical analysis, patients who died of disease or were transitioned to palliative care were combined to reach a composite endpoint.

Results: Of 253 patients with follow-up data, 184 had no evidence of disease with a mean follow-up time of 61.8 months (+/- 54.7), 13 were alive with disease, 22 died of disease, and 34 were transitioned to palliative care. LR and DR occurred in 28 and 76 cases. On univariate survival analyses (Table 1), T stage ($P<0.001$), N stage ($P=0.019$), and use of chemotherapy ($P<0.001$) were significantly associated with LR; T stage ($P<0.001$), N stage ($P<0.001$), overall stage ($P<0.001$) and CAIX expression ($P<0.001$) were significantly associated with DM; and grade ($P=0.028$), T stage ($P<0.001$), N stage ($P<0.001$), overall stage ($P<0.001$) and CAIX expression ($P=0.003$) were associated with OS (Figure 1). On multivariate analysis, overall stage (HR CI $P<0.001$) and CAIX expression (HR CI $P=0.011$) were independent predictors of DM; only overall stage (HR CI $P<0.001$) was an independent predictor of OS.

	LR			DM			DOD + Palliative Care					
	95% CI			95% CI			95% CI					
	HR	Lower	Upper	P	HR	Lower	Upper	P	HR	Lower	Upper	P
Age	1.145	0.523	2.505	0.735	0.764	0.479	1.217	0.257	0.760	0.445	1.298	0.315
K5 >10%	1.842	0.813	4.171	0.143	1.279	0.766	2.136	0.346	1.377	0.773	2.453	0.278
Grade (3 vs. 2/1)	0.786	0.325	1.898	0.592	1.642	0.857	3.146	0.135	2.818	1.118	7.101	0.028
Overall Stage												
2 vs. 1	0.994	0.423	2.336	0.988	3.667	1.707	7.877	0.001	4.904	1.720	13.982	0.003
3 vs. 1	1.055	0.278	4.000	0.937	16.04	7.131	36.082	<0.001	18.069	6.027	54.174	<0.001
T stage												
2 vs. 1	0.898	0.372	2.171	0.812	3.604	1.849	7.025	<0.001	4.256	1.767	10.253	<0.001
3 vs. 1	8.839	2.974	26.277	<0.001	26.274	12.151	56.812	<0.001	31.175	12.176	79.817	<0.001
N stage												
1 vs. 0	1.550	0.578	4.156	0.384	2.733	1.543	4.84	0.001	2.838	1.445	5.574	0.002
2 vs. 0	0.757	0.095	6.058	0.793	4.741	2.055	10.936	<0.001	3.905	1.442	10.575	0.007
3 vs. 0	6.294	1.357	29.178	0.019	7.985	3.434	18.567	<0.001	9.832	3.857	25.066	<0.001
Mutation												
AR	1.357	0.438	4.206	0.597	1.047	0.505	2.17	0.901	1.213	0.484	3.042	0.68
Chemotherapy	2.557	1.157	5.649	<0.001	1.049	0.58	1.894	0.875	1.013	0.510	2.013	0.971
CAIX	1.663	0.562	4.922	0.358	2.750	1.605	4.71	<0.001	2.555	1.387	4.707	0.003
Vimentin	1.106	0.452	2.711	0.825	1.086	0.608	1.939	0.780	0.920	0.475	1.785	0.806
p16	1.366	0.613	3.044	0.446	1.125	0.702	1.802	0.625	1.376	0.792	2.388	0.257
p53	1.507	0.645	3.521	0.344	1.146	0.668	1.966	0.622	1.226	0.615	2.444	0.563
RB1	1.028	0.452	2.338	0.947	1.082	0.656	1.786	0.756	1.183	0.674	2.077	0.559
Ki67	1.727	0.700	4.258	0.235	1.390	0.745	2.592	0.301	1.369	0.667	2.810	0.391

Figure 1 - 152

Survival Functions



Conclusions: Expression of the transmembrane protein CAIX, known to be upregulated in hypoxia, is associated with disease progression in TNBC. This marker may be used as a prognostic marker and potential therapeutic target for TNBC.

153 Reproducibility and Concordance of Local vs Central IHC4 Score Compared to EndoPredict Score in Invasive ER+ HER2- Early Breast Cancer: A GEFPICS' Retrospective Study

Juliette Haudebourg¹, Jocelyn Gal¹, Gaetan Macgrogan², Lounes Djerroudi³, Aurelie Maran-Gonzalez⁴, Lucie Tixier⁵, Veronique Verriele⁶, Laurent Arnould⁷, Anne Vincent-Salomon³, Janice Barros-Monteiro⁸, Jerome Lemonnier⁹, Camille Franchet¹⁰, Magali Lacroix-Triki¹¹

¹Centre Antoine Lacassagne, Centre de lutte contre le cancer, Nice, France, ²Institut Bergonié, Lyon, France, ³Institut Curie, Paris, France, ⁴ICM (Institut du Cancer de Montpellier), Nantes, France, ⁵Centre Jean Perrin, Clermont Ferrand, France, ⁶Angers, France, ⁷Centre Georges-François Leclerc, Dijon, France, ⁸Roche Diagnostics France, Meylan, France, ⁹Unicancer, Paris, France, ¹⁰University Cancer Institute - Oncopole, Toulouse, France, ¹¹Gustave Roussy, Cancer Campus, Grand Paris, Villejuif, France

Disclosures: Juliette Haudebourg: None; Jocelyn Gal: None; Gaetan Macgrogan: None; Lounes Djerroudi: None; Aurelie Maran-Gonzalez: None; Lucie Tixier: None; Veronique Verriele: None; Laurent Arnould: None; Anne Vincent-Salomon: None; Janice Barros-Monteiro: None; Jerome Lemonnier: None; Camille Franchet: None; Magali Lacroix-Triki: None

Background: IHC4 score may be used to guide treatment decision in invasive breast cancer (BC), provided that the score has been validated beforehand in the laboratory, and if multigene prognostic assays are not available. The derived IHC4+C is a prognostic algorithm combining IHC4 (based on ER, PR, HER2, Ki67 immunohistochemistry) and clinical parameters (lymph node status, tumor size, histological grade, age, type of endocrine therapy). Despite low cost and wide availability, the use of IHC4+C remains limited, mainly due to lack of validation of IHC4 in decentralized "real life" conditions. Our study aimed at evaluating: (i) the IHC4+C score concordance between local and central technique, (ii) the inter-observer reproducibility between both techniques, and (iii) the concordance between IHC4+C and EndoPredict (EP) multigene prognostic assay.

Design: This retrospective study included 155 patients selected from the National EndoPredict database, with a balanced repartition between low and high EPclin scores (48.5% and 51.5% respectively). Participating laboratories (n=6) provided for each of their case: 1 HE and 4 local IHC slides (ER, PR, HER2, Ki67), and unstained slides for central testing. All slides were digitized. After a training session, 7 pathologists were asked to score ER (H-score), PR (% stained cells), HER2 (positive vs negative) and Ki67 (% stained cells). Two pathologists scored the whole local and central series, and 5 pathologists scored 30 selected cases, both locally and centrally stained. The equivalence between local and central technique was defined as a ≥90% concordance rate.

Results: Comparison of risk category obtained by IHC4 +C on local IHC for 155 cases scored by 2 pathologists showed an agreement for 145 (93.5%) patients ($\kappa=0.76$). The 10 discordant cases presented with a 10-yr risk of recurrence near the 10% cut off (-3.8% to +2.5%). Preliminary results for 3 out of 5 pathologists on the 30 selected cases showed a 90% inter-observer concordance rate on central IHC technique, vs 93% concordance rate on the local technique. For the 5 discordant cases, the maximum 10-yr risk deviation between observers ranged from 0.9 to 3.1%. Full concordance analysis between IHC4+C local/central scores and EPclin scores is still ongoing and will be presented.

Conclusions: Preliminary inter-observer analysis showed a good concordance ($\geq 90\%$) for IHC4+C scoring on local and central IHC, supporting its technical validity for a real-life use.

154 Effect of Paraffin Sections Preservation Time on HER2 Expression in Invasive Breast Cancer

Jiankun He¹, Hongbo Liu¹, Yueping Liu¹

¹The Fourth Hospital of Hebei Medical University, Shijiazhuang, China

Disclosures: Jiankun He: None; Hongbo Liu: None; Yueping Liu: None

Background: The antigen immune reaction in paraffin sections will change with time, and the storage time of paraffin sections will affect the results of immunohistochemistry. With the emergence of new therapeutic drugs ADCs, accurate detection of HER2 low affects the prognosis of these patients. Therefore, it is necessary to explore the expression of HER2 in breast cancer paraffin sections with different storage times.

Design: A total of 240 invasive breast cancer cases were selected. 128 cases were paraffin sections of surgical specimens. There were 47 paraffin sections with initial status of HER2 1+ and 40 cases of HER2 2+ and 41 cases of HER2 3+. To simulate the study of biopsy tissue, the 112 cases were fabricated as tissue microarray sections with a diameter of 2 mm. There were 31 paraffin sections with initial status of HER2 1+ and 46 cases of HER2 2+ and 35 cases of HER2 3+. All cases were serially sectioned. HER2 staining was performed at weekly intervals. A total of 8 weeks of HER2 staining was performed.

Results: For paraffin sections of surgical specimens, HER2 expression in sections stored for 1 week and 2 weeks was highly consistent with that in fresh sections ($Kappa \geq 0.800$). The HER2 expression in the slices stored for 3 weeks to 7 weeks was consistent with that in fresh slices ($Kappa \geq 0.600$). For tissue microarray sections simulating needle biopsy tissue, HER2 expression in sections stored for 1 week was highly consistent with that in fresh sections ($Kappa = 0.815$). The HER2 expression in the slices stored for 2 weeks to 3 weeks was consistent with that in fresh slices ($Kappa \geq 0.600$). The HER2 expression in the slices stored for 4 weeks to 5 weeks was moderately consistent with that in fresh slices ($Kappa \geq 0.400$). With the increase of storage time of paraffin sections, the expression level of HER2 gradually decreased. HER2 expression in tissue microarray sections decreased faster with time than in paraffin sections of surgical specimens. Sections with HER2 expression of 2+ had the highest rate of change, followed by 1+. Sections with HER2 3+ had the most stable HER2 expression levels. All cases were divided into HER2 low and HER2 positive. The decline in patients with HER2 low was higher than that in HER2-positive patients.

Figure 1 - 154

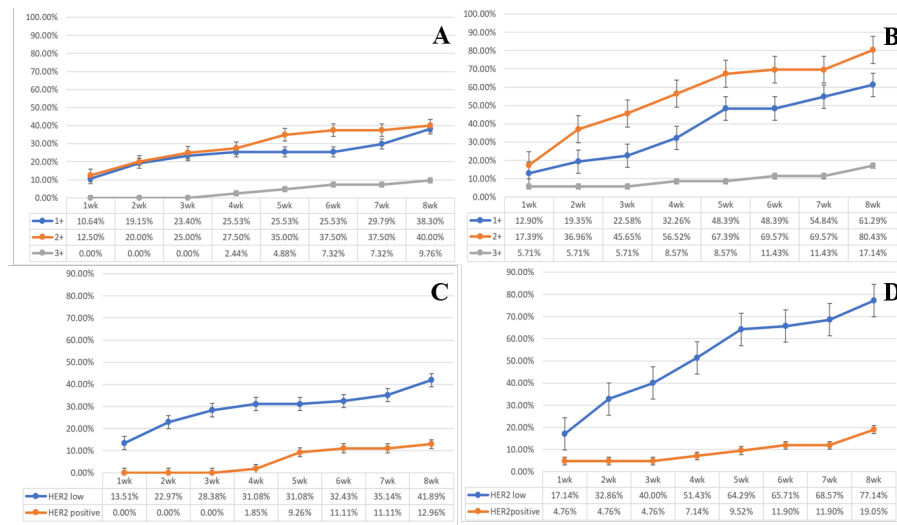


Fig.1 Change rate of HER2 expression in paraffin sections at different storage times
A and C are the rate of change of HER2 expression in paraffin sections of surgical specimens. B and D are the rate of change of HER2 expression in tissue microarray sections.

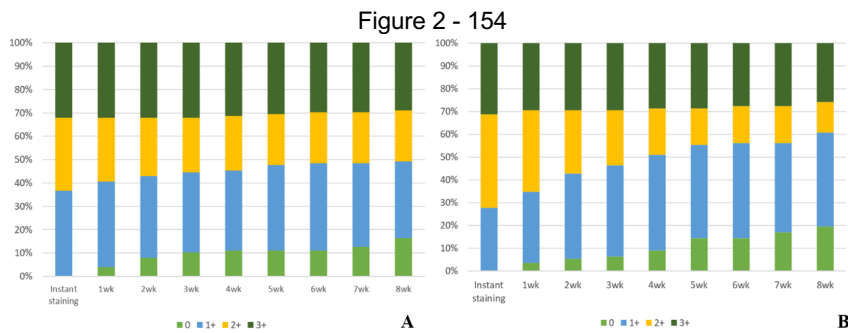


Fig.2 The proportion of HER2 expression in the cohort of patients with different storage times of paraffin sections
A is the proportion of patients with paraffin sections of surgical specimens. B is the proportion of patients with tissue microarray sections.

Conclusions: Long-term storage of paraffin sections can lead to decreased HER2 expression levels, especially in patients with HER2 low. Compared with surgical specimens, the HER2 expression level decreased more in biopsy tissue.

155 Deep Learning-Based, Fully Automated Analysis of Whole Slide Images Can Detect Invasive Breast Carcinoma and Count Ki-67 Easily and Precisely

Akira Hida¹, Jeppe Thagaard², Takahiro Watanabe³, Thomas Ramsing², Agnete Overgaard², Yumi Oshiro⁴, Takuya Moriya⁵

¹Matsuyama Shimin Hospital, Matsuyama, Japan, ²Visiopharm A/S, Horsholm, Denmark, ³Hyogo College of Medicine, Nishinomiya, Japan, ⁴Matsuyama Red Cross Hospital, Matsuyama, Japan, ⁵Kawasaki Medical School, Kurashiki, Japan

Disclosures: Akira Hida: None; Jeppe Thagaard: None; Takahiro Watanabe: None; Thomas Ramsing: None; Agnete Overgaard: None; Yumi Oshiro: None; Takuya Moriya: None

Background: The basic treatment of hormone-receptor(HR) positive breast carcinoma(BC) is anti-hormonal therapy. Recently, cyclin-dependent kinases 4/6 inhibitor called abemaciclib, has been approved for high risk patients after surgery, together with Ki-67 IHC MIB-1 pharmDx(Dako Omnis) for the patient selection. However, there remains concerns about reproducibility, and a development of automated image analysis is desired.

Design: Random 100 cases were collected from a previous study [Histopathology. 2020;77(3):471-480]. Resected specimen of primary breast invasive carcinoma(HR positive and HER2 negative) had been stained with Ki-67(MIB-1; Dako, Autostainer Link 48; Agilent), and digitized by NanoZoomer-XR(Hamamatsu Photonics K.K.). Two board-certified pathologists evaluated Ki-67 following the recommendations from the International Working Group. We also performed original scoring using a deep learning(DL)-based Ki-67(Breast, AI APP, research use only; Visiopharm) in a fully automated approach with no manual input or review. We compared the continuous output score with Spearman's correlation analysis, and calculated agreement with the clinically relevant cut-off of 20% for treatment with adjuvant abemaciclib.

Results: Median/mean value of each pathologist and automated analysis were 11.7/15.1(AIH, Path 1), 8.4/12.0(TW, Path 2) and 6.5/9.4 respectively. Every pair showed statistically positive correlations of Ki-67(figure 1-2), and the highest value was yielded by Path 1 and the software($R^2=0.9112$). Time needed for pathologist to evaluate 100 cases ranged from 328(Path 2) to 562 minutes(Path 1). The software counted 385,985 cells on average within the full-face slides. When we set the threshold of Ki-67 at 20% by pathologist 1 and calculated 13% by software, the sensitivity and specificity of our new algorithm is 88.9% and 97.6% respectively.

Figure 1 - 155

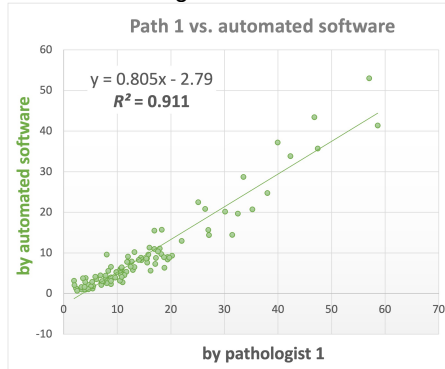
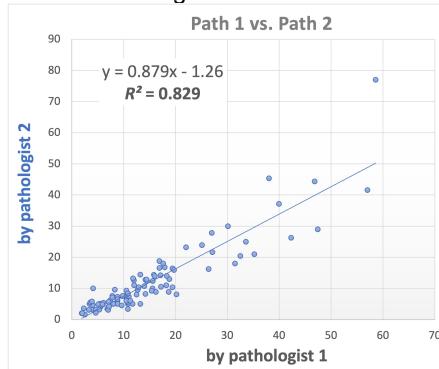


Figure 2 - 155



Conclusions: Here, we have created a fully automated software to analyze Ki-67, which includes DL-based algorithm to detect invasive BC nest and count a large amount of cells quickly. It has probed to have concordant result with experienced breast pathologists, although the prognostic value needs to be confirmed. As the software tends to have lower value than pathologists, we have to pay attention to the cut-off value. However, fully automated analysis can be performed by a technician or an engineer, and allow pathologists to focus on another task. This objective method would help clinicians and patients to select the optimal treatment based on the tumor biology.

156 Solitary Fibrous Tumor of Breast and Axilla: Clinicopathologic Profile of Five Cases

Raza Hoda¹, Lauren Duckworth², John Van Arnam², Patrick McIntire¹, Hannah Gilmore³, Xiaoyan Cui¹, Gloria Zhang¹, J. Jordi Rowe¹, Karen Fritchie¹, Elizabeth Azzato², Erinn Downs⁴

¹Cleveland Clinic, Cleveland, OH, ²Cleveland Clinic Foundation, Cleveland, OH, ³University Hospitals Case Medical Center, Case Western Reserve University, Cleveland, OH, ⁴Mayo Clinic Arizona, Phoenix, AZ

Disclosures: Raza Hoda: None; Lauren Duckworth: None; John Van Arnam: None; Patrick McIntire: None; Hannah Gilmore: None; Xiaoyan Cui: None; Gloria Zhang: None; J. Jordi Rowe: None; Karen Fritchie: None; Elizabeth Azzato: None; Erinn Downs: None

Background: Solitary fibrous tumor (SFT) is a rare fibroblastic tumor with malignant potential that is underpinned by a recurrent inv12(q13q13)-derived *NAB2-STAT6* fusion. Breast and axilla are exceptionally uncommon locations for this entity, with approximately 50 such cases reported in the literature. A SFT risk stratification model has been developed, and studies suggest *NAB2-STAT6* fusion variants correlate significantly with anatomic site and clinical behavior. However, such studies include limited examples from breast and axilla. Herein we describe clinical, pathologic, and molecular features of SFT in these sites.

Design: Surgical pathology records of 2 large academic centers were electronically searched for 'SFT' and 'hemangiopericytoma' from 1989-2022. Clinical information, pathologic diagnoses, immunohistochemical (IHC) profile, next-generation sequencing (NGS) fusion panel results, treatment, and outcome data, if available, were reviewed. SFTs were classified according to the risk stratification model from Demicco et al.¹

Reference: Demicco EG et al. *Mod Pathol* 2017;30:1433-42.

Results: Clinicopathologic parameters of 5 patients with SFT are shown in Table 1. All patients were women, and median age at time of diagnosis was 57 years (range, 21-74 years). Patients presented with either palpable mass (4 cases) or radiographic abnormalities (1 case). Surgical procedures were excisional biopsies in all cases. Diagnosis of 'SFT' was rendered in 4 cases, and 'malignant SFT' in 2 cases. Using the risk stratification model, 3 cases were scored as 'low risk,' 2 as 'intermediate risk,' and 1 as 'high risk,' the latter case recurred. IHC stains were supportive of SFT, where performed (Figure 1). NGS was attempted in 4 cases; quality was sufficient in 3 cases and confirmed all to harbor the characteristic *NAB2-STAT6* fusion with different variants (Table 1). Clinical follow-up was available for 4 patients (median, 58 months; range, 10-163 months). All patients were surgically managed. Three patients showed no evidence of disease; however, 1 patient developed local recurrence 4 months after initial procedure and underwent extensive resection.

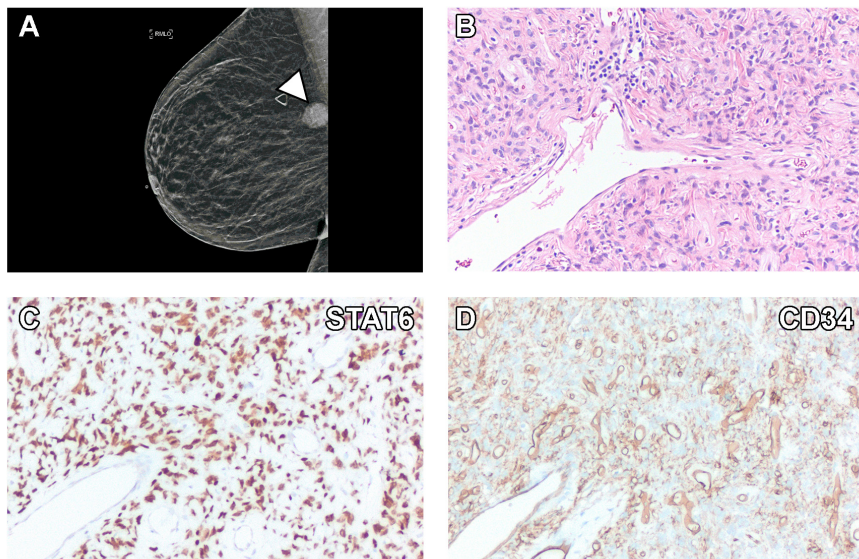
Table 1. Clinical and pathologic profile of 5 cases of solitary fibrous tumor of breast and axilla.

Case No.	Sex	Age at Diagnosis (y)	Site	Laterality	Histologic Diagnosis	Tumor Size (cm)	STAT6 IHC	CD34 IHC	<i>NAB2-STAT6</i> Fusion Variant	Risk score*	Locoregional Treatment	Systemic Treatment	Follow-up, months
1	F	57	Breast	R	SFT	2.4	Positive	Positive	Exon 5-Exon 16	Intermediate	Excision	None	NED, 15
2	F	21	Breast	L	SFT	2.5	Positive	Positive	NA	Low	Excision	None	NA
3	F	61	Breast	R	Malignant SFT	2.8	QNS	QNS	QNS	Intermediate	Excision	None	NED, 163
4	F	49	Axilla	R	SFT	1.9	Positive	Positive	Intron 6-Exon 16	Low	Excision	None	NED, 100
5	F	74	Axilla	R	Malignant SFT	11.0	Positive	Positive	Exon 6-Exon 16	High	Excision	None	Alive with recurrent disease, 10

Abbreviations: F, female; M, male; NA, information not available; NED, no evidence of disease; QNS, quality not sufficient; y, years;

* Risk score is calculated using the risk stratification model as described in Demicco et al. (2017).

Figure 1 - 156



Conclusions: While many breast and axillary SFT cases remain clinically indolent; a subset may develop local recurrence. Applying the current SFT risk model may help identify such cases with aggressive clinical behavior. Further molecular studies are warranted to identify additional predictive markers.

157 Clinicopathological Features and Fluorescent in Situ Hybridization Profile of HER2-Low Breast Carcinoma

Yan Hu¹, Dan Jones², Weiqiang Zhao², Gary Tozbekian¹, Anil Parwani¹, Zaibo Li¹

¹The Ohio State University Wexner Medical Center, Columbus, OH, ²The Ohio State University, Columbus, OH

Disclosures: Yan Hu: None; Dan Jones: None; Weiqiang Zhao: None; Gary Tozbekian: None; Anil Parwani: None; Zaibo Li: None

Background: A new therapeutically relevant category of breast carcinoma, HER2-low, defined by immunohistochemistry (IHC) HER2 score of 1+ or 2+ with no high-level HER2 amplification by fluorescent in situ hybridization (FISH)/chromogenic ISH (i.e., FISH negative) using the 2018 American Society of Clinical Oncology and the College of American Pathologists testing guidelines has shown response to the anti-HER2 drug, trastuzumab deruxtecan (T-DXd). Given that up to 60% of breast carcinomas can be HER2-low, there is a need for rigorous evaluation of this category. These goals can include recategorizing/reevaluating our testing methods and reporting cutoffs in cases with lower HER2 expression. HER2 gene amplification (copy number and/or HER2/CEP17 ratio) has been known to be well-correlated to HER2 protein expression, when HER2 IHC 0 and 3+, and lowest for cases with HER2 IHC 1+ and 2+. Using a large historical series, we characterize HER2-low category and reassess the correlations of HER2 copy number and/or HER2/CEP17 ratio in the breast carcinomas with low HER2 protein expression as a first step in developing reliable criteria for HER2-low scoring criteria.

Design: We have collected IHC and FISH data from 1309 invasive breast carcinoma biopsy cases diagnosed from 2018 to 2021 comprising 465 HER2 0, 844 HER2-low cases. Clinicopathological features (including estrogen receptor (ER) and progesterone receptor (PR) status), the HER2 copy number and HER2/CEP17 ratio were compared between HER2 0 and HER2-low groups.

Results: There were no significant differences in age distribution or tumor subtypes between HER2 0 and HER2-low groups. The HER2 0 group was significantly associated with higher Nottingham grade (grade 3), more ER-negative, PR-negative and triple negative breast carcinomas than the HER2-low group. There were significant increases in the average copy number of the HER2 gene and HER2/CEP17 ratio in HER2-low group when compared to HER2 0 group (Table 1).

Table 1. Comparison of clinicopathological features, HER2 gene copy number and HER2/CEP17 ratio between HER2 0 and HER2-low groups.

	HER2 0		HER2-low		p-value
	#/Average	%/Range	#/Average	%/Range	
Case #	465		844		
Age	60.7	29-94	61.18	26-94	No significance (NS)
Invasive ductal carcinoma, no special type	323	69.5%	596	70.6%	NS
Grade 3	129	27.7%	138	16.4%	0.0002
Triple negative	121	26.0%	97	11.5%	<0.0001
ER-negative	121	26.0%	97	11.5%	<0.0001
PR-negative	159	34.2%	191	22.6%	<0.0001
HER2 copy #	2.71	0.8-5.6	3.05	0.9-5.6	<0.0001
HER2/CEP17 ratio	1.06	0.6-1.4	1.11	0.4-1.9	<0.0001

Conclusions: Breast carcinoma with HER2-low group has fewer triple-negative, ER-negative and PR-negative cases than those with HER2 0 group. There is significantly increased HER2 copy number and HER2/CEP17 ratios in the HER2-low group providing support for reliable discrimination of HER2-Low cases using existing immunohistochemical methods. Large studies correlating pattern of HER2-low expression with response to T-DXd may be useful in further refining scoring criteria.

158 HER2-Low/Estrogen Receptor-Positive Early-Stage Breast Carcinomas: Association with Clinicopathologic Features, Oncotype DX Recurrence Scores and HER2 RNA Expression Scores

Yan Hu¹, Dan Jones², Weiqiang Zhao², Anil Parwani¹, Zaibo Li¹

¹The Ohio State University Wexner Medical Center, Columbus, OH, ²The Ohio State University, Columbus, OH

Disclosures: Yan Hu: None; Dan Jones: Grant or Research Support: AstraZeneca; Weiqiang Zhao: None; Anil Parwani: None; Zaibo Li: None

Background: Recently, the Food and Drug Administration approved fam-trastuzumab deruxtecan-nxki (T-DXd, Enhertu, Daiichi Sankyo, Inc.) for patients with unresectable or metastatic HER2-low breast carcinoma (i.e., immunohistochemical (IHC) HER2 score of 1+ or 2+ with no high-level HER2 amplification by *in situ* hybridization using the 2018 American Society of Clinical Oncology and the College of American Pathologists testing guidelines) who have received prior chemotherapy in the metastatic setting or developed disease recurrence. Given that up to 60% of breast carcinomas can be HER2-low, characterization of this newly proposed HER2-low category becomes very important. The goal of our study is to evaluate the clinicopathological features, Oncotype DX recurrence scores and HER2 RNA expression scores in HER2-low, estrogen receptor-positive (ER+), early-stage breast carcinomas.

Design: A total of 438 ER+ with HER2-negative scores early-stage breast carcinomas with available Oncotype DX results were included. The cases were subdivided into two subgroups: HER2 0/ER+ and HER2-low/ER+. Clinicopathologic features, ER/progesterone receptor (PR) qualitative and semi-quantitative results, Oncotype DX recurrence scores, and HER2 RNA expression scores were compared between the two groups.

Results: HER2-low/ER+ cases showed significantly lower Nottingham grades ($p=0.04$), higher ER+ percentages ($p=0.02$), and more PR-positive cases than HER2 0/ER+ cases ($p=0.04$), with no significant differences in age distribution, histologic type, tumor size, lymph node metastasis or American Joint Committee on Cancer (AJCC) stage. The average Oncotype DX recurrence score was significantly lower in HER2-low/ER+ group than in the HER2 0/ER+ group (17.3 vs 19.6, $p=0.0332$). HER2 RNA expression score was significantly higher in HER2-low/ER+ group than in the HER2 0/ER+ group (9.2 vs 8.6, $p<0.0001$) (Table 1).

Table 1. Clinicopathologic characteristics of HER2 0/ER+ and HER2-low/ER+ early-stage breast carcinomas.

		HER2 0/ER+		HER2-low/ER+		p-value
		#/value	%/Range	#/value	%/Range	
Case #		107		331		
Age		58.6	31-84	57.9	31-84	No significance (NS) NS
Histologic type	Ductal	79	73.8%	252	76.1%	
	Lobular	17	15.9%	51	15.4%	
	Mixed	7	6.5%	16	4.8%	
	Other	4	3.7%	12	3.6%	
Nottingham grade	Overall grade 3	29	27.1%	64	19.3%	0.0473
	Tubule formation 3	82	76.6%	208	62.8%	0.0108
	Nuclear pleomorphism 3	28	26.2%	84	25.4%	NS
	Mitotic rate 3	16	15.0%	44	13.3%	NS
ER		% of stained cells	90.7	2-100	93.4	30-100
PR		Negative case #	11	10.3%	18	5.4%
Lymph node (LN)	+ macrometastasis	21	19.8%	55	17.0%	NS
	+ micrometastasis	6	5.7%	25	7.7%	
	+ isolated tumor cells	4	3.8%	11	3.4%	
AJCC T stage	T1	71	66.4%	232	70.1%	NS
	T2	35	32.7%	93	28.1%	
	T3	1	0.9%	6	1.8%	
Oncotype DX	Recurrence score (RS)	19.6	0-58	17.3	0-61	0.0332
	HER2 RNA expression score	8.6	7.6-9.9	9.2	8-11.8	<0.0001

Conclusions: IHC evaluation in HER2-low/ER+ versus HER2 0/ER+ breast carcinomas correlates with the HER2 RNA expression score by Oncotype DX. Given its association with lower Nottingham grade and lower Oncotype DX recurrence score, HER2-low/ER+ early-stage breast carcinoma could represent a less-aggressive variant.

159 Effect of Activating Cancer-associated Fibroblasts Biomarker TNC on Immune Cell Infiltration and Prognosis in Breast Cancer

Ting Huang¹, Di Zhu¹, Yuanzhi Lu¹

¹Guangzhou, China

Disclosures: Ting Huang: None; Di Zhu: None; Yuanzhi Lu: None

Background: Cancer-associated fibroblasts (CAFs) are critical components of the tumor microenvironment (TME) and definitely involved in tumor initiation, invasion, metastasis, and drug resistance. CAFs usually display a distinctly activated phenotype. It has been reported that CAFs-expressing biomarkers may contribute to remodeling the TME and serve as prognostic factors for predicting clinical outcomes in patients with various solid cancers. However, the predictive value of CAFs-expressing biomarkers such as Tenascin-C (TNC) in breast cancer is incompletely elucidated. This study sought to determine the correlation of CAFs-expressing biomarkers with the immune cell infiltration and survival of patients with breast cancer (BC).

Design: The RNA-sequencing data and survival information for breast cancer patients were downloaded from The Cancer Genome Atlas (TCGA) in R software. The clusterProfiler package was used for GO and KEGG enrichment analysis, the ssGSEA algorithm was used to analyze the correlation between platelet-derived growth factor receptor-alpha (PDGFRA), platelet-derived growth factor receptor-beta (PDGFRB), Tenascin-C (TNC) and immune cells, and the survminer package was used to evaluate the prognostic role of appealing genes. Immunohistochemical (IHC) staining was used to determine expression levels of TNC in 160 breast cancer samples pathologically diagnosed as invasive ductal carcinoma, not otherwise specified (IDC-NOS).

Results: Pathway enrichment displayed that overexpression of CAFs-related genes mainly enriched in focal adhesion and PI3K-AKT signaling pathway. Immune infiltration analysis suggested that high expression of CAFs-related genes was significantly positively correlated with the infiltration of B cell naive, dendritic cell resting, and inversely correlated with macrophages cell infiltration. In addition, high expression of TNC in tumor cells was associated with most adverse clinicopathological features and reduced metastasis-free survival (MFS) (hazard ratio 0.574, 95% confidence interval 0.404-0.815, P=0.035), and independent of ER status, blood vessel invasion and T stage in breast cancer.

Figure 1 - 159

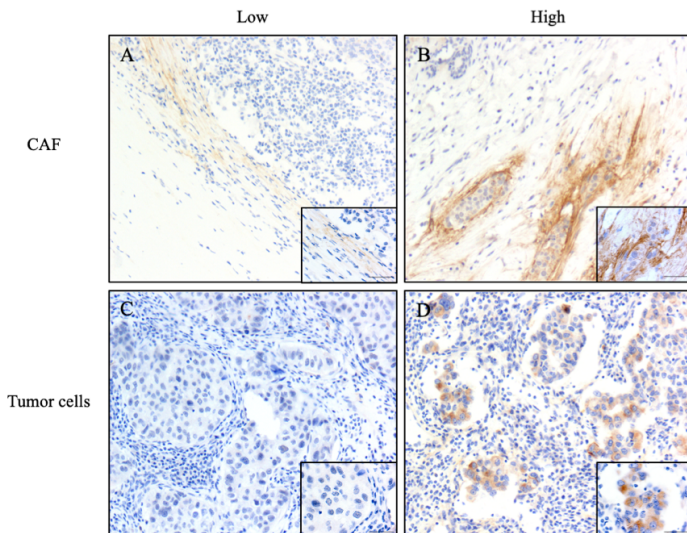
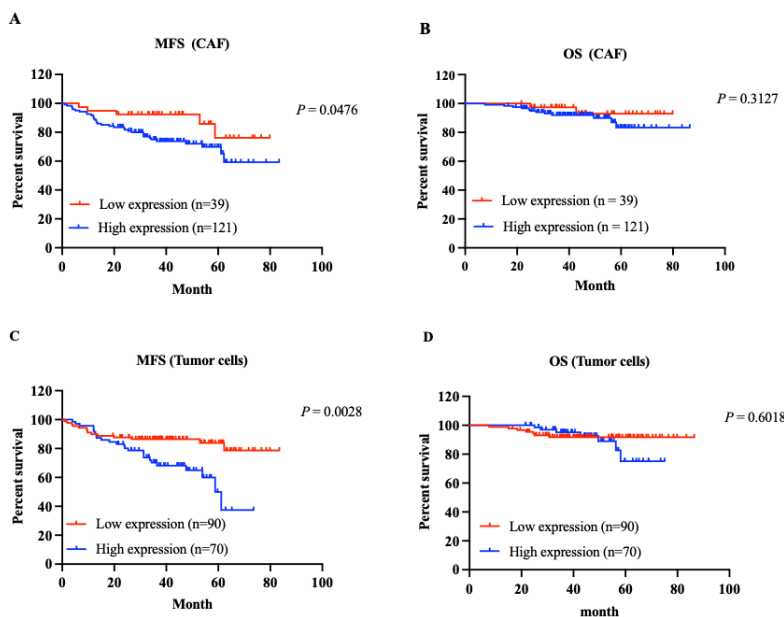


Figure 2 - 159



Conclusions: In this study, we found that CAFs may participate in immunosuppression and regulate tumor cell proliferation and invasion through the focal adhesion and PI3K-AKT pathway. High TNC expression was associated with several adverse clinicopathological features, and high TNC expression in tumor cells was identified as an independent prognostic factor for IDC-NOS.

160 Atypical Apocrine Adenosis Diagnosed on Breast Core Biopsy Shows No Upgrade to Ductal Carcinoma In Situ or Invasive Carcinoma on Excision

Helena Hwang¹, Cecilia Dusek¹, Sunati Sahoo¹, Venetia Sarode¹, Yan Peng¹, Yisheng Fang¹, Barbara Susnik²

¹UT Southwestern Medical Center, Dallas, TX, ²University of Miami Hospital, Miami, FL

Disclosures: Helena Hwang: None; Cecilia Dusek: None; Sunati Sahoo: None; Venetia Sarode: None; Yan Peng: None; Yisheng Fang: None; Barbara Susnik: None

Background: Atypical apocrine adenosis (AAA) in the breast is defined as apocrine cells with cytologic atypia involving sclerosing adenosis or nodular adenosis and is rare. Cytologic atypia in apocrine cells include threefold variation in nuclear size, hyperchromasia, and pleomorphic nucleoli. The diagnosis of AAA may be challenging and should be distinguished from apocrine atypical ductal hyperplasia (ADH) and apocrine ductal carcinoma in situ (DCIS). Atypical apocrine adenosis should lack the

architectural complexity seen in apocrine ADH and DCIS and should not have necrosis. The incidence of AAA on core biopsy is very low with no clear guidelines on the management of these lesions. The purpose of this study was to determine the upgrade rate when AAA is found on breast core biopsy.

Design: After institutional review board approval, the databases of three different hospitals were searched for AAA for a period ranging from 2010-2022. All breast core biopsies with AAA were identified and those with concomitant diagnoses of invasive carcinoma, DCIS, ADH, and non-classic lobular carcinoma in situ (LCIS) were excluded. The excisions of included AAA cases were identified and correlated with the biopsy. In each case, patient age, breast laterality, the lesion being targeted, the method of breast biopsy, history of breast cancer, and follow up were recorded. Cases without follow up for at least one year were excluded.

Results: A total of 19 cases involving 18 patients were identified. Fourteen cases were in the right breast and five cases in the left. The age range was 33-71 years with a median age of 60. The imaging target was as follows: mass=11, architectural distortion=5, calcifications=3. Fifteen of the 19 cases were excised with no upgrade to DCIS or invasive carcinoma on excision. The patients who did not undergo excision had follow up ranging from 2-7 years with no breast cancer subsequently diagnosed.

Conclusions: This study shows no upgrade to DCIS or invasive carcinoma of AAA diagnosed on breast core biopsy. Only a few studies have been performed on this topic and show varying results. While the number of cases in this study is small, with careful radiologic-pathologic correlation performed to ensure that the targeted lesion is adequately sampled, routine excision of atypical apocrine adenosis may not be necessary.

161 Clinical, Histopathological and Molecular Characterization of the Spectrum of Pseudo-lactational Breast Lesions: From benign to *in situ* pseudo-lactational carcinoma, a mysterious milky way

Natacha Joyon¹, Thomas Grinda¹, Sophie Cotteret¹, Alexander Valent, Nadja Alsadoun², Camille Franchet³, Laurent Arnould⁴, Gaetan Macgrogan⁵, Anne Vincent-Salomon⁶, Magali Lacroix-Triki¹

¹Gustave Roussy, Cancer Campus, Grand Paris, Villejuif, France, ²Institut de pathologie multisite des Hospices civils de Lyon, Lyon, France, ³University Cancer Institute - Oncopole, Toulouse, France, ⁴Centre Georges-François Leclerc, Dijon, France, ⁵Institut Bergonié, Lyon, France, ⁶Institut Curie, Paris, France

Disclosures: Natacha Joyon: None; Thomas Grinda: None; Sophie Cotteret: None; Alexander Valent: None; Nadja Alsadoun: None; Camille Franchet: None; Laurent Arnould: None; Gaetan Macgrogan: None; Anne Vincent-Salomon: None; Magali Lacroix-Triki: None

Background: Pseudo-lactational hyperplasia (PLH) is an incidental lesion discovered in biopsies from women who, curiously, are neither pregnant nor lactating. PLH is typically recognizable by its irregular oval acinar structures with pale luminal eosinophilic secretions and lined by hobnail-shaped cells containing vacuolated clear cytoplasms. Although PLH is a benign lesion, some atypical and *in situ* forms have been described suggesting a spectrum. Little is known regarding the histopathological and molecular aspects of PLH. We assembled a multicenter series of PLH cases, encompassing PLH lesions ranging from benign to malignant, and aimed at deciphering their clinical, histopathological and molecular characteristics.

Design: We retrospectively collected cases displaying PLH from seven cancer centers and performed immunohistochemical (IHC) and molecular analysis using SNParray and next generation sequencing (panel of 66 genes).

Results: We included 15 patients displaying PLH diagnosed between 2017 and 2020. All cases were female. The mean age at diagnosis was 46 years. Most lesions were revealed by microcalcifications on mammography (12/15) with a majority of BI-RADS 4 lesions (10/15). We report five cases of PLH, three cases of atypical PLH and seven cases of pseudo-lactational carcinoma *in situ*. Atypical PLH and carcinoma *in situ* showed a complex morphological pattern: cribriform, papillary and micropapillary structures, associated with moderate to high nuclear atypia and with an increased number of mitoses. One case of carcinoma *in situ* showed necrosis. 11 cases were intermingled with cystic hypersecretory lesion. One patient showed a recurrence 1 year later with an invasive carcinoma. All cases expressed hormone receptors. Reactivity for estrogen receptor was diffuse with moderate to strong intensity in 9/16 cases. Only one case had diffuse reactivity for progesterone. One case showed an overexpression of the HER2 protein (3+ staining) but without HER2 amplification by FISH. p53 IHC showed an aberrant phenotype in 7/16 cases: 1 atypical PLH and in 6 carcinoma *in situ*. Molecular analysis confirmed a TP53 mutation in 6 out of these 7 cases. In atypical PLH and in carcinoma *in situ*, SNParray analysis showed recurrent gains of 1q and 8q and losses of 14q (1q+8q+14q-).

Conclusions: We herein describe for the first time the molecular alterations associated with atypical PLH and pseudo-lactational carcinoma *in situ*, characterized by recurrent TP53 mutations and 1q+8q+14q- genomic pattern.

162 Assessment of Reproducibility of HER2 IHC Scoring in a HER2-low Breast Cancer Enriched Cohort among Breast Subspecialized Pathologists

Cansu Karakas¹, Haley Tyburski², Bradley Turner¹, Xi Wang², Linda Schiffhauer², Hani Katerji¹, Elena Liu¹, David Hicks¹, Huina Zhang¹

¹University of Rochester Medical Center, Rochester, NY, ²University of Rochester, Rochester, NY

Disclosures: Cansu Karakas: None; Haley Tyburski: None; Bradley Turner: None; Xi Wang: None; Linda Schiffhauer: None; Hani Katerji: None; Elena Liu: None; David Hicks: None; Huina Zhang: None

Background: With the significant clinical benefits of novel HER2-targeting antibody-drug conjugates in HER2-low breast cancers, accurate and reproducible assessment of lower levels of HER2 expression becomes crucial. We assessed the reproducibility of HER2 IHC scoring among breast specialized pathologists in a HER2-low enriched cohort which were stained by two commonly-used HER2 IHC kits.

Design: 114 breast cancer cases were stained by both HercepTest and PATHWAY 4B5, and scored by six breast subspecialized pathologists independently using 2018 ASCO/CAP HER2 testing guideline. Level of agreement was evaluated by Cohen's Kappa analysis.

Results: The overall inter-observer agreement rates for HercepTest and 4B5 were 74.3% and 64.1%, and average weighted Kappa values were 0.76 and 0.65 respectively, which was statistically significant ($p<0.01$) (Fig. 1). The overall inter-antibody agreement rate between HercepTest and 4B5 was 57.8%, with a weighted Kappa of 0.58 (moderate agreement). Inter-observer concordance with 100% agreement rate were achieved in 44.7% (51) cases by HercepTest and in 45.6% (52) cases by 4B5. Disagreement was highest in IHC 0 cases by both HercepTest (7 cases, 5%) and 4B5 antibody (10 cases, 9%) (Fig. 2). Absolute agreement rates on HercepTest increased from 78.1% for IHC score of 0-1+ cases to 91.9% for cases with IHC score of 2-3+. On 4B5 antibody, it increased from 72.2% for IHC score of 0-1+ to 86.3% for cases with IHC score of 2-3+. Additionally, average absolute agreement on HercepTest showed moderate agreement for cases of 0+-1+ (Kappa value:0.53), substantial agreement for cases of 1+-2+ (Kappa value:0.61) and almost perfect agreement for cases of 2+-3+ (Kappa value:0.84). 4B5 clone also showed a similar trend, with moderate agreement for cases of 0-1+ (Kappa value:0.41) and 1+-2+ (Kappa value:0.38), while almost perfect agreement for cases of 2+-3+ (Kappa value:0.72).

Figure 1 - 162

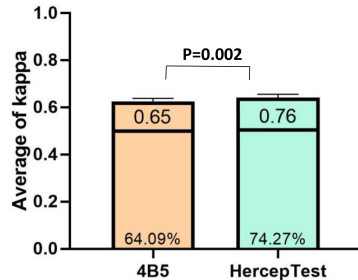
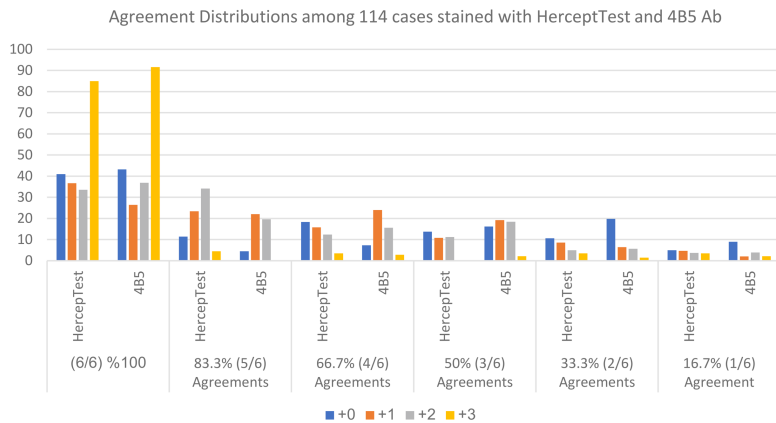


Figure 2 - 162



Conclusions: Our results demonstrated notable inter-observer and inter-antibody variation for evaluating HER2 IHC, especially in cases with scores of 0-1+, although the performance was much more improved among breast specialized pathologists with the awareness of HER2-low concept. More accurate and reproducible methods are urgently needed for selecting patients who may benefit from the newly-approved HER2-targeting agent on HER2-low breast cancers.

163 Dynamic Changes of HER2 Expression in Breast Cancers after Neoadjuvant Chemotherapy with the Inclusion of HER2-low Category

Cansu Karakas¹, Haley Tyburski², Elena Liu¹, David Hicks¹, Huina Zhang¹

¹University of Rochester Medical Center, Rochester, NY, ²University of Rochester, Rochester, NY

Disclosures: Cansu Karakas: None; Haley Tyburski: None; Elena Liu: None; David Hicks: None; Huina Zhang: None

Background: Low-levels of HER2 expression is an emerging promising biomarker for the treatment of advanced breast cancers with novel HER2-targeted agents. In this study, we analyzed the HER2 expression between primary breast cancers and matched resection specimens after neoadjuvant chemotherapy (NAC) as well as the likelihood of pathologic complete response (pCR), disease free survival (DFS) and overall survival (OS) in HER2-zero, HER2-low and HER2-positive subgroups.

Design: 139 breast cancer cases with available pre- and matched post-NAC samples between 2008-2018 at our institution were included. HER2 IHC was performed by HercepTest and was re-evaluated by consensus scoring according to 2018 ASCO/CAP HER2 testing guideline. Tumors were re-classified into HER2-0 (IHC 0+), HER2-low (IHC 1+ or 2+/ISH-negative) and HER2-positive (IHC 3+ or 2+/ISH positive) subgroups.

Results: The pCR rate was significantly higher in HER2-positive (44%) compared with HER2-low (23.1%) and HER2-0 (17.5%) tumors, while there was no significant difference between HER2-0 and HER2-low tumors (By Fisher Exact test, Fig 1). In 99 patients with residual disease (RD) after NAC, the proportion of HER2-low cases were 21.2% (21/99) in pre-NAC biopsies and 18.2% (18/99) in RD samples. The overall rate of HER2 evolution from pre-NAC biopsy to post-NAC excision specimen was 30.9%. Among patients with HER2-0 expression on pre-NAC biopsy, 22.5% (9/40) experienced a conversion to HER2-low, while 40.3% (21/52) of HER2-low tumors showed a conversion in the opposite direction. For HER2-positive group, 28.8% (13/45) of patients converted to either HER2-low (13.3%, 6/45) or HER2-0 (15.5%, 7/45) (Table 1). Exploratory survival analysis based on the baseline HER2 expression did not reveal any significant difference in DFS among three groups. There was no significant difference in OS between HER2-0 and HER2-low groups, while both appeared to have inferior OS compared to HER2-pos group (Fig 2).

Table 1: Incidences of HER2-0, HER2-low and HER2-positive breast cancers pre-and post-NAC treatment

Incidence	Post-NAC					
	HER2-0	HER2-low	HER2-pos	pCR	NA	Total
Pre-NAC						
HER2-0	23	9	0	7	1	40
HER2-low	21	18	0	12	1	52
HER2-pos	7	6	6	20	6	45
NA	1	0	0	1	0	2
Total	53	32	6	40	8	139

NAC Neoadjuvant chemotherapy; N/A Not available; pCR Pathologic complete response

Figure 1 - 163

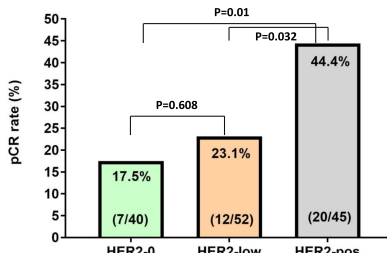
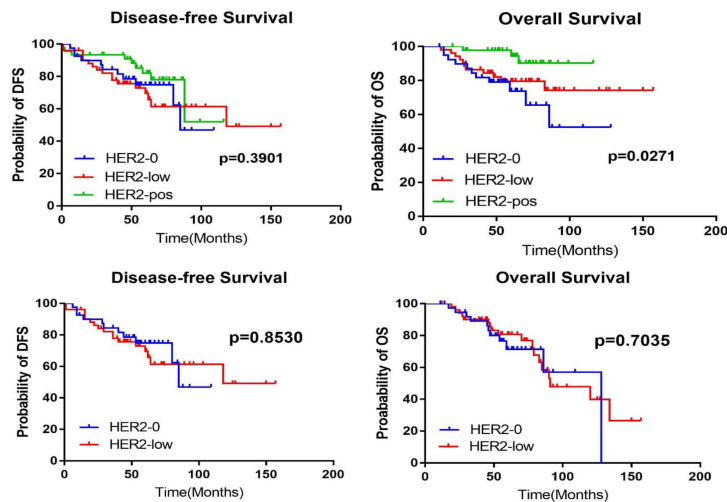


Figure 2 - 163



Conclusions: Our results with HER2 consensus re-review demonstrated a high dynamic change of HER2 expression after NAC in breast cancers, mostly driven by cases switching from and to HER2-low. The findings of this study may suggest re-testing HER2 expression in patients with residual disease after NAC might help enhancing the access to potentially effective drugs in patients at high-risk of relapse, especially in the era of rapid development of HER2-targeted agents in HER2-low expressing breast cancers.

164 The Histologic and Genomic Features of Breast Cancers Harboring Genetic Alterations in RecQ DNA Helicases

Gagandeep Kaur¹, Pier Selenica¹, Andrea Gazzo¹, Lorraine Colon Cartagena¹, Fayed Daaboul¹, Higinio Dopeso¹, Edaise M. da Silva¹, Dara Ross¹, Hong (Amy) Zhang¹, Hannah Wen¹, Sarat Chandarlapaty¹, Mark Robson¹, Diana Mandelker¹, Simon Powell¹, Larry Norton¹, Edi Brogi¹, Jorge Reis-Filho¹, Fresia Pareja¹

¹Memorial Sloan Kettering Cancer Center, New York, NY

Disclosures: Gagandeep Kaur: None; Pier Selenica: None; Andrea Gazzo: None; Lorraine Colon Cartagena: None; Fayed Daaboul: None; Higinio Dopeso: None; Edaise M. da Silva: None; Dara Ross: None; Hong (Amy) Zhang: None; Hannah Wen: None; Sarat Chandarlapaty: None; Mark Robson: None; Diana Mandelker: None; Simon Powell: None; Larry Norton: None; Edi Brogi: None; Jorge Reis-Filho: None; Fresia Pareja: None

Background: RecQ DNA helicases play key roles in maintenance of genomic stability and homologous recombination (HR) DNA repair. Alterations in these genes are associated with cancer predisposition syndromes, such as Bloom (*BLM*) and RAPADILINO (*RECQL4*) syndromes. Their role in breast cancer (BC) development is poorly understood. We sought to characterize the histologic and genomic features of BCs with pathogenic alterations in these genes.

Design: We identified BCs harboring germline or somatic pathogenic genetic alterations in *BLM*, *RECQL* and *RECQL4* among 8,571 BCs previously subjected to targeted sequencing. A histologic review was conducted following the WHO criteria; tumor infiltrating lymphocytes (TILs) were assessed according to the International TILs working group. Estrogen receptor (ER)/HER2 status was retrieved from medical records. Mutational signatures were inferred using synonymous and non-synonymous mutations using SigMA in cases with ≥ 5 SNVs.

Results: The study cases include 69 BCs, including 34 primary (pBC) and 35 metastatic (mBC) BCs with germline (n=32) or somatic (n=37) alterations in *RECQL4* (n=36), *BLM* (n=22) or *RECQL* (n=11). *RECQL4/BLM/RECQL* were affected by loss-of-function mutations (n=54) or rearrangements (n=15) and were altered in a mutually exclusive manner. Bi-allelic inactivation as loss-of-heterozygosity of the wild-type allele (LOH) was seen in 21% of pBCs and 17% of mBCs. Most of the 34 *RECQL4/BLM/RECQL*-altered pBCs were invasive ductal carcinomas of no special type (IDC-NST, 82%), of histologic grade 3 (62%) and ER+/HER2- (47%) or ER-/HER2- (38%). Most of the 35 mBCs were IDC-NSTs (89%), poorly differentiated (83%) and ER+/HER2- (60%). Median TIL infiltration was 10% for pBCs and mBCs. No differences in TIL extent were seen between BCs with mono- vs bi-allelic alterations ($P>0.05$). Most pBCs (79%) and mBCs (68%) lacked a dominant HR deficiency (HRD) mutational signature; instead, a dominant APOBEC signature was detected in 67% of pBCs and 75% of mBCs with bi-allelic *RECQL4/BLM/RECQL* alterations.

Conclusions: BCs harboring pathogenic alterations in RecQ helicases are enriched for ER+/HER2- high-grade tumors and display low TIL levels. In contrast to BRCA1/2 BCs, most RecQ helicases-altered BCs lack a dominant HRD mutational signature. Genomic features of these tumors might deviate from those of BCs with inactivation of canonical HRD genes, or the back-up DNA repair mechanisms elicited by loss of *RECQL4/BLM/RECQL* may differ from those triggered by loss of *BRCA1/2*.

165 Breast Biomarkers Evolution from Primary to Recurrent Breast Cancer Based on the Newly Recognized Clinical Subtypes

Maha Khedr¹, Mohamed Desouki¹, Thaer Khoury¹

¹Roswell Park Comprehensive Cancer Center, Buffalo, NY

Disclosures: Maha Khedr: None; Mohamed Desouki: None; Thaer Khoury: None

Background: Treatment decisions in primary breast cancer patients and/or disease recurrence are based on hormone receptors (HR) and HER2 status. The emerging new medications, mandates to categorize those patients to guarantee the appropriate treatment delivery. The aim of our study is to evaluate the HR and HER2 evolution among primary BC and recurrence including the distant metastasis.

Design: We retrieved ER, PR and HER2 results from the pathology reports in our database for BC patients with disease recurrence (local or distant metastasis). HER2 status was reported based on the American Society of Clinical Oncology/College of American Pathologists. We excluded contralateral BC without other sites of recurrence and solitary bone metastasis. The ER and PR data were pooled together as HR as follows, HR positive is designated when either ER or PR were positive and HR negative when ER and PR were both negative. The HER2 was subclassified into HER2-negative [0+ by immunohistochemistry (IHC)], HER2-low [(IHC1+ or 2+ with negative in situ hybridization (ISH)], and HER2-positive [(IHC3+ or 2+ with positive ISH)]. The final categories for the HR/HER2 groups were as follows: HR-positive/HER2-0, HR-positive/HER2-low, HR-negative/HER2-0, HR-negative/HER2-1 and HR positive or negative/HER2-positive. We studied the rate of discordance in the above categories between primary BC and the disease recurrence including distant metastasis.

Results: A total of 287-patients who underwent tissue confirmation of locoregional recurrence or distant metastasis were included. The time range from original diagnosis to disease recurrence was 4.4 years. Primary BC was positive for HR in 215 (75%) cases. The rate of switching was 14% from HR-positive to HR-negative, and 7% from HR-negative to HR-positive. The distribution according to the primary tumor phenotypes and the recurrent tumor including local recurrence and distant metastasis combined is presented in Table 1. The overall discordance among the different categories was 34%. The highest rate of discordance was observed in the HR-negative/HER2-negative switching to HR-negative/HER2-low (64%).

Table 1: Distribution of HR and HER2 status among primary breast cancer and recurrence including local and distant metastasis

Primary Breast cancer	Combined locoregional recurrence and distant metastasis					
	HR+/HER2 negative	HR+/HER2 low	HR-/HER2 negative	HR-/HER2 low	HR/HER2 +	Total
HR+/HER2 negative	5 (19%)	12 (44%)	2 (7.4%)	6 (22.2%)	2 (7.4%)	27(9%)
HR+/HER2 low	15 (9.1%)	118 (72%)	4 (2.4%)	12 (7.3%)	15(9.2%)	164(57%)
HR-/HER2 negative	0 (0%)	1 (9%)	3 (27%)	7 (64%)	0 (0%)	11(4%)
HR-/HER2 low	0 (0%)	3 (6%)	6 (13%)	39 (81%)	0 (0%)	48(17%)
HR/HER2 +	1 (2.7%)	9 (24.3%)	1 (2.7%)	1 (2.7%)	25(67.6%)	37(13%)
Total	21 (7%)	143 (50%)	16 (5%)	65(23%)	42 (15%)	287(100%)

Concordant cases are in bold font.

Conclusions: The evolution in breast biomarker results between the primary tumor and the recurrence is not uncommon. We present the rate of switching based on five clinical and molecular groups instead of the traditionally known three groups to highlight the rate of change in the treatment plan in each category.

166 HER2 Evolution from Primary to Recurrent Breast Cancer: The Importance of Sampling the Recurrent Tumor

Maha Khedr¹, Mohamed Desouki¹, Thaer Khoury¹

¹Roswell Park Comprehensive Cancer Center, Buffalo, NY

Disclosures: Maha Khedr: None; Mohamed Desouki: None; Thaer Khoury: Consultant: AstraZeneca; AstraZeneca

Background: The eligibility criteria for metastatic breast carcinoma (BC) patients to receive Trastuzumab Deruxtecan is for the tumor to be HER2-low. The clinical trial accepted the results of any sample to be eligible, regardless of the origin, previous primary tumor or current metastatic carcinoma. The aim of this study is to evaluate the HER2 evolution from primary BC to locoregional recurrence or distant metastasis.

Design: Our database was searched for BC patients with recurrence (local or distant metastasis) with available HER2 results scored based on the American Society of Clinical Oncology/College of American Pathologists. We excluded cases with contralateral BC without other sites of recurrence and solitary bone metastasis. HER2 status was abstracted from the pathology reports and sub-classified into 3 categories: HER2-negative [0+ by immunohistochemistry (IHC)], HER2-low [(IHC1+ or 2+ with negative in situ hybridization (ISH)], and HER2-positive [(IHC3+ or 2+ with positive ISH)]. We compared all cases with the three staining categories. We focused on the HER2-negative versus HER2-low between primary BC, locoregional recurrence and distant metastasis, as combined and separate groups. The rate of discordance was compared in terms of the site of the metastasis.

Results: A total of 287-patients who had tissue confirmation of locoregional recurrence or distant metastasis were included. HER2 distribution and evolution in the primary tumor and locoregional recurrence or distant metastasis are shown in Table 1. Overall HER2 discordance between primary BC and locoregional recurrence or distant metastasis was 28% (24% locoregional and 30% distant metastasis), mostly driven from switching HER2-negative to HER2-low in 26/38 (68.4%) (39% locoregional and 91% metastasis). The rates of HER2 switching from HER2-low or positive to HER2-negative were 25/212 (12%) and 2/37 (5%), respectively. Among the discordant metastatic cases (n=41) for HER2-negative/HER2-low, 12%, 32%, 22%, 12%, 7% and 15% were in brain, liver, lung, pleural fluid, lymph nodes and others, respectively. Among each organ site, the discordance rate was 38%, 29%, 56%, 25%, 40% and 32%, respectively.

Table 1: HER2 distribution and evolution from primary BC to locoregional recurrence or distant metastasis

Primary breast cancer	Combined locoregional recurrence and distant metastasis			
	Negative, n (%)	Low, n (%)	Positive, n (%)	Total
Negative, n (%)	10 (26.2%)	26 (68.4%)	2 (5.3%)	38 (13%)
Low, n (%)	25 (12%)	172 (81%)	15 (7%)	212 (74%)
Positive, n (%)	2 (5%)	10 (27%)	25 (68%)	37 (13%)
Total	37 (13%)	208 (72%)	42 (15%)	287 (100%)

Concordant cases are in bold font

Conclusions: Management based on a previous sample result may deny eligible patients and at the same time may have no benefit to others, as a good proportion of the cases convert from HER2-negative to HER2-low or from HER2-low to HER2-negative, respectively. Therefore, we recommend sampling the recurrent tumor when possible and testing for HER2

167 Clinicopathologic Evaluation of Triple Negative Breast Cancer Treated with Neoadjuvant Immune- and Chemo- Therapy: Attempt to De-Escalate Treatment

Thaer Khoury¹, Gary Tozbikian², Oluwole Fadare³, Yisheng Fang⁴, Samira Syed⁴, Kristopher Attwood¹, Shipra Gandhi¹

¹Roswell Park Comprehensive Cancer Center, Buffalo, NY, ²The Ohio State University Wexner Medical Center, Columbus, OH, ³UC San Diego School of Medicine, La Jolla, CA, ⁴UT Southwestern Medical Center, Dallas, TX

Disclosures: Thaer Khoury: Consultant: AstraZeneca; AstraZeneca; Gary Tozbikian: Advisory Board Member: AstraZeneca; Daiichi-Sankyo; Eli Lilly; Speaker: Roche; Oluwole Fadare: None; Yisheng Fang: Consultant: Integro Theranostics/KINGDOM CAPITAL; Samira Syed: None; Kristopher Attwood: None; Shipra Gandhi: Advisory Board Member: AstraZeneca

Background: Immunotherapy (IT) with checkpoint inhibition along with chemotherapy (CT) were accepted to treat patients with triple negative breast cancer (TNBC) in the neoadjuvant (NA) setting (KEYNOTE-522). Pembrolizumab is associated with several immune related toxicities. With NACT alone, around 40% patients achieve pathologic complete response (pCR). Therefore, there is a serious concern that we are potentially overtreating many of our patients in this setting, who can be cured just with CT alone. We aim to, 1. compare the response rate between two cohorts (CT+IT vs. CT alone), and 2, define clinicopathologic variables to specify certain patients who may benefit from adding IT.

Design: The database of four collaborating institutions is searched for patients treated with CT and IT (n=54) based on KEYNOTE-522 in the NA setting. The following variables were recorded, patient's age and race, clinical AJCC (c-AJCC) stage, CT regimen/number of cycles, and IT regimen/number of cycles. Then, the cases were matched 1:1 with patients treated with CT alone, including the following variables, age range (10-years), CT regimen, c-AJCC stage, and histologic type (no special type, metaplastic). For all cases, the proceeding core needle biopsy (CNB) to the surgical resection was reviewed, and histologic type, degree of necrosis and the percentage of tumor infiltrating lymphocytes (TILs) were recorded. The resected tumor was reviewed, and the following variables were recorded, residual cancer burden class (RCB) [0-pathologic complete response (pCR), I, II, and III], the RCB score, and pathology AJCC (p-AJCC) stage.

Results: pCR was achieved in 26 (48.1%) patients treated with CT + IT vs. 16 (29.6%) treated with CT alone ($p=.075$) (Table). In CT alone group, pCR correlated with TILs with mean/standard deviation (SD) 40.3%/24% in pCR group vs. 24.1%/17.4% in non-pCR group ($p=0.017$). In CT + IT group, pCR correlated with TILs with mean/SD 39.2%/22.4% in pCR group vs. 19.6%/22.8% in

non-pCR group ($p < .001$). For c-stage III cases, 6 of 28 (21.4%) patients had pCR when treated with CT alone vs. 11 of 23 (47.8%) when treated with CT/IT ($p=0.07$). Two of 5 metaplastic carcinoma had pCR in CT + IT group.

Distribution of cases based on the various types of measuring the response to CT + IT vs. CT alone					
		CT/IT	CT alone	Overall	P value
RCB Class	0	54 (50)	54 (50)	108 (100)	
	1	26 (48.1)	16 (29.6)	42 (38.9)	0.058
	2	6 (11.1)	7 (13.0)	13 (12)	
	3	17 (31.5)	16 (29.6)	33 (30.6)	
RCB Score	Median (range)	5 (9.3)	15 (27.8)	20 (18.5)	
	0	2.1 (0,6.0)	1.3 (0,6.0)	0.005	
	I	26 (48.1)	16 (29.6)	42 (38.9)	
	II	12 (22.2)	7 (13.0)	19 (17.6)	
Path AJCC	III	12 (22.2)	13 (24.1)	25 (23.1)	
	IV	4 (7.4)	18 (33.3)	22 (20.4)	
	non-pCR	28 (51.9)	38 (70.4)	66 (61.1)	0.075
	pCR	26 (48.1)	16 (29.6)	42 (38.9)	

Conclusions: These results show potential variables that can be used to direct therapy with CT + IT vs. CT alone; that is to offer the maximum benefit to the patient with the least side effects. Larger number of cases is warranted to evaluate these findings.

168 The Role of Axillary Lymph Node Residual Cancer Burden in the Survival of Triple Negative Breast Cancer Patients Treated with Neoadjuvant Chemotherapy

Thaer Khoury¹, Kristopher Attwood¹, Shipra Gandhi¹

¹Roswell Park Comprehensive Cancer Center, Buffalo, NY

Disclosures: Thaer Khoury: None; Kristopher Attwood: None; Shipra Gandhi: None

Background: In breast cancer (BC) treated with neoadjuvant chemotherapy (NAT), measuring the size of the metastatic carcinoma to the axillary lymph node (ALN) with therapy-related changes could be challenging. The aim of the study is to investigate whether the residual cancer burden in the largest ALN (RCB_{met}) correlates with the clinical outcomes; therefore, have the potential to improve existing RCB calculator.

Design: We conducted pathologic review of 85 patients who had triple negative BC (TNBC) and had residual disease, diagnosed between 2002 and 2016. RCB of the primary tumor (RCB_{prim}) is calculated as follows: $\sqrt{d_{1prim} d_{2prim}} \times f_{prim}$, where d_{1prim} and d_{2prim} are the two dimensions of the primary tumor bed, and f_{prim} is the tumor/tumor bed ratio. Then, RCB class and score were calculated utilizing published formula. The two dimensions of the largest involved ALN were combined as follows: $\sqrt{d_1 d_2}$. We estimated the largest involved LN tumor/tumor bed ratio (f_{met}). RCB_{met} was calculated as follows: $\sqrt{d_1 d_2} \times f_{met}$. Pathology-stage (p-stage) and clinical-stage (c-stage) were recoded following AJCC staging system. Clinicopathologic variables were correlated with the recurrence free survival (RFS) and overall survival (OS). Multivariate analysis with hazard ratio (HR) and 95% confidence interval (95% CI) were calculated.

Results: p-stage-I was identified in 28 (32.9%) cases, II in 21 (24.7%), and III in 36 (42.4%). 20 (23.5%) patients died from disease after 5-years, and 23 (27.1%) after 10. In the univariate analysis, the following variables were statistically significantly correlated with RFS and OS including, RCB score (but not class), RCB_{prim} , p-stage, c-stage, lymphovascular invasion (LVI) (extent and location), and RCB_{met} . In the multivariate analysis including p-stage and RCB_{met} , RCB_{met} correlated with OS [HR and 95% CI 1.71 (1.25, 2.34) per standard deviation increment (SD inc) ($p=.0008$)], while p-stage did not. RCB_{met} correlated with RFS [HR and 95% CI 1.79 (1.31, 2.43) per SD inc ($p=0.0002$)]. p-stage correlated with RFS with HR and 95% CI of 1.23 (0.14, 10.53) for p-stage II vs. I, and 4.16 (0.55, 31.64) for p-stage III vs. I ($p=.033$). When RCB_{met} and RCB score were included, only RCB_{met} correlated with both RFS and OS with HR and 95% CI of 1.96 (1.47, 2.6) per SD inc ($p<.0001$) and 2.02 (1.50, 2.70) per SD inc ($p<.0001$), respectively.

Conclusions: RCB_{met} could improve the predictability power of the existing formula that calculates the RCB index for TNBC treated with NAT

169 High PPFIA1 Expression Could Promote Cancer Survival by Suppressing CD8+ T cells in Breast Cancer: drug discovery and machine learning approach

Dong-Hoon Kim¹, Kyueng-Whan Min², Jinah Chu³, Byoung Kwan Son⁴

¹Kangbuk Samsung Hospital, Sungkyunkwan University School of Medicine, Seoul, South Korea, ²Hanyang University Guri Hospital, Hanyang University College of Medicine, ³Kangbuk Samsung Hospital, Sungkyunkwan University School of Medicine, South Korea, ⁴Eulji General Hospital, Eulji University School of Medicine

Disclosures: Dong-Hoon Kim: None; Kyueng-Whan Min: None; Jinah Chu: None; Byoung Kwan Son: None

Background: PTPRF Interacting Protein Alpha 1 (PPFIA1) plays an important role as a regulator of cell motility and tumor cell invasion and is frequently amplified in breast cancer. The aim of this study was to investigate the clinicopathologic features, survival, anticancer immunities and specific gene sets related to high PPFIA1 expression in patients with breast cancer. We verified the importance of PPFIA1 and survival rate using machine learning, and suggested drugs that can effectively reduce breast cancer cells with high PPFIA1 expression. PTPRF Interacting Protein Alpha 1 (PPFIA1) plays an important role as a regulator of cell motility and tumor cell invasion and is frequently amplified in breast cancer. The aim of this study was to investigate the clinicopathologic features, survival, anticancer immunities and specific gene sets related to high PPFIA1 expression in patients with breast cancer. We verified the importance of PPFIA1 and survival rate using machine learning, and suggested drugs that can effectively reduce breast cancer cells with high PPFIA1 expression.

Design: This study analyzed clinicopathologic factors, survival rates, immune profiles and gene sets according to PPFIA1 expression in 3,457 patients with breast cancer from the Kangbuk Samsung Medical Center cohort (456 cases), the Molecular Taxonomy of Breast Cancer International Consortium (1,904 cases) and The Cancer Genome Atlas (1,097 cases). We applied gene set enrichment analysis (GSEA), in silico cytometry, pathway network analyses, in vitro drug screening, and gradient boosting machines (GBM).

Results: High PPFIA1 expression in breast cancer was associated with worse prognosis with reduced tumor-infiltrating lymphocytes, especially CD8+ T cells, and increased PD-L1 expression. In pathway network analysis, PPFIA1 was linked directly to the tyrosine-protein phosphatase pathway and indirectly to immune pathways. The importance of PPFIA1 associated with survival rate in GBM was higher than that of perineural and lymphovascular invasion. In vitro drug screening, erlotinib effectively suppressed the proliferation of breast cancer cell lines.

Table. Disease-free and disease-specific survival analyses according to PPFIA1 expression from KBSMC cohort

Disease-free survival	Univariate ¹	Multivariate ²	HR	95% CI
PPFIA1 (low vs. high)	<0.001	<0.001	2.378	1.509 3.746
T stage (1, 2 vs. 3)	<0.001	0.004	2.675	1.359 5.265
N classification (0, 1, 2 vs. 3)	<0.001	<0.001	3.868	2.182 6.854
Histological grade (1 vs. 2, 3)	0.001	0.112	1.993	0.851 4.667
Lymphovascular invasion (absence vs. presence)	<0.001	0.064	1.568	0.975 2.524
Perineural invasion (absence vs. presence)	<0.001	<0.001	2.541	1.625 3.972
HER2 (negative vs. positive)	0.001	0.174	1.380	0.867 2.195
Disease-specific survival	Univariate ¹	Multivariate ²	HR	95% CI
PPFIA1 (low vs. high)	<0.001	0.028	1.758	1.062 2.909
T classification (1, 2 vs. 3)	<0.001	0.015	2.458	1.187 5.089
N classification (0, 1, 2 vs. 3)	<0.001	<0.001	3.750	2.035 6.908
Histological grade (1 vs. 2, 3)	<0.001	0.034	3.553	1.101 11.473
Lymphovascular invasion (absence vs. presence)	<0.001	0.418	1.233	0.742 2.050
Perineural invasion (absence vs. presence)	<0.001	<0.001	2.547	1.568 4.139
HER2 (negative vs. positive)	0.015	0.02	1.804	1.096 2.971

HER2, human epidermal growth factor receptor 2

¹Log rank test

²Cox proportional hazard model

p < 0.05 is shown in bold.

Figure 1 - 169

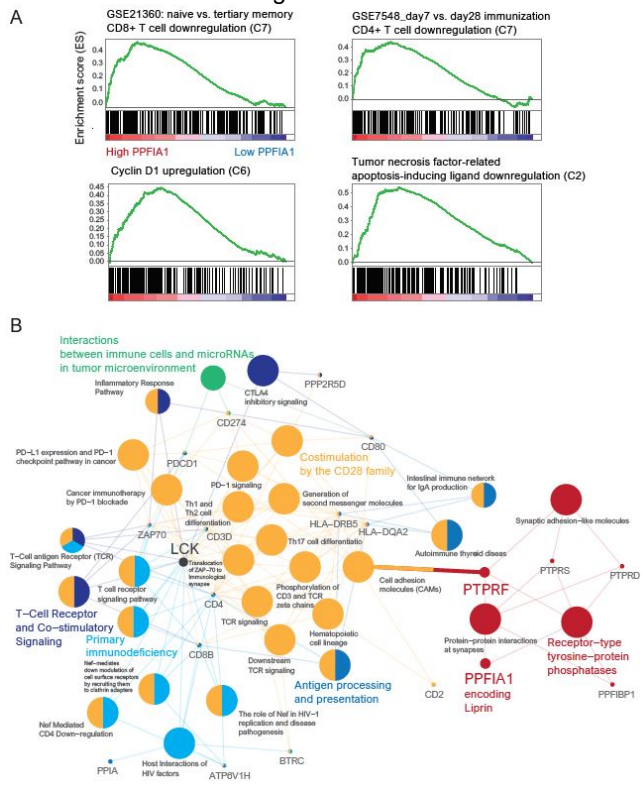


Figure 2 - 169

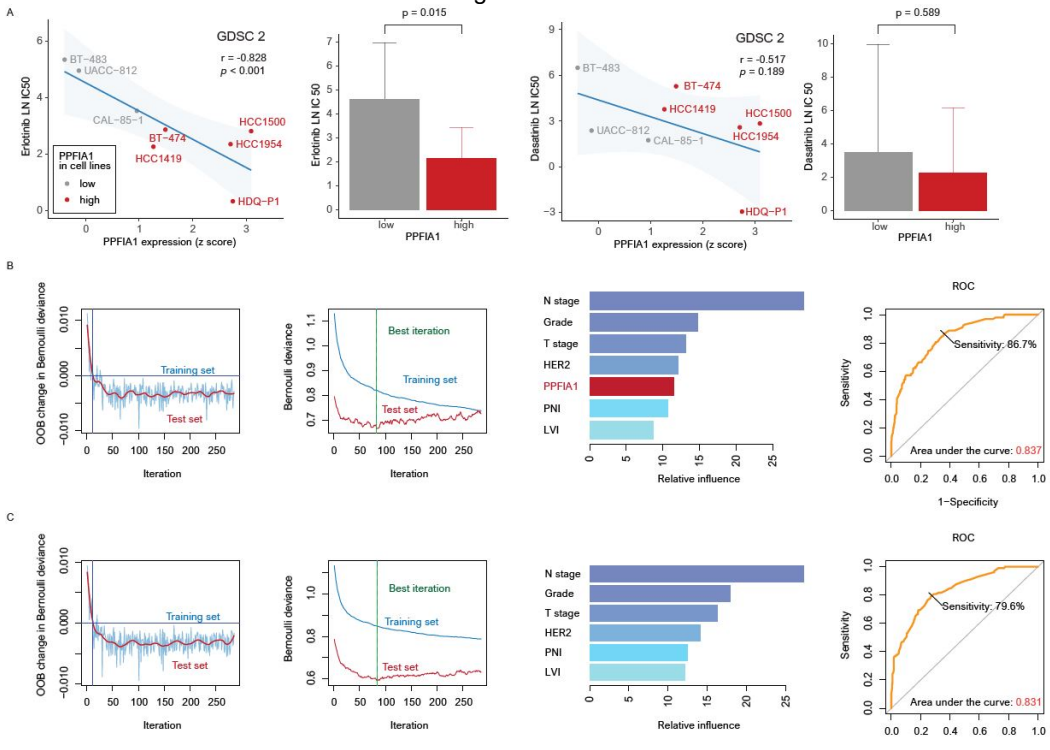


Figure 5

Conclusions: High PPFIA1 in patients with breast cancer is related to poor prognosis and decreased anticancer immune response, and erlotinib may enhance the therapeutic effect.

170 Utility of Pan-TRK Immunohistochemistry in Triple Negative Breast Cancers

Aisha Kousar¹, Samaneh Motanagh², Li Chen², Gloria Carter², Beth Clark², Jeffrey Fine³, Lakshmi Harinath², Tatiana Villatoro⁴, Jing Yu², Rohit Bhargava²

¹Magee-Womens Hospital, University of Pittsburgh Medical Center, Pittsburgh, PA, ²UPMC Magee-Womens Hospital, Pittsburgh, PA, ³University of Pittsburgh, Pittsburgh, PA, ⁴University of Pittsburgh Medical Center, Pittsburgh, PA

Disclosures: Aisha Kousar: None; Samaneh Motanagh: None; Li Chen: None; Gloria Carter: None; Beth Clark: None; Jeffrey Fine: None; Lakshmi Harinath: None; Tatiana Villatoro: None; Jing Yu: None; Rohit Bhargava: None

Background: Somatic chromosomal rearrangements involving *NTRK* genes often results in oncogenic fusion protein that can be detected via Pan-TRK immunohistochemistry. Pan-TRK IHC has been reported to be a sensitive and specific test for confirming the diagnosis of secretory breast carcinoma; however, the number of breast cancers analyzed to date have been limited. The aim of our study was not to identify secretory carcinomas but rather survey a large cohort of well characterized triple negative breast cancers (TNBCs) for high Pan-TRK expression which may then be amenable to targeted therapy.

Design: Five tissue microarrays containing 245 untreated TNBCs (not subjected to neoadjuvant chemotherapy) represented in triplicate were evaluated with Pan-TRK IHC (clone EPR17341, Ventana). Staining in any cellular compartment and with an H-score of 1 was considered a positive result. H-score of 1-100 was considered low, 101-200 intermediate, and 201-300 as high expression. Semi-quantitative expression was correlated with tumor morphology. Recurrence-free survival (RFS) and breast cancer-specific survival (BCSS) were evaluated with respect to Pan-TRK results.

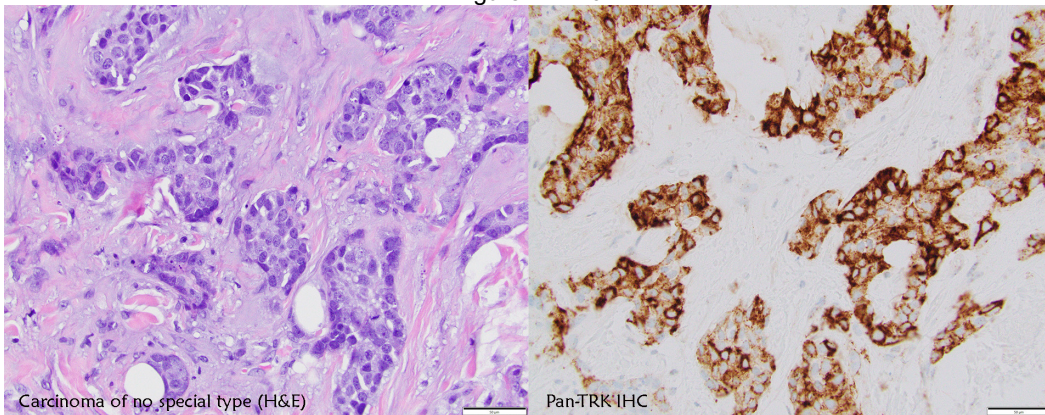
Results: Pan-TRK expression was seen in 47% cases (table 1). None of the cases showed nuclear expression, which is expected in secretory carcinomas with *ETV6-NTRK3* fusions. Low expression is common in TNBC but likely does not correlate with *NTRK* gene fusion (as per prior studies). Intermediate to high expression was seen in 9 cases (4%, figure 1). These latter cases may have *NTRK* gene fusions with partner gene other than *ETV6*. None of these cases had morphology of secretory carcinoma. There was no difference in RFS (log rank test p-value 0.973) or BCSS (p-value 0.215) with respect to Pan-TRK results.

Table 1: Tumor morphology and Pan-TRK expression

Morphology	Negative	Low	Intermediate	High	Total
Adenoidcystic			2		2
AFNST	17	6			23
Apocrine (ductal)	7	1			8
Apocrine (lobular)	4	1			5
Apocrine (mixed)	1				1
Atypical MGA-like	1				1
Fibromatosis-like		1			1
Histiocytoid (lobular)	2	1			3
Lobular-pleomorphic		1			1
Low grade adenosquamous	1	2			3
Matrix producing+NST		4			4
Metaplastic matrix producing	1	5			6
Metaplastic spindle cell	1	2			3
Micropapillary+NST		1			1
Mixed ductal & lobular	5	2			7
Carcinoma of NST	87	71	6	1	165
Osteoclast-like giant cells		1			1
Solid basaloid growth (NST)		2			2
Spindle+AFNST		1			1
Squamous+AFNST	1				1
Squamous+NST	2	2			4
Squamous cell	1	1			2
Total (%)	131 (53.4%)	105 (42.8%)	8 (3.2%)	1 (0.4%)	245

NST: no special type; AFNST: no special type with apocrine features; MGA: microglandular adenosis

Figure 1 - 170



Conclusions: While low expression with Pan-TRK is common in TNBC, intermediate to high expression is rare (<5%). Carcinomas with no special type morphology and intermediate to high Pan-TRK expression should be tested for fusion transcript for potential therapeutic value.

171 Comprehensive Immunohistochemical Analysis of Metaplastic Breast Carcinoma Subtypes

Gregor Krings¹, Gregory Bean², Christopher Schwartz¹, Eliah Shamir¹, Guofeng (George) Gao³, Megan Troxell⁴, Yunn-Yi Chen¹

¹University of California, San Francisco, San Francisco, CA, ²Stanford Medicine/Stanford University, Stanford, CA, ³Stanford University School of Medicine, Stanford, CA, ⁴Stanford University Medical Center, Stanford, CA

Disclosures: Gregor Krings: None; Gregory Bean: None; Christopher Schwartz: None; Eliah Shamir: None; Guofeng (George) Gao: None; Megan Troxell: None; Yunn-Yi Chen: None

Background: Metaplastic breast carcinomas (MBC) are aggressive tumors with molecular features that broadly align with cell lineage. Many markers have been studied by immunohistochemistry (IHC), especially to differentiate MBC from phyllodes tumor or sarcoma. Whether expression varies among MBC subtypes has not been evaluated in detail, but may be useful diagnostically and elucidate oncogenic drivers. We evaluated IHC markers across MBC subtypes and correlated expression patterns with genetics.

Design: 55 MBC were studied: 12 chondroid matrix-producing (CMC), 11 spindle cell (SPC), 8 squamous cell (SQC), 9 mixed spindle/squamous (MSSC), 15 mixed with chondroid +/- osseous differentiation (diff) (MCOD). IHC was performed for TRPS1, SOX10, P63, GATA3, P53, RB, P16, beta-catenin (BCAT) and SATB2. MBC were scored by percent positive tumor cells (focal [F] 1-9%, patchy [P] 10-49%, diffuse [D] >49%) and H-score (HS). Next generation DNA sequencing (NGS) was performed using an assay targeting exons of 480 cancer genes.

Results: TRPS1 was positive in 57% MBC (n=35), including 100% MCOD and 89% CMC compared to only 20% SQC, 17% SPC and 17% MSSC ($p<.001$). MCOD (100%) and CMC (67%) were often TRPS1 P or D, in contrast to SQC (20%), SPC (0%) or MSSC (0%) ($p<.05$ each). SOX10 was positive (and P or D) in 100% CMC but only 13% MSSC and 0% SQC or SPC ($p<.001$). P63 was positive in 94% MBC (n=49) and was D in 57% SQC and 40% SPC vs 0% CMC or MCOD. P63 mean HS was higher in SQC and SPC than CMC and MCOD ($p<.05$ each). GATA3 was more often P or D in SQC (67%) than SPC (0%), CMC (9%) or MCOD (8%) ($p<.05$ each), and mean HS was higher in SQC and MSSC than other subtypes ($p=.002$). BCAT was nuclear (n) in 47% MBC (n=38) but was F in most (89%). MCOD (90%) more often had nBCAT than CMC (33%, $p=.02$) or SPC/SQC/MSSC (32%, $p=.005$). SATB2 staining in >70% cells was restricted to MBC with osseous diff (100% vs 0% other MBC, $p<.001$). RB was negative in 53% MCOD and 25% CMC compared to 0% in other subtypes ($p<.05$). P16/CDK4/RB aberrations were identified by IHC and/or NGS in 73% MCOD and 50% CMC (vs 33% SQC, 10% SPC and 22% MSSC, each $p<.002$ vs MCOD). P53 was intact by IHC and/or NGS in 100% SPC but aberrant in 100% MCOD, 91% CMC, 71% SQC and 56% MSSC ($p<.05$ each).

	TRPS1		SOX10		P63		GATA3		BCAT (nuclear)		RB	RB/CDK4/P16	TP53
	Positive	mean HS (SD)	Positive	mean HS (SD)	Positive	mean HS (SD)	Positive	mean HS (SD)	Pos	Avg % positive cells (SD)	Negative	Aberrant IHC and/or NGS	Aberrant IHC and/or NGS
CMC	89% (8/9)	105 (97)	100% (12/12)	196 (95)	90% (9/10)	19 (24)	45% (5/11)	8 (8)	33% (3/9)	1 (<1)	25% (3/12)	50% (6/12)	91% (10/11)
MCO D	100% (9/9)	90 (86)	29% (4/14)	145 (63)	93% (13/14)	24 (20)	62% (8/13)	4 (5)	90% (9/10)	2 (1)	53% (8/15)	73% (11/15)	100% (14/14)
SQC	20% (1/5)	88 (-)	0% (0/6)	-	86% (6/7)	133 (107)	100% (6/6)	53 (54)	0% (0/5)	-	0% (0/6)	33% (2/6)	71% (5/7)
SPC	17% (1/6)	3 (-)	0% (0/10)	-	100% (10/10)	119 (91)	33% (3/9)	4 (2)	43% (3/7)	10 (16)	0% (0/8)	10% (1/10)	0% (0/9)
MSS C	17% (1/6)	3 (-)	13% (1/8)	52 (-)	100% (8/8)	130 (100)	43% (3/7)	32 (34)	43% (3/7)	25 (23)	0% (0/7)	22% (2/9)	56% (5/9)
Total	57% (n=35)		34% (n=50)		94% (n=49)		54% (n=46)		47% (n=38)		23% (n=48)	42% (n=52)	68% (n=50)

Conclusions: Expression of common IHC markers in MBC varies by subtype. MCOD and CMC are usually TRPS1 positive, and CMC are SOX10 positive. P63 is more often D in SQC and SPC, and GATA3 is more often P/D in SQC. nBCAT is usually focal across subtypes. Awareness of these staining patterns may be useful for diagnosis of primary or metastatic MBC. Along with PI-3 kinase and TP53, differential aberrations in the RB/CDK4/P16 axis reflect distinct oncogenic pathways between subtypes that may have treatment implications.

172 Clinical Validation of a Fully Automatic Artificial Intelligence Solution for Accurate HER2 IHC Scoring in Breast Cancer

Savitri Krishnamurthy¹, Yuval Globerson², Lilach Bien², Jonathan Harel², Giuseppe Malle², Geraldine Sebag², Maya Grinwald², Manuela Vecsler², Chaim Linhart², Judith Sandbank³

¹The University of Texas MD Anderson Cancer Center, Houston, TX, ²Ibex Medical Analytics, Tel Aviv, Israel, ³Maccabi Health Services, Kiriat Ono, Israel

Disclosures: Savitri Krishnamurthy: None; Yuval Globerson: None; Lilach Bien: None; Jonathan Harel: None; Giuseppe Malle: None; Geraldine Sebag: None; Maya Grinwald: None; Manuela Vecsler: None; Chaim Linhart: None; Judith Sandbank: None

Background: Visual interpretation of IHC HER2 staining is subjective, leading to intra- and inter-pathologist variability. Recent findings on the efficacy of HER2-targeted therapy on HER2-low patients raises the need for accurate and reproducible scoring. This study aimed to validate the use of an artificial intelligence (AI)-based solution for reviewing and reporting HER2 scores in breast samples in comparison to standard practice of manual scoring based on ASCO/CAP 2018 guidelines.

Design: We developed a fully automated AI-based solution for HER2 scoring. The AI solution performs three steps: 1) It runs an AI model detecting areas of invasive carcinoma within the HER2 slide; 2) It then employs another AI model that identifies individual tumor cells and classifies their staining pattern; 3) Finally, it counts cells and determines the HER2 score according to ASCO/CAP 2018 guidelines. The AI models were trained on >770,000 image samples annotated by a team of senior pathologists in a large, diverse set of slides from multiple labs and scanners. A two-arm retrospective reader study comparing the performance of pathologists using the HER2 AI-based solution with pathologists reviewing digitally with manual scoring was performed. Both arms were compared to rigorous ground truth (GT) established by consensus of breast subspecialists. Rates of discrepancies between each arm and GT were compared.

Results: The HER2 algorithm showed very high performance for detecting areas of invasive cancer in HER2-stained IHC slides (AUC=0.967) and for determining the type and staining pattern of individual cells – e.g., tumor vs. non-tumor cells (AUC=0.931) and negative vs. stained tumor cells (AUC=0.936) (results were measured with 4-fold cross validation). The study endpoints included accuracy of the HER2 scoring by pathologists with and without the AI system compared to the GT, and pathologists' feedback on the performance and potential benefits of the AI solution.

Figure 1 - 172

Figure 1. Example of IDC with HER2 score 1+ and identified by the AI as Her2 1+ (A); AI identifies the invasive tumor (B), identifies DCIS areas (C) and counts HER2 stained cells only in the invasive areas, ignoring DCIS areas with higher HER2 staining intensity (D)

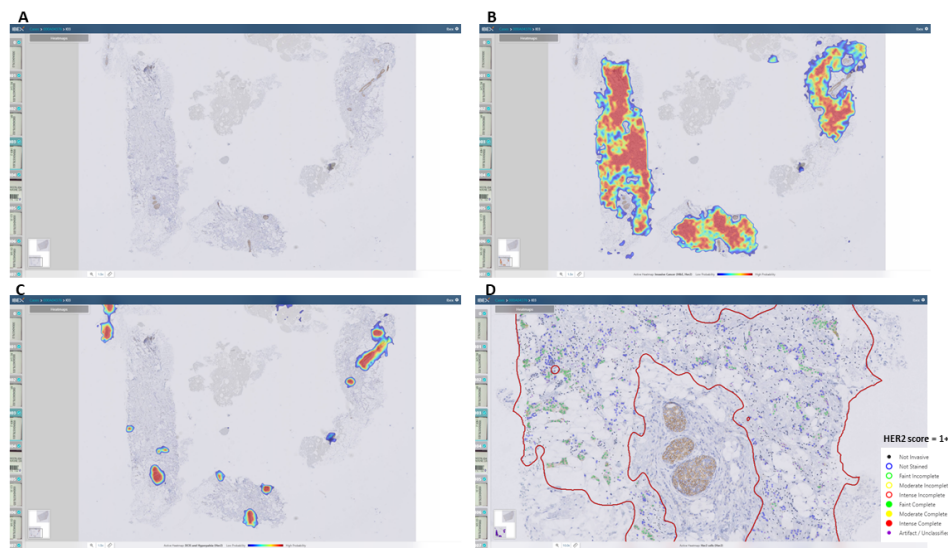
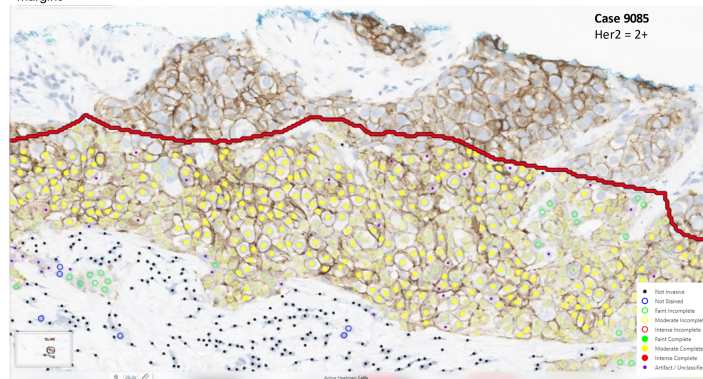


Figure 2 - 172

Figure 2. Example of IDC with HER2 score 2+ and identified by the AI as Her2 2+; AI identifies and counts tumor cells in the invasive area, classifying each cell to its staining pattern and ignoring non-invasive cells and the tumor margins



Conclusions: This study reports the successful validation of an AI-based solution for accurate IHC HER2 scoring in breast cancer. AI solutions, such as the one reported here, could be used as decision-support tools for pathologists in routine clinical practice, enhancing the reproducibility and consistency of HER2 scoring, thus enabling optimal treatment pathways and better patient outcomes. Accurate and automatic IHC scoring solutions can also contribute to the development of new prognostic, predictive and companion diagnostic tools.

173 Prognostic Value of Programmed Cell Death 1 Ligand 2 (PD-L2) Immune Infiltrates and mRNA Expression in Triple-negative Breast Cancer

Dong Yeul Lee¹, Bennett Lee², Clara Ong³, Joe Yeong⁴, Puay Hoon Tan⁴, Jabeed Iqbal⁵

¹Nanyang Technological University, Singapore, Singapore, ²Singapore Immunology Network, Agency for Science, Technology and Research (A*STAR), Singapore, Singapore, ³SGH Anatomical Pathology, Singapore, Singapore, ⁴Singapore General Hospital, Singapore, Singapore, ⁵Singapore General Hospital, Bukit Merah, Singapore

Disclosures: Dong Yeul Lee: None; Bennett Lee: None; Clara Ong: None; Joe Yeong: None; Puay Hoon Tan: None; Jabeed Iqbal: None

Background: Recent advances in immunotherapy have shown promising results in triple-negative breast cancer (TNBC). In particular, studies regarding programmed death ligand 1 (PD-L1) and programmed cell death protein 1 (PD-1) co-inhibitory pathway observed that PD-L1 expressing TNBCs had better prognosis and increased response to PD-1 checkpoint blockade. However, there are few studies on programmed cell death 1 ligand 2 (PD-L2) and its relationship to PD-L1/PD-1 co-inhibitory pathway.

Design: 319 TNBC cases diagnosed between 2003 and 2013 in Singapore General Hospital were used in this study. Tissue microarray blocks (TMAs) was stained with anti-PD-L2 antibody (D7UHC). Immunostaining was scored based on expression in tumour infiltrating lymphocytes (TILs) and positivity was defined as ≥ 2 TILs count. A total of 874 immune/hypoxia-associated genes in the NanoString panel were tested for significant differential expression between sample groups using Welch's t-tests with multiple testing corrections. *PDCD1LG2* expression association with survival outcomes and identification of differentially expressed genes were also assessed in METABRIC and TCGA.

Results: PD-L2 TILs positivity was observed in 22.3% (71/319) cases, where higher densities of PD-L2 TILs is significantly associated with better disease-free survival (DFS, $P = 0.044$) and histological subtype ($P = 0.001$). Within the same cohort, high *PDCD1LG2* transcript levels reported significantly improved survival rates [DFS: $P < 0.001$, OS: $P < 0.001$] and association with tumor size ($P = 0.043$). Similarly in METABRIC, high *PDCD1LG2* conferred significantly better relapse-free survival ($P = 0.03323$). Top-10 key hub genes were identified between sample groups in PDL2 TILs (SGH: *PTPRC*, *CD4*, *CD8A*, *IL10RA*, *CTLA4*, *ITGB2*, *LCP2*, *SELL*, *IFNG*, *TYROBP*) and *PDCD1LG2* (SGH/METABRIC/TCGA: *CD4*, *PTPRC*, *CD86*, *CD80*, *IRF8*, *IL1B*, *ITGB2*, *CD274*, *IL10RA*, *IFNG*). Interestingly, all hub genes were markedly downregulated in negative PD-L2 TILs or low *PDCD1LG2* sample groups, and is significantly associated with poorer survival rates within 3 TNBC databases.

Figure 1 - 173
PD-L2 TILs expression

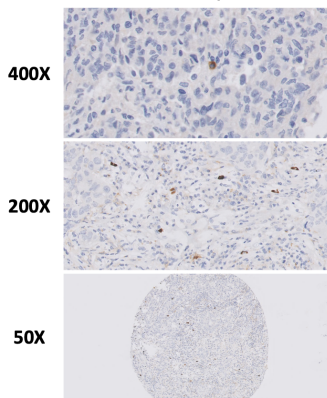
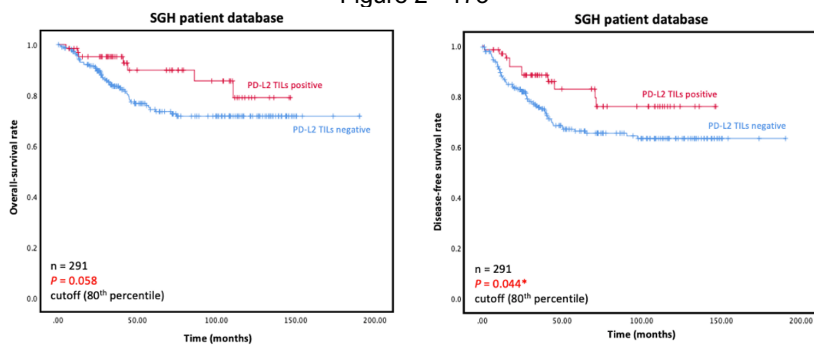


Figure 2 - 173



Conclusions: Our results demonstrate PD-L2 expression in TILs to be significantly associated with better prognosis in TNBCs. Furthermore, our data suggest that PD-L2 could function independently of PD-L1 expression with key regulatory roles in identified immune genes signatures. However, further studies are required to review the prognostic signature of PD-L2 and its role in the tumour microenvironment and immune response.

174 Clinical and Histopathological Characteristics of HER2 Low-Expressing Breast Cancer

Soo Hyun Lee¹, Kristen Young², Adeyemi Sofoluwe², Isa Jacoba¹, Ramya Narasimhan², Qing Zhao¹, Tao Zuo³

¹Boston University School of Medicine/Boston Medical Center, Boston, MA, ²Boston Medical Center, Boston, MA, ³Boston University Mallory Pathology Associates, Boston, MA

Disclosures: Soo Hyun Lee: None; Kristen Young: None; Adeyemi Sofoluwe: None; Isa Jacoba: None; Ramya Narasimhan: None; Qing Zhao: None; Tao Zuo: None

Background: It is well-established treatment strategy for anti-HER2 therapy in patients with HER2 3+ and 2+ with amplification in situ hybridization (ISH) results. Furthermore, a promising response has recently been shown for anti-HER2 therapy in patients with

HER2 low-expressing breast cancers (i.e., HER2 1+ and HER2 2+/ISH unamplified tumors). However, the clinicopathologic characteristics and biology of HER2-low breast cancers are not well understood.

Design: A total of 299 patients with first diagnosed breast cancer between January 2015 and December 2017 in the authors' institute were evaluated for histological and clinical parameters.

Results: The number of patients with HER2 IHC 0, 1+, 2+, and 3+ was 204 (69%), 51 (17%), 18 (6%), and 26 (9%), respectively. Among patients with HER2 2+ tumors, ISH was unamplified in 7 (39%) and amplified in 11 (61%). The estimated mean relapse free survival (RFS) according to HER2 expression are as follows: 87, 78, 76, 72, and 67 months in patients with HER2 IHC 0, 1+, 2+/ISH unamplified, 2+/ISH amplified, and 3+, respectively ($P=0.012$, Fig 1). In HER2-low and negative (score 0) cases, there was no statistical difference in age, tumor size, TNM stage, and histologic grades. After excluding triple negative breast cancers, the percentage of tumor cells with positive ER and PR expression were significantly lower in patients with HER2 2+/ISH unamplified than those with HER2 0, 1+ group (ER: 90.4%, 81.2%, 31.4%, $P<0.001$; PR: 65.6%, 44.4%, 13.3%, $P<0.001$ in HER2 0, 1+, 2+/ISH unamplified respectively, Fig 2), however the level of Ki67 was not different ($P=0.678$).

Figure 1 - 174

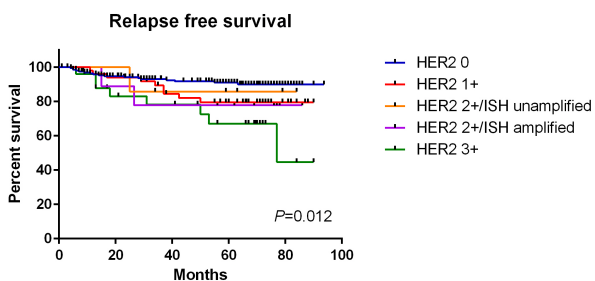
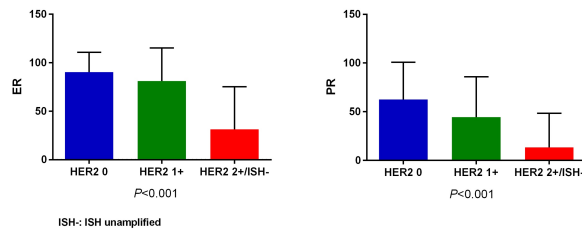


Figure 2 - 174



Conclusions: The significant prognostic implication of HER2 overexpression was shown in our study. In HER2-low expressing breast cancers, the levels of ER and PR inversely correlated with HER2 levels, which may have clinical impact on tailored treatments for anti-HER2 and hormonal therapy in patients with HER2 low breast cancers. The clinical and prognostic implication of HER2 low breast cancer needs to be further validated in larger cohort prospective studies.

175 Impact of Neoadjuvant Chemotherapy on Biomarker Expression in Breast Cancer

Su Ji Lee¹, Ahrong Kim², Jee Yeon Kim, Kyung Un Choi, Soon Wook Kwon¹, Yury Lee¹, Jihyun Ahn, Se Jin Jung¹, Kyungbin Kim, Gi Yeong Huh¹, Chang Hun Lee¹, Dong Hoon Shin³

¹Pusan National University Hospital, Busan, South Korea, ²Pusan National University, South Korea, ³Pusan National University Yangsan Hospital

Disclosures: Su Ji Lee: None; Ahrong Kim: None; Jee Yeon Kim: None; Kyung Un Choi: None; Soon Wook Kwon: None; Yury Lee: None; Jihyun Ahn: None; Se Jin Jung: None; Kyungbin Kim: None; Gi Yeong Huh: None; Chang Hun Lee: None; Dong Hoon Shin: None

Background: Neoadjuvant chemotherapy (NAC) has an important role in management of breast cancer patients. Biomarker changes according to NAC has variably reported previously. Here, we investigated the impact of NAC on biomarker expression in breast cancer patients.

ABSTRACTS | BREAST PATHOLOGY

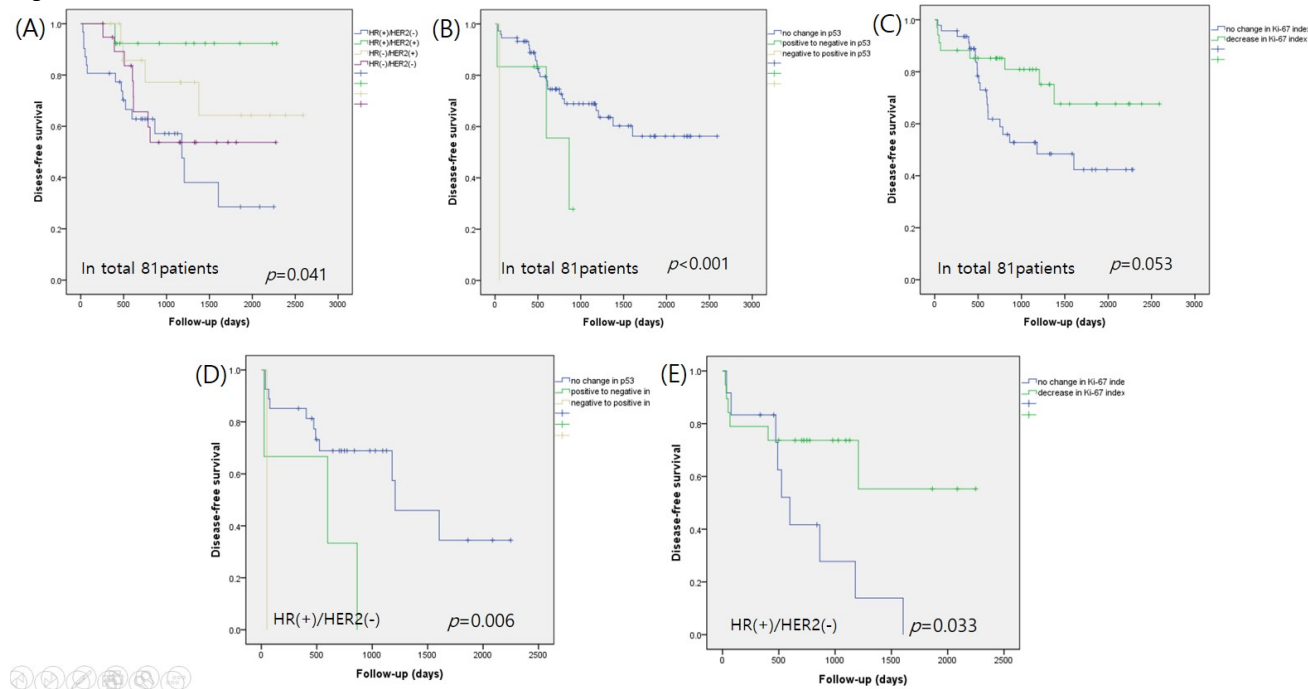
Design: We reviewed pathologic reports of 106 patients who had paired biopsy and post-NAC resection samples from 2016 to 2022. Total 106 cases of invasive breast carcinoma were included. The results of ER, PR, HER2, p53, and Ki-67 proliferation index were collected and survival analysis was performed.

Results: After NAC treatment, 81 (76.4%) out of 106 patients had any residual disease. 68 (83.9%) patients had any changes in at least one biomarker. Among 68 patients with residual disease, 31 (38.3%) patients were hormone receptor HR(+)/HER2(-), 13 (16.0%) patients were HR(+)/HER2(+), 17 patients (21.0%) were HR(-)/HER2(+), and the other 20 (24.7%) patients were HR(-)/HER2(-). The status of ER, PR, HER2, p53 and Ki-67 index had significant difference in total patient group ($p<0.001$, $p<0.001$, $p<0.001$, $p<0.001$, and $p=0.01$, respectively) before and after NAC. There was no case of increase of Ki-67 index after NAC. In 31 HR(+)/HER2(-) patients, expression of ER, PR and p53 showed significant difference according to NAC ($p=0.002$, $p=0.006$, and $p<0.001$, respectively). Among 13 patients of HR(+)/HER2(+) group, significant difference was identified in expression of HR and p53 ($p=0.033$ and $p=0.002$, respectively). In group of 17 HR(-)/HER2(+) patients, p53 status had significant difference according to NAC ($p<0.001$). In 20 patients with HR(-)/HER2(-), p53 status and Ki-67 index had significant difference before and after NAC ($p<0.001$, $p=0.002$). In total 81 patients with residual disease, patients of HR(+)/HER2(-) in pre-NAC biopsy had worst DFS ($p=0.041$). Negative to positive change of p53 was associated with worst DFS, no change of p53 had best DFS, and positive to negative change of p53 had intermediate outcome in DFS ($p<0.001$) and decrease in Ki-67 index after NAC correlated with better DFS though it was not statistically significant ($p=0.053$). In HR(+)/HER2(-) patients, negative to positive change of p53 was associated with worst DFS, no change of p53 had best DFS, and positive to negative change of p53 had intermediate outcome in DFS ($p=0.006$). Among HR(+)/HER2(-) group, decrease in Ki-67 index was correlated with better DFS ($p=0.033$).

				Tota l (N= 81)			HR(+) HER2(-) (n=31)			HR(+)/HE R2(+)(n=13)			HR(-) HER2(+)(n=17)			HR(-) HE R2(-)(n= 20)		
				Tota l (N= 81)			HR(+) HER2(-) (n=31)			HR(+)/HE R2(+)(n=13)			HR(-) HER2(+)(n=17)			HR(-) HE R2(-)(n= 20)		
				positive	neg ativ e	p- val ue	posi tive	negati ve	p- val ue	pos itiv e	negati ve	p- val ue	posi tive	negativ e	p- val ue	posi tive	negativ e	p- val ue
	ER	posi tive	35(8 3.3)	5(12 .8)	<0. 00 1	28(1 00.0)	2(66.7)	0.0 02	7(1 00.0)	3(50.0)	0. 03 3	0(0. 0)	0(0.0)		0(0. 0)	0(0. 0)		
		neg ativ e	7(16 .7)	34(8 7.2)		0(0. 0)	1(33.3)		0(0. 0)	3(50.0)		5(10 0.0)	12(100. 0)		2(10 0.0)	18(1 00.0)		
	PR	posi tive	27(8 4.4)	10(2 0.4)	<0. 00 1	21(9 5.5)	5(55.6)	0.0 06	6(1 00.0)	5(71.4)	0. 15 5	0(0. 0)	0(0.0)		0(0. 0)	0(0. 0)		
		neg ativ e	5(15 .6)	39(7 9.6)		1(4. 5)	4(44.4)		0(0. 0)	2(28.6)		3(10 0.0)	14(100. 0)		1(10 0.0)	19(1 00.0)		
Bio psy* *	HE R2	posi tive	24(9 6.0)	6(10 .7)	<0. 00 1	0(10 0.0)	0(0.0)		9(1 00.0)	4(100.0)		15(1 00.0)	2(100.0)		0(0. 0)	0(0. 0)		
		neg ativ e	1(4. 0)	50(8 9.3)		0(10 0.0)	31(100 .0)		0(0. 0)	0(0.0)		0(0. 0)	0(0.0)		1(10 0.0)	19(1 00.0)		
	p5 3	posi tive	33(9 7.1)	6(12 .8)	<0. 00 1	6(85 .7)	3(12.5)	<0. 00 1	6(1 00.0)	1(14.3)	0. 00 2	9(10 0.0)	1(12.5)	<0. 00 1	12(1 00.0)	1(12 .5)	<0. 00 1	
		neg ativ e	1(2. 9)	41(8 7.2)		1(14 .3)	21(87 .5)		0(0. 0)	6(85.7)		0(0. 0)	7(87.5)		0(0. 0)	7(87 .5)		
	Ki 67	posi tive	41(1 00.0)	34(8 5.0)	0. 0 1	7(10 0.0)	19(79. 2)	0.1 87	7(1 00.0)	6(100.0)		9(10 0.0)	8(100.0)		18(1 00.0)	1(50 .0)	0. 0 02	
		neg ativ e	0(0. 0)	6(15 .0)		0(0. 0)	5(20.8)					0(0. 0)	0(0.0)		0(0. 0)	1(50 .0)		

*post neoadjuvant **pre neoadjuvant

Figure 1 - 175



Conclusions: Biomarker expression change after NAC do occur and it has prognostic effects. Biomarker re-evaluation after NAC should be performed to predict the prognosis and provide the best management of the breast cancer patients.

176 Integrating Histological Images and Clinical Information for Predicting the Pathological Complete Response for Breast Cancer Receiving Neoadjuvant Chemotherapy

Fengling Li¹, Yongquan Yang¹, Yuanyuan Zhao², Jing Fu³, Xiuli Xiao⁴, Hong Bu⁵

¹West China Hospital, Chengdu, China, ²Shanxi Cancer Hospital, Taiyuan, China, ³Sichuan Academy of Medical Sciences & Sichuan Provincial People's Hospital, Chengdu, China, ⁴Luzhou, China, ⁵West China Hospital, Sichuan University, Chengdu, China

Disclosures: Fengling Li: None; Yongquan Yang: None; Yuanyuan Zhao: None; Jing Fu: None; Xiuli Xiao: None; Hong Bu: None

Background: Neoadjuvant chemotherapy (NAC) is a common therapeutic option for locally advanced breast cancer. In breast cancer patients receiving NAC, a pathological complete response (pCR) is regarded as a proxy goal for favorable survival. Clinicians currently mainly rely on empirical clinical risk stratification to make decisions about patients who should receive NAC. However, the routinely used pretreatment determination method is not accurate enough, and the demand for efficient prediction tools of pCR is still quite high.

Design: We enrolled 1035 breast cancer patients receiving NAC from four centers in China, and the largest cohort (N=695) was designated as the primary cohort (PC), with the other three serving as validation cohorts (VCs). Deep learning (DL) was used to generate predictive scores from tumor epithelium (TE), tumor-stroma (TS), and representative tumor regions (TR) respectively based on three different basal DL architectures. The only combination of region and architecture was selected in PC and then inference was performed in VCs. Integrated prediction-model (IPM), a random forest model that incorporates the histology score and important clinical parameters, was created to predict pCR. Additionally, we comprehensively tested the IPM.

Results: The combination of inceptionV4 architecture and TR generated score, called TR-score, showed an AUC of 0.735 (95%CI 0.692-0.777) and was determined. The TR-score showed AUCs of 0.757 (95%CI 0.670-0.843), 0.636 (95%CI 0.521-0.750), and 0.627 (95%CI 0.447-0.806) in VCs respectively. To create the IPM for better pCR prediction, significant clinical parameters such as T-stage, HR, HER2, Ki67, and grade were integrated with TR-score. The AUCs were 0.808 (95%CI 0.775-0.841) in PC, 0.810 (95%CI 0.763-0.855) in V1, 0.792 (95%CI 0.767-0.832) in V2, and 0.733 (95%CI 0.698-0.782) in V3, indicating that the IPM demonstrated effective discrimination of pCR across all cohorts. In PC and VCs, IPM demonstrated strong sensitivity and specificity; particularly, the NPVs for predicting pCR were 0.916 and 0.890, respectively. IPM divided patients into NAC-sensitive (SEN) and NAC-insensitive (INSEN), with the NAC-SEN group showing a higher pCR rate than the NAC-INSEN group ($P<0.05$).

Table 1 The prediction performance of IPM in PC and VCs datasets

	PC		VCs	
	Values	95% CI	Values	95% CI
Accuracy	0.735	0.708-0.772	0.724	0.690-0.754
Sensitivity	0.743	0.691-0.812	0.680	0.609-0.750
Specificity	0.733	0.696-0.768	0.736	0.698-0.782
PPV	0.421	0.375-0.472	0.421	0.381-0.472
NPV	0.916	0.885-0.938	0.890	0.864-0.916
AUC	0.808	0.775-0.841	0.789	0.750-0.829

Figure 1 - 176

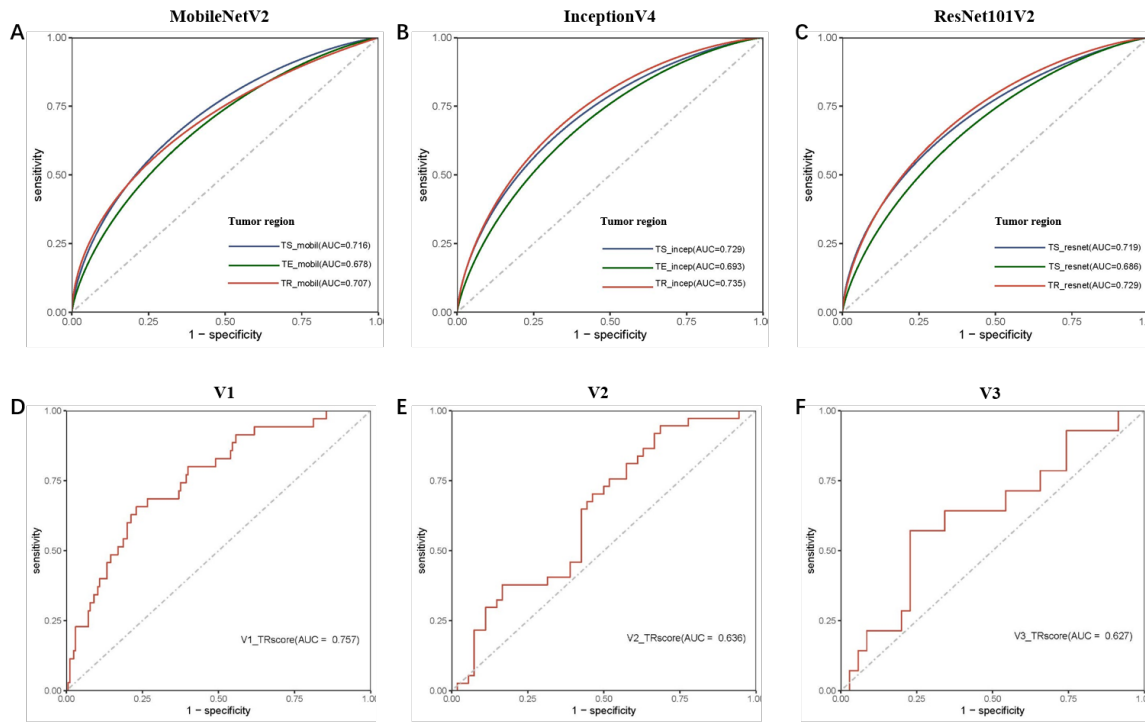


Figure 1 Predictive effect of different combinations of tissue regions and basal DL architectures on pCR. A-C Using MobileNetV2, Inception-V4 and ResNet101-V2 as the algorithm base to predict pCR from different tissue regions, respectively. D-F The prediction effect of TR-score developed by Inception-V4 based on tumor regions on pCR in three external validation sets.

Figure 2 - 176

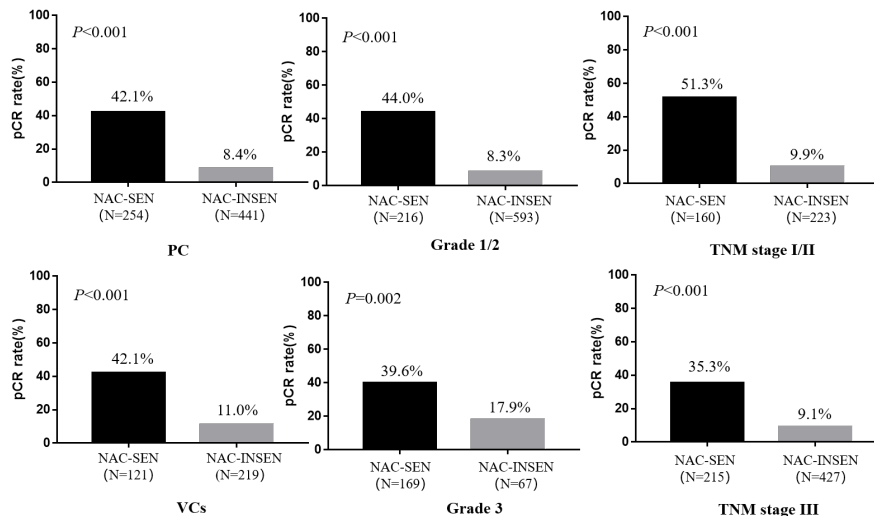


Figure 2 Comparison of pCR rates between sensitive and non-sensitive groups of IPM classification in different breast cancer subgroups

Conclusions: The DL-based model integrated histological and clinical information had good predictive value for pCR, IPM could provide predictive information for individual treatment decision-making of breast cancer receiving NAC.

177 Clinicopathological Implication and Immunotherapy Response Predictive Potential of T cell Exhaustion Signature in Triple Negative Breast Cancer: A Machine Learning Case

Jian-Di Li¹, Ming-Jie Li¹, Yu-Xing Tang¹, Wei Zhang¹, Rong-Quan He¹, Zhi-Guang Huang¹, Gang Chen¹

¹The First Affiliated Hospital of Guangxi Medical University, Nanning, China

Disclosures: Jian-Di Li: None; Ming-Jie Li: None; Yu-Xing Tang: None; Wei Zhang: None; Rong-Quan He: None; Zhi-Guang Huang: None; Gang Chen: None

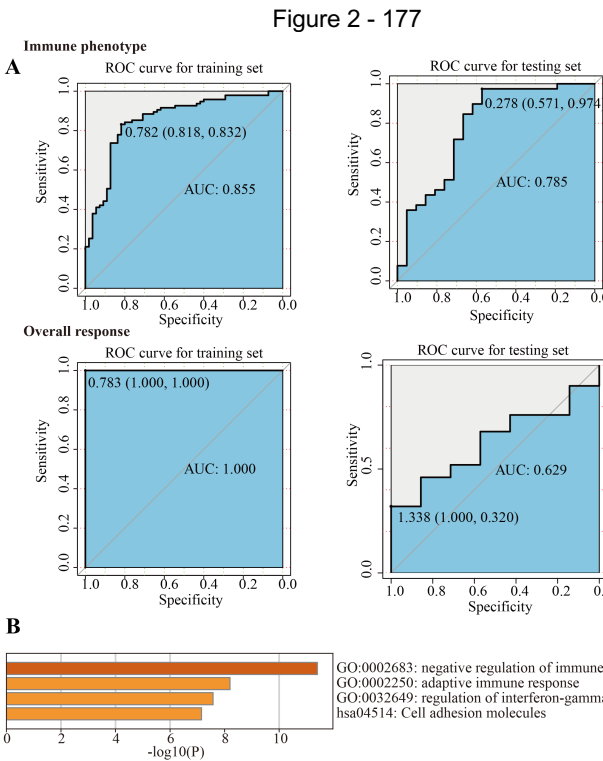
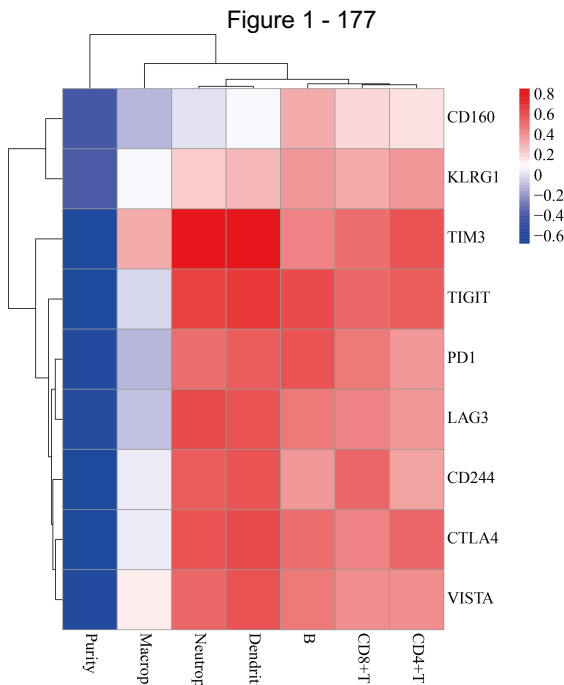
Background: T cell exhaustion (Tex) belongs to a state of T cell dysfunction, which enables cancer cells to develop immune escape, thus forming a barrier to anti-cancer immunotherapy. However, the molecular basis of T cell exhaustion in triple-negative breast cancer (TNBC) remains unclear. Herein, we are dedicated to exploring the expression abundance and its potential molecular mechanisms of the Tex signature in TNBC.

Design: Multi-centered microarray and RNA-sequencing datasets of BC tissue samples were obtained from GEO, TCGA, Metabric, and ArrayExpress. The comprehensive expression statuses of nine Tex markers were compared between distinct BC molecular subtypes by calculating standardized mean difference (SMD). Kaplan-Meier and Cox survival analyses were performed, and the prognostic value of Tex signature was comprehensively assessed by pooling hazard ratios (HR). Based on a TIMER algorithm, the association between Tex signature and tumor microenvironment was quantified. The potential of Tex signature in forecasting anti-PDL-1 immunotherapy response was evaluated in the IMvigor210 cohort by using a support vector machine (SVM) learning. Potential therapeutic agents for treating TNBC were predicted by targeting Tex signature in Cellminer.

Results: Compared to non-cancerous breast tissue and non-TN BC tissue, a total of six Tex markers were significantly upregulated in TNBC tissue samples ($SMD > 0$, $p < 0.05$). Among them, PD1, CTLA4, TIM3, and LAG3 may be potent risk factors for relapse-free survival of BC patients. All the Tex markers were positively correlated to the infiltration levels of B cells in TNBC tissue ($R > 0.30$, $p < 0.05$) but negatively correlated to the tumor purity of TNBC tissue ($R < -0.30$, $p < 0.05$). Additionally, the majority of Tex markers were positively associated with the infiltrations of CD8⁺ T, CD4⁺ T, neutrophil, and dendritic cells (Figure 1) ($R > 0.30$, $p < 0.05$). Moreover, Tex signature might have the potential in predicting the immunotherapy response and immune phenotype in the IMvigor210 cohort (Figure 2A) (immune phenotype: training set AUC=0.855, testing set AUC=0.785; overall response: training set AUC=1.000, testing set AUC=0.629). Moreover, the Tex signature was predicted to participate in negative regulation of the immune system process (Figure 2B). TAK-632, Vemurafenib, and FLX-8394 were anticipated to be putative anti-cancer agents by targeting TIM3 and CTLA4.

Table: The comprehensive expression level and prognostic value of T cell exhaustion signature in triple-negative breast cancer

Marker	SMD			HR
	BRCA vs non-cancerous	TNBC vs non-cancerous	TNBC vs non-TN	
PD1	ns	1.25	0.64	2.91
CTLA4	ns	0.90	0.33	2.03
TIM3	0.66	0.95	0.19	2.83
LAG3	0.43	1.23	0.65	2.14
TIGIT	0.77	1.55	0.35	ns
VISTA	-0.78	ns	ns	ns
CD160	ns	-0.53	ns	1.91
CD244	ns	0.48	0.38	ns
KLRG1	ns	ns	ns	ns



Conclusions: A Tex signature might be helpful in predicting the immunotherapy response and immune phenotype of cancer patients.

178 Neoadjuvant Chemotherapy for Luminal Androgen Receptor (LAR) Breast Cancer: Potential Predictive Biomarkers and Genetic Alterations

Ming Li¹, Hong Lv¹, Shuling Zhou¹, Hongfen Lu¹, Ruohong Shui¹, Yufan Cheng¹, Bao-Hua Yu¹, Rui Bi², Xiaoli Xu¹, Wentao Yang¹

¹Fudan University Shanghai Cancer Center, Shanghai, China, ²Fudan University Shanghai Cancer Center, Shanghai Medical College, Fudan University, Shanghai, China

Disclosures: Ming Li: None; Hong Lv: None; Shuling Zhou: None; Hongfen Lu: None; Ruohong Shui: None; Yufan Cheng: None; Bao-Hua Yu: None; Rui Bi: None; Xiaoli Xu: None; Wentao Yang: None

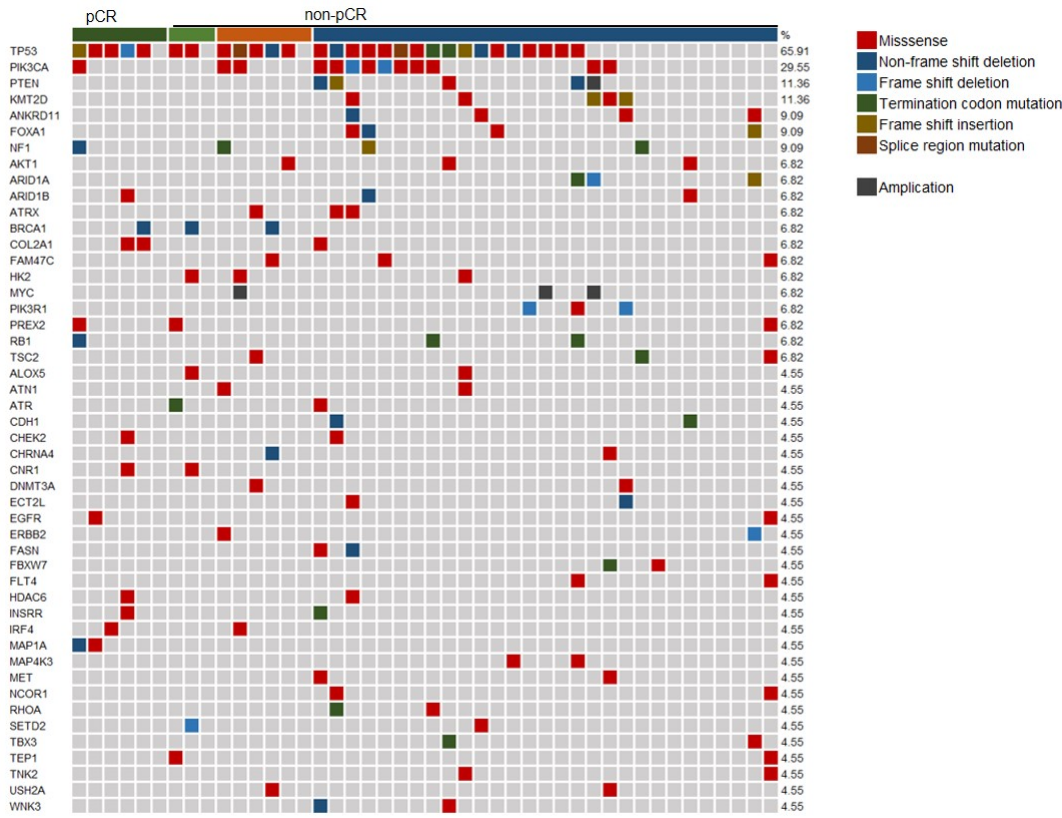
Background: Triple negative breast cancer (TNBC) is a highly heterogeneous group of cancers. The luminal androgen receptor (LAR) subtype is characterized by the expression of the Androgen Receptor (AR) and its downstream effects. The aim of this study was to determine the appropriate threshold of AR positive TNBC, investigate whether AR status affects the efficacy of neoadjuvant chemotherapy (NACT) in TNBC patients, and determine the landscape of mutations associated with pathological complete response (pCR) in LAR cases.

Design: AR and FOXC1 was evaluated by immunohistochemistry on core-needle biopsy (CNB) specimen before NACT in 226 TNBC patients between 2018 and 2022. Response was evaluated in terms of pCR in the subsequent mastectomy or breast conservation specimens. 44 LAR cases were further investigated by next-generation sequencing (NGS).

Results: Among 226 TNBC patients, the percentage of AR negative, AR<10% and AR≥10% cases were 61.50% (139), 5.75%(16), and 26.99%(71), respectively. AR≥10% tumors demonstrated distinct clinical and pathological features compared to AR negative patients, while no significant difference was seen between AR negative and AR<10% cases. Thus, AR≥10% was defined as AR positivity. Of the 226 TNBC patients, pCR was observed in 62 cases (27.43%). Tumors with LAR phenotype(AR positive TNBC) presented a pCR rate of 12.68% compared to 34.19% of the AR negative group ($p < 0.001$). In TNBC, the multivariate analysis indicated that FOXC1 was an independent predictor of pCR ($p = 0.042$), while AR was not. The pCR rate was higher in tumors with FOXC1 expression compared to FOXC1 negative TNBC patients (34.44% vs. 3.13%, $p < 0.001$). In the LAR subgroup, patients with FOXC1 expression showed higher Ki-67 expression ($p = 0.011$) and higher histologic grade ($p < 0.001$). In addition, patients with FOXC1 expression showed a higher rate of pCR as compared to FOXC1 negative patients (28.00% vs. 0.00%,

p=0.01). The identified alterations in non-pCR LAR cases were mainly categorized into PI3K/mTOR pathway alterations (loss or mutation of PTEN, mutations in PIK3CA, PIK3R1, TSC2 or AKT1).

Figure 1 - 178



Conclusions: This study indicated that the LAR phenotype is associated with lower rates of pCR after NACT. Our results suggest that assessment of FOXC1 in LAR patients may be applied as a predictive marker for the efficacy of NACT, and highlights the genetic basis in non-pCR LARs and provides a rationale for the AR inhibitor and PI3K/AKT/mTOR inhibitors in these tumors.

179 Novel Immune Biomarkers Identified in Triple Negative Breast Carcinoma (TNBC) Using Spatially-Resolved Highly Multiplexed Protein Quantification

Xiaomo Li¹, Mingtian Che¹, V Krishnan Ramanujan¹, Shikha Bose¹

¹Cedars-Sinai Medical Center, Los Angeles, CA

Disclosures: Xiaomo Li: None; Mingtian Che: None; V Krishnan Ramanujan: None; Shikha Bose: None

Background: TNBC is an aggressive subtype of breast carcinoma. While immunotherapy has improved its outcome, the suboptimal response rates (10-40%), significant toxicity, and high cost underscore the need to elucidate the important factors in the tumor microenvironment and identify biomarkers that would help stratify patients for immunotherapy. Recent studies have revealed a TNBC subset characterized by a robust host immune response evidenced by increased tumor-associated lymphocytes (TILs) and increased immune cell and cytokine signaling. However, the importance of lymphocyte subsets and associated protein expression in the tumor microenvironment is incompletely understood. This study aims to identify candidate biomarkers in immune cell rich TNBC that may allow for a better selection of patients for immunotherapy.

Design: 16 treatment-naïve TNBCs were selected including good (GP, DFS>5 years, n=8) and poor prognosis (PP, never disease-free or DFS < 5 years, n=8) groups. All cases showed associated TILs. Tissue sections were imaged using three-color immunofluorescence (PanCK, CD45, DNA) for regions of interest (ROI) selection (Figure 1). Six ROIs were selected in each case localizing stromal lymphocytes. 50 immune-related proteins (Immune cell type, activation status, immunotherapy targets) were quantified in all ROIs using the GeoMx Protein Assay in NanoString Digital Spatial Profiling (DSP) platform. GeoMx DSP Analysis Suite was used for normalization and background correction.

Results: 15 of 50 proteins showed statistically significant ($p < 0.05$) differential expression in the two groups (Figure 2A). High expression of checkpoint inhibitors PDL-1, PD-L2, and IDO1 were noted in GP. Additionally, GP also demonstrated high expression of CD3, CD4, CD68, CD45RO, CD40, ICOS, and STING indicating a Th1 skewed tumor microenvironment. PP group demonstrated high expression of fibronectin and CD66b, and CD127 possibly indicating T cell exhaustion. Linear regression analysis demonstrated a positive correlation of STING, ICOS, and IDO1 with PD-L1 (Figure 2B).

Figure 1 - 179

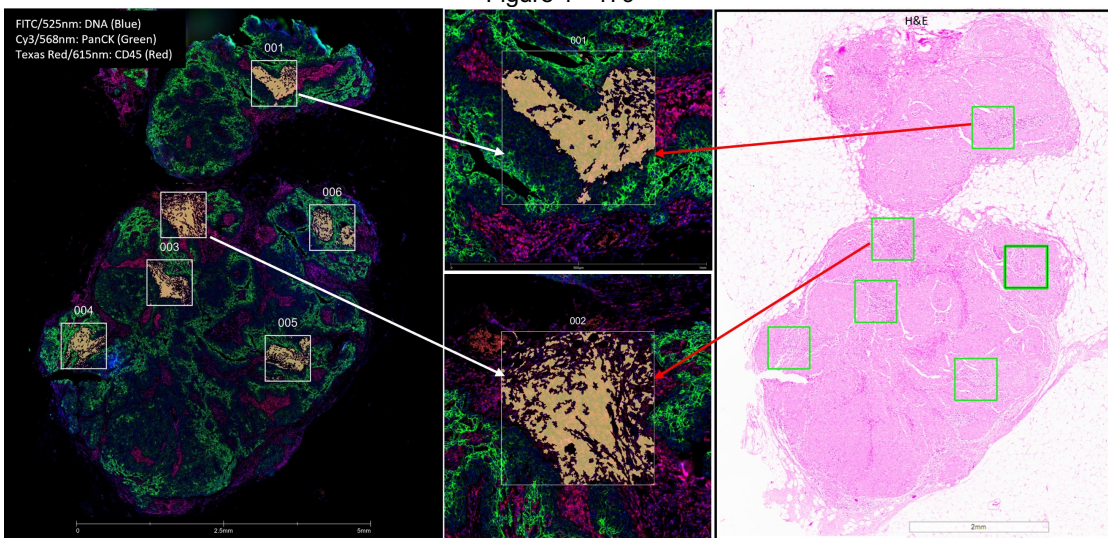
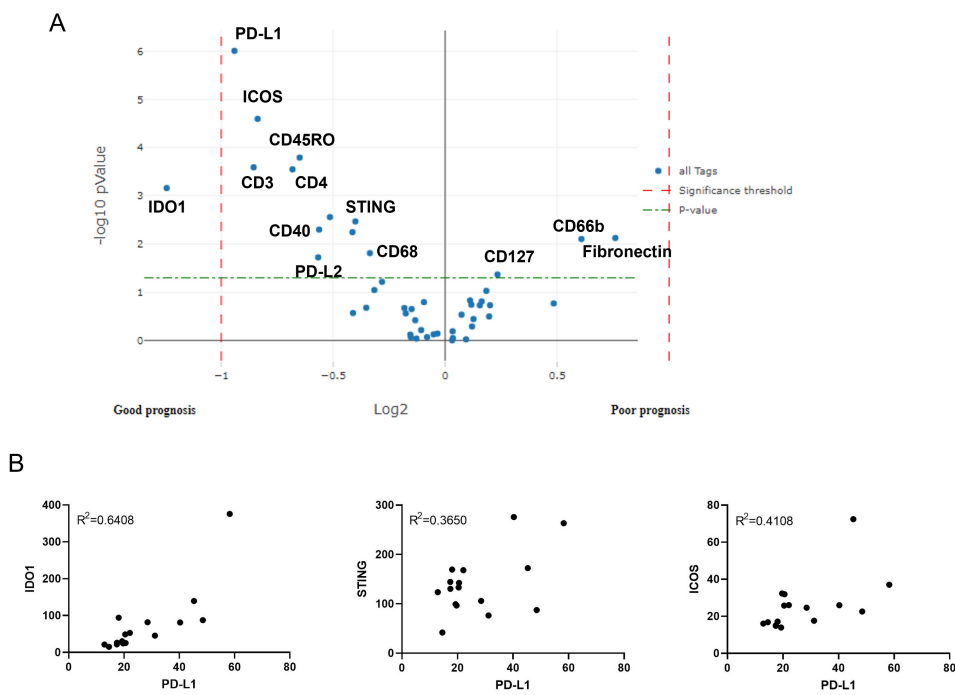


Figure 2 - 179



Conclusions: Our results showed that good prognosis TNBC cases displayed an acute inflammation microenvironment (Th1 type) seen in tumors during the elimination phase. Poor prognosis TNBC cases showed T cell exhaustion. IDO1, STING, CD40, CD45Ro, CD127 and CD66b are potential novel biomarkers. Additional studies are needed to determine the prognostic and predictive value in isolation or in combination for immunotherapy and patient selection.

180 High Tumor Infiltrating Lymphocytes are Significantly Associated with Pathologic Complete Response in Triple Negative Breast Cancer When Treated with Neoadjuvant KEYNOTE-522 RegimensXiaoxian Li¹, Yuan Gao¹, Sarah Wood¹, Ji-Hoon Lee², Qun Wang¹, Sadaf Ilyas¹, Jane Meisel¹¹Emory University, Atlanta, GA, ²Georgia Institute of Technology, Atlanta, GA**Disclosures:** Xiaoxian Li: None; Yuan Gao: None; Sarah Wood: None; Ji-Hoon Lee: None; Qun Wang: None; Sadaf Ilyas: None; Jane Meisel: None**Background:** For patients with locally advanced triple negative breast cancer (TNBC), the standard of care is to administer the neoadjuvant KEYNOTE-522 regimen (K522), including chemotherapy and immune-blockade therapy (pembrolizumab). Pathologic complete response (pCR) is more likely in patients who receive the K522 regimen than standard chemotherapy, and previous studies have shown that pCR is a strong predictor of long-term disease-free survival. However, factors predicting pCR to K522 are not well understood.**Design:** We retrospectively retrieved tissues from 59 patients treated with the K522 regimen at our institution. Twenty nine pre-treatment biopsies had slides that were available for pathologic review. Nuclear grade, Nottingham histologic grade, Ki-67, and tumor infiltrating lymphocytes (TIL) of the biopsy specimens were evaluated for these 29 cases. For the cases that did not have available slides, these variables were retrieved from pathology reports. In addition, tumor size and lymph node status by imaging evaluation before K522 and BMI at the time of biopsy of all 59 cases were retrieved from patients' charts. Binary logistic regression models were used to correlate these variables with pathologic complete response (pCR).**Results:** Of the 59 cases, 54 were invasive ductal carcinoma, NOS, 4 metaplastic carcinoma and 1 invasive lobular carcinoma. Thirty-five patients underwent surgery following completion of K522 and 16 (45.7%) achieved pCR. In univariate analysis, only TIL was significantly associated with pCR ($p=0.0448$); whereas other variables including age, race, nuclear grade, Nottingham grade, Ki-67, BMI, pre-treatment tumor size and lymph node status were not associated with pCR ($p>0.1$).**Conclusions:** Our real-world data shows a lower pCR rate than what was seen in the KEYNOTE-522 trial (45.7% vs 64.8%). Reasons for this are being investigated. High TIL is significantly associated with pCR rate in our cohort and may potentially serve as a biomarker to select patients for the optimal regimens. Larger studies are warranted to investigate the role of immune cells in TNBC response to K522 and other treatment regimens.**181 Subspecialized Breast Pathologists have Moderate Interobserver Agreement in Ki-67 Evaluation Using 20% as the Cutoff**Xiaoxian Li¹, Yuan Gao¹, Di (Andy) Ai¹, Abdulwahab Ewaz¹, Sandra Gjorgova Gjeorgjievski¹, Qun Wang¹, Thi Nguyen², Chao Zhang³, Gulisa Turashvili¹¹Emory University, Atlanta, GA, ²Emory University School of Medicine, Atlanta, GA, ³Winship Cancer Institute, Falls Church, VA**Disclosures:** Xiaoxian Li: None; Yuan Gao: None; Di (Andy) Ai: None; Abdulwahab Ewaz: None; Sandra Gjorgova Gjeorgjievski: None; Qun Wang: None; Thi Nguyen: None; Chao Zhang: None; Gulisa Turashvili: None**Background:** Abemaciclib has been approved for treatment of ER+/HER2- node positive breast cancer with high risk and $\geq 20\%$ Ki-67 expression. Therefore, accurate Ki-67 evaluation is important for optimal patient care. The International Ki-67 in Breast Cancer Working Group (IKWG) developed an algorithm to improve interobserver variability. However, this algorithm is tedious and time consuming. We modified the IKWG algorithm and assessed interobserver agreement.**Design:** Six subspecialized breast pathologists (practice experience <5 years: 4, ≥ 5 years: 2) evaluated 57 immunostained Ki-67 slides. Each pathologist assessed the percentage of positive cells with any staining intensity in 5% increments (<1%, 1-5%, 6-10%, 11-15%, 16-20%, 21-25%, 26-30% and $>30\%$). The time spent on each slide was recorded. Our modified IKWG algorithm used eyeballing method at 40x to estimate the Ki-67 percentage instead of counting 100 tumor nuclei. Two rounds of ring study were performed before and after training with the modified algorithm after a 4-week washout period. Concordance was assessed using Kendall's coefficient for all categories with 5% increments and Kappa coefficient for binary categories based on 20% as the cutoff (<20% vs $\geq 20\%$).**Results:** Analysis of ordinal scale ratings for all categories with 5% increments showed almost perfect agreement in round 1 (0.821), with substantial agreement among senior and junior pathologists (0.718 vs 0.649). With our modified algorithm, agreement for all categories with 5% increments slightly decreased to substantial in round 2 (0.793), and was similar among seniors and juniors (0.756 vs 0.658). Agreement in round 1 vs round 2 remained substantial for both seniors (0.718 vs 0.756) and juniors (0.649 vs 0.658). In dichotomous scale analysis using 20% as cutoff, the overall agreement remained moderate (round 1: 0.437, round 2: 0.479). Agreement also remained moderate among juniors (round 1: 0.445, round 2: 0.505) and seniors (round 1: 0.436, round 1: 0.437). Average scoring time per case was 37 seconds in round 1 and 71 seconds in round 2.

Conclusions: In our study, overall interobserver agreement among subspecialized breast pathologists is almost perfect in evaluating Ki-67 using the conventional eyeballing method. The modified algorithm yields moderate (binary data) to substantial (categorical data) agreement among junior and senior pathologists. A better algorithm, probably with machine learning, is needed to accurately evaluate Ki-67 expression for optimal patient care.

182 Detection of Metastatic Breast Carcinoma in Sentinel Lymph Node Frozen Section Using Artificial Intelligence-Assisted System

Wen-Yih Liang¹, Chih Yi Hsu¹, Hsiang Sheng Wang²

¹Taipei Veterans General Hospital, Taipei, Taiwan, ²Chang Gung Memorial Hospital, Linkou, Linkou, Taiwan

Disclosures: Wen-Yih Liang: None; Chih Yi Hsu: None; Hsiang Sheng Wang: None

Background: Intraoperative frozen section of the sentinel lymph node is used for evaluating the nodal status of patients with breast cancer. However, the sensitivity is low for micrometastasis. We develop an automatic method using the convolutional neural network to help identify the metastases in whole slide images (WSI) within 2 minutes.

Design: A total of 954 sentinel lymph nodes frozen section examinations were performed from 2021/01/01 to 2022/09/27, including 732 (76.7%) negative, 4 (0.4%) isolated tumor cells, 49 (5.1%) micrometastases, and 169 (17.7%) macrometastases. The glass slides were scanned by Hamamatsu S360 in 20x and seventy-two WSIs were selected and annotated for training the model (50 macrometastases, 16 micrometastases and 6 negatives). All annotated WSIs were sent for training by a self-developed platform (EasyPath). Our system was built under R 4.1.3 accompanied by python 3.7 using the reticulate package. Another 105 metastatic cases were collected to validation test the algorism.

Results: The results of the validation test were shown in table 1. Ninety-eight percent of the metastases were identified by our algorism in a very short time (average 87.3 seconds). The time spent, including slide scanning (taking about 1-2 minutes) and artificial intelligence (AI) processing, can be completed in less than 4 minutes. The two missed cases are due to severely crushed artifacts. (figure 1). Two macro-metastases and six micro-metastases were missed in the original frozen sections and were identified in the algorism. The performance of AI algorism was significantly better than that of original pathologists ($p = 0.005$), especially for identifying micrometastasis ($p = 0.014$).

	Original	AI Algorism	P (McNemar's test)
All metastatic case			0.005
Positive	95	103	
Negative	10	2	
Type of metastasis			
Macrometastases			0.157
Positive	83	85	
Negative	2	0	
Micrometastases			0.014
Positive	12	18	
Negative	8	2	
Time spent for diagnosis (seconds)		87.3 (39-190)	

Figure 1 - 182

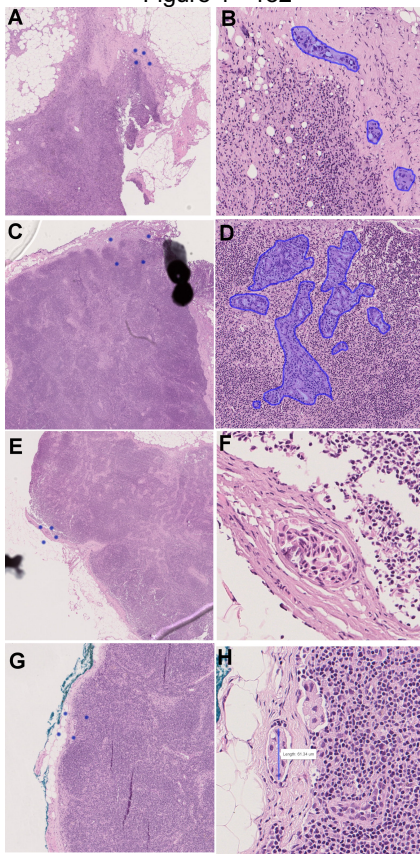


Figure 1: (A-D, AC) Low power, BD High power and labelled by algorithm
Micrometastases identified by algorithm and missed in original frozen section examined. (EF) Micrometastases missed by algorithm only. (GH)
Micrometastases missed by both original frozen section and algorithm.

Conclusions: Our AI system can work in a reasonable time, meeting the requirement of the frozen section. Especially for micrometastases, the AI system performs better than pathologists. With the assistance of the AI system, pathologists can improve the accuracy of the intraoperative frozen section of the sentinel lymph node.

183 Mucocele-Like Lesions without Atypia on Breast Core Biopsy Performed for Indeterminate Calcifications Do Not Require Surgical Excision

Chad Livasy¹, Shayna DeSando², Daniel Coldren³

¹Atrium Health, Charlotte, NC, ²Wake Forest Baptist Health, Winston-Salem, NC, ³Wake Forest Baptist Medical Center, Winston-Salem, NC

Disclosures: Chad Livasy: None; Shayna DeSando: None; Daniel Coldren: None

Background: Mucocele-like lesions (MLLs) of the breast are rare findings in core biopsy specimens and consist of dilated mucin-filled ducts associated with extravasation of mucin into stroma. Most MLLs are clinically occult and identified in biopsies performed for indeterminate calcifications. Several studies have described an association between MLLs and presence of atypia or carcinoma. Differing opinions exist on the need for surgical excision of MLLs identified in core biopsy specimens. This study was initiated to specifically focus on upgrade rate and need for surgical excision for MLLs without associated atypia identified in stereotactic core biopsies for indeterminate calcifications.

Design: After institutional review board approval, our system database was searched to identify all cases of mucocele-like lesion identified on stereotactic core biopsy for indeterminate calcifications. Cases with associated atypia or carcinoma in the core biopsy were excluded. All cases were reviewed by a subspecialty breast pathologist to confirm the diagnosis of MLL. All imaging studies were performed by radiologists with subspecialty expertise in breast imaging. Available excision pathology reports were reviewed. An upgrade was defined by the presence of ductal carcinoma in-situ (DCIS) or invasive carcinoma in the excision specimen. The frequency of any atypia in the excision specimen was also recorded.

Results: MLLs were identified in 132 patients undergoing core biopsy for indeterminate calcifications. A total of 74 cases were excluded either due to presence of associated atypia/carcinoma in the core biopsy or lack of follow-up excision. Of the remaining 58 cases, there were no cases (0%) that were upgraded to invasive carcinoma or DCIS. Atypia in the excision specimen was identified in 7 cases (12%) consisting of 3 flat epithelial atypia, 1 atypical lobular hyperplasia and 3 atypical ductal hyperplasia.

Conclusions: Mucocele-like lesions without atypia identified in stereotactic core biopsies for indeterminate calcifications have an extremely low upgrade rate to DCIS or invasive carcinoma on excision. Breast imaging surveillance rather than immediate surgical excision is a reasonable option for these patients.

184 Clinical and Pathological Features of CHEK2 Mutation Carriers in Breast Cancer

Christopher Lloyd¹, Heather Rocha², Nicole Ortiz², Chelsea Mehr³

¹Geisinger Commonwealth School of Medicine, Scranton, PA, ²Geisinger Medical Center, Danville, PA, ³Geisinger Health, Wilkes-Barre, PA

Disclosures: Christopher Lloyd: None; Heather Rocha: None; Nicole Ortiz: None; Chelsea Mehr: None

Background: Cancers in patients who are *CHEK2* mutation carriers have become a target for research in the hopes of yielding information that can assist patients and providers in determining cancer risk and treatment plans. Data are still lacking in regards to the breadth of the disease profile, particularly prevalence of different cancer types as well as pathologic features of breast cancers (BCs) in *CHEK2* mutation carriers. The aim of this study is to collect clinical and pathologic data from a cohort of *CHEK2* mutation carriers.

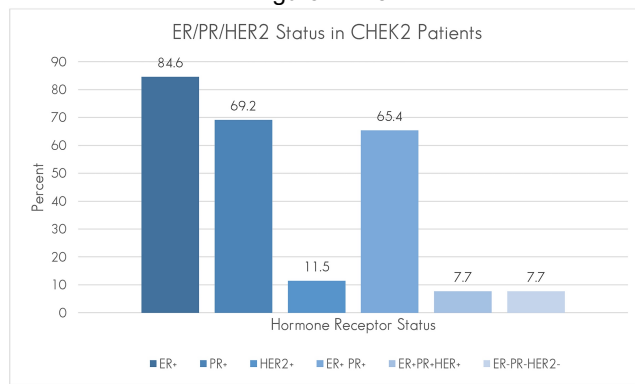
Design: Genetic testing data was analyzed for patients that had previously undergone screening and tested positive for a germline *CHEK2* mutation predisposing them to cancer. Patients' demographic and family history of malignancy were recorded. If the patient had a history of BC, surgical pathology data including tumor type, grade, lymph node involvement, estrogen receptor (ER), progesterone receptor (PR) and HER2 status were obtained.

Results: Of the 120 patients, 25.8% (31/120) had a history of BC. The mean age of initial diagnosis was 49.4 years old. Of note, 87.5% (21/24) of tumors biopsied were high grade (grades 2 & 3). A subset had lymph node involvement (8/24; 33.3%) at the time of diagnosis. Invasive ductal carcinoma (IDC) accounted for the majority of BC at 58% (18/31) with an average age at diagnosis of 54.6 years. Ductal carcinoma in situ (DCIS) was much less common at 13% (4/31) with an earlier age at diagnosis of 38.2 years (Table 1). The majority of carcinomas were ER (84.6%) and PR (69.2%) positive and HER2 negative (88.5%) (Figure 1). Regarding family histories of malignancies, 43.3% (52/120) of patients had a 1° family member with BC. This rate was higher than family history rates of other cancers (Table 1). Complete pathological records were not available for 7 patients.

Table 1: Clinical and Pathologic Features of *CHEK2* Mutation Carriers

	N/Total	Percent
Positive Breast Cancer	31/120	25.8%
Lymph Node Involvement/ Metastases	8/24	33.3%
Tumor Grade		
Grade 1	3/24	12.5%
Grade 2	10/24	41.7%
Grade 3	11/24	45.8%
Tumor Types		
IDC (Invasive Ductal Carcinoma)	18/31	58.0%
LCIS (Lobular Carcinoma In Situ)	5/31	16.1%
DCIS (Ductal Carcinoma In Situ)	4/31	12.9%
ILS (Invasive Lobular Carcinoma)	2/31	6.5%
Other	2/31	6.5%
Family History		
1° family members with breast cancer	52/120	43.3%
1° family members with colon cancer	14/120	11.7%
1° & 2° family members with colon cancer	31/120	25.8%
1° & 2° family members with ovarian cancer	12/120	10.0%
1° & 2° family members with prostate cancer	19/120	15.8%
1° & 2° family members with stomach cancer	10/120	8.3%

Figure 1 - 184



Conclusions: Our cohort of patients with *CHEK2* mutations predisposing them to carcinoma had a 25.8% rate of breast cancer. The cancers tended to be invasive ductal carcinoma, high grade (grade 2/3) and ER/PR positive. These patients also had higher rates of breast cancer in their family history than other cancers. These findings provide insight into this patient population and can ultimately guide surveillance and treatment for patients who test positive for *CHEK2* germline mutations.

185 BRCA Status and Clinicopathological Characteristics in Mexican Patients with Invasive Breast Cancer and High Risk of Hereditary Carcinoma

Carlos A. Lopez-Garcia¹, Dulce López Sotomayor¹, Andrea Leal Lopez¹, Antonio Dono², Qingqing Ding³, Servando Cardona-Huerta¹, Cynthia Villarreal-Garza¹, Dione Aguilar y Mendez¹, Pablo Josafat Avalos Montes¹, Jorge Novo⁴, Gabriela Sofia Gomez Macias⁵

¹Escuela de Medicina y Ciencias de la Salud TecSalud, Monterrey, Mexico, ²The University of Texas Health Science Center at Houston McGovern Medical School, Houston, TX, ³The University of Texas MD Anderson Cancer Center, Houston, TX, ⁴Northwestern University Feinberg School of Medicine, Chicago, IL, ⁵TecSalud, Hospital San José, Hospital Universitario de la UANL, Mexico

Disclosures: Carlos A. Lopez-Garcia: None; Dulce López Sotomayor: None; Andrea Leal Lopez: None; Antonio Dono: None; Qingqing Ding: None; Servando Cardona-Huerta: None; Cynthia Villarreal-Garza: None; Dione Aguilar y Mendez: None; Pablo Josafat Avalos Montes: None; Gabriela Sofia Gomez Macias: None

Background: The most common cause of hereditary breast cancer is an inherited mutation in either *BRCA1* or *BRCA2* genes, which are associated with DNA repair. This study aims to identify the influence of *BRCA1* and *BRCA2* mutations on clinicopathological characteristics in Mexican breast cancer patients at risk of hereditary invasive carcinoma focusing on tumor-infiltrating lymphocytes (TILs), complete pathologic response (pCR), and prognosis.

Design: A retrospective study of 168 Mexican females at high risk of hereditary carcinoma, according to NCCN criteria, and diagnosed with invasive breast cancer between 2011 and 2019 were included. Age, sex, tumor location, extent of resection, molecular subtype, WHO grade, TILs (according to International TILs Working Group), NAT (neoadjuvant therapy), recurrence, and death were collected. All cases were tested for *BRCA1* or *BRCA2* genes by NGS. A comparison between patients with mutations on *BRCA1* or *BRCA2* and patients without these or other mutations was performed. Disease-free survival (DFS) and overall survival (OS) were analyzed using a Log-rank test.

Results: Out of 168 patients, 24 (14.3%) showed *BRCA1* mutation, 15 (8.9%) *BRCA2* mutation, 129 (76.8%) no mutations. The most prevalent molecular subtype was TN (triple negative) for the mutated group (28/39, 71.8%), and luminal for the non-mutated group (78/129, 60.5%) ($p<0.0001$). The mutated group was predominantly Nottingham grade 3 (31/39, 79.5%) and the non-mutated group was grade 2 (66/129, 51.2%) ($p=0.0002$). Clinical stage between groups was no different ($p=0.16$). Median TILs in patients with and without mutations (23.9 vs 17.9, $p=0.06$) were not different. There were no significant differences in DFS and OS. One-hundred patients received NAT. From the mutated group treated with NAT (27/100), 18 (66.7%) achieved pCR, while in the non-mutated group (73/100), 29 (39.7%) reached pCR ($p=0.02$). Multivariate analysis showed that *BRCA1/BRCA2* mutations are a predictive factor for pCR (OR 5.196, CI 95% 1.746-15.462, $p=0.003$).

Conclusions: Our findings suggest the relevance of the mutational status as an independent predictive factor to NAT in the presence of pathogenic *BRCA* variants in a Mexican population with breast cancer and a high risk of hereditary carcinoma. Although there was a tendency for higher TILs in *BRCA* mutated tumors, the difference was not statistically significant. The prognosis seems to be similar among both groups of patients.

186 Mutational Landscape of HER2-low Breast Carcinoma

Georgi Lukose¹, Carlos Munoz-Zuluaga¹, Laura Munoz-Arcos², Olivier Michaud², Massimo Cristofanilli¹, Syed Hoda³, James Solomon¹

¹New York-Presbyterian/Weill Cornell Medicine, New York, NY, ²New York-Presbyterian/Weill Cornell Medical Center, New York, NY, ³Weill Cornell Medicine, New York, NY

Disclosures: Georgi Lukose: None; Carlos Munoz-Zuluaga: None; Laura Munoz-Arcos: None; Olivier Michaud: None; Massimo Cristofanilli: None; Syed Hoda: None; James Solomon: None

Background: Trastuzumab deruxtecan has been effective in metastatic breast carcinomas with low expression of HER2 (Modi, et al. NEJM 2022). The molecular characteristics of this cohort is still unknown. We sought to characterize mutational landscapes in HER2-low breast carcinoma cases, and identify differences in HER2-negative, HER2-low, and HER2-positive breast cancers.

Design: We performed retrospective review of advanced stage breast carcinomas sequenced using Oncomine Comprehensive Assay (ThermoFisher), an in-house next-generation sequencing (NGS) based assay. Immunohistochemical (IHC) staining performed for ER, PR, HER2, and HER2 FISH results were recorded. HER2-low was defined as 1+ staining on IHC or 2+ staining with negative FISH. NGS variants were tiered using the AMP/ASCO/CAP system to reflect targetability and oncogenicity. Cases with unknown or unclear HER2 status were excluded.

Results: NGS was performed on 147 formalin fixed paraffin embedded (FFPE) tissues, from 140 patients, 108 (74%) samples from metastatic sites and 39 (26%) from primary/locally recurrent sites. The most common metastatic sites were liver (32, 22%), bone (26, 18%), and brain (11, 8%). There were 19 (12%) HER2-positive, 64 (44%) HER2-low, and 64 (44%) HER2-negative cases (Table 1). Variants in 73 genes were identified. Common tier 1 variants in HER2-positive cases occurred in *ERBB2* (74%, 100% amplification) and *PIK3CA* (16%), while tier 1 variants occurred in *PIK3CA* and *ESR1* in HER2-low (33% and 16%) and HER2-negative (38% and 13%) groups. *ERBB2* variants occurred in 9% of HER2-low cases (50% amplification and 50% single nucleotide variant/ insertions and deletions [SNV/indels]) and 3% of HER2-negative cases(50% amplification and 50% SNV/indels). *CCND1* amplification was more common in HER2-low cases (27%), compared to HER2-positive (11%) and HER2-negative (16%), but was not statistically significant.

Table 1. Clinical, pathological, and molecular characteristics of the study cohort

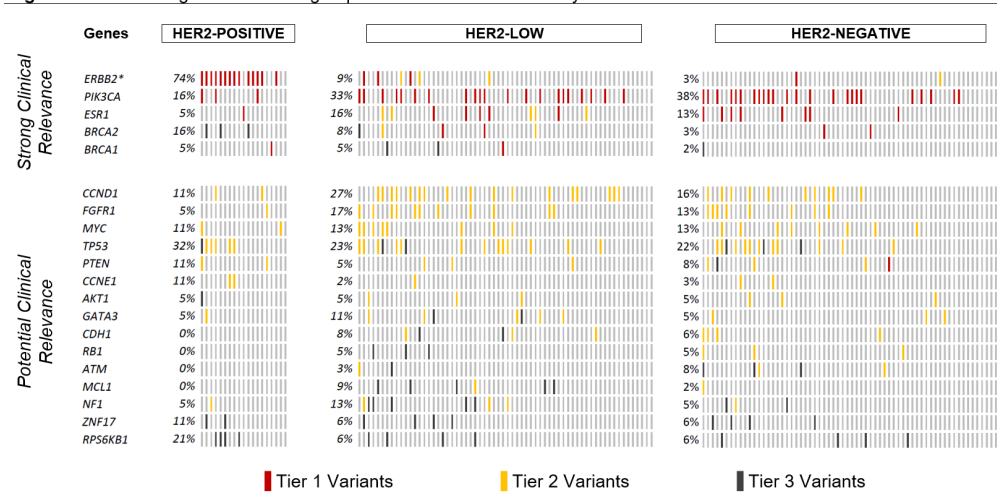
Characteristic	Total	HER2-positive	HER2-low	HER2-negative
Total cases, n (%)	147(100)	19(12)	64(44)	64(44)
Age, mean ± SD [range]	60 ± 13 [30 - 86]	58 ± 14 [39 - 86]	60 ± 12 [30 - 80]	60 ± 13 [31 - 85]
Source of tissue, n (%)				
Breast	21(14)	4(21)	10(16)	7(11)
Lymph node	18(12)	5(26)	6(9)	7(11)
Metastatic disease	108(74)	10(53)	48(75)	50(78)
Hormone Receptor Status, n (%)				
ER-positive	111(76)	11(58)	55(86)	45(70)
PR-positive	61(42)	8(42)	28(44)	25(39)
HER2 Status, n (%)				
HER2: 0	64(44)	0(0)	0(0)	64(0)
HER2: 1+	33(22)	0(0)	33(52)	0(0)
HER2: 2+	31(21)	0(0)	31(48)	0(0)
HER2: 2+ / FISH-positive	6(4)	6(32)	0(0)	0(0)
HER2: 3+	13(9)	13(68)	0(0)	0(0)
ERBB2 copy number when tumor %>20*, (n=107)				
Median Copy Number (Q1 - Q3)	1.75 (1.3 - 2.43)	16.5 (6.3 - 19.8)	1.8 (1.5 - 2.1)	1.4 (0.8 - 2.2)
% of tumor in sample for NGS, median (Q1 - Q3) [range]	60 (30 - 70) [5-90]	50 (20-60) [5-80]	60 (35 - 73) [5-9]	60 (30 - 70) [10-90]
Cases with at least one variant identified, n (%)	132(90)	18(95)	58(91)	56(88)
Tier 1 variants, n (%)				
<i>PIK3CA</i>	48(33)	3(16)	21(33)	24(38)
<i>ERBB2</i> amplification	18(12)	14(74)	3(5)	1(2)
<i>ERBB2</i> mutation	4(3)	0(0)	3(5)	1(2)
<i>ESR1</i>	19(13)	1(5)	10(16)	8(13)

*Cases with tumor percentage <20% where excluded from the *ERBB2* copy number calculations

ER: Estrogen receptor, HER2: Human epidermal growth factor receptor 2, NGS: Next generation sequencing, Progesterone receptor, Q1: Quartile 1, Q3: Quartile 3, SD: Standard deviation

Figure 1 - 186

Figure 1. Variants in genes with strong or potential clinical relevance by HER2 status



*Tier 1 variants in *ERBB2* are amplifications (n=18/22) while tier 2 variants are single nucleotide variation (n=2/22) or insertions (n=2/22).

Conclusions: Precision medicine to identify molecularly targetable alterations is rapidly becoming standard of care in oncology. In our breast cancer cohort, 44% of cases were HER2-low, which is concordant with previous reports. Interestingly, these cases appear also enriched of actionable mutations in *PIK3CA*. Molecular characterization of breast carcinomas in disease subtypes, including those defined as HER2-low may further expand potential treatment options and further the understanding of HER2 expression in tumorigenicity and treatment response.

187 HER2 Low-Amplified Breast Cancer: The Efficacy of Anti-HER2 Therapy in Neoadjuvant Setting

Hong Lv¹, Qianming Bai¹, Ruohong Shui¹, Xiaoli Xu¹, Bao-Hua Yu¹, Rui Bi², Yufan Cheng¹, Xiaoyu Tu¹, Xiaoyan Zhou², Wentao Yang¹

¹Fudan University Shanghai Cancer Center, Shanghai, China, ²Fudan University Shanghai Cancer Center, Shanghai Medical College, Fudan University, Shanghai, China

Disclosures: Hong Lv: None; Qianming Bai: None; Ruohong Shui: None; Xiaoli Xu: None; Bao-Hua Yu: None; Rui Bi: None; Yufan Cheng: None; Xiaoyu Tu: None; Xiaoyan Zhou: None; Wentao Yang: None

Background: In HER2-positive breast carcinoma, different HER2 average copy number and ratio of HER2/CEP17 may lead to different response to HER2 targeted therapy. Our aim is to explore the response of invasive breast carcinoma patients with low HER2 amplification (HER2/CEP17 \geq 2.0 & <3.0, HER2 average copy number \geq 4.0 & <6.0) to HER2 targeted therapy in neoadjuvant setting.

Design: The clinicopathological data of patients with HER2-positive breast cancer who underwent chemotherapy and HER2-targeted neoadjuvant therapy in Fudan University Shanghai Cancer Centre from January 2015 to July 2022 were collected. Patients were divided into four groups according to different results of fluorescence in situ hybridization (FISH). Group A: HER2/CEP17<2.0, HER2 average copy number \geq 6.0; Group B: HER2/CEP17 \geq 2.0 and <3.0, HER2 average copy number \geq 4.0 and <6.0; Group C: HER2/CEP17 \geq 2.0 and <3.0, HER2 average copy number \geq 6.0; Group D: HER2/CEP17 \geq 3.0, HER2 average copy number \geq 4.0. Group B was defined as HER2 low amplification group according to literature. The clinicopathological characteristics and the efficacy of anti-HER2 neoadjuvant therapy of HER2-positive breast cancer patients with different FISH results were analyzed.

Results: A total of 173 patients with HER2-positive breast cancer underwent anti-HER2 targeted neoadjuvant therapy were collected. The age of the patients ranged from 27 to 69 years (mean, 51.0 years). According to different FISH results, there were 12 cases (6.9%) in group A, 32 cases (18.5%) in group B (low amplification group), 30 cases (17.3%) in group C and 99 cases (57.2%) in group D. There were no significant differences in age(p=0.356), lymph node metastasis(p=0.129), MP grade(p=0.055), ER(p=0.195), PR(p=0.733), and Ki67(p=0.351) expression among the four groups. However, the low-amplified group B was enriched with HER2 2+ patients(27/32,84.4%) and no HER2 3+ cases(0.0%) were identified. The pCR rate of group B was only 3.1% (1/32), which was the lowest among the 4 groups (p <0.001).

	The pCR rate of different groups					χ^2	p
	Group A	Group B (HER2 low amplification)	Group C	Group D			
Total number	12(6.9%)	32 (18.5%)	30 (17.3%)	99(57.2%)			
non-pCR	8(66.7%)	31(96.9%)	17(56.7%)	68(68.7%)	16.573	<0.001	
pCR	4(33.3%)	1(3.1%)	13(43.3%)	31(31.3%)			

Conclusions: This study suggests different response to HER2-targeted therapy within HER2-FISH positive breast cancers. Low HER2-amplified breast cancers are enriched with HER2 2+ cases and less responsive to HER2-targeted treatment. Thus, it might be of clinical significance in subclassification of HER2-FISH positive breast cancers. Larger prospective studies are vital to obtain more accurate prognostic information in HER2 low-amplified breast cancers.

188 Biomarker Changes After Neoadjuvant Chemotherapy for Breast Cancer

Aoife Maguire¹, Andrew Hudson¹, Jacob Jagas¹, Cecily Quinn¹

¹St. Vincent's University Hospital and Irish National Breast Screening Programme, Dublin, Ireland

Disclosures: Aoife Maguire: None; Andrew Hudson: None; Jacob Jagas: None; Cecily Quinn: None

Background: Changes in breast cancer (BC) hormone receptor (HR) and HER2/neu (HER2) phenotype may occur following neoadjuvant chemotherapy (NACT). This may be due to tumor heterogeneity, NACT-related selective pressure or technical issues. Currently, there is no consensus regarding biomarker re-assessment on residual tumor post NACT. This study aimed to determine if repeating biomarker studies in this setting identifies clinically actionable changes.

Design: A retrospective review was conducted of tumor biomarker profile from 240 BC patients who received NACT followed by definitive surgery from 2019 to mid 2022. The biomarker profile (estrogen receptor [ER], progesterone receptor [PR], and HER2) of residual tumor post NACT was compared with that of the pre-treatment core needle biopsy.

Results: Complete pathological response was seen in 72 patients (30%) and biomarkers were not repeated in a further 7 (3%) due to insufficient residual tumor. Repeat biomarker testing was performed on the post NACT surgical resection specimen from 161 patients (67%). Changes in biomarker profile were observed in 36/161 (22%). PR changed in 16/36 patients (14 positive to negative; 2 negative to positive, 1 of which also expressed ER). ER changed in 9/36 cases (6 positive to negative; 3 negative to positive). Changes in both ER and PR were identified in 2 patients (positive to negative). HER2 status changed in 9/36 cases (7 positive to negative; 2 negative to positive).

Conclusions: A change in biomarker profile post NACT was identified in 22% of patients with a tendency towards decreased expression. In 6 patients (4% of tumors tested) there was a positive change in biomarker status (2 with HER2 positivity, 4 with HR positivity) with potential to introduce new adjuvant treatment options. This study adds to the evidence that repeat biomarker testing post NACT may have a significant impact on therapeutic management in a small group of patients with BC. Whether re-testing of residual tumor should be performed as routine in all patients post NACT or be subject to specific selection criteria remains a matter of debate.

189 HER2-low Breast Cancer Incidence, Immunohistochemical (IHC) Staining, FISH Group Stratification, and Oncotype Dx Recurrence Score (RS): A Retrospective Review

Lily Mahler¹, Laura Collins², Liza Quintana¹, Gabrielle Baker¹

¹Beth Israel Deaconess Medical Center, Boston, MA, ²Beth Israel Deaconess Medical Center, Harvard Medical School, Boston, MA

Disclosures: Lily Mahler: None; Laura Collins: None; Liza Quintana: None; Gabrielle Baker: None

Background: With the advent of antibody-drug conjugate (ADC) therapy such as trastuzumab deruxtecan, further elucidation of the HER2-low category of invasive breast cancer (IBC) is necessary given the promising benefits of ADCs in this newly defined group (IHC score 1+ or 2+ and FISH negative).

Design: We retrospectively reviewed paired H&E and HER2 IHC (HercepTest™) slides for 350 cases (2015-2017), FISH-negative by 2018 ASCO/CAP guidelines. Consensus was determined by two breast pathologists (BP), with a third senior BP as arbiter in challenging cases that would be of clinical significance (16%, 56/350). IHC and FISH are performed on all IBC at our institution.

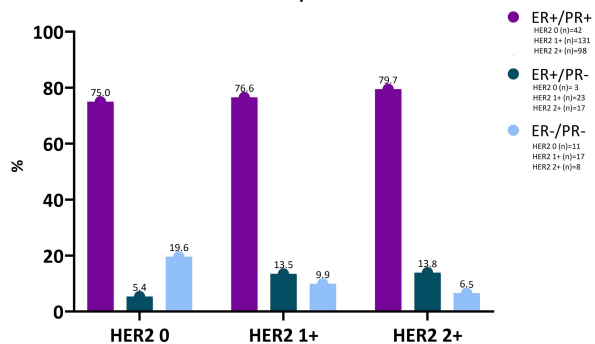
Results: Of the 350 cases, 16% (n=56) were 0, 48.9% (n=171) were 1+, and 35.1% (n=123) were 2+. On review, 84% (n=294) were classified as HER2-low. Histologic grade (see table) and ER/PR status (see figure) were recorded by HER2 score. The majority of HER2-low and HER2 0 IBC were FISH group 5 (see table). Of note, 6.5% (19/294) of the HER2-low cases were assigned to the non-classical FISH groups (groups 2-4) as compared to 1.8% (1/56) of the HER2 0 cases. Of the HER2-low cases

91.5% (n=269) were ER+ as compared to 80.4% (n=45) of HER2 0 cases. Oncotype DX was performed on 40.9% (n=110) of ER+ HER2-low cases with a mean RS of 15.8 (range=0-58); for HER2 0 IBC (42.2%, n=19) cases the mean RS was 14.7 (range=5-27).

HER2 IHC	Grade	Grade	Grade	FISH	FISH	FISH	FISH
				Group 5	Group 4	Group 3	Group 2
	%,(n)	%,(n)	%,(n)	%,(n)	%,(n)	%,(n)	%,(n)
0	37%(20)	33.3%(18)	29.6%(16)	98.2%(55)	0	0	1.8%(1)
1+	36.8%(63)	43.9%(75)	19.3%(33)	96.5%(165)	1.8%(3)	0.6%(1)	1.2%(2)
2+	33.3%(41)	48.8%(59)	17.9%(22)	89.4%(110)	9.8%(12)	N/A	0.8%(1)

Figure 1 - 189

Hormone Receptor Status



Conclusions: In our cohort, a majority of cases (84%; 294/350) that were originally classified as HER2 negative by the 2018 ASCO/CAP guidelines were classified as HER2-low, qualifying them for HER2-targeted ADC therapy in the appropriate clinical setting. As triple-negative IBC (TN; ER/PR/HER2 negative by current guidelines) has limited treatment options, the observation that a majority of TN IBC in this cohort (69.4%; 25/36) were classified as HER2-low raises the possibility that these patients may derive clinical benefit from HER2-targeted ADCs. This study adds to the limited literature available for this newly defined category. Additional evaluation is warranted to further assess the clinical benefit of treating HER2-low IBC with HER2-targeted ADCs. As acknowledged by others, the authors note that the distinction between 0 and 1+ is challenging, as such an alternate assay/methodology to reliably detect low HER2 expression is an important imperative for biomarker evaluation.

190 Biomarker Testing in Microinvasive Carcinoma (T1mi) of the Breast: A Study of 79 Cases Highlights Need for Clinicopathologic Guidelines

Olivier Michaud¹, Ami Patel², Syed Hoda³

¹New York-Presbyterian/Weill Cornell Medical Center, New York, NY, ²New York-Presbyterian/Weill Cornell Medicine, New York, NY, ³Weill Cornell Medicine, New York, NY

Disclosures: Olivier Michaud: None; Ami Patel: None; Syed Hoda: None

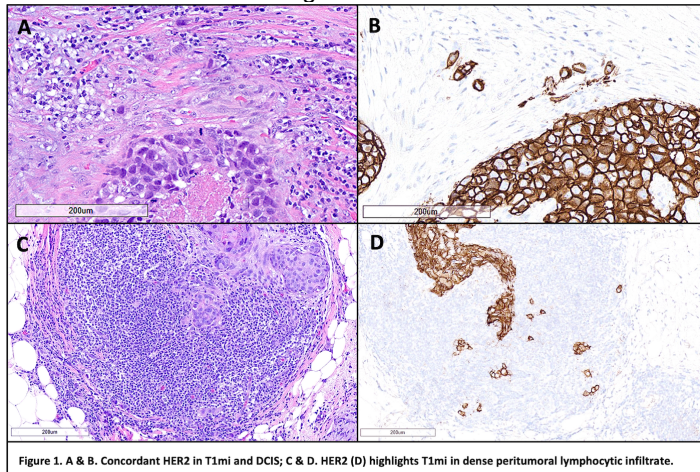
Background: Per NCCN 2022 (PMID: 35714673) and St. Gallen 2021 Guidelines (PMID: 34242744), the optimal clinical management of T1mi (≤ 0.1 cm) and the role of biomarkers in T1mi remain unclear. Emerging data suggest that T1mi and T1a (1- ≤ 5 mm) tumors show similar clinical behavior (PMID: 31342393) and that patients with T1mi benefit from anti-HER2 therapy (PMID: 34830989); however, data on biomarkers assessment and its relevance in T1mi remains limited.

Design: All relevant histopathological material and clinical data of consecutive cases of T1mi, diagnosed over 2 years: 07/20 to 06/22, were reviewed. Diagnosis of T1mi was confirmed. Immunohistochemical-based biomarker preparations (ER, PR, HER2 & Ki-67) were re-assessed in T1mi and concurrent *in situ* carcinoma.

Results: During the study period, 105 T1mi were diagnosed. 26 T1mi were not tested and excluded (larger invasive carcinoma or other T1mi elsewhere). 79 T1mi cases were studied (45 lumpectomies, 15 mastectomies, & 19 core biopsies; 61 ductal, 14 lobular & 4 mucinous). Nuclear grade was 2 in 43 cases, and 3 in 32 cases; with nuclear grade of concurrent *in situ* carcinoma being similar or lower in 63 of 65 cases with DCIS. T1mi comprised of <50 cells in 45 (57%) cases and >100 cells in 20 (25%) cases. ER, PR & HER2 assessment was possible in 60 (76%), 59 (75%) and 59 (75%) cases respectively; of which 38 (63%) were ER (+), 26 (33%) PR (+), and 25 (42%) HER2 (+). 2 of 6 HER2-equivocal (2+) cases were tested via FISH; one showed no amplification, and the other was inadequate (paucicellular). T1mi was no longer identified in slides from cases stained for ER (n:19), PR (n:20) and HER2 (n:20). 19 of these 20 cases comprised <100 cells. Assessment of proliferation was complicated or precluded by co-staining of Ki-67 in peritumoral lymphocytes and by paucicellularity. ER and HER2 status were concordant in T1mi

and concurrent *in situ* carcinoma in 96% and 93% of cases, respectively. Endocrine and HER2-targeted therapies varied in the cohort.

Figure 1 - 190



Conclusions: In this study of 79 T1mi, results for ER, PR and HER2 could be obtained in about 3/4 of cases. Loss of T1mi in immunostained slides was the main obstacle to the assessment of biomarkers, mostly in cases with <100 cells. ER & HER2 results in T1mi and associated DCIS were concordant in 96% and 93% of cases respectively. Ki-67 testing, when assessed, was complicated by co-staining of peritumoral lymphocytes and paucicellularity. Guidelines for testing and clinical utilization of biomarkers in T1mi are needed.

191 Can We Avoid Routine Excision for Atypical Ductal Hyperplasia Diagnosed on Breast Core Biopsy?

Nicolas Millan¹, Jamie Spoont², Omar Aljuboori¹, Barbara Susnik³

¹Jackson Memorial Hospital/ University of Miami Hospital, Miami, FL, ²University of Miami, Miami, FL, ³University of Miami Hospital, Miami, FL

Disclosures: Nicolas Millan: None; Jamie Spoont: None; Omar Aljuboori: None; Barbara Susnik: None

Background: In addition to long-term increased risk of breast carcinoma, atypical ductal hyperplasia (ADH) diagnosed on core biopsy (CB) is associated with an upgrade to invasive or ductal carcinoma *in situ* (DCIS) on follow-up surgical excision. Although single institution studies of ADH upgrades have shown that observation and surveillance can be a safe approach in a select subgroup of patients with well-sampled lesions, currently most patients with ADH on CB undergo surgical excision of the CB site. The aim of our study is to characterize features associated with upgrade of ADH at our institution and to establish criteria to identify a subset of patients with a low risk of upgrade, who may avoid surgical intervention.

Design: After institutional review board approval, we retrospectively collected imaging, clinical and pathologic data from January 2020 to June 2022 on patients with image-guided in-house performed CB with a diagnosis of ADH without coexistent invasive carcinoma or DCIS. Cases without excision at our hospital or lacking complete follow-up were excluded.

Results: A total of 44 patients were identified, aged 41 to 77 (median 56.5). Prior or synchronous carcinoma was established in 9 patients. Imaging target was: mass or asymmetry (17/44), calcifications (21/44), and MRI enhancement (7/44). 41 were vacuum-assisted biopsies and 43 used 9 or 12-gauge CB. Excluding a case of apocrine ADH with an upgrade to apocrine DCIS, all upgrades were ER-positive DCIS (6/43), and grade 1 or 2 (measuring 3 to 20 mm). The upgrades were seen in 3/21 CB targeting calcifications, 3/17 targeting masses (1/3 asymmetries), and 1/7 of MRI enhancements. In all upgrades of CB that targeted calcifications, calcifications were larger than 3 cm and were less than 50% removed by the CB procedure. Only the upgraded cases showed all three histological features in CB: at least two foci of ADH, complete duct involvement, and size no less than 2 mm.

Conclusions: The upgrade of ADH is limited to borderline and small low to intermediate grade DCIS and is related to the size of the targeted lesion, adequacy of sampling, and qualitative and quantitative extent of ADH in the CB. With the inclusion of additional cases and with careful pathologic-radiologic correlation we anticipate defining a subset of ADH with a low risk of upgrade. Our preliminary data based on a limited number of cases supports the non-surgical management of ADH in a subset of patients who may benefit from observation and surveillance instead of surgery.

192 Study of Pre-analytical effects on Breast Cancer Biomarkers

Mariel Molina¹, Pragya Virendrakumar Jain², Chandler Cortina², Ellen Schneider³, Yunguang Sun³, Hallgeir Rui³, Julie Jorns³

¹Froedtert and the Medical College of Wisconsin, Milwaukee, WI, ²Medical College of Wisconsin Affiliated Hospitals, Milwaukee, WI, ³Medical College of Wisconsin, Milwaukee, WI

Disclosures: Mariel Molina: None; Pragya Virendrakumar Jain: None; Chandler Cortina: None; Ellen Schneider: None; Yunguang Sun: None; Hallgeir Rui: None; Julie Jorns: None

Background: In recent years, breast cancer (BC) operations have largely become outpatient procedures. The decision for BC systemic therapy relies significantly upon the expression of three key biomarkers: estrogen receptor (ER), progesterone receptor (PR) and human epidermal growth factor receptor-2 (HER2). One drawback of outpatient BC procedures is that there may be no physical on-site pathology presence for punctual specimen processing, and therefore, delays in specimen transport and processing can have significant negative impacts on BC biomarker expression (i.e., false negatives), potentially resulting in omission of targeted systemic therapy. We aimed to evaluate the effect of practical alternatives, such as refrigeration and freezing, on BC biomarker expression.

Design: Benign prophylactic mastectomy specimens from five patients were rapidly delivered to pathology, and from each, 4 "mock lumpectomies" were procured and assigned to one of 4 arms: room temperature (20-22°C) without formalin, room temperature (20-22°C) with formalin, (pre-chilled) refrigerated formalin (4°C), and freezer (-18°C) without formalin. Excision into and submission of central tissue to create tissue blocks was done at 3 timepoints: 30-60 minutes, >90<120 minutes and 12-18 hours. Immunohistochemical (IHC) stains for ER, PR, HER2, and Ki-67 were performed. IHC was blindly quantitated using digital pathology software (QuPath®). The room temperature formalin arm was used as the "standard" control arm and compared with the remaining arms using two-tailed T-tests. Small tissue fragments were procured for future RNA analysis.

Results: The median age of patients was 54 (range 30-66 years), median "mock lumpectomy" volume 25 cm³ (range 14.9-36.7 cm³) and median weight 13.8 g (range 6.4-22.1 g). The refrigerated formalin study arm showed statistically significant preservation of ER expression compared to the room temperature formalin control arm ($p=.027$). Other study arms did not show differences in ER expression (Figures 1-2). Similarly, the refrigerated formalin arm alone showed preservation of Ki-67 that approached statistical significance ($p=.07$). Statistical analysis of PR and HER2 is pending.

Figure 1 - 192

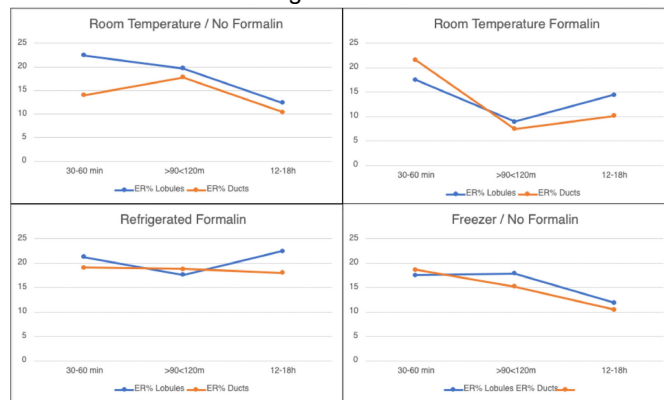
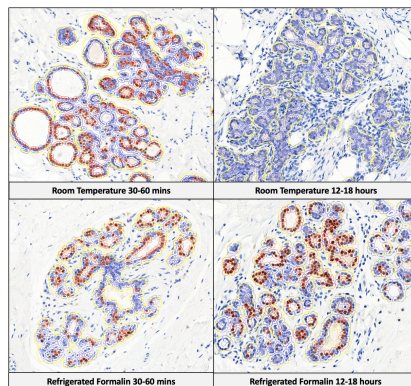


Figure 2 - 192



Conclusions: Our novel pilot study shows promising results suggesting refrigerated formalin as the best alternative to preserve ER expression when surgical specimens may not be able to be rapidly triaged or grossed. However, larger scale studies utilizing BC specimens are needed to assess the reproducibility of these findings.

193 HER2 0, HER2 1+ and HER2 2+/FISH Negative Breast Cancers Are Biologically Different

Khin Su Mon¹, Hui Zhang¹, Alessa Aragao², Ping Tang¹

¹Loyola University Medical Center, Maywood, IL, ²Mayo Clinic, Rochester, MN

Disclosures: Khin Su Mon: None; Hui Zhang: None; Alessa Aragao: None; Ping Tang: None

Background: The results of DESTINY-Breast04 trial reported at ASCO 2022 have established that Trastuzumab Deruxtecan, the anti-HER2 antibody drug conjugate, is a new standard of care for HER2-low metastatic breast cancer. HER2-low is defined as HER2 1+ or 2+ by IHC analysis and negative by FISH analysis, and HER2 negative breast cancer, including HER2 0 and HER2-low subgroup, consisting of roughly 85% of all breast cancer, which was not previously eligible for HER2 target therapy. Thus, this newly developed HER2 target therapy can potentially help a significant portion of breast cancer patients.

Design: We identified 2683 consecutive HER2 negative breast cancer treated in our institution during last 20 years, to determine the frequency of HER2-low breast cancer (HER2 1+ or HER2 2+/FISH negative). We also compared the clinical and pathological features among these three groups (HER2 0, HER2 1+ and HER2 2+/FISH negative) of HER2 negative breast cancer.

Results: Among these 2683 cases of HER2 negative breast cancer, 46% (1229 cases) belonged to HER2-low subgroup (Table). 13% of HER2-low breast cancer are ER/PR negative, compared to 20% in HER2 0 subgroup. These three groups of HER2 negative breast cancer are significantly different in patient age, tumor size, and tumor types. Histologic grade and tumor markers are also different among these three groups with significantly more high grade and >20% Ki-67 cancers in HER2 2+/FISH negative subgroup. More importantly, HER2 2+/FISH negative subgroup has significantly more >3 node metastasis and local or/and distant recurrence compared to HER2 0 or HER2 1+ subgroup.

	HER2 0	HER2 1+	HER2 2+	p-value
Case No.	1454	819	410	2683
Age (y)	25-98	24-101	28-96	0.0219
<40	75 (5%)	21 (3%)	13 (3%)	
40-60	594 (41%)	361 (44%)	167 (41%)	
>60	785 (54%)	437 (53%)	230 (56%)	
Tumor size (cm)				0.0046
<2.1	1011 (*28) (70%)	541 (*47) (66%)	246 (*38) (60%)	
2.1-5	288 (*40) (19%)	186 (*39) (23%)	109 (*18) (27%)	
>5	54 (4%)	43 (*3) (5%)	17 (*3) (4%)	
No data ****	101 (7%)	49 (6%)	38 (9%)	
Tumor type				<0.0001
IDC	1154 (** 122) (80%)	610 (**112) (75%)	345 (**42) (84%)	
ILC	217 (**23) (15%)	94 (**15) (11%)	51 (**7) (12%)	
Other	35 (**2) (2%)	115 (**2) (14%)	14 (**1) (4%)	
No data ****	48 (3%)	0	0	
Histologic grade				<0.0001
1	291 (20%)	166 (20%)	45 (11%)	
2	682 (47%)	441 (54%)	199 (48%)	
3	441 (30%)	201 (25%)	155 (38%)	
No data ****	40 (3%)	11 (1%)	11 (3%)	
Tumor markers				
ER/PR negative	300 (21%)	90 (11%)	67 (16%)	<0.0001
ER/PR low***	21 (1%)	6 (0.7%)	6 (2%)	
ER/PR positive	1128 (78%)	717 (88%)	337 (82%)	
No data ****	5 (0.1%)	6 (0.7%)	0	
Ki67				0.0029
<20%	839 (58%)	496 (61%)	211 (51%)	
>20%	507 (35%)	268 (33%)	175 (43%)	
No data ****	108 (7%)	55 (6%)	24 (6%)	
LN				0.0154
0	913 (63%)	483 (59%)	231 (57%)	
1-3	273 (19%)	170 (21%)	70 (17%)	
>3	78 (5%)	52 (6%)	38 (9%)	
No data ****	190 (13%)	114 (14%)	71 (17%)	
Recurrence				0.0004
Yes	141 (10%)	88 (11%)	68 (17%)	
No	1313 (90%)	731 (89%)	342 (83%)	

* Number of cases that are multifocal

** Number of cases that received neoadjuvant treatment, not including all PCR cases

*** ER/PR low defined as either ER or PR with an Allred Score of 3, while the other marker is negative or Allred score of 3

**** For statistical purpose, cases with no data were excluded from the analysis

Conclusions: This study has clearly demonstrated the biological difference among the three subgroups of HER2 negative breast cancer: HER2 0, HER2 1+, and HER2 2+/FISH negative. It provides the biological basis for the new HER2 target treatment of anti-HER2 antibody and drug conjugate.

194 Phyllodes Tumor of The Breast, A 18 Year Experience of a Single Institution

Khin Su Mon¹, Hui Zhang¹, Alessa Aragao², Ping Tang¹

¹Loyola University Medical Center, Maywood, IL, ²Mayo Clinic, Rochester, MN

Disclosures: Khin Su Mon: None; Hui Zhang: None; Alessa Aragao: None; Ping Tang: None

Background: Phyllodes tumor (PT) is a rare biphasic breast tumor, consisting of <1% of all breast tumors. It ranges from benign to borderline and malignant subtypes based on its morphologic features, which can overlap among themselves and with subtypes of fibroadenomas (FA). Recent findings of the recurrence mutation of mediator complex subunit 12 (MED12) and telomerase reverse transcriptase (TERT) hotspot mutation in PT and FA have not only shed light on their pathogenesis but also can serve as great tools for differential diagnosis of them. Biologically, PT can be locally aggressive; thus, historically, 1cm surgical margins were recommended for all subtypes of PT. However, breast surgeons across the country often do not follow this radical recommendation, as it may significantly compromise the cosmetic result of surgery. Based on recent data, NCCN (version 2.2022) has revised its recommendation for PT treatment: simple excision for benign PT and wide excision with 1cm margin for borderline and malignant PT.

Design: We have retrospectively identified 75 cases of PT diagnosed and treated in our institution for last 18 years, in an effort to find the practice pattern, and the relationship between local recurrence and margin status, tumor size, and patients' age.

Results: Among the 75 cases of PT treated in our institution for 18 years; all were treated with surgical excision only (Table). The benign, borderline and malignant PT consisted of 87%, 7%, and 5% of these tumors respectively. 12% (9 cases) of PT were in patients 18 years of age or younger, and 84% of cases with tumors 5cm or smaller. Three patients (4%) had recurrence, all occurred within 3 years of original diagnosis, only one with close <1mm margin, and 45% of cases with positive or close (<1mm) margins did not recur. Two patients with local recurrence were from benign PT and one patient with lung metastasis was from malignant PT. Both local recurrence cases occurred in patients with benign PT >2cm in size, occurred within 1 year (with negative margin) and 3 years (with <1mm margin) after original diagnosis. One malignant PT metastasized to lung only one year after original diagnosis (with negative margins) in a 64-year-old with a 5.5cm tumor. None of the patients aged 18 years old or younger have recurrence.

	PT no recurrence	PT with recurrence	P value
Case No.	72	3	
Age	12-74	38-64	1.000
<18	9 (13%)	0	
>18	63 (87%)	3 (100%)	
PT subtype			0.3785**
Benign*	63 (87%)	2 (67%)	
Borderline*	5 (7%)	0	
Malignant	3 (4%)	1 (33%)	
Unclassified	1 (2%)	0	
Size			0.4032
<2*	26 (35%)	0	
2-5*	35 (49%)	2 (67%)	
>5	11 (16%)	1 (33%)	
Margins			0.8647**
Positive*	21 (30%)	0	
<1mm*	11(16%)	1 (33%)	
>1mm or negative	38 (54%)	2 (67%)	

*Groups combined for statistically analysis

** P-value with Yates correction

Conclusions: Benign PT can recur, often associated with larger tumors and older patients. The recurrence of PT is not associated with margin status.

195 Serum Inflammatory Profiles in Immunophenotypes of Breast Carcinoma: Correlation with Clinicopathological Factors

Yoel G Montoyo-Pujol¹, Pascual Martínez-Peinado², Sandra Pascual-García², Ana Belén López-Jaén², Elena Castellon-Molla¹, Silvia Delgado-García¹, Tina Martin¹, Hortensia Ballester Galiana¹, Angela Ramos-Montoya³, Jose Ponce⁴, Inmaculada Lozano-Cubo³, José Miguel Sempere Ortells², Gloria Peiro¹

¹Dr. Balmis University General Hospital, Alicante Institute for Health and Biomedical Research (ISABIAL), Alicante, Spain, ²University of Alicante, Alicante, Spain, ³University General Hospital of Alicante, ISABIAL, Alicante, Spain, ⁴University General Hospital of Alicante, ISABIAL-FISABIO, Alicante, Spain

Disclosures: Yoel G Montoyo-Pujol: None; Pascual Martínez-Peinado: None; Sandra Pascual-García: None; Ana Belén López-Jaén: None; Elena Castellon-Molla: None; Silvia Delgado-García: None; Tina Martin: None; Hortensia Ballester Galiana: None; Angela Ramos-Montoya: None; Jose Ponce: None; Inmaculada Lozano-Cubo: None; José Miguel Sempere Ortells: None; Gloria Peiro: None

Background: Inflammation is essential to induce an effective immune response and mediates tumor initiation and promotion. Maintenance of serum inflammatory mediators (IM) has been related to immunosuppressive cell recruitment and immune checkpoint expression. In breast cancer (BC), their release has been linked to tumor invasion, progression, metastasis and treatment resistance. However, little is known about their serum profile in BC phenotypes.

Design: Pretreatment serum from 204 BC patients (23% Luminal A, 23.6% Luminal B/HER2-, 22.5% Luminal B/HER2+, 10.3% HER2-enriched and 20.6% Triple-Negative/Basal-like -TNBL-) and 50 healthy donors was collected. Measurement of 62 IM was performed using LEGENDplex immunoassay. Fluorescence intensity was quantified by flow cytometry. The results were correlated with clinicopathological factors (age, tumor size and grade, vascular invasion, necrosis, immunophenotype, tumor-infiltrating lymphocytes -TILs-, lymph-node status and Ki67). Statistical analysis was done by Student's t-test and Mann-Whitney U test.

Results: Compared to the healthy group, BC patients showed higher levels of SCF, MIP3α, EPO and 4-1BB but lower levels of IL-2RA, IL-8, IL-12p40, IL-18, IL-23, IL-27, PDGF-AA, Galectin9, PDGF-BB, B7.2, MIP1β and PD1. Furthermore, IL-23, IL-27 and EPO correlated with younger age ($p \leq 0.041$), in contrast to Galectin9, MCP1, IL-2RA and MIP1β ($p \leq 0.003$). IL-12p40 and IFNγ were elevated in grade I ($p \leq 0.05$) and, in addition to IL-11 and IL-27, in low Ki67 tumors ($p \leq 0.030$). Moreover, IL-12p40 and IL-23 were associated with positive lymph nodes ($p \leq 0.031$). In Luminal tumors we detected high IL-12p40, IL-15, IL-23, IL-27 and IFNγ ($p \leq 0.048$), but only PDGF-BB in non-Luminal ($p = 0.040$). IL-12p40, IL-18, IL-23, IL-27, SCF and EPO were mainly higher in Luminal A, while PDGF-AA in Luminal B/HER2-. Likewise, Luminal B/HER2+ serum was elevated for MIP1β, MIP3α and EPO, whereas Galectin9, PDGF-BB, IL-2RA, B7.2, SCF, 4-1BB and PD1 were found in TNBL, with no specific profile for HER2-enriched.

Conclusions: Our results showed a specific serum profile of IM among BC phenotypes. Moreover, IL-12p40 and IL-23 were correlated with unfavourable characteristics in Luminal tumors, especially in Luminal A.

Supported by Grant (SEAP-Proyecto Semilla; Expt. 200042); Biobank HGUA (21-154) and HUB-ICO-IDIBELL (PT17/0015/0024).

196 Clinicopathologic Features and Prognosis in Metastatic or Recurrent Breast Carcinoma with ESR1 Genetic Abnormalities

Jennifer Moreira-Dinze¹, Haiying Zhan¹, Uma Krishnamurti¹, Malini Harigopal², Yuanxin Liang²

¹Yale School of Medicine, Yale New Haven Hospital, New Haven, CT, ²Yale School of Medicine, New Haven, CT

Disclosures: Jennifer Moreira-Dinze: None; Haiying Zhan: None; Uma Krishnamurti: None; Malini Harigopal: None; Yuanxin Liang: None

Background: Approximately 80% of breast cancers are estrogen receptor (ER) positive making endocrine therapy the first line of treatment and current standard of care. Despite therapy, 20% of patients develop resistance after long-term therapy. There are many genetic alterations associated with endocrine resistance including Estrogen Receptor 1 (ESR1) alterations. In this study, we analyze clinicopathologic features and prognosis in metastatic or recurrent breast carcinoma with ESR1 genetic abnormalities.

Design: We evaluated 81 breast carcinoma patients with available Oncomine genetic profile on metastatic or recurrent tumors. They had undergone standard therapy according to their clinicopathologic stage and subsequently developed tumor metastasis or recurrence. The mean follow-up time was 63 months (range 0-315.8). The follow-up endpoint was defined as metastasis or recurrence. Clinicopathological evaluation and survival analysis was performed to compare the groups of ESR1 mutation (ESR-MUT), ESR1 wild-type with positive ER (ESR-WT ER+), and ESR1 wild-type with negative ER (ESR-WT ER-).

Results: There was no statistical difference of age, gender, laterality, histological types, pathologic stages and tumor biomarkers among the groups of ESR-MUT, ESR-WT ER+ and ESR-WT ER-. All the ESR-MUT breast cancer cases were ER positive and well to moderately differentiated, while ESR-WT ER+ and ESR-WT ER- breast cancers were poorly differentiated in 31% and 85%

cases, respectively. Among the ER positive breast cancers, although ESR1-MUT breast cancer showed significantly lower (1-2) Nottingham grade (100% vs. 69% in ESR-WT ER+ cases, $p<0.0262$), ESR-MUT patients' disease-free survival time appeared to be shorter than ESR-WT ER+ patients (median 51.7 months vs. 57.8 months, $p>0.05$). ESR-WT ER- patients had shorter survival time with no statistical significance ($p>0.05$) (Fig. 1). The most common (7/12) ESR1 mutation was D538G variant, 5 out of these 7 cases had liver and/or bone metastasis.

Table1: The clinicopathological characteristic summary of ESR1				P value	
	ESR1-MUT (n=12)	ESR1-WT (n=66)			
		ER pos (n=52)	ER neg (n=14)		
Median age (range)	54 (31-89)	56 (31-70)	63 (25-79)	0.8138	
Gender	Female	12	51	0.7540	
		0	1		
Laterality	Left	7	23	0.9483	
	Right	7	28		
Histologic type:	Ductal*	7	36	0.3030	
	Lobular	1	13		
Nottingham Grade	Grade 1-2	100% (13/13) **	69% (33/48)**	<0.0001 (multiple groups) 0.0262 (ESR1 vs. ER pos) <0.0001 (ESR1 vs. ER neg)	
	Grade 3	0% (0)	31% (15/48)		
Initial T stage (\geq pT2) ***	71.4% (5/7)	35.5% (11/31)	50% (2/4)	0.2117	
Lymph node metastasis (N) at initial diagnosis	80% (4/5)	53.3% (16/30)	55.6% (5/9)	0.5354	
Distant metastasis (M) at initial diagnosis	20% (3/15)	7.7% (4/52)	14.3% (2/14)	0.3756	
Disease free interval, months (median, range)	51.7 (0-232.4)	57.8 (0-315.8)	31.8 (0-178.4)	0.2378	
ER positive	100% (15/15)	100%	0%	0.0613	
Her2 positive	6.7% (1/15)	3.9% (2/51)	7.1% (1/14)	0.8403	
Because of the remote history of resection and/or resection in an outside institution, the entire information may not be available on all cases.					
* One invasive ductal carcinoma case with neuroendocrine differentiation.					
** One well differentiated carcinoma in ESR1 group, two well differentiated carcinoma in ER pos group.					
*** Neoadjuvant cases were excluded from the statistical analysis on the initial T stage.					

Figure 1 - 196

Survival

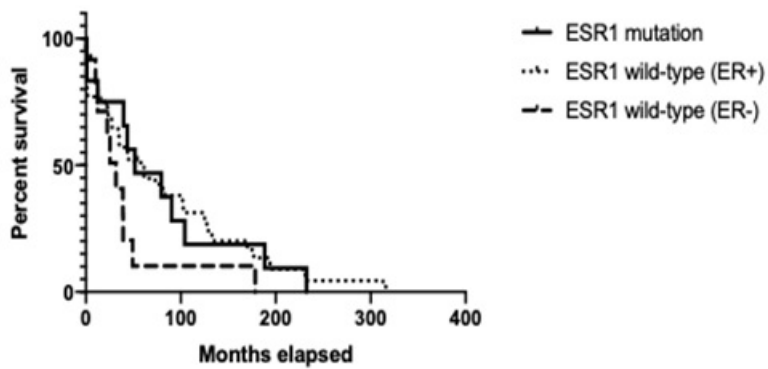


Figure 1: The disease-free survival of ESR1-mutation, ESR1-wild-type ER positive and ESR1-wild-type ER negative groups.

Conclusions: Endocrine therapy resistance is a main concern in ESR1 mutated breast cancer. It probably explains that although patients with ESR1 mutation had lower grade cancer, they did not show longer survival time. Therefore, endocrine therapy alone is not favored in ESR1 mutated breast cancer, instead combination with other chemotherapeutic agents is now being considered as the new standard of care. ESR1 genetic abnormalities may need to be tested in metastatic or recurrent breast cancer, especially when the primary tumor is well to moderately differentiated.

197 Upgrade Rates of Pleomorphic and Florid Lobular Carcinoma in Situ Diagnosed on Core Needle Biopsy: One Healthcare Network's Experience

Doaa Morrar¹, Sudarshana Roychoudhury², Reham Al-Refai¹, Yousstina Salib¹, Liana Kataw³, Ziya Karimov⁴, Shabnam Jaffer¹, Sabina Hajiyeva¹

¹Northwell Health Lenox Hill Hospital, New York, NY, ²Donald and Barbara Zucker School of Medicine at Hofstra/Northwell, New York, NY, ³Seton Hall University, South Orange, NJ, ⁴Ege University Faculty of Medicine, Izmir, Turkey

Disclosures: Doaa Morrar: None; Sudarshana Roychoudhury: None; Reham Al-Refai: None; Yousstina Salib: None; Liana Kataw: None; Ziya Karimov: None; Shabnam Jaffer: None; Sabina Hajiyeva: None

Background: Lobular carcinoma in situ (LCIS) is a group of mammary in situ carcinomas that occur in terminal duct lobular units (TDLU) and is characterized by loss of cellular cohesion. Classic LCIS (c-LCIS) is characterized by small dyscohesive cells with uniform hyperchromatic nuclei to slightly larger vesicular nuclei with mild variability, filling and expanding more than half of TDLU. When c-LCIS creates a confluent mass-like architecture with little to no intervening stroma between markedly distended TDLU and/or expands acinus or duct by filling an area equivalent to 40-50 cells in diameters, it is classified as Florid LCIS (f-LCIS). Pleomorphic LCIS (p-LCIS) is characterized by large dyscohesive cells with marked nuclear pleomorphism with nuclear size over four times the size of a lymphocyte (equivalent to the cells of high-grade ductal carcinoma in situ (DCIS)).

Design: We retrospectively identified all in-house core needle biopsies (CNB) obtained between January 2011- June 2022 with f-LCIS and/or p-LCIS. We reviewed all CNB slides and assessed radiologic-pathologic concordance. The biopsy target, imaging modality, size of the target, gauge of the biopsy needle, type of surgery, and outcomes were reviewed. An upgrade on excision was defined as invasive carcinoma (IC) and DCIS in the excision material. The excision slides of all upgraded cases were re-reviewed.

Results: Out of ~32000 consecutive CNBs in the study period, 122 CNBs yielded f-LCIS, p-LCIS, or combined p-LCIS and f-LCIS, with classic lobular neoplasia. We excluded 60 CNBs with prior/concurrent carcinoma and 16 without available excisional material. After re-review, we reclassified 6 cases, one from DCIS to p-LCIS and 5 "extensive" c-LCIS to f-LCIS. The final p/f - LCIS study cohort consisted of 46 CNBs. The CNB targeted mammographic calcifications in 33 (71.7%) cases, MRI non-mass enhancement in 6 (13%), and 3 (6.5%) sonographic mass. All CNBs were deemed radiologic-pathologic concordant. Excision yielded 10 (21.7%) invasive carcinomas, spanning 1-12 mm, and 5 (10.8%) cases of DCIS. One additional case showed atypical ductal hyperplasia on excision.

Figure 1 – 197

Figure 1: Summary of study design and results

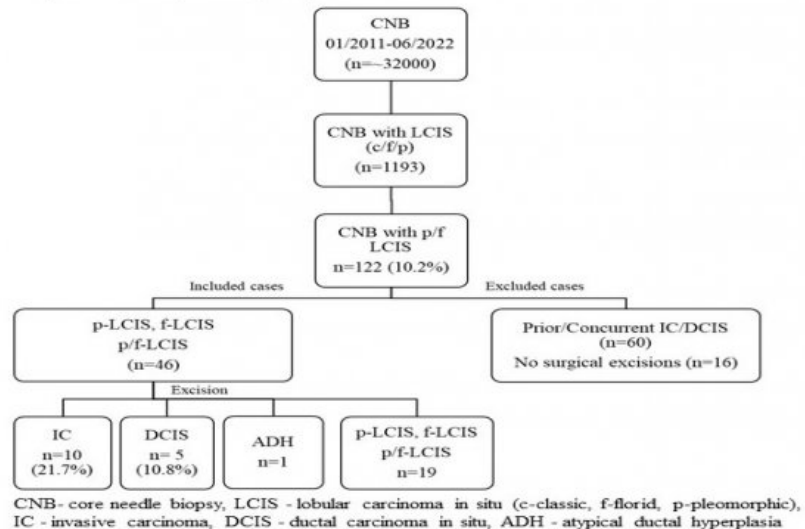
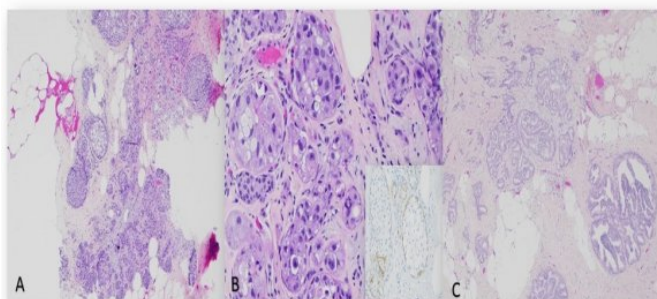


Figure 2 – 197

Figure 2: Example of pleomorphic LCIS with an upgrade at excision

A: Core needle biopsy with p-LCIS (H&E 40X);
B: High power showing nuclear features (H&E 200X), inset: E-cadherin
C: Tissue from excision specimen with focus of invasive carcinoma (H&E 40X)

Conclusions: The upgrade rate of p/f-LCIS was 32.6%. Compared to c-LCIS, most of the cases in the study cohort were imaging targets and not incidental. Previously reported by our group, the upgrade rate of c-LCIS on excision was 3.8%. We conclude that surgical management should be recommended for any non-classic LCIS (p-LCIS and f-LCIS) diagnosed on CNB.

198 A Retrospective Analysis of Clinical and Pathologic Variables Predict Recurrence in Ductal Carcinoma *in Situ*

Matthew Mullally¹, Sean Hacking², Christine Yu³, Evgeny Yakirevich⁴, Yihong Wang⁵

¹Brown University, Rhode Island Hospital, Lifespan, Providence, RI, ²Laboratory Medicine Program, Departments of Anatomical Pathology, University Health Network and University of Toronto, Toronto, ON, ³Brown University Lifespan Academic Medical Center, Providence, RI, ⁴Rhode Island Hospital, Providence, RI, ⁵Brown University, Rhode Island Hospital, Providence, RI

Disclosures: Matthew Mullally: None; Sean Hacking: None; Christine Yu: None; Evgeny Yakirevich: None; Yihong Wang: None

Background: The incidence of ductal carcinoma *in situ* (DCIS) has risen mainly due to improved capabilities of non-invasive detection through mammographic screenings. Risk in patients with DCIS following breast-conserving surgery primarily involves recurrence. Various clinical and pathological variables are implicated in prediction of the risk of recurrence outcomes in women diagnosed with DCIS.

Design: In a retrospective study of 446 patients diagnosed with DCIS between 2006 and 2011, with first recurrence greater than 6months after initial DCIS treatment and with >10 years of follow-up were included in this study. Clinical and pathological variables were reviewed in relation to the recurrence of DCIS. "Low-risk" was defined as disease-free since the DCIS diagnosis and surgery; while "high-risk" included recurrence of ipsilateral DCIS and ipsilateral invasive breast carcinoma (IBC).

Results: Of the 446 patients, 9 had a local DCIS recurrence, 17 had an IBC recurrence, and one had both. The mean time to recurrence was 107 months, median 112 months and range 14 -185 months. These 27 cases were collectively grouped as "High Risk." When looking at patients as high or low risk, surgical margin was found as significant ($P = 0.0354$), Table 1. Notably, when comparing DCIS and invasive recurrences separately, ipsilateral DCIS recurrence was found to be more strongly associated with positive margin ($P = 0.0019$). When comparing those with invasive recurrence to those without, high DCIS grade was significantly associated with recurrence ($P = 0.0270$). For clinical variables, race was significantly associated with recurrence, with those of African American descent have a higher relative incidence ($P = 0.0282$). Kaplan Meier curves demonstrated hormone treatment ($P = 0.0050$) and Radiation ($P = 0.0369$) to be associated with improved recurrence-free survival (RFS).

	High Risk vs. Low Risk	
	High Risk	Low Risk
Number	27	419
Age	$P = 0.8433$	
High (≥ 65)	12	200
Low (<65)	15	219
Racial Origins	$P = 0.5008$	
African Decent	2	15
Asian Decent	0	5
European Decent	25	388
Unknown	0	11
Hispanic Origin	$P = 1.000$	
Hispanic Origin	0	11
non-Hispanic	26	388
Unknown	1	20
Tobacco Use History	$P = 0.6353$	
No Tobacco Use	11	185
Previous Tobacco Use	9	112
Unknown	7	122
Tumor Size	$P = 0.3834$	
High ($\geq 25\text{mm}$)	2	62
Low ($<25\text{mm}$)	16	228
Hormone Treatment vs. No Treatment	$P = 0.1362$	
Hormone Treatment	12	127
No Hormone Treatment	15	292
Estrogen Receptor	$P = 0.5502$	
Negative	2	57
Positive	19	262
Radiation Treatment vs No Radiation	$P = 0.3178$	
No Radiation	16	204
Radiation	10	197
Surgical Margins	$P = 0.0354$	
Negative	12	201
Close	5	86
Positive	7	30
Grade	$P = 0.1120$	
Low	1	48
Intermediate	15	145
High	9	156
Mastectomy Vs. Partial or Less	$P = 0.4642$	
Partial Mastectomy or Less	19	296
Total Mastectomy	7	79

High Risk Individuals In Relation to Various Clinical and Pathological Variables.

Conclusions: Pathological variables such as surgical margin appear to have a significant impact on recurrence. Despite having less significance with clinical variables, it was interesting to see the association of AA race with recurrence in our patient population. Future prospective studies are necessary to determine variables which lead to recurrence in diverse patient populations.

199 Assessment of Size of Locally Advanced Breast Carcinoma After Neoadjuvant Chemotherapy (NACT): A Retrospective Study of 44 Cases Evaluating Extent of 'Tumor Bed' by Imaging Techniques, Gross & Microscopic Examination

Carlos Munoz-Zuluaga¹, Olivier Michaud², Laura Munoz-Arcos², Syed Hoda³

¹New York-Presbyterian/Weill Cornell Medicine, New York, NY, ²New York-Presbyterian/Weill Cornell Medical Center, New York, NY, ³Weill Cornell Medicine, New York, NY

Disclosures: Carlos Munoz-Zuluaga: None; Olivier Michaud: None; Laura Munoz-Arcos: None; Syed Hoda: None

Background: Assessment of 'tumor bed' size (TB) by imaging (I-TB) is clinically crucial in the management of breast carcinoma (ca) in patients undergoing NACT. TB must also be pathologically assessed via gross exam (G-TB) and microscopic exam (M-TB) for calculation of Residual Cancer Burden (RCB, <http://www3.mdanderson.org/app/medcalc/>). However, the measurement of TB can be problematic when the microscopic and gross extents differ. In this study, we compared the tumor size at presentation by imaging (I-preNACT), to I-TB, G-TB and M-TB.

Design: All relevant clinicopathologic material of patients with invasive breast ca s/p NACT over a 11-month period (08/21-06/22) was reviewed. I-preNACT, I-TB, G-TB & M-TB were analyzed and compared, using the largest dimension as a surrogate for TB.

Results: A total of 44 patients (median age: 52 [26-95]) were studied. Of these patients, 37 (84%) presented with invasive ductal ca, 32 (72%) were grade 3 and 17 (39%) had multifocal or multicentric disease before initiation of NACT. On pre-NACT testing: 14 (32%) were ER-/PR-/HER2+, 13 (30%) were triple-negative, 12 (27%) were ER+/PR+/HER2-, and 5 (11%) were triple-positive.

Median interval from diagnosis to surgery (mastectomy in 23 (52%) and lumpectomy in 21 (48%)), was 6 months (interquartile range (IQR): 5-7). Median I-preNACT was 2.4 cm (n: 44, IQR: 1.8-3.6) and median I-TB was 0.2 cm (n: 41, IQR: 0-1.8). Regardless of the presence of residual ca, median G-TB was 2.0 cm (n: 42, IQR: 0.7-3.3) and median M-TB was 1.8 cm (n: 40, IQR: 1.4-3.0). Twenty-three (52%) cases showed residual invasive ca with median largest contiguous focus (ypT, per AJCC/TNM System) of 1.0 cm (IQR: 0.4-1.8) with associated median M-TB of 2.1 cm (IQR: 1.5-3.3).

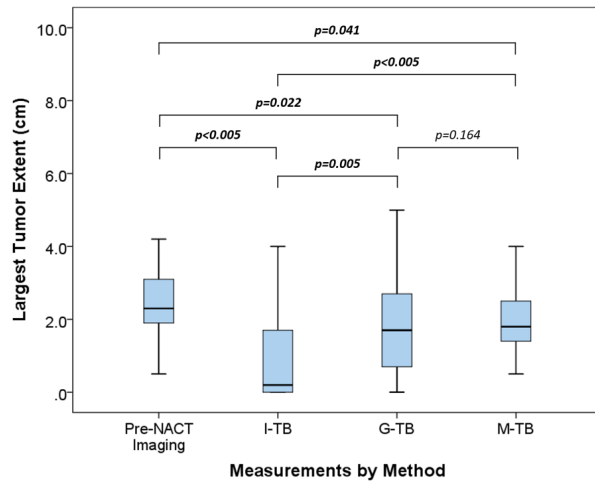
Table 1. Changes in largest dimension of tumor size/bed between different measurement methods of invasive breast carcinomas undergoing neoadjuvant chemotherapy				
Tumor Size	I-preNACT to	I-preNACT to	I-preNACT to	G-TB to
Change	I-TB	G-TB	M-TB	M-TB
Increased	2 (5%)	11 (26%)	9 (22%)	12 (30%)
No change	1 (2%)	5 (12%)	10 (24%)	20 (50%)
Decreased	38 (93%)	26 (62%)	22 (54%)	8 (20%)

I-preNACT: tumor size at presentation by any imaging modality, I-TB: Imaging tumor bed, G-TB: Gross tumor bed, M-TB: microscopic tumor bed.

Table based on available data

Figure 1 - 199

Figure 1. Comparison of largest tumor extent pre-neoadjuvant chemotherapy (NACT), post-NACT by imaging, by gross and microscopic exam



I-TB: Imaging tumor bed, G-TB: Gross tumor bed, M-TB: microscopic tumor bed
Wilcoxon Rank Sum Test was used to determine significant differences between groups

Conclusions: In this study, (1) I-TB did not correlate with either G-TB or M-TB, (2) There was no statistically significant difference between G-TB and M-TB. (3) ypT per AJCC/TNM criteria differed from TB size per RCB criteria in all cases studied. Assessment of TB can be a complicated matter in some cases.

200 Genome-Wide Analysis of the DNA Methylation Profile Reveals a Prognostic CpG Island Methylator Phenotype in Advanced Breast Tumors

Eva Musulen¹, Aleix Noguera-Castells², Patricia Villagrassa³, Jordi Canes⁴, Tomás Pascual⁵, Patricia Galvan⁵, Aleix Prat⁵, Eva Ciruelos⁵, Sonia Pernas⁶, Manel Esteller²

¹Hospital Universitari General de Catalunya, Institut de Recerca contra la Leucèmia Josep Carreras, Barcelona, Spain,

²Institut de Recerca contra la Leucèmia Josep Carreras, Badalona, Spain, ³REVEAL GENOMICS, SL., Barcelona, Spain,

⁴SOLTI Breast Cancer Research Group, Barcelona, Spain, ⁵Hospital Clínic de Barcelona, Barcelona, Spain, ⁶Catalan Institute of Oncology (ICO), Barcelona, Spain

Disclosures: Eva Musulen: None; Aleix Noguera-Castells: None; Patricia Villagrassa: None; Jordi Canes: None; Tomás Pascual: None; Patricia Galvan: None; Aleix Prat: None; Eva Ciruelos: None; Sonia Pernas: None; Manel Esteller: None

Background: In the era of multiomics data there is still no classification based on breast cancer (BC) epigenetics. Therefore, the establishment of an epigenetic signature based on DNA methylation for classifying BC patients with clinical outcome would be essential to better classify BC.

Design: The present study aimed to assess the feasibility of a molecular screening program of advanced BC to facilitate the access to matched-targeted therapies. DNA sequencing of 74 cancer-related genes was performed using FFPE tumor samples. Gene expression was evaluated using a custom 55-gene panel on the nCounter. Intrinsic subtypes were determined by the

research-based PAM50 predictor. DNA methylation profiles was performed using the Infinium Methylation EPIC Kit (Illumina, Inc, San Diego, CA) (~850,000 CpG sites). Survival analysis using Kaplan-Meier curves and Cox regression analysis were performed.

Results: Methylation data were obtained from 113 (37%) patients, 76 primary and 37 non-paired metastatic tumors. According to the IHC subtype, 83 (74%) were HR+/HER2; 13 (11%) HER2+ and 17 (15%) triple-negative (TNBC). The PAM50 subtypes were 30 (26%) Luminal A, 21 (19%) Luminal B, 19 (17%) basal-like, HER2-enriched 15 (13%), 10 normal-like (9%), and 18 (16%) were not available. An unsupervised consensus clustering analysis of the top 1% most variable CpG probes was performed, and 3 groups of patients were established according to CpG island methylator phenotype (CIMP) as CIMP-low, CIMP-intermediate(int) and CIMP-high (Fig. 1). The BC CIMP-low was enriched with the TNBC, basal-like subtypes and mutation in *TP53*, and was associated with a worse OS compared to CIMP-int/high tumors (Fig. 2). We established a CIMP epigenetic signature, and with only 15 CpG probes from the CIMP signature a machine learning algorithm (MLA) was trained to predict methylation BC subtypes in ABC tumors. The MLA classified with high specificity (0.939) and sensitivity (0.909) CIMP-low tumors of an external validation cohort from the TCGA.

Figure 1 - 200

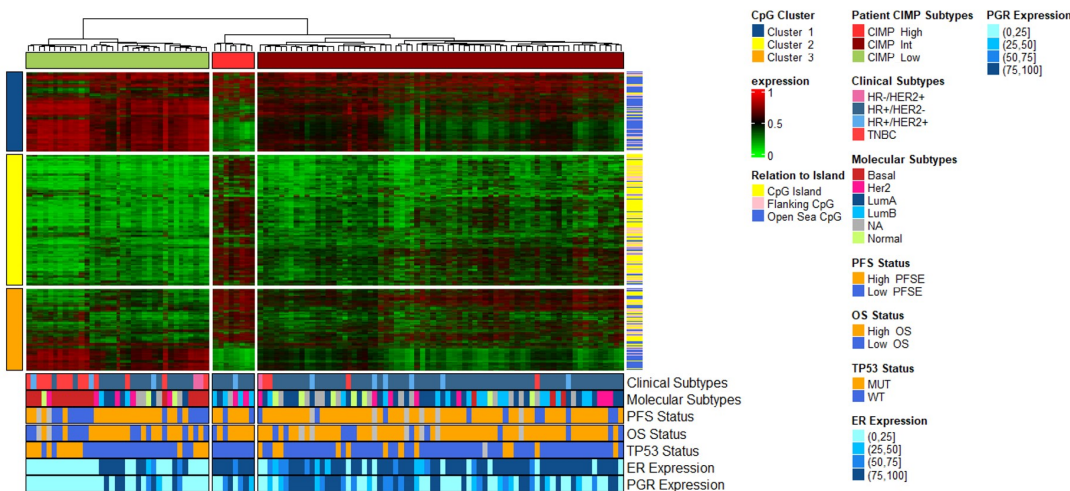
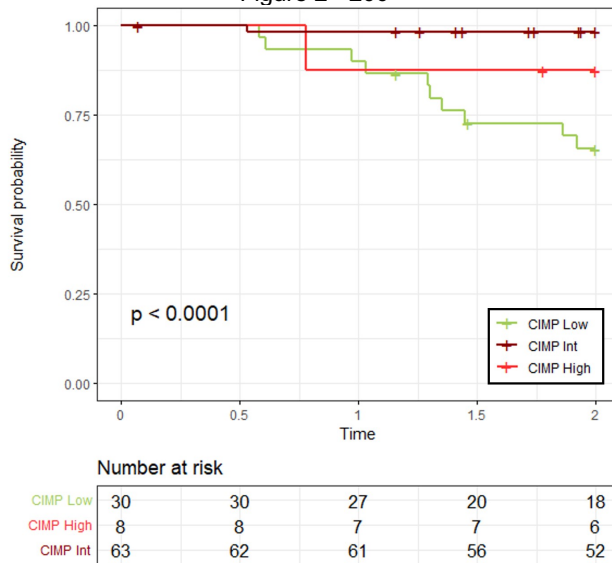


Figure 2 - 200



Conclusions: The epigenetic classification of BC according to the CIMP has an important prognostic value. Our epigenetic signature is useful to classify CIMP-low tumors with high specificity and sensitivity.

201 Breast Cancers Negative for HER2 Over-Expression/Amplification Have Inconsistent HER2 IHC Results from Primary to Metastatic Samples: Can We Trust Metastatic Site IHC 0 Results?

Parisa Najafzadeh¹, Gregory Bean², Grace Allard³, Aihui Wang², Kimberly Allison¹

¹Stanford University School of Medicine, Stanford, CA, ²Stanford Medicine/Stanford University, Stanford, CA, ³Feinberg School of Medicine/Northwestern University, Chicago, IL

Disclosures: Parisa Najafzadeh: None; Gregory Bean: None; Grace Allard: None; Aihui Wang: None; Kimberly Allison: Consultant: Mammatome

Background: The antibody drug-conjugate trastuzumab-deruxtecan (T-DXd) was originally FDA approved as a treatment option for metastatic breast cancers testing positive for HER2 over-expression/amplification. In August of 2022 the FDA expanded this approval to include HER2 IHC 1+ or 2+/ISH negative metastatic cancers, based on the results of the DESTINY-Breast04 trial. While HER2 IHC 0 cases were not included in this trial, the difference between an IHC 0 and a non-zero result is now clinically relevant. We sought to determine if breast cancers have consistent HER2 IHC 0 vs 1-2+/ISH- results with metastatic progression and to determine how frequently metastatic IHC 0 results occur in the setting of primaries with 1-2+ expression.

Design: This is a cohort study on both tissue microarray (TMA) breast cancer samples and a retrospective search for all HER2 not over-expressed/FISH negative metastatic breast carcinomas. A total number of 50 patients with case-matched primary and metastatic sites were included.

Results: 40% of primary vs 58% of metastatic samples were IHC 0 (vs 1-2+/ISH-). Overall, 38% of case-matched primary vs metastatic breast cancer samples had a change in HER2 IHC expression between the IHC 0 and 1-2+ categories. Primary IHC 1-2+ cancers with matched metastatic IHC 0 results occurred in 28% of cases. Primary IHC 0 results with matched metastatic IHC 1-2+ results occurred in 10% of cases. An IHC 0 primary remained IHC 0 in the metastatic sample in 30% of cases. Importantly, when a metastatic sample tested IHC 0, 48% of the time it was 1-2+ in the prior matched primary sample. In contrast, when a primary tested IHC 0, only 26% of the time did it become 1-2+ in the metastatic site (74% remained IHC 0). Metastatic samples may not always follow the pre-analytic tissue handling requirements that primary breast samples do, which may contribute to the greater probability of an IHC 0 result in a metastatic site when the breast primary tested 1-2+/ISH- (vs heterogeneity).

Conclusions: HER2 non-amplified cancers have inconsistent IHC 0 vs 1-2+ results in primary vs metastatic samples with metastatic samples more often testing IHC 0. These results suggest that low levels of HER2 expression are not reliably tested by IHC across sample types (or are heterogeneous) and raise concern about using metastatic sample IHC 0 results for T-DXd access.

202 Upregulated mRNA Expression and Protein Overexpression of Alpha-Methylacyl-CoA Racemase (AMACR) in Breast Carcinoma with Apocrine Differentiation are Associated with Peroxisomal β-oxidation

Harumi Nakamura, Osaka International Cancer Institute, Osaka, Osaka, Japan

Disclosures: Harumi Nakamura: None

Background: We reported at USCAP in 2022 that most breast carcinomas with apocrine differentiation (AC) are positive for anti-alpha-methylacyl-CoA racemase (AMACR) antibodies; AMACR gene expression was significantly higher in carcinomas with apocrine differentiation than in non-AC ($p<0.001$). AMACR is localized in peroxisomes and mitochondria and is involved in β-oxidation. Here, we conducted an immunohistochemical investigation of the peroxisomal and mitochondrial enzymes involved in β-oxidation and associated fatty acid metabolism.

Design: We used surgically obtained formalin-fixed paraffin-embedded specimens from 35 cases of AC, 21 cases of ER+/HER2- carcinoma, 12 cases of ER+/HER2+ carcinoma, 19 cases of ER-/HER2+ carcinoma, and 8 cases of triple negative breast carcinoma (TNBC). Immunohistochemical staining was performed for the following: acyl-CoA oxidase 1 (ACOX1), acyl-CoA oxidase 2 (ACOX2), peroxisome proliferator-activated receptor γ (PPARγ), catalase, acyl-CoA dehydrogenase short chain (ACADS), cytochrome c, long chain fatty acyl-CoA synthetase (ACSL1), fatty acid synthase (FASN), and CD36. Those with significantly more intense staining than normal adipose tissue and mammary gland tissue were deemed positive (i.e., overexpression).

Results: The results of immunohistochemical staining are summarized in Table 1 (where there were untested specimens, the actual number of specimens was recorded as the denominator). The positive (overexpression) rates of ACOX1, catalase, ACSL1, and FASN were significantly higher in ACs than in non-ACs ($p<0.001$). In contrast, the expression of ACOX2, ACADS, cytochrome c, and CD36 did not significantly change in AC.

Table 1. A summary of the results immunostaining results; number of cases exhibiting high expression and positive rate

Groups	n	FASN (%)	ACOX1 (%)	ACOX2 (%)	Catalase (%)	ACADS (%)	Cytochrome c (%)	PPARγ (%)	CD36 (%)	ACSL1 (%)
AC	35	31 (88.6)	23 (65.7%)	3/34 (8.8)	16/31 (51.6)	8 (22.9)	3/32 (9.4)	4/34 (11.8)	3/34 (8.8)	14/18 (77.8)
non-AC	60	32 (53.3)	7 (11.7)	3/57 (5.3)	4/56 (7.1)	20 (33.3)	3/59 (5.1)	4/59 (6.8)	2 (3.3)	1/28 (3.6)
ER+/HER2-	21	7 (33.3)	0 (0.0)	2/20 (10.0)	1/19 (5.3)	9 (42.9)	0/20 (0.0)	0/20 (0.0)	1 (4.8)	0/11 (0.0)
ER+/HER2+	12	8 (66.7)	0 (0.0)	0/10 (0.0)	0/11 (0.0)	3 (25.0)	0 (0.0)	1 (8.3)	0 (0.0)	0/5 (0.0)
ER-/HER2+	19	12 (63.2)	7 (36.8)	1 (5.3)	1/18 (5.6)	6 (31.6)	0 (0.0)	3 (15.8)	0 (0.0)	1/7 (14.3)
TNBC	8	5 (62.5)	0 (0.0)	0 (0.0)	2 (25.0)	2 (25.0)	3 (37.5)	0 (0.0)	1 (12.5)	0/5 (0.0)

Conclusions: This study suggested that upregulated mRNA expression and protein overexpression of AMACR in AC are associated with peroxisomal β-oxidation, but not mitochondrial β-oxidation.

203 Comparative Analysis of Four Immunohistochemical Assays for HER2 Expression in Breast Carcinoma – Correlation with HER2 Gene Amplification and Perspectives for HER2 Low Expression

Søren Nielsen¹, Diana Wang², Valeria Montalvo Calero², Jared LaMar², Ashish Saxena², Rina Decamillis², Mia Stensballe¹
¹Aalborg Pathology Department, Aalborg, Denmark, ²Sakura Finetek USA, Inc., Torrance, CA

Disclosures: Søren Nielsen: None; Diana Wang: None; Valeria Montalvo Calero: None; Jared LaMar: None; Ashish Saxena: None; Rina Decamillis: None; Mia Stensballe: None

Background: Accurate HER2 status based on immunohistochemistry (IHC) is required to select patients for existing and newly developed HER2-targeting treatments. Patients with HER2 gene-amplified and/or HER2 IHC overexpressing breast carcinomas (BCs) are eligible for treatment with anti-HER2 drugs as trastuzumab. Recently, BC patients with HER2 low expression (IHC 1+ or 2+ without HER2 gene amplification) may be offered new anti-HER2 antibody-drug-conjugates as trastuzumab deruxtecan. Since patient stratification for anti-HER2 drugs primarily is based on IHC, our goal is to compare the analytical accuracy of HER2 overexpression and concordance rate for HER2 low expression in BC amongst four different HER2 IHC assays.

Design: 98 human formalin fixed paraffin embedded resection BC specimens from five microarrays were analyzed by four different IHC assays: (1) HercepTest SK001, Agilent, (2) HercepTest GE001, Agilent, (3) PATHWAY 4B5, Roche and (4) HER2 EP3, Sakura Finetek. The gene amplification status for all specimens were confirmed by fluorescence in situ hybridization (FISH) analysis. IHC results were evaluated by three reviewers and a consensus result was obtained for each specimen analyzed. IHC and FISH results were scored accordingly to the 2018 ASCO/CAP guidelines.

Results: A total of 33 BC specimens exhibited HER2 amplification by FISH. A higher positive predictive value to FISH analysis of 94% was observed for HercepTest GE001, PATHWAY 4B5 and HER2 EP3 when compared to HercepTest SK001 (91%). All four IHC assays resulted in a negative predictive value to FISH of 100%. 21% of the non-amplified BCs were categorized as HER2 low expression by HercepTest GE001 and HER2 EP3 compared to 19% and 14% for HercepTest SK001 and PATHWAY 4B5, respectively.

Conclusions: This was to our knowledge, the first study to evaluate the inter-assay performance of two well-established HER2 IHC assays (HercepTest SK001 and PATHWAY 4B5) with two relatively new IHC assays (HercepTest GE001 and HER2 EP3). A high accuracy and concordance for HER2 overexpression was obtained by the four different IHC assays; however, HercepTest SK001 exhibited 3% more false negative results. A reduced concordance was seen for HER2 low expression BCs amongst the different assays; therefore, future comparative studies with an enriched number of HER2 low and HER2 negative BCs must be performed to evaluate the concordance rate for HER2 low expression in BC amongst these IHC assays.

204 Correlation between a Manual Count and an Automated System of Estimation of Ki67 in Breast Cancers in Danbury Hospital

Oluwole Odujoko¹, Fnu Sandeep², Oluwaseyi Olayinka³, Ramapriya Vidhun⁴, Samuel Barasch⁴

¹Obafemi Awolowo University Teaching Hospitals Complex, ²Danbury Hospital, Danbury, CT, ³The University of Texas MD Anderson Cancer Center, Houston, TX, ⁴Western Connecticut Health Network, Danbury Hospital, Danbury, CT

Disclosures: Oluwole Odujoko: None; Fnu Sandeep: None; Oluwaseyi Olayinka: None; Ramapriya Vidhun: None; Samuel Barasch: None

Background: Immunohistochemical characterization of breast cancers with biomarkers including Ki67 are required for contemporary oncologic care. Manual estimation of Ki67 expression in breast cancer is unappealing for Pathologists. Automated methods minimize variability and time spent with manual estimation with the hypothesis that correlation between a manual estimate and automated count is acceptable.

Design: Breast cancer cases diagnosed between March, 2020 and August, 2021 were retrospectively reviewed and random selection of 40 biopsy cases was done. The H&E and Ki67 slides of the selected cases were retrieved from the archives. Images of the Ki67 slides were taken with Olympus camera (U-TV0.63XC). The score was estimated by two residents and subsequently, a scoring application (QuPath, 0.2.3) was used on the same images. Manual estimation was calculated as the average of the scores from the two residents. The QuPath application settings were made to minimize interference of tumor Ki67 staining estimation by stromal and inflammatory cell Ki67 staining. This was done by selecting the hotspot of tumor cell staining and irregular polygon annotation of hotspots. Manual method estimation was performed prior to automated count for all cases. Correlation of tumor grades as well as manual and automated scoring systems was performed (Linear regression analysis, Excel 2016).

Results: Forty cases were reviewed for the study. About 70% of the breast cancer cases studied were invasive ductal carcinoma (70%) followed by Invasive lobular carcinoma (19%). Majority of the cases (37.5%) were grade 1 carcinomas. There was a good level of correlation between the manual methods of Ki67 estimation compared to the automated method with a R^2 of 0.86 (Fig. 1). Grade 1 and 2 tumors were found to have a higher level of correlation (R^2 of 0.88 and 0.84 respectively) compared to grade 3 tumors with a R^2 of 0.69 (Fig. 2).

Figure 1 – 204

Figure 2 – 204

All grades and histologic types.

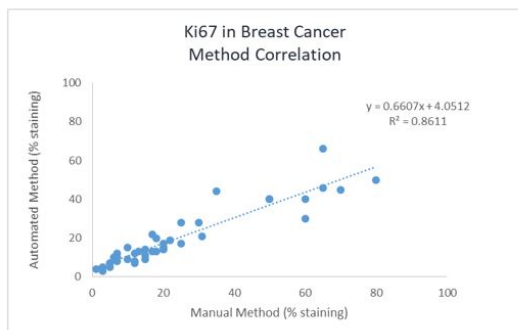


Figure 1: Correlation between manual estimation of Ki67 and automated calculation of Ki67.

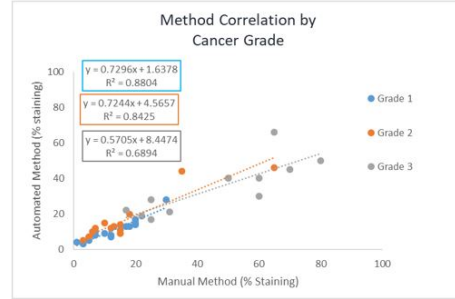


Figure 2: Correlation between manual estimation of Ki67 and automated estimation of Ki67 between the different grades of tumor.

Conclusions: Automated methods such as QuPath are helpful in reducing the intra and inter-observer variability in Ki67 scoring. We noticed a higher correlation in cases that had lower Ki67 scores than those with higher scores. Line plots of correlation show a slope less than 1 for all tumor classifications. This indicates that Ki67 was over-estimated with manual method compared with the automated method even when an average count was taken between two observers.

205 Detection of Invasive Lobular Carcinoma Using an Artificial Intelligence Algorithm Based on Genetic Ground Truth

Fresia Pareja¹, Higinio Dopeso¹, Yikan Wang², Marc Goldfinger², Andrea Gazzo¹, Fatemeh Derakhshan³, Edaise M. da Silva¹, Pier Selenica¹, Thais Basili¹, Share Danielle¹, David Brown¹, Jillian Sue², Qiqi Ye⁴, Arnaud Da Cruz Paula¹, Monami Banerjee², Matthew Lee², Ran Godrich², Adam Casson², Britta Weigelt¹, Hannah Wen¹, Edi Brogi¹, Matthew Hanna¹, Jeremy Kunz², Christopher Kanan², David Klimstra², Thomas Fuchs², Jorge Reis-Filho¹

¹Memorial Sloan Kettering Cancer Center, New York, NY, ²Paige.AI, New York, NY, ³Columbia University Irving Medical Center, New York, NY, ⁴The University of Texas MD Anderson Cancer Center, Houston, TX

Disclosures: Fresia Pareja: None; Higinio Dopeso: None; Yikan Wang: None; Marc Goldfinger: None; Andrea Gazzo: None; Fatemeh Derakhshan: None; Edaise M. da Silva: None; Pier Selenica: None; Thais Basili: None; Share Danielle: None; David Brown: None; Jillian Sue: None; Qiqi Ye: None; Arnaud Da Cruz Paula: None; Monami Banerjee: None; Matthew Lee: None; Ran Godrich: Employee: Paige AI; Adam Casson: Employee: Paige.AI; Britta Weigelt: Grant or Research Support: Repare Therapeutics; Hannah Wen: None; Edi Brogi: None; Matthew Hanna: None; Jeremy Kunz: Employee: Paige.ai; Christopher Kanan: None; David Klimstra: Employee: Paige.AI; Thomas Fuchs: Employee: Paige.ai Inc.; Jorge Reis-Filho: None

Background: Invasive lobular carcinoma (ILC) is characterized by a dis-cohesive growth pattern, mainly due to bi-allelic *CDH1* inactivation, present in up to 80% of ILCs. Bi-allelic *CDH1* alterations, however, are vanishingly rare in other histologic types of breast cancer (BC). Although ILCs show inferior response rates to chemotherapy and SERMs relative to other BC subtypes, the high inter-observer variability in ILC diagnosis, precludes its incorporation in therapeutic decisions. Artificial intelligence (AI)-based models have the potential to improve pathologic diagnoses. Histologic diagnoses, however, which might be confounded by human subjectivity, are often used as ground truth (GT) for training. We sought to develop an AI-based algorithm for detection of ILC using *CDH1* biallelic mutations as GT.

Design: We developed an AI-based model to detect *CDH1* biallelic mutations (i.e., inactivating mutation and loss of heterozygosity (LOH) of the wild-type allele, or two inactivating mutations), using diagnostic whole slide images (WSI) from 1057 primary BCs with available MSK-IMPACT targeted sequencing data. The model was developed using a 10-fold cross validation system. *CDH1* gene promoter methylation assessment was conducted in a subset of cases using digital droplet PCR.

Results: The AI-based algorithm trained utilizing *CDH1* bi-allelic mutations as the GT predicted the presence of *CDH1* 'bi-allelic mutations' with an AUC of 0.966, accuracy of 0.95, positive predictive value (PPV) of 0.77 and negative predictive value (NPV) of 0.98. Re-analyses of the misclassified cases revealed that most (74%; 25/34) false positives (FPs) harbored *CDH1* inactivation through different mechanisms, including promoter methylation (n=21), homozygous deletion (n=3) or intragenic deletion with LOH (n=1). The performance of the algorithm for detection of a 'lobular phenotype' (i.e., ILC (classic or variant) or mixed lobular and ductal BC) regardless of *CDH1* status had an AUC of 0.974, accuracy of 0.94, PPV of 0.97 and NPV of 0.93. Most (66%) cases with a 'lobular phenotype' not detected by the algorithm were mixed ductal and lobular BCs (n=33; 53%) or ILC variants (n=8; 13%), whereas only a subset of them (n=21; 34%) were classic ILCs.

Conclusions: An AI algorithm trained to detect 'CDH1 biallelic mutations' as GT, instead of labels based on histologic diagnosis of ILC can detect ILC robustly. These findings represent a paradigm shift for the use of orthogonal GT in the development of AI-based cancer classification systems.

206 Whole Genome Landscape of Male Breast Cancer

Andy Phan¹, Majd Al Assaad², Aditya Deshpande³, Kevin Hadi³, Jyothi Manohar⁴, Michael Sigouros⁴, Ahmed Elsaeed⁴, Andrea Sboner⁴, Juan Medina-Martínez³, Syed Hoda⁴, Olivier Elemento⁴, Juan Miguel Mosquera⁴

¹New York-Presbyterian/Weill Cornell Medical Center, New York, NY, ²New York-Presbyterian/Weill Cornell Medicine, New York, NY, ³New York, NY, ⁴Weill Cornell Medicine, New York, NY

Disclosures: Andy Phan: None; Majd Al Assaad: None; Aditya Deshpande: Employee: Isabl Inc; Isabl Inc; Isabl Inc; Isabl Inc; Isabl Inc; Kevin Hadi: Employee: Isabl, Inc.; Isabl, Inc.; Isabl, Inc.; Isabl, Inc.; Isabl, Inc.; Isabl, Inc.; Jyothi Manohar: None; Michael Sigouros: None; Ahmed Elsaeed: None; Andrea Sboner: None; Juan Medina-Martínez: Employee: Isabl Inc.; Syed Hoda: None; Olivier Elemento: None; Juan Miguel Mosquera: None

Background: Male breast cancer (MBC) is extremely rare, accounting for less than 1% of all breast cancers and 0.5% of all cancers in males. Current treatment for MBC is based on protocols and research on female breast cancer. Pathogenic variants in cancer-predisposing genes are a likely etiology in 4% to 40% of MBC cases, and it is currently advised that all MBC patients be offered genetic counseling. The goal of this project was to characterize the genomic landscape of this rare cancer via whole-genome sequencing (WGS).

Design: We performed WGS on matched tumor/normal tissues from 10 localized invasive ductal MBCs. By IHC these were 10 ER-positive, 8 PR-positive, and 10 HER2-negative, i.e., 80% luminal A-like, 20% luminal B-like, and 0% basal-like cases. The median age at diagnosis was 77 years of age.

Results: Table 1 summarizes the histopathologic characteristics of the ten patients with identified targets/biomarkers and associated treatments. The ten cases were found to have an average tumor mutational burden (TMB) of 4.97/Mb, Coding TMB 11.70/Mb, structural variant counts (SVs) 87, and 55% tumor purity. Seven of the ten cases were found to have *at least* one molecular target. Four cases harbored *FGFR1* amplification and another set of five cases were identified to have high TMB. One case was identified to have borderline *ERBB2* amplification with HER2 IHC showing 1+ scoring, which may support this case to be classified as HER2-low (a new proposed categorization of receptor status) (Figure 1). Mutational signatures associated with homologous recombination deficiency (HRD) were identified in one case (Figure 2). A pathogenic *BRCA2* germline mutation was identified in one patient.

Case	Age	Stage	Grade (Bloom-Richardson Score)	Targets / Biomarkers	Treatments	Select Signatures
1	53	ypT2N1a	Moderately differentiated (2,2,2)	<i>ERBB2</i> amp, <i>FGFR1</i> amp, <i>PIK3CA</i> H1047R, high TMB	<i>FGFR</i> inhibitors, estrogen receptor antagonist, Pembrolizumab	
2	68	pT1aN0	Moderately differentiated (3,2,1)			
3	84	pT1cN1a	Moderately differentiated (3,2,2)	<i>FGFR1</i> amp; HR/NER deficiency, <i>ESR1</i> E380Q	<i>FGFR</i> inhibitors, estrogen receptor antagonist	HRD
4	77	pT2N0	Moderately differentiated (3,2,2)	<i>FGFR1</i> amp and high TMB	<i>FGFR</i> inhibitors, Pembrolizumab	
5	80	pT1cN1	Moderately differentiated (2,2,2)			
6	73	pT4bN1	Poorly differentiated (3,3,3)	<i>MET</i> amp, <i>PIK3CA</i> E542K	Tyrosine kinase receptor inhibitors, PIK3 inhibitors	
7	78	pT2N1mi	Poorly differentiated (3,2,3)			
8	51	pT1bN0	Moderately differentiated (3,2,1)	High TMB and MSI-H	Pembrolizumab	
9	79	pT2N0	Poorly differentiated (3,3,2)	High TMB and <i>BRCA2</i> deletion	Pembrolizumab, PARP inhibitors	
10	80	pT1cN0	Moderately differentiated (3,2,1)	<i>FGFR1</i> amp, High TMB	<i>FGFR</i> inhibitors, Pembrolizumab	

Table 1: Cohort of ten invasive ductal carcinomas of male breast interrogated by whole genome sequencing. Clinical, pathologic and molecular details. HRD = homologous recombination deficiency; TMB = tumor mutational burden

Figure 1 - 206

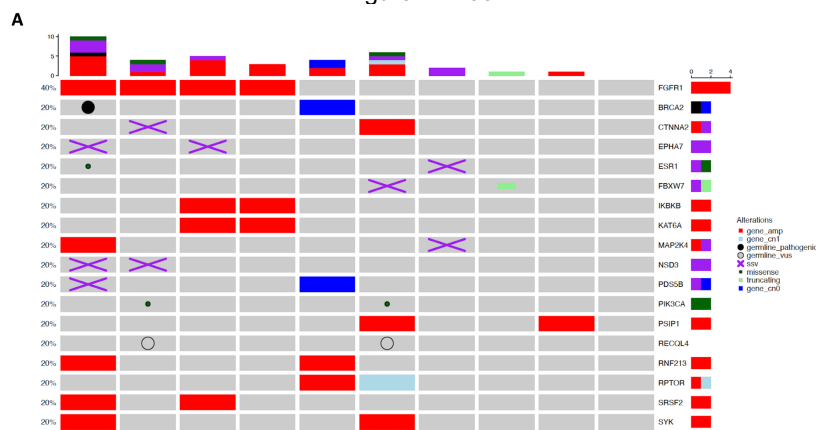


Figure 2 - 206

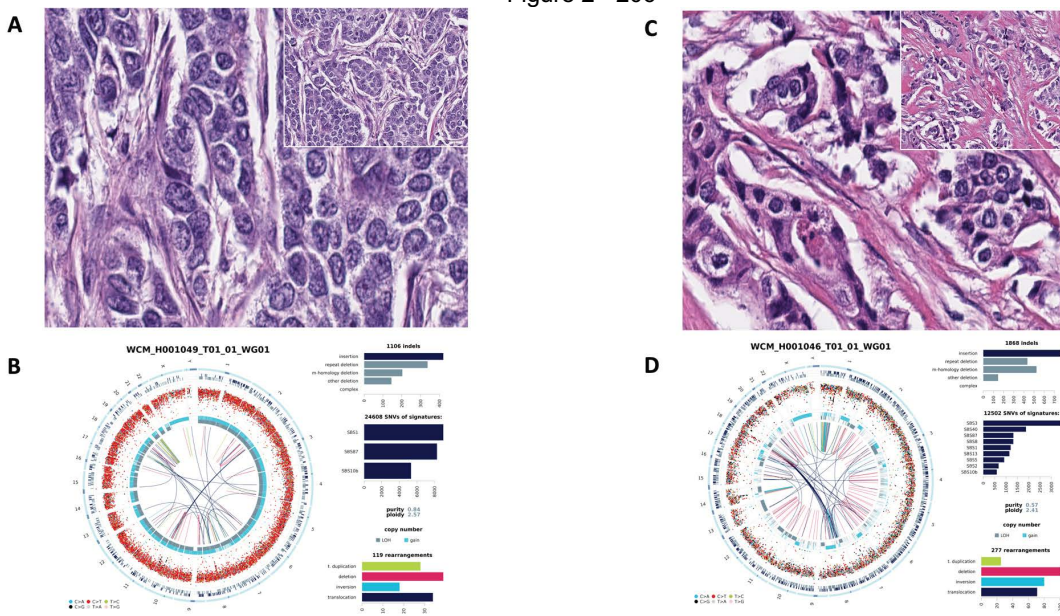


Figure 2. Whole genome sequencing of two poorly differentiated invasive ductal male breast carcinomas. A. Representative H&E images B. Circos plot and major findings that included *ERBB2* and *MET* amplifications, and *PIK3CA* E542K. C. Representative H&E images. D. Circos plot and major findings that included *FGFR1* amplification and *ESR1* E38Q.

Conclusions: Comprehensive WGS analysis has empowered us to further characterize the genomic landscape of male breast cancer, which appears to harbor molecular differences when compared to its female counterpart. Employing a single WGS assay and state-of-the-art analytic pipelines, we detected known targets, pathogenic germline mutations, high TMB, and genomic signatures associated with an HRD phenotype.

207 Whole Genome Sequencing (WGS) of Locally Advanced and Metastatic Breast Carcinoma Unravels Relevant Molecular Signatures and Novel Events

Andy Phan¹, Majd Al Assaad², Gunes Gundem³, Max Levine³, Jyothi Manohar⁴, Michael Sigouros⁴, Ahmed Elsaeed⁴, Andrea Sboner⁴, Syed Hoda⁴, Juan Medina-Martínez³, Olivier Elemento⁴, Juan Miguel Mosquera⁴

¹New York-Presbyterian/Weill Cornell Medical Center, New York, NY, ²New York-Presbyterian/Weill Cornell Medicine, New York, NY, ³New York, NY, ⁴Weill Cornell Medicine, New York, NY

Disclosures: Andy Phan: None; Majd Al Assaad: None; Gunes Gundem: *Consultant*: Isabl Technologies; Isabl Technologies; Isabl Technologies; Max Levine: *Employee*: Isabl Inc.; Isabl Inc.; Isabl Inc.; Jyothi Manohar: None; Michael Sigouros: None; Ahmed Elsaeed: None; Andrea Sboner: None; Syed Hoda: None; Juan Medina-Martinez: *Employee*: Isabl Inc.; Olivier Elemento: None; Juan Miquel Mosquera: None

Background: Patients with metastatic breast carcinoma portends to a poor prognosis, especially for patients who fail first line therapies. Molecular sequencing has allowed us to provide additional information to guide targeted and salvage therapies. The aim of this study is to profile locally advanced and metastatic breast carcinomas via WGS to identify novel events that may unearth new biomarkers and potential targets of the disease.

Design: WGS was performed on 48 tumor/normal DNA pairs of locally advanced and metastatic breast carcinoma from 34 patients including 20 local/regional/axillary lymph node metastases and 28 distant metastases. Three cases were excluded due to sequencing artifacts. We employed the Isabl GxT analytic platform and manually curated single base substitution (SBS) molecular signatures and structural variants (SV) that involved tumor suppressor genes and oncogenes.

Results: The IHC hormone receptor profile was: 22 (65%) ER positive, 16 (47%) PR positive and 5 (15%) HER2 positive. Seven (24%) were triple negative breast carcinomas. Histologically, 31 (91%) were ductal, 2 (6%) lobular and 1 (3%) was metaplastic carcinoma. Twenty-two out of 31 patients (71%) had actionable/clinically relevant alterations including SV impacting *BRCA1*, *PIK3CA* hotspot, *FGRF1* and *ERBB2* amplifications, among others (Table 1). Gene fusions included *TBL1XR1::PIK3CA* (described in a metastatic pancreatic ductal adenocarcinoma) and *ESR1::EP300* (novel event) (Figure 1). Interestingly, of 7 patients which tumors had strong evidence of homologous recombination deficiency (HRD), i.e. excess tandem duplications or short, small deletions and annotation by the Classifier of HOMologous Recombination Deficiency (CHORD) algorithm, 6 patients did not have pathogenic *BRCA1/2* mutations or SVs altering these genes (Figure 2). Remarkably, 4 out of those 6 patients (67%) responded to chemotherapy, including 2 with complete remission and lack of pathogenic variants in HRD genes. In contrast, only 7 out of the 18 patients (39%) which tumors lacked HRD responded to treatment.

Case?	Molecular targets and Biomarkers?	Select SBS Signatures?
1*	?-	HRD
2?	<i>ERBB2</i> amp, <i>PIK3CA</i> H1047L	-?
3?	? <i>ERBB2</i> amp	<i>POLE</i> exonuclease domain mutation
4?	<i>MET</i> amp	-
5?	<i>FGFR2</i> Y375C	-
6?	? <i>PIK3CA</i> E545Q, <i>ESR1</i> Y537S, TMB-H	?HRD
7?	?-	<i>POLE</i> exonuclease domain mutation
8?	<i>PIK3CA</i> H1047R	-?
9*	<i>PTEN</i> del	HRD
10?	<i>NF1</i> G1511Efs*42, <i>AKT1</i> E17K	-
11	<i>FGFR1</i> amp	HRD
12	?-	HRD
13	? <i>PIK3CA</i> G118D	-
15	<i>PIK3CA</i> A1066V	-?
16*	?	HRD
17	<i>ERBB2</i> amp, <i>PIK3CA</i> H1047R	?-
18	?	-
19	<i>PIK3CA</i> H1047R	?-
20	? <i>FGFR1</i> amp, <i>MET</i> amp, <i>ESR1::EP300</i> Fusion	-
21*	-	?-
22	? <i>CDKN2A</i> del	-
23	? <i>FGFR1</i> amp, <i>ERCC2</i> del	HRD
26	-?	-
27	<i>PIK3CA</i> E545Q, TMB-H	?-
28	-?	?-
29	<i>ERCC2</i> del	HRD
30*	?-	?-
31*	<i>PIK3CA</i> R115Q	?HRD
32	<i>FGFR1</i> amp	-
33	<i>PIK3CA</i> Q546R	-
34	<i>AKT1</i> E17K	?-

Table 1. Summary of the molecular targets and single base substitution (SBS) molecular signatures. Examples of tumors with molecular signatures associated with homologous recombination deficiency (HRD) include Case 31 with a pathogenic germline variant in *BRCA2*, Case 9 with a *BRCA1* VUS, which was also confirmed to be pathogenic. multiple tumors from Case 4 that harbored HRD signatures but only a SV impacting *RAD51B* was detected. (*) denotes cases with DNA structural evidence of HRD (excess of tandem duplications); TMB-H denotes tumor mutational burden-high.

Figure 1 - 207

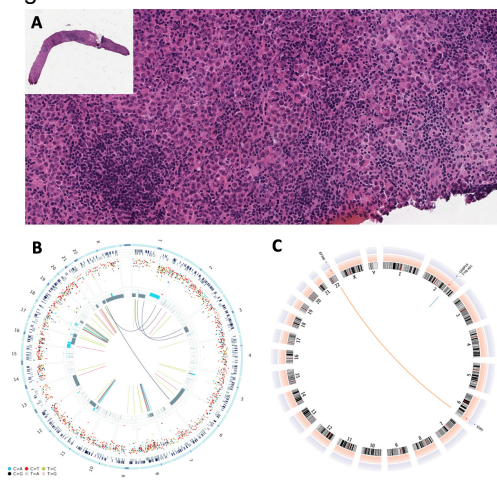


Figure 1. Novel *ESR1::EP300* fusion event in breast cancer may cause therapeutic resistance. A. Metastatic lobular carcinoma to lymph node (Case 20). H&E of low and high magnification. B. Genome circos plot. C. Fusion circos plot.

Figure 2 - 207

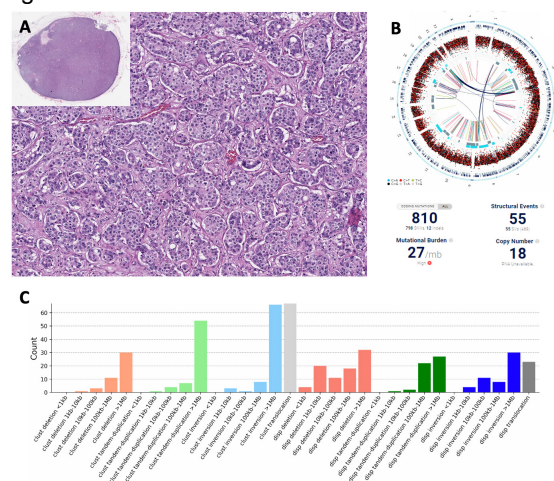


Figure 2. Metastatic ductal carcinoma to lymph node with potentially relevant molecular phenotype. A. H&E of low and high magnification (Case 6). B. Genome circos plot and some WGS analysis results. C. Mutational bar plot with a large tandem duplication phenotype (no *CDK12/CCNE1* events detected).

Conclusions: WGS of locally advanced and metastatic breast carcinoma empowered by state-of-the-art analysis elucidates significant molecular signatures and relevant structural variants that may provide additional biomarkers and open therapeutic avenues. These include patients with tumors featuring high TMB and HRD phenotype, and their potential susceptibility to checkpoint and poly adenosine diphosphate-ribose polymerase (PARP) inhibitors.

208 Comparison Between Nottingham Histologic Grade of Invasive Ductal Carcinoma Diagnosed on Core Needle Biopsy and Excision Specimen

Peter Podany¹, Reza Golestani¹, Susan Fineberg², Kamaljeet Singh³, Malini Harigopal⁴

¹Yale School of Medicine, Yale New Haven Hospital, New Haven, CT, ²Montefiore Medical Center, Bronx, NY, ³Women and Infants Hospital, Providence, RI, ⁴Yale School of Medicine, New Haven, CT

Disclosures: Peter Podany: None; Reza Golestani: None; Susan Fineberg: None; Kamaljeet Singh: None; Malini Harigopal: None

Background: Core needle biopsy (CNB) is an accurate method for detection of invasive ductal carcinoma with a high degree of concordance with surgical excision. CNB is used to provide valuable information that can be used in presurgical decision making. In this study we investigated the value of CNB in assessment of Nottingham histologic grade in comparison to final histologic grade assessed on excision.

Design: All cases of breast excision for invasive ductal carcinoma between September 2020- August 2021 that had in-house biopsies were included in this study. All cases with preoperative neoadjuvant chemotherapy were excluded. Nottingham histologic grade with total scores, tubule formation, nuclear pleomorphism, and mitotic activity were compared between CNB and excision.

Results: A total of 216 cases with histologic grade diagnosed on CNB were included. Rates of well-, moderately-, and poorly differentiated carcinomas on CNB were 27.8%, 60.2%, and 12.0%, respectively, and on excision 27.8%, 50.5%, and 21.7%, respectively. Changes in final grades and individual components are summarized in Figure 1A. Final total score was changed in 37.0% of cases (28.2% upscore, 8.8% downscore) (Figure 1B). Grades were changed in 19.0% of cases (13.9% upgrade, 5.1% final downgrade) (Figure 2A). Tubule formation score was changed in 14.3% (5.1% increase, 9.2% decrease), nuclear score was changed in 12.0% (8.3% increase, 3.7% decrease), and mitosis score was changed in 26.4% of cases (24.1% increase, 2.3% decrease) (Figures 2B-1D). Table 1 shows the factors responsible for changes in Nottingham scores. There was no difference between tumor size/extent on CNB cases with grade changes (0.63 ± 0.33 cm) and without grade changes (0.63 ± 0.32 cm, $p = 0.99$).

		Due to score change in							
	Count	Tubule	Nuclei	Mitosis	Tubule & Nuclei	Tubule & Mitosis	Nuclei & Mitosis	All three	
Down grade	11	6	3	1	0	1	0	0	
Upgrade	30	8	1	14	0	2	5	0	
Total	41	14	4	15	0	3	5	0	

Table 1: Summary of the changes in grade components that are responsible for final grade change.

Figure 1 - 208

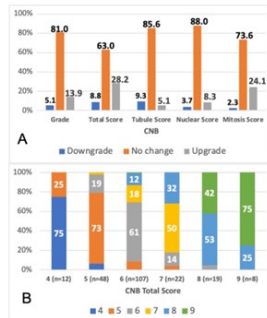


Figure 1. A) Total changes in invasive ductal carcinoma grades and grade components in core needle biopsy versus excision. B) Changes in core needle biopsy total score in comparison with final total score. CNB: Core needle biopsy.

Figure 2 - 208

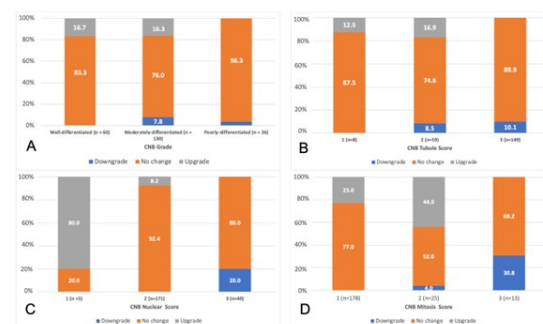


Figure 2. Changes in final grade (A), tubule formation score (B), nuclear pleomorphism score (C), and mitotic activity score (D) in different categories of grades and scores on core needle biopsy. CNB: core needle biopsy.

Conclusions: Nottingham grade, diagnosed on CNB was changed in one fifth of breast excisional biopsies. Mitosis score was the least reliable histologic variable on CNB and its changed on final excision resulted in 47% of Nottingham score downgrades. Although, tubule formation score was relatively stable between CNB and excision, its changes on final excision was responsible for a majority of Nottingham score upgrades (51%). We propose that nuclear grade and tubule point score on CNB without mitotic count score will result in better concordance with surgical excision.

209 Changes in Expression of Breast Cancer Tumor Markers Between Primary Tumors and Corresponding Metastatic Sites: Common Patterns and Relationships with Survival

Lauren Postlewait¹, Yi Liu¹, Stephanie Jou¹, Sha Yi², Limin Peng¹, Xiaoxian Li¹

¹Emory University, Atlanta, GA, ²Brody School of Medicine at East Carolina University, Greenville, NC

Disclosures: Lauren Postlewait: None; Yi Liu: None; Stephanie Jou: None; Sha Yi: None; Limin Peng: None; Xiaoxian Li: None

Background: Tumor markers estrogen receptor (ER), progesterone receptor (PR), and HER2 are key in predicting breast cancer (BC) outcomes and selecting appropriate treatment. Differences in ER/PR/HER2 between the primary tumor (PT) and metastatic site (MET) have been observed. We aimed to describe patterns of ER/PR/HER2 on PTs and corresponding METs and to assess the relationship between expression patterns and overall survival (OS).

Design: Patients with BC (2011-2020) with a PT and MET from a single institution were included. Those with missing data points were excluded. ER/PR expression was stratified by % staining [$<1\%$ (-), 1-10% (+), or $>10\%$ (+)] on immunohistochemistry, and HER2 was classified as positive or negative by ASCO/CAP recommendation. Kaplan-Meier curves and log-rank tests were used to compare OS based on change of receptor expression.

Results: 440 patients were assessed: 18% had a synchronous MET and 82% a metachronous MET. Location of MET included 20% brain, 36% bone, 20% lung, 17% liver, 5% distant lymph node, and 2% other site. Detailed tumor marker data for the PT with corresponding MET were available in 188 cases (Table). Patients whose PT was ER- (n=60) or PR- (n=92) commonly had a MET with ER- (n=53/60, 88%) or PR- (n=81/92, 88%). These ER- or PR- PTs rarely had a MET that was ER+ (n=7/60, 12%) or PR+ (n=11/92, 12%). In contrast, those who had PT that was ER+ (n=128) or PR+ (n=96) frequently had a MET with loss of ER (n=29/128, 23%) or PR (n=48/96, 50%). HER2+ PTs (n=44) had HER2- MET in 18% (8/44), while HER2- PTs (n=144) had only 9% HER2+ MET (13/144). There were no additional patterns noted between tumor markers expression on the PT and MET in patients stratified by MET site of disease. Decrease in ER expression between the PT and MET was associated with decreased OS ($p=0.043$, Figure 1). A similar trend was observed with worse OS in patients with decreased PR expression in the MET ($p=0.23$, Figure 2). Differences in HER2 expression were not associated with changes in OS ($p=0.52$).

Patterns of Breast Cancer Marker Expression of Primary Tumor and Corresponding Metastatic Site

ER		MET ER: <1%		MET ER: 1-10%		MET ER: >10%	
		Total (n)	n	%	n	%	n
PT ER: <1%		60	53	88	2	3	5
PT ER: 1-10%		7	5	71	0	0	2
PT ER: >10%		121	24	20	6	5	91
							75
PR		MET PR: <1%		MET PR: 1-10%		MET PR: >10%	
		Total (n)	n	%	n	%	n
PT PR: <1%		92	81	88	6	7	5
PT PR: 1-10%		14	10	71	2	14	2
PT PR: >10%		82	38	46	12	15	32
							39
HER2		MET HER2: neg		MET HER2: pos			
		Total (n)	n	%	n	%	
PT HER2: neg		144	131	91	13	9	
PT HER2: pos		44	8	18	36	82	

ER- estrogen receptor, MET- metastatic site, neg- negative, pos- positive, PR- progesterone receptor, PT- primary tumor

Figure 1 - 209

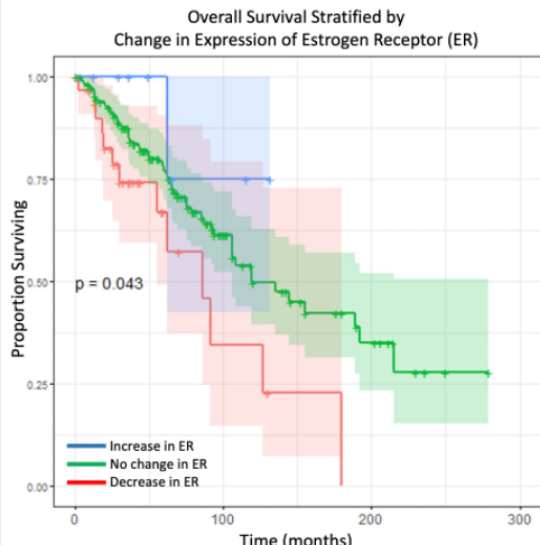
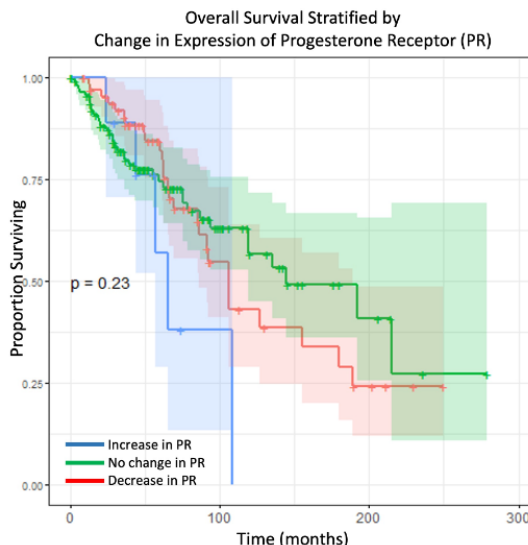


Figure 2 - 209



Conclusions: The tumor expression of ER/PR/HER2 in patients with BC can differ between PTs and corresponding METs. Loss of ER/PR expression is common, and decrease in ER expression is associated with worse OS. This observation merits additional investigation. Re-evaluating tumor markers at the metastatic site could potentially inform prognosis and therapeutic decision-making.

210 Indeterminate Fibroepithelial Lesions of the Breast Diagnosed by Percutaneous Core Needle Biopsy (CNB): Clinicopathologic Features and Predictive Criteria of Phyllodes Tumor

João Henrique Quintão¹, Caio Vasconcellos¹, Nicolai Gomes¹, Gabriel Oliveira¹, Bruno Maran¹, Guilherme Pellissari¹, Leonardo Romaniello Gama de Oliveira¹, Fabiana Makdissi¹, Solange Sanches¹, Luciana Graziano¹, Almir Bitencourt¹, Cynthia Osorio¹, Marina De Brot¹

¹A.C.Camargo Cancer Center, Sao Paulo, Brazil

Disclosures: João Henrique Quintão: None; Caio Vasconcellos: None; Nicolai Gomes: None; Gabriel Oliveira: None; Bruno Maran: None; Guilherme Pellissari: None; Leonardo Romaniello Gama de Oliveira: None; Fabiana Makdissi: None; Solange Sanches: None; Luciana Graziano: None; Almir Bitencourt: None; Cynthia Osorio: None; Marina De Brot: None

Background: Fibroepithelial lesions (FELs) of the breast are biphasic neoplasms for which the precise diagnosis entails an integrated evaluation of both epithelial/stromal components and this may generate issues in core needle biopsy (CNB) due to limited sampling. Here, we sought to establish clinical, radiological and histological parameters on CNB of indeterminate FELs that can predict a diagnosis of phyllodes tumors (PTs) at excision.

Design: Consecutive cases of FELs with overlapping features between fibroadenoma (FA) and PT diagnosed on CNB from 2014-2022 at a Cancer Center were selected and clinicopathological data were collected. Findings were correlated with subsequent excisions and sensitivity/specificity of the histologic parameters were calculated.

Results: Of 148 FELs from 145 female patients, 83/56% underwent surgical excision, with a final diagnosis of FA in 52/63% cases; benign PT in 12/15%; borderline PT in 5/6%; other benign lesions in 4/5% women. For 10/12% tumors, a clear distinction could not be made at excision and the term "benign fibroepithelial neoplasm" was used. Compared to FA, PT patients had an older average age at diagnosis (44 yo PT vs 36 yo FA; $p=0.019$) and a larger tumor size (3 cm PT vs 2 cm FA; $p=0.019$) - Table. Additionally, PT cases exhibited more frequently a leaf-like pattern (41% vs 33%; $p=0.56$) and stromal hypercellularity (88% vs 75%; $p<0.001$), particularly moderate hypercellularity (58.8% vs 7.7%; $p<0.001$). Stromal overgrowth was absent in all FAs, while it was found in 12% of PTs, all borderline. Mild/moderate stromal atypia was observed in 6% and 59% of FA/PT cases, respectively ($p<0.001$). No cases showed marked stromal hypercellularity/atypia. All lesions demonstrated a low mitotic rate, with a mean count in PTs greater than in FAs ($p=0.004$). Stromal hypercellularity on CNB was highly sensitive for the diagnosis of PT at surgical excision, whereas stromal atypia and mitotic activity were highly specific. In 32/39% cases, the diagnosis of FA vs PT was suggested in a note in the CNB report and it was concordant with the surgical diagnosis in 24. Follow-up data were obtained for 133 (90%; mean 12 mos) patients and 9 women developed new breast nodules. Only one was submitted to CNB, which revealed a FA.

		Diagnosis at surgical excision	p-value	Sensitivity	Specificity
Clinical, radiological and histological features on CNB	Fibroadenoma n=52	Phyllodes tumor n=17			
Mean age	36.5 yo	44.0 yo	0.019	N/A	N/A
Mean size in cm (at imaging)	2.1	3.1	0.019	N/A	N/A
Leaf-like architecture - n (%)	17 (32.7)	7 (41.2)	0.566	N/A	N/A
Stromal hypercellularity - n(%)	39 (75.0) 4 (7.7)	15 (88.2) 10 (58.8)	0.0004 <0.001	88.8% 88.8%	18.1% 18.1%
Mild to moderate					
Moderate					
Stromal atypia - n (%)	3 (5.8)	10 (58.8)	<0.001	58.8%	92.4%
Mitotic rate - mean/10 HPFs	0.038	0.47	0.0041	18.8%	98.5%

Conclusions: Our findings indicate that in indeterminate FELs detected by CNB a combination of key clinicopathological features, such as age, tumor size, stromal cellularity/atypia, and a higher mitotic rate are predictive of a PT diagnosis after excision.

211 TRPS-1 Immunohistochemical Staining in Breast Carcinomas and Carcinomas of Other Organ Sites with Emphasis on Triple-Negative Breast Cancers and Gynecologic Tumors

Rayan Rammal¹, Thing Rinda Soong², Gloria Carter³, Beth Clark³, Esther Elishaev⁴, Jeffrey Fine², Lakshmi Harinath³, Mirka Jones², Lauren Skvarca¹, Tatiana Villatoro¹, Jing Yu³, Chengquan Zhao³, Rohit Bhargava³

¹University of Pittsburgh Medical Center, Pittsburgh, PA, ²University of Pittsburgh, Pittsburgh, PA, ³UPMC Magee-Womens Hospital, Pittsburgh, PA, ⁴University of Pittsburgh School of Medicine, Pittsburgh, PA

Disclosures: Rayan Rammal: None; Thing Rinda Soong: None; Gloria Carter: None; Beth Clark: None; Esther Elishaev: None; Jeffrey Fine: None; Lakshmi Harinath: None; Mirka Jones: None; Lauren Skvarca: None; Tatiana Villatoro: None; Jing Yu: None; Chengquan Zhao: None; Rohit Bhargava: None

Background: The trichorhinophalangeal syndrome 1 (TRPS1) gene is a GATA transcription factor family member that has been found to play a role in breast carcinogenesis. Given the dearth of highly sensitive and specific markers for triple-negative breast carcinomas (TNBCs), interest in TRPS1 as a potential immunochemical (IHC) marker for TNBCs has grown. Recent data suggests high expression of TRPS1 in TNBCs and low or absent expression in carcinomas of other organs including gynecologic (GYN) carcinomas. Our aim was to explore the performance of TRPS-1 as an IHC diagnostic marker, find the optimal conditions for its use within breast carcinomas with an emphasis on TNBCs and compare to carcinomas of a select few organ sites with an emphasis on gynecologic tumors.

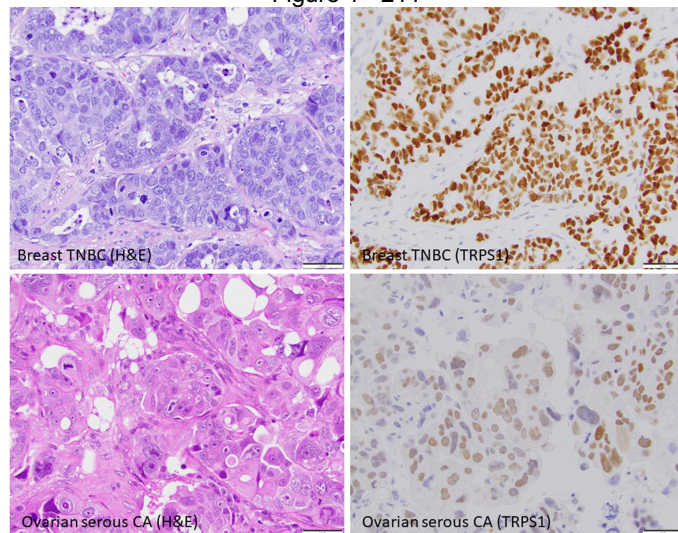
Design: Tissue microarrays (TMAs) from breast carcinomas (n=197); endometrial endometrioid adenocarcinoma (n=69); ovarian tumors (n=250); vulvar squamous cell carcinomas (n=96); pancreatic ductal adenocarcinoma (n=20); gastric adenocarcinoma (n=12) were stained with TRPS-1 using different conditions. Breast carcinomas consisted of hormone receptor positive (HR+)/HER2-negative (n=53); HR+/HER2-positive (n=6) and TNBCs (n=138). Ovarian tumors consisted of endometrioid (n=5); high grade serous (n=55), low grade serous (n=24), clear cell (n=25) carcinomas, serous borderline tumors (n=135) and carcinoma NOS (n=3). After trying >30 different staining conditions, two staining protocols (with intense reactivity in breast cancers, minimal reactivity in endometrium with no background staining) were chosen for staining (see table 1).

Results: A total of 644 tumors were tested for TRPS1 using two selected protocols (table 1). In our cohort, comparing TRPS1 result in breast carcinomas versus tumors from other tested organ sites, the sensitivity of TRPS1 was 89.13% and 84.74% while the specificity was 64.82% and 72.77% for protocol 1 and 2, respectively. For TNBCs versus GYN tumors, the sensitivity of TRPS1 was 91.37% and 86.8% while the specificity was 62.75% and 71.81% for protocols 1 and 2, respectively.

TMAs and tumors	Protocol 1-High pH: +ve/total (%)	Protocol 2-Low pH: +ve/total (%)	Protocol 1 TRPS1 H-score median and range on positive cases; IQR	Protocol 2 TRPS1 H-score median and range on positive cases; IQR
Breast carcinoma (TNBC)	123/138 (89%)	117/138 (85%)	230; 1-300; 130-270	170; 1-300; 100-225
Breast carcinoma (HR+ / HER2-neg)	51/53 (96%)	48/53 (91%)	180; 1-300; 105-240	140; 5-280; 85-200
Breast carcinoma (HR+ / HER2+)	6/6 (100%)	6/6 (100%)	190; 110-290; 150-253	135; 80-280; 80-220
Endometrial endometrioid adenocarcinoma	49/69 (71%)	46/69 (67%)	25; 2-170; 10-70	30; 1-150; 10-58
Ovarian tumors	43/250 (17%)	38/250 (15%)	15; 1-110; 5-25	7.5; 1-120; 5-40
Vulvar squamous cell carcinoma	54/96 (56%)	29/57 (30%)	30; 1-140; 10-60	20; 1-120; 10-50
Pancreatic ductal adenocarcinoma	2/20 (10%)	2/20 (10%)	22.5; 5-40; 14-31	22.5; 5-40; 14-31
Gastric adenocarcinoma	4/12 (33%)	0/12 (0%)	7.5; 2-10; 4-10	Not applicable

For both protocols 1 and 2: TRPS-1 Antibody clone: PA5-84874 (Invitrogen/Thermo Fisher, Waltham, MA); Staining Platform: Leica Bond III; Detection: Bond Polymer Refine DAB; Antigen Retrieval Temp: 100 °C; Primary Antibody Temp: room temperature.
 Protocol 1: Pre-treatment-ER2 (pH 9.0), 20 minutes, dilution-1 in 1000, primary antibody incubation time-30 minutes
 Protocol 2: Pre-treatment-ER1 (pH 6.0), 20 minutes, dilution-1 in 300, primary antibody incubation time-15 minutes

Figure 1 - 211



Conclusions: Under the conditions used, TRPS-1 stains 85-100% of breast carcinomas but also up to 71% of gynecological carcinomas, albeit with a weaker median expression (figure 1). Our data shows that while TRPS1 is a highly sensitive marker for TNBCs, it is not as highly specific as previously reported. Our protocol #1 had the maximum sensitivity with minimal compromise of the specificity and is currently approved for clinical use at our institution.

212 Secretory Cancer of Breast: A Clinicopathologic Analysis of Twenty-three Cases and Literature Review

Huayan Ren¹, Xin He¹, Huifen Huang¹, Yuqiong Liu¹, Huixiang Li¹

¹The First Affiliated Hospital of Zhengzhou University, Zhengzhou, China

Disclosures: Huayan Ren: None; Xin He: None; Huifen Huang: None; Yuqiong Liu: None; Huixiang Li: None

Background: Secretory breast carcinoma is an uncommon subset of breast cancer that usually has a favorable outcome. Although initially described in children, it also occurs in adults where it may metastasize, possibly resulting in death.

Design: The clinicopathological data and prognostic information of 23 patients with secretory breast cancer diagnosed by the Department of Pathology of the First Affiliated Hospital of Zhengzhou University from 2014 to 2022 were collected, and their clinical characteristics, histological structure, immunophenotype and molecular characteristics were analyzed.

Results: There were 21 female patients and 2 male patients, ranging from 12 to 63 years old, with a median age of 43 years. 9 cases in left breast and 14 cases in right breast. The clinical manifestations were mainly painless breast masses. Generally, most of them were relatively well-defined nodules, gray and hard. Microscopically, the tumor cells were mainly arranged in microcysts and tubular, and a few were in solid nest and papillary structures. The cytoplasm of tumor cells was eosinophilic granules or foam like. Introcytoplasmic and extracellular eosinophilic or amphophilic secretions were consistently present. Most cases are accompanied by sclerotic stroma. An in situ component often present. Immunohistochemically, 23 cases showed S100 and pan-TRK diffuse strong positive, 14 cases showed ER, PR and HER2 triple negative expression, 9 cases showed a small amount or weak positive ER, and Ki67 proliferation index was 3%-30%. FISH detection in 6 cases showed that NTRK3 gene was broken. Treatment and prognosis: 23 patients received surgical treatment, 14 of them received postoperative adjuvant chemotherapy. all 23 patients were followed up for 2-96 months, and 1 patient had pulmonary metastasis after 1 year. all 23 patients survived.

Figure 1 - 212

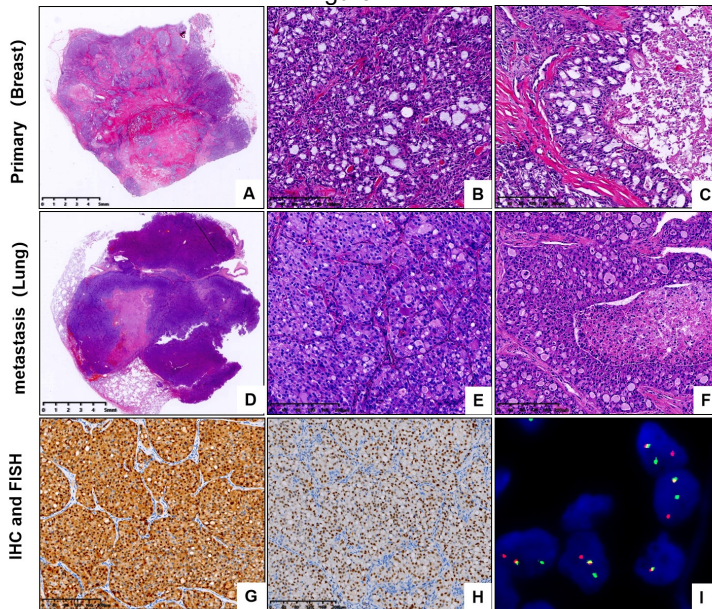


Figure 1. Secretory carcinoma of breast metastasizes to lung. (A) Primary focus of breast. (B) Microcysts and solid nest. (C) Focal necrosis. (D) Pulmonary metastasis. (E) Microcysts and solid nest. (F) Focal necrosis. (G,H) Immunohistochemical staining of S100 and pan-TRK, both are diffuse strong positive. (I) FISH: NTRK3 gene break (positive).

Conclusions: Secretory breast carcinoma is a rare invasive carcinoma, most of which show indolent biological behavior, but a few cases can also have lymph node and distant metastasis. The cases with solid structure, increased mitotic figures, necrosis and high proliferative activity in histology may indicate a higher tendency of recurrence or metastasis. The application of specific immunological marker pan-TRK and FISH detection of NTRK gene can assist in the diagnosis of secretory breast carcinoma. With the popularization and application of NTRK inhibitors, new treatment options will be provided for patients with recurrent or metastatic secretory breast carcinoma.

213 A Deep Learning Artificial Intelligence Algorithm Helps Pathologists Improve Diagnostic Accuracy and Efficiency in The Detection of Lymph Node Metastases in Breast Cancer Patients

Juan Retamero¹, Emre Gulturk¹, Jillian Sue¹, Alican Bozkurt¹, Julian Viret¹, Kasper Malfroid¹, Brandon Rothrock¹, David Klimstra¹

¹Paige.AI, New York, NY

Disclosures: Juan Retamero: None; Emre Gulturk: None; Jillian Sue: None; Alican Bozkurt: None; Julian Viret: None; Kasper Malfroid: None; Brandon Rothrock: None; David Klimstra: None

Background: The detection of metastases to lymph nodes constitutes an essential task in breast cancer staging, which is done by pathologists worldwide. However, this is tedious and time-consuming, and the sensitivity of pathologists at this task is suboptimal. The literature shows that pathology review by experts results in a change of nodal status in up to 24% of patients. The literature also shows that artificial intelligence (AI) tools can help pathologists in detecting breast cancer metastases to lymph nodes, which could potentially improve their diagnostic accuracy and alleviate workload issues. We set out to study how the diagnostic performance of pathologists varied when they were aided by a tumor detection AI tool.

Design: An AI algorithm was trained using multiple instances learning, a weakly supervised deep learning approach whereby the digitized glass slide image (known as whole slide image or WSI) is paired with its corresponding pathology report. More than 32,000 breast sentinel lymph node WSIs from more than 8,000 patients were used to train this algorithm, which is designed to highlight areas suspicious to harbor metastasis in digitized WSIs of lymph node tissue. Three pathologists were asked to review a challenging dataset comprising 167 breast sentinel lymph node WSIs, of which 69 harbored cancer metastases of different sizes, enriched for challenging cases. Ninety eight slides were benign. The pathologists read the dataset twice, both digitally without AI assistance and with AI assistance, staggered to control for reading order bias, after a three week washout period. They were asked to record their slide level diagnosis, and were timed during their reads.

Results: The average sensitivity of the pathologists during the unassisted phase in this challenging dataset was 81% which improved to 93% during the assisted phase. Specificity was non-inferior during the assisted phase, and remained at 98%. The average reading time was 131 seconds per slide during the unassisted phase compared with 58 seconds per slide during the aided

phase, resulting in an overall efficiency gain of 55% when the pathologists were assisted by AI. These shorter reading times applied to both benign and malignant WSIs regardless of metastasis size.

Conclusions: This study highlights how AI can help pathologists improve their diagnostic performance, as measured by sensitivity improvements to detect metastases of any size. In addition, AI helped pathologists reduce their reading times by more than half.

214 Targeting Cell Cycle Dystopia in Breast Cancer

Hanna Rosenheck¹, Sidney Mahan¹, Jianxin Wang¹, Vishnu Muthuraj Kumarasamy¹, Agnieszka Witkiewicz¹

¹Roswell Park Comprehensive Cancer Center, Buffalo, NY

Disclosures: Hanna Rosenheck: None; Sidney Mahan: None; Jianxin Wang: None; Vishnu Muthuraj Kumarasamy: None; Agnieszka Witkiewicz: None

Background: Cell cycle control is tightly coordinated by Cyclin-dependent kinase (CDK) family activities, which are frequently deregulated in cancer. The CDK4/6 action is targeted by compounds that are FDA-approved in the context of HR+/HER2- breast cancer, while a number of CDK2 inhibitors are in the early-stage clinical development. Here, we sought to define means to identify tumors with specific configurations of CDK and Cyclin proteins expression using multispectral profiling to define precision approaches for these inhibitors.

Design: A combination of gene perturbation and biochemical approaches were used to define requirement for different CDK and Cyclins in driving cancer cell cycles. These dependencies were linked to specific alterations in the expression of select Cyclin and CDK genes. Multispectral immunofluorescence panels were applied to >500 clinical cases to define protein markers associated with sensitivity to CDK4/6 or CDK2 inhibitors. Cell cycle states in breast cancer were compared to those in genitourinary, and gynecological malignancy tissue microarrays. Results were benchmarked against xenograft models of known sensitivity to these agents.

Results: The differential requirements for specific CDK or Cyclins associated with tumor origin and genetic alterations, revealing substantial heterogeneity within and between different tumor types. This variability in cell cycle dependences can be predicted in clinical specimens by analyses of multispectral immunofluorescence expression data. Unbiased statistical analyses indicated specific protein configurations that are associated with sensitivity to CDK4/6 vs. CDK2 inhibitors. Benchmark experiments using xenograft models of known resistance and sensitivity profiles supported specific marker configurations associated with pharmaceutical sensitivities.

Conclusions: The cell cycle states define sensitivity to FDA-approved CDK4/6 inhibitors as well as the emerging CDK2 inhibitors and could provide precision medicine approach to treatment.

215 TRPS1 Immunohistochemical Evaluation of Paget Disease

Cooper Rutland¹, Aihui Wang², Gregor Krings³, Gregory Bean²

¹Stanford Pathology, Stanford, CA, ²Stanford Medicine/Stanford University, Stanford, CA, ³University of California, San Francisco, San Francisco, CA

Disclosures: Cooper Rutland: None; Aihui Wang: None; Gregor Krings: None; Gregory Bean: None

Background: TRPS1 is a GATA family transcription factor and recent work has demonstrated the utility of TRPS1 immunohistochemistry (IHC) in the clinicopathologic evaluation of breast carcinoma. TRPS1 has been shown to be a highly sensitive marker for triple-negative breast carcinoma, including tumors which do not express immunohistochemical markers GATA3 and SOX10. Such high-grade lesions may be an underlying carcinoma in mammary Paget disease (PD), with >95% of PD patients harboring a concurrent high-grade ductal carcinoma in situ (DCIS) or invasive carcinoma. Histologic mimics of PD, including Toker cell hyperplasia and Bowen disease, and the immunohistochemical overlap of these entities, can represent a diagnostic challenge.

Design: Cases of mammary PD and mimics were stained with TRPS1, including 24 cases of PD (9 ER-HER2+, 5 ER+HER2-, 5 ER+HER2+ and 5 ER-HER2-), 5 cases of Toker cells/Toker cell hyperplasia, and 1 case of Bowen disease. Additionally, TRPS1 and GATA3 IHC was performed on 15 cases of extramammary PD (5 perianal, 5 vulvar and 5 scrotal) to explore any potential immunohistochemical differences from mammary PD.

Results: TRPS1 consistently demonstrated strong (22/24) to moderate (2/24) nuclear staining of Paget cells in mammary PD cases from all four ER/HER2 expression profiles. Moreover, TRPS1 IHC demonstrated improved differential staining of Paget cells from surrounding keratinocytes, with minimal to absent staining of background epidermis compared to GATA3. For extramammary PD, a similarly positive staining pattern was demonstrated in scrotal (5/5) and vulvar (5/5) cases. Interestingly, however,

PD cases from perianal skin demonstrated faint (3/5) to no (2/5) nuclear expression of TRPS1. Lastly, TRPS1 also positively highlighted Toker cells of nipple skin (5/5), while Bowen disease was negative.

Conclusions: These data suggest a potential use of TRPS1 immunohistochemistry, combined with ER and HER2, in the evaluation of mammary PD. Paget (and Toker) cells are more easily distinguished from keratinocytes using TRPS1 compared to GATA3. Though beyond the scope of this study, these data also suggest a molecular divergence in the pathogenesis of extramammary Paget disease arising in genital versus perianal skin.

216 End-to-End Deep Neural Network for Ki-67 Stained WSI Automatic Hotspot Detection and Proliferation Index (PI) Quantification for Breast Cancer Tissue

Joseph Rynkiewicz¹, Yahia Salhi², Céline Bossard³, Jérôme Chetritt³, Sanae Salhi⁴

¹Paris, France, ²DiaDeep, Lyon, France, ³IHP GROUP, Nantes, France, ⁴Lyon, France

Disclosures: Joseph Rynkiewicz: None; Yahia Salhi: None; Céline Bossard: None; Jérôme Chetritt: None; Sanae Salhi: None

Background: The advent of digitalisation of immunostained slides and recent progress in artificial intelligence emphasised the development of computer-assisted quantification, assessment and analysis of whole-slide images (WSI). In this paper, we shed light on the nuclear protein Ki-67 assessment, which is one of the main prognostic factors for tumor progression and treatment in breast cancer. The main objective is to propose an end-to-end pipeline based on a deep neural network for the hotspot detection on Ki-67 stained WSI as well as proliferation rate quantification.

Design: We developed a supervised deep neural network on histopathology annotated squared images (tiles) of size 256 pixels of the publicly available dataset SHIDC-BC-Ki-67, which consists of 2356 images from 23 patients, labelled by expert pathologists. For each tile, cell annotations were available in three different classes of immunopositive, immunonegative, and tumor infiltrating lymphocytes. A U-Net architecture with an adequate backbone network is investigated and trained and validated on 1656 tiles. Testing was carried on a left-out set of size 701 of the same database originating from 23 patients. The performance of the model is investigated and compared to the original PathoNet architecture, among others.

Results: Ki-67 PI prediction was evaluated using the root mean squared errors (RMSE) at the tile and patient level. Our pipeline has an RMSE of 0.035 at the patient level, which outperforms the benchmark, on the same data split, that has an RMSE of 0.048. The model also outperforms other state of the art frameworks. The hotspots are implicitly and accurately inferred on the basis of outcomes of this prediction. Regarding the classification of the patients with respect to the cut-off thresholds: 16% and 30%, the accuracy is 95.96% over 23 patients on the left-out set SHIDC-BC-Ki-67 database. Finally, the pipeline is challenged using an external dataset of 65 cases, which were independently screened by experienced pathologists, with the same performance.

Conclusions: Development of artificial intelligence models for WSI treatment is generally task-specific and is based on casting possibly complex processing pipelines. Thus, unlike most of the available algorithms, the proposed end-to-end approach identifies the hotspot and quantifies the PI, on a single end-to-end step with promising performance. The model can be easily generalized to other prognostic and/or nuclear biomarkers in a quick and straightforward manner.

217 Inter-Observer Variability in the Diagnosis of Breast Atypical Glandular Proliferations on Core Needle Biopsy

Lamees Saeed¹, Bing Han², Zena Jameel¹, Erika Baardsen¹, Sarah Hugar¹, Reza Eshraghi³, Saeed Bajestani⁴, Saira Shah⁵, Marilin Rosa¹

¹H. Lee Moffitt Cancer Center & Research Institute, Tampa, FL, ²Tulane School of Medicine, New Orleans,

LA, ³Northwestern University Feinberg School of Medicine, Chicago, IL, ⁴Louisiana State University Health Sciences Center, ⁵Quest Diagnostics, Tampa, FL

Disclosures: Lamees Saeed: None; Bing Han: None; Zena Jameel: None; Erika Baardsen: None; Sarah Hugar: None; Reza Eshraghi: None; Saeed Bajestani: None; Saira Shah: None; Marilin Rosa: None

Background: The diagnosis of atypia in the breast is subject to inter and intraobserver variability. In addition, this diagnosis is impacted by other factors such as clinical and radiological findings, type and quality of the biopsy sampling, and lesion characteristic, among others.

Design: To evaluate diagnostic variability within our team of 7 breast pathologists, we performed a search of our system to identify lesions with the undetermined/borderline diagnoses of "atypical intraductal proliferation" and "atypical glandular proliferation" on CNB between 2010 and 2021. Slides were reviewed independently and blindly to the original interpretation and available follow-up.

Clinical and radiological information was provided at the time of review. Interobserver variability was evaluated using Fleiss multi-rater kappa analysis and possible associations underwent Chi-square testing.

Results: Forty cases with available slides for review were included. Relevant follow-up data were collected. In 62.5% of cases (25/40) a follow-up diagnosis of atypia or carcinoma was made upon excision. Of these, 52% of cases (13/25) had overt invasive or in-situ carcinoma (*upgraded group*) and 48% (12/25) were diagnosed with atypical lesions (*no change/atypical group*). In 27.5% of cases (11/40) an atypical or malignant lesion was not present on follow-up (*downgraded group*). Four cases (10%) did not undergo excision. A statistically significant agreement of 0.866 ($p<0.001$) on calling a lesion atypical on CNB was found. Interobserver agreement for the diagnosis of atypia on CNB was 0.93 ($p=0.42$) for the upgraded group, 0.86 ($p<0.001$) for the no change/atypical group, and 0.79 ($p<0.001$) for the downgraded group. The most cited reasons for being unable to make a definitive diagnosis on CNB included: 1) limited focus, 2) borderline features, 3) apocrine features, however none were statistically significant when Chi-square was applied.

Figure 1 - 217

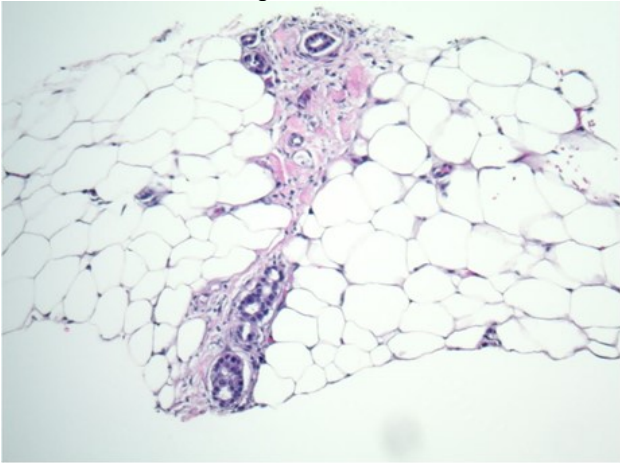


Figure 1: Case diagnosed as atypical glandular proliferation on CNB. A limited number of infiltrating glands suspicious for invasive carcinoma is present. The area of interest is not available on deeper sections for further characterization. Follow-up was invasive carcinoma (HE, x100)

Figure 2 - 217

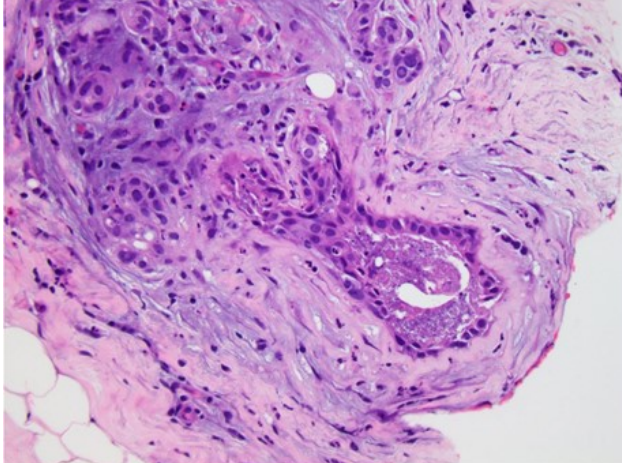


Figure 2: Case diagnosed as "atypical intraductal proliferation" on CNB shows a few ducts with apocrine features, cytologic atypia, and necrosis. Follow-up excision did not show atypical or malignant findings (HE, x200)

Conclusions: During this retrospective study, we evaluated our experience with atypical and borderline breast lesions diagnosed on core needle biopsy in correlation with surgical or clinical follow-up and we statistically measured the interobserver variability where a significant interrater agreement ($p<0.001$) was observed. The seeming lack of definitive associations with the definition of atypicality calls for consensus agreement which showed very good kappa measurement in our study.

218 A Comparative Evaluation of TRPS1 and GATA3 in Adenoid Cystic, Acinic Cell, and Secretory Carcinomas of the Breast and Salivary Glands

Alireza Salem¹, Cody Han¹, Yun Wu¹, Constance Albarracin¹, Lavinia Middleton¹, Hui Chen¹, Aysegul Sahin¹, Qingqing Ding¹

¹The University of Texas MD Anderson Cancer Center, Houston, TX

Disclosures: Alireza Salem: None; Cody Han: None; Yun Wu: None; Constance Albarracin: None; Lavinia Middleton: None; Hui Chen: None; Aysegul Sahin: None; Qingqing Ding: None

Background: Salivary gland-type neoplasms of the breast are uncommon and are comprised of a collection of entities with distinct biology and clinical behavior, sharing analogies to salivary glands carcinomas. Most of these tumors are triple-negative breast carcinoma (TNBC) with a low risk of metastasis. While GATA3 is the most widely used breast marker, its utility is limited in diagnosing TNBC. In this study, we have investigated the expression of a new breast marker, TRPS1, in the subset of salivary gland-type tumor of breast and head & neck (H&N) and compared its utility to GATA3.

Design: We collected 37 breast cases (28 adenoid cystic carcinoma [AdCC], 7 secretory carcinoma [SC], 2 acinic cell carcinoma [ACC] and 24 H&N cases (16 AdCC, 2 SC, and 4 ACC) between 2015-2022. Immunohistochemical staining for TRPS1 and GATA3 were performed. Only nuclear staining was considered as positive. The immunoreactivity scores were calculated semi-quantitatively and categorized as negative (<1%), low positive (1-10%), intermediate positive (11-50%), and high positive (>50%).

Results: In the breast AdCC, TRPS1 was positive in 100% of solid type, and mixed cribriform and solid type, but only positive in 50% of cribriform type; conversely, GATA3 was negative in majority of all types of breast AdCC. In the H&N AdCC, TRPS1 was positive in 100% of solid, 67% of mixed, and only 30% of cribriform type; GATA3 was also predominately negative in these tumors.

Both TRPS1 and GATA3 were positive in 100% of secretory carcinomas of breast and H&N, while both TRPS1 and GATA3 were negative in all breast ACC and majority of ACC of H&N (75%). (Figure 1)

Figure 1 - 218

	TRPS1			GATA3				Total
	Negative (n, %)		Positive (n, %)	Negative (n, %)	Positive (n, %)		High	
	Low	Intermediate	High	Low	Intermediate	High	Total	
Breast AdCC								
Cribiform	3 (50%)	2 (33%)	1 (17%)	0	4 (67%)	2 (33%)	0	6
Mixed	0	3 (37.5)	4 (50%)	1 (12%)	6 (75%)	2 (25%)	0	8
Solid	0	2 (14%)	0	12 (86%)	13 (93%)	1 (7%)	0	14
H&N AdCC								
Cribiform	7 (70%)	3 (30%)	0	0	7 (70%)	0	2 (20%)	1 (10%)
Mixed	1 (33%)	1 (33%)	1 (33%)	0	2 (67%)	1 (33%)	0	3
Solid	0	1 (33%)	2 (67%)	0	3 (100%)	0	0	3
Breast SC	0	0	0	7 (100%)	0	0	0	7
H&N SC	0	0	0	2 (100%)	0	0	0	2
Breast ACC	2 (100%)	0	0	0	2 (100%)	0	0	2
H&N ACC	3 (75%)	1 (25%)	0	0	3 (75%)	1 (25%)	0	4

Conclusions:

- TRPS1 exhibited high expression in AdCC with solid component (solid and mixed types) of both breast and H&N, while GATA3 was predominantly negative or weak positive in all AdCCs.
- TRPS1 & GATA3 showed similar pattern in SC and ACC of both breast and H&N.
- TRPS1 does not differentiate breast salivary gland-type tumor from H&N counterparts, which may provide evidence of genetic analogies between these entities.

219 Prognostic Impact of NOTCH1 Expression in Primary Breast Adenoid Cystic Carcinoma

Alireza Salem¹, Yun Wu¹, Qingqing Ding¹, Lavinia Middleton¹

¹The University of Texas MD Anderson Cancer Center, Houston, TX

Disclosures: Alireza Salem: None; Yun Wu: None; Qingqing Ding: None; Lavinia Middleton: None

Background: Adenoid cystic carcinoma (AdCC) of the breast is a rare subtype of TNBC, characterized by proliferation of two cell types: luminal and myoepithelial with either a cribriform or solid growth pattern. Most AdCCs harbor a characteristic chromosomal translocation resulting in an *MYB:NFIB* fusion gene and the overexpression of MYB. *NOTCH1* mutations are found in approximately 14% of patients with salivary gland AdCC and patients harboring *NOTCH1* mutations have shorter relapse free and overall survival. The purpose of this study was to explore the effects of *NOTCH1* pathway on the clinical behavior of patients with primary breast AdCC by examining *NOTCH1* immunoreactivity.

Design: We reviewed 24 cases of breast AdCC in patients diagnosed at a single institution from 2015-2022. Immunohistochemical staining for NOTCH1 was performed. Only nuclear expression of NOTCH-1 considered as positive. Results were assessed on a four-tier scale: negative indicated no staining (<1%), low positive (<20%), intermediate positive (20-50%), and high positive (>50%). Clinical features were reviewed. Follow-up data was available in all 24 patients and median follow-up was 23 months (range 1-127 mo).

Results: In 70% (7 of 10) of patients with metastasis or recurrences NOTCH1 showed 20% or more nuclear expression (intermediate and high positive) and in 30% (3 of 10) NOTCH1 was negative. In patients without metastasis/recurrence NOTCH1 was negative in 21.5% (3 of 14), low positive in 57% (8 of 14), and intermediate positive in only in 21.5% (3 of 14). These results show overexpression of NOTCH1 ≥ 20% in AdCCs is associated with aggressive clinical features. Fisher exact test 0.0351, p <0.05. MYB expression was documented in 12 cases. In 50% of which, NOTCH1 was expressed more than 20% (intermediate or high positive) and in the remaining 50 % NOTCH1 was either negative or low positive (<20%). NOTCH1 was predominantly expressed in tumor cells with reticular and cribriform growth patterns.

NOTCH1 expression in breast AdCC, Fisher exact test 0.0351, p <0.05		
	NOTCH1 Intermediate/ High positive	NOTCH1 Low positive/ negative
AdCC with recurrence / metastasis	7	3
AdCC without recurrence /metastasis	3	11

Conclusions:

- Our study demonstrates that in patients with breast AdCC, overexpression of NOTCH $\geq 20\%$ is associated with aggressive clinical outcomes.
- NOTCH1 inhibitor may have potential therapeutic effect in patients with breast AdCC, by inhibiting cancer cell growth in recurrence and metastasis.

220 Predicting Response to CDK4/6 Inhibitors in Breast Cancer

Emily Schultz¹, Deanna Hamilton¹, Jianxin Wang¹, Agnieszka Witkiewicz¹

¹Roswell Park Comprehensive Cancer Center, Buffalo, NY

Disclosures: Emily Schultz: None; Deanna Hamilton: None; Jianxin Wang: None; Agnieszka Witkiewicz: None

Background: In spite of widespread use and known mechanism of action, predictive biomarkers for the use of CDK4/6 inhibitors (CDK4/6i) in conjunction with endocrine therapy have yet to emerge. Here a cohort of patients treated with standard-of-care combination regimens was utilized to explore features of disease and determinants of progression-free survival (PFS).

Design: In this cohort of 235 patients, >90% of patients were treated with Palbociclib in combination with either an aromatase inhibitor (AI) or fulvestrant (FUL). The PFS mirrored that observed in randomized clinical trials. A total of 151 patient tumor tissues were used for targeted gene expression analyses with the HTG-Oncology Biomarker Panel. The association of disease state and gene expression analyses were interrogated for disease evolution and association with PFS using Cox PH regression.

Results: HER2 immunohistochemistry (0, 1+, 2+) was not associated with PFS in full cohort, or AI and FUL subgroup analyses. The lack of progesterone receptor was associated with shorter PFS in the full patient cohort ($p=0.012$) and selectively in patients treated with AI ($p=0.005$), but not FUL. Gene expression-based subtyping indicated that the majority of patients had luminal breast cancer; the predominant subtypes changed with treatment and disease evolution. Primary tissue from tumor resection was dominated by luminal A subtype, which diminished with metastatic disease, and was rare in post progression. The luminal B, HER2, and basal subtypes exhibited shorter PFS in CDK4/6i combinations (AI, $p=0.01$; FUL, $p=0.03$). Existing clinically developed breast cancer signatures (e.g. breast cancer index) had variable associations with PFS; however high expression of gene signatures associated with cell cycle were broadly associated with short PFS. Concordantly, utilizing unbiased analyses, gene expression programs linked to cell cycle were associated with short PFS, while interferon response processes were associated with longer PFS. Algorithms that incorporated standard pathological and clinical variables with the gene expression data were developed that exhibited potent predictive power.

Conclusions: Tumor evolution occurs on treatment with CDK4/6i; however, analyses of pretreatment biopsies can inform the duration of PFS. These data support discrete biological processes associated with sensitivity/resistance. Predictive algorithms could be developed to inform features of treatment decision which will require prospective validation which is ongoing.

221 Clinicopathologic and Genetic Characteristics of Breast Cancers in Patients with CHEK2 Alterations

Christopher Schwartz¹, Nikka Khorsandi¹, Amie Blanco², Rita Mukhtar¹, Yunn-Yi Chen¹, Gregor Krings¹

¹University of California, San Francisco, San Francisco, CA, ²UCSF Medical Center, San Francisco, CA

Disclosures: Christopher Schwartz: None; Nikka Khorsandi: None; Amie Blanco: None; Rita Mukhtar: None; Yunn-Yi Chen: None; Gregor Krings: None

Background: Germline alterations in checkpoint kinase 2 (CHEK2) are associated with a moderately increased risk of breast cancer (BC). While it is known that BC arising in the context of CHEK2 mutation are estrogen receptor (ER) and/or HER2 positive, the clinical and genetic features of these BC are lacking.

Design: A cohort of 64 patients with heterozygous high-risk germline CHEK2 alterations that underwent breast sampling was assembled. All pathology slides were reviewed. Clinicopathologic and outcome data were retrieved. Targeted next generation DNA sequencing (NGS) was performed on a subset (21 BC, 18 patients) with an assay targeting 529 cancer genes.

Results: Of 64 patients, 36 (56%) had invasive BC. Median age at diagnosis was 45 years (range 25-71). Mean tumor size was 1.5 cm (range <0.1 to 9.4). Lymph node metastases were present in 31% (10/32). Most BC were invasive ductal carcinomas (81%, 29/36) and grade 2 (61%, 22/36) or 3 (19%, 7/36). Nearly all tumors (92%, 33/36) were ER+, and 28% (10/36) were HER2+ (8 ER+, 2 ER-). Mammprint scores (MP) were equally high (50%) and low (50%) risk (n=12). 21-gene recurrence scores (RS) were low (<17) in 50%, intermediate (18-30) in 33%, and high (>30) in 17% (n=12). Of 13 patients treated with neoadjuvant chemotherapy, 31% had pathologic complete response, with 15% RCB-I, 46% RCB-II and 8% RCB-III. One patient (3%, 1/33) had

disease progression, with overall event free survival rate of 93% (mean follow up 3.4 years, range 0.4-13.9). There were no differences in clinical or pathologic data between HER2- and HER2+ groups, aside from higher Ki-67 (>25%) in the HER2+ group ($p=.01$). By NGS, 57% (12/21) BC had biallelic CHEK2 inactivation, due to loss of heterozygosity (LOH) of the germline allele in 92% (11/12). One patient with multifocal BC had a somatic CHEK2 mutation as a second hit in 1 tumor. Three patients also had germline mutations in other BC risk genes (ATM, PALB2, RAD50), 2 with CHEK2 LOH and 1 also with ATM LOH. Most CHEK2 BC had a luminal genetic profile with aberrations in GATA3 (24%), PIK3CA (24%), CCND1 (24%), and FGFR1 (19%). TP53 alteration was infrequent (10%).

Conclusions: Most BC arising in high-risk CHEK2 carriers are ER positive and were clinicopathologically heterogeneous in our cohort. In addition to a luminal genetic profile, most BC had biallelic CHEK2 inactivation, supporting CHEK2 as a dominant oncogenic driver. No differences were identified between HER2+ and HER2- BC, but larger studies with longer follow-up are required.

222 Evolution and Clinical Significance of HER2 Status after Neoadjuvant Therapy for Breast Cancer

Jiuyan Shang¹, Yueping Liu¹

¹The Fourth Hospital of Hebei Medical University, Shijiazhuang, China

Disclosures: Jiuyan Shang: None; Yueping Liu: None

Background: The emergence of HER2 antibody-drug conjugates provides new treatment decisions for breast cancer patients, especially those with low HER2 expression. In order to explore the biological characteristics of breast cancer with low HER2 expression, the HER2-Low category in primary breast cancer and residual tumor after neoadjuvant therapy was investigated to reflect the evolution of HER2 expression. Comparing the clinicopathological features of HER2-low and negative breast cancer.

Design: HER2 was assessed according to the latest ASCO/CAP guidelines. The cut-off value for staining of HER2-positive cells was >10%. HER2-negative cases were divided into HER2 low expression (IHC=1+/2+ and no ISH amplification) and HER2-0 (IHC=0), and the clinicopathological characteristics of the cases were collected.

Results: This study included 1140 patients with invasive breast cancer who received preoperative neoadjuvant therapy from 2018 to 2021, of which 365 patients achieved pCR and 775 were non-pCR. In the non-pCR cohort, HER2-Low cases accounted for 59.61% of primary tumors and 55.36% of residual tumors. Among HER2-negative cases, HR-positive tumors had a higher incidence of low HER2 expression compared with triple-negative tumors (80.27% vs 60.00% in primary tumors and 72.68% vs 50.77% in residual tumors). The inconsistency rate of HER2 expression was 21.42%, mainly manifested as the conversion of HER2-Low cases to HER2-0 (10.19%) and the conversion of HER2-0 to HER2-Low (6.45%) (Fig.1). Among the HER2-negative cases in the primary tumor, the HER2 discordance rate of HR-positive cases was lower than that of triple-negative cases (23.34% VS 36.92%) (Fig.2). This difference was mainly caused by the case switching from HER2-Low to HER2-0. Compared with HER2 0 cases, there were statistically significant differences in RCB grade, MP grade and the number of metastatic lymph nodes in HER2 low expression cases. Patients with low HER2 expression had a lower pathological response rate and a higher number of metastatic lymph nodes.

Figure 1 - 222

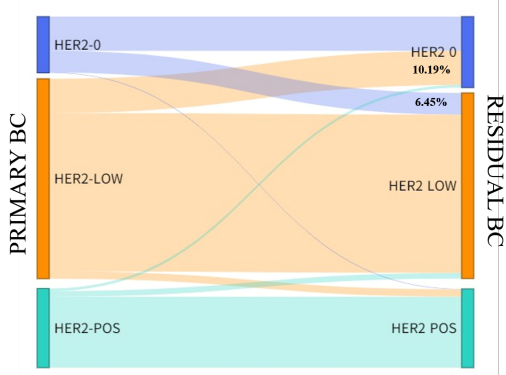


Fig.1 Evolution of HER2 status from primary tumor to residual tumor before and after neoadjuvant therapy in breast cancer

Figure 2 - 222

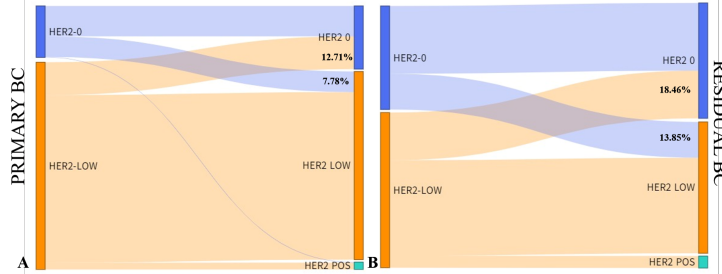


Fig.2. Evolution from primary tumor to residual tumor in the HER2-negative cohort.
A. Hormone receptor positive (HR+); B. Hormone receptor negative (HR-).

Conclusions: Low expression of HER2 is highly unstable during disease evolution and has certain biological characteristics. Re-detection of HER2 in breast cancer after neoadjuvant therapy may lead to new treatment opportunities for a certain proportion of patients.

223 DNAJC12 Causes Breast Cancer Chemotherapy Resistance by Repressing Doxorubicin-Induced Ferroptosis and Apoptosis via Activation of AKT

Mengjia Shen¹, Libo Yang², Feng Ye, Hong Bu¹

¹West China Hospital, Sichuan University, Chengdu, China, ²West China Hospital, Sichuan University, China/The University of Texas MD Anderson Cancer Center, USA, Abidjan

Disclosures: Mengjia Shen: None; Libo Yang: None; Feng Ye: None; Hong Bu: None

Background: Although chemotherapy is the most effective treatment for breast cancer (BC), some patients are chemoresistant. Elimination of chemotherapy resistance would improve the overall survival for BC patients. This study aims to screen essential chemoresistant factors, clarify the corresponding mechanism, and ultimately try to reverse this process.

Design: Samples from the Gene Expression Omnibus (GEO) and West China Hospital were used to screen and validate chemoresistant candidate genes. MDA-MB-231 cells and MCF-7 cells were mainly used to conduct gain-of or loss-of function studies. RNA-seq was used to screen the underlying mechanism. Interactions among DNAJC12, HSP70 and AKT were explored by coimmunoprecipitation (Co-IP) assay. Mouse xenograft models were generated to validate the molecular mechanism *in vivo*.

Results: DNAJC12 expression was closely correlated with the response to taxane and anthracycline-based neoadjuvant chemotherapy in GEO datasets and our clinical cases, which was confirmed to be anthracycline. Doxorubicin (DOX, a typical anthracycline) could induce cell death via ferroptosis, which could be inhibited by ferroptosis inhibitors. DNAJC12 inhibited both DOX-induced ferroptosis and apoptosis, and the combined apoptosis and ferroptosis inhibitors entirely reversed this DOX resistance. RNA-seq enrichment revealed that overexpression of DNAJC12 activated the PI3K-AKT pathway. An AKT inhibitor reversed DNAJC12-induced DOX resistance by restoring DOX-induced apoptosis and ferroptosis. Furthermore, we confirmed that DNAJC12 increased AKT phosphorylation in an HSP70-dependent manner. HSP70 inhibition could also relieve DNAJC12-induced DOX resistance by recovering apoptosis and ferroptosis. Finally, in a subcutaneous tumor-bearing mouse model, we used an AKT inhibitor to reverse DNAJC12-induced DOX resistance *in vivo*.

Conclusions: DNAJC12 expression is strongly associated with chemoresistance in BC patients. The DNAJC12-HSP70-AKT signaling axis plays an essential role in chemotherapy resistance by inhibiting DOX-induced ferroptosis and apoptosis. Our results reveal a potential therapeutic target for BC chemoresistance.

224 Artificial Intelligence for Mitosis Count Assistance in Invasive Breast Carcinoma: a clinical study

Clara Simmat¹, Stephane Sockeel¹, Nicolas Pozin¹, Sophie Prévot¹, Magali Lacroix-Triki², Catherine Miquel¹, Marie Sockeel¹, Loris Guichard¹

¹Paris, France, ²Gustave Roussy, Cancer Campus, Grand Paris, Villejuif, France

Disclosures: Clara Simmat: None; Stephane Sockeel: None; Nicolas Pozin: None; Sophie Prévot: None; Magali Lacroix-Triki: None; Catherine Miquel: None; Marie Sockeel: None; Loris Guichard: None

Background: The Elston-Ellis modification of Scarff-Bloom-Richardson (SBR) grading system is a major prognostic factor for invasive breast carcinoma (IC). Its determination requires the evaluation of a mitotic score which is subject to low intra and inter reproducibility. The mitotic count shall be performed in the most proliferative area of the tumor, which determination is hard but critical. Artificial intelligence based tools could help pathologists to detect mitosis on whole slide images (WSI). We developed an automatic detection pipeline along with an interactive interface to ease mitotic score determination. Here we present a clinical study designed to measure the help brought to practitioners by this tool.

Design: The algorithm locates mitosis in IC regions. Localization is a two-step process : a first brick detects candidate objects resembling mitosis, the selection is then refined by a classifier. It is trained on a set of invasive breast carcinoma slides containing 2838 labeled mitoses from various medical centers. Mitosis density on the slide is then measured and the densest regions are shown to the pathologist along with detected objects. The pathologist can then establish a score. For this study, three expert pathologists determined a ground truth mitotic score on fifty slides in a consensual manner. Those slides were also submitted to two junior pathologists who evaluated the mitotic score of each slide twice, with and without the assistance of the algorithm, with a four weeks wash-out period. The help brought by our tool was measured by evaluating the scores obtained with, and without assistance, compared to the ground truth.

Results: AI improves both pathologists' reproducibility and diagnostic accuracy. Mitotic score accuracy is increased by 14%, from 62% without IA (resp. 64%) to 76% with IA (resp. 78%) for both junior pathologists. Kappas are increased from 0.457 (resp. 0.378) to 0.726 (resp. 0.629). Intraclass Correlation Coefficient (ICC) for the mitotic count between junior pathologists is increased from 0.591 to 0.883.

Conclusions: A clinical study confirmed that our mitotic detection can assist pathologists in their daily practice.

225 Clinicopathological Features of HER2 Expressing Lobular Carcinoma of Breast

Maher Sughayer¹, Majd Khader¹

¹King Hussein Cancer Center, Amman, Jordan

Disclosures: Maher Sughayer: None; Majd Khader: None

Background: Invasive lobular carcinoma (ILC) comprises about 10% of invasive breast carcinomas (IBC) and is considered the most common special subtype of invasive breast carcinoma. The vast majority (95%) of classical ILC express estrogen receptors (ER+) and progesterone receptors (PR+) but lack HER2 overexpression. On the other hand 30% of pleomorphic ILC are reported to be HER2+. In a previous study we found that ILC represents 7.1% of all IBC and that HER2 was overexpressed in 3.6% of them. The aim of this study is to assess the histopathologic features of ILC that show overexpression of HER2.

Design: This study was carried out at the King Hussein Cancer Center department of pathology. The archives were retrospectively searched for cases of invasive lobular carcinoma that exhibited HER2 overexpression between the years (2008-2019). H&E slides were retrieved. The histopathologic features of the invasive carcinomas were reviewed looking for any morphological deviation from the classical features of lobular carcinomas. The following features were specifically looked for: nuclear pleomorphism, signet ring cell morphology, and apocrine features in order to see if these tumors can be classified as pleomorphic lobular carcinoma

Results: A total of twenty-eight cases were found. Ten cases displayed all three histopathologic criteria that were studied (nuclear pleomorphism, signet ring cell morphology, and apocrine features), 12 cases showed pleomorphism and signet ring cell morphology, 3 cases showed pleomorphism and apocrine features, 2 cases showed pleomorphism only, and 1 case did not show any of the features. Twenty two cases were ER+ (78.6%), while only 16 cases (57.1%) were PR+. The patients were followed up over an average duration of 47 months. At 60 months, the overall survival was 40.7%. At time of last follow-up, of the twenty-eight patients, seven patients were alive (35%), four were alive with advanced disease (metastasis) (20%), and nine were dead (45%). Eight patients had no outcome data available. Out of the seven alive patients, three had a pathologic stage of ypT0N0 (43%) at time of presentation

Conclusions: The vast majority of HER2+ invasive lobular carcinomas are of the pleomorphic variant. In addition they tend to have signet ring cell morphology and apocrine features. Compared to the classical variant they have decreased overall survival rates and tend to have less expression of estrogen and progesterone receptors.

226 Clinicopathologic Features of 96 Pure Invasive Apocrine Carcinoma of the Breast

Xiangjie Sun¹, Ke Zuo¹, Xiaoli Xu¹, Yufan Cheng¹, Rui Bi², Bao-Hua Yu¹, Xiaoyu Tu¹, Ruohong Shui¹, Wentao Yang¹

¹Fudan University Shanghai Cancer Center, Shanghai, China, ²Fudan University Shanghai Cancer Center, Shanghai Medical College, Fudan University, Shanghai, China

Disclosures: Xiangjie Sun: None; Ke Zuo: None; Xiaoli Xu: None; Yufan Cheng: None; Rui Bi: None; Bao-Hua Yu: None; Xiaoyu Tu: None; Ruohong Shui: None; Wentao Yang: None

Background: Pure invasive apocrine carcinoma (IAC) is a rare type of primary breast cancer, constituting approximately 1% of all breast cancers. Most pure IACs are triple negative, while the rest are HER2-enriched. The clinical outcome of pure IACs varies among different studies due to limited cases and other reasons such as the criteria of the diagnosis. Therefore, we analyzed the clinicopathologic features of 96 pure IACs to investigate the characteristics of this population.

Design: 96 pure IAC patients who underwent breast surgery at Fudan University Shanghai Cancer Center between 2009-2021 were collected. Clinicopathologic characteristics including age, tumor size, lymph node status, histological grade, immunophenotype, pTNM stage, local recurrence and metastasis status were analyzed.

Results: All IAC patients were female, with a median age at diagnosis of 61 years (ranging from 38 to 83 years). The largest diameter of these tumors ranged from 0.8 to 7.5 cm. 86.8% of cases were diagnosed as histological grade II, and 13.2% as grade III. 25% of patients had nodal metastases at diagnosis, and the number of positive lymph nodes ranged from 1 to 14. The majority of patients in this cohort presented at an early TNM stage (I:51.0%; II:41.7%; and III:7.3%). 86.5% of patients were TNBC while only 10.4% were HER2 positive. The mean Ki-67 index was 12.9% (ranging from 3 to 50%). All cases exhibited diffuse nuclear staining for AR and GCDP15. 41.4% of cases showed a distinctive granular cytoplasm staining pattern for HER2, and most of them (93.1%) were of TNBC subtype. After a median follow-up of 49 months, six patients (6.3%) died, four of whom developed disease-related mortality, and the other 2 died from other diseases. One (1.0%) patient suffered from local recurrence, and six (6.3%) experienced distant metastases. The most common metastatic sites were bone and lung. Twenty-five triple negative apocrine carcinomas were further investigated by next-generation sequencing (NGS), and the top ranked genomic alterations were PIK3CA (68%), TP53 (32%) and PTEN (28%) mutation.

Conclusions: To the best of our knowledge, this study is the largest clinicopathologic cohort for pure IACs. In our study, most pure IACs were TNBC with a relatively good clinical outcome compared with other aggressive subtypes of TNBC. NGS revealed the most common clinical relevant genomic alteration for triple negative IACs was PIK3CA mutation. Longer follow-up is vital to obtain more accurate prognostic information for IAC patients.

227 Clinical and Histopathologic Correlation of MRI-Guided Breast Biopsies: Experience in a Tertiary Care Hospital

Steffanie Charlyne Tamayo¹, Evi Abada², Gregory Tatevian¹, C. James Sung², Kamaljeet Singh¹

¹Women and Infants Hospital, Providence, RI, ²Women & Infants Hospital/Alpert Medical School of Brown University, Providence, RI

Disclosures: Steffanie Charlyne Tamayo: None; Evi Abada: None; Gregory Tatevian: None; C. James Sung: None; Kamaljeet Singh: None

Background: Breast magnetic resonance imaging (MRI) is currently used for screening high risk patients, pre-surgical planning, assessment of eligibility for and response to neoadjuvant chemotherapy, and resolution of lesions with discordant pathology. It has high sensitivity (> 90%) compared to conventional breast imaging methods (i.e., mammography) but is a time-consuming procedure that requires specific equipment and highly trained staff. More importantly, it has variable specificity (range 30-90%) and low positive predictive value, thereby increasing cost of care, patient anxiety, and time to treatment. This study explores the common clinical indications whereby MRI-guided breast biopsy is performed in our institution, as well as the histopathologic findings in these biopsies.

Design: A retrospective electronic database search for MRI-guided breast biopsies performed in our institution between January 1, 2016 and December 31, 2021 was conducted. Clinical indications and MRI findings were correlated with final histopathology and tested for statistical significance.

Results: A total of 655 MRI biopsies (bx) from 548 patients were identified: 455 patients with 1 bx and 93 patients with more than 1 bx. The MRI findings were: mass/mass-like enhancement (MLE) = 230 (35%), non-MLE = 214 (33%), enhancement = 118 (18%), and others = 93 (14%). Indications for bx were: post-mammogram dense breast = 19 (3%), high risk screening 267 (41%), concurrent breast cancer = 294 (45%), and others = 75 (12%). The bx histological findings included: 415 (63%) benign proliferative changes, 105 (16%) high-risk histology, 68 (10%) DCIS, 66 (10%) invasive carcinoma, and 1 (0.2%) mastitis. Malignancy was significantly higher in a setting of concurrent breast cancer ($p<0.001$, Figure 1). The prevalence of high risk/ borderline lesions was similar in all the clinical settings and ranged from 10.5% to 18%. MRI bx in the setting of nipple discharge revealed malignancy and high risk lesion in 13% and 7% of cases, respectively (Figure 2). The histological diagnosis of malignancy was independent of MRI findings, ranging from 19% to 22% among the 4 aforementioned categories.

Figure 1 - 227

	Germline mutation	History of breast cancer	History of atypia	Nipple discharge	> 1 risk factor	Family history	Others
Histology							
Malignancy	2 (8%)	8 (28%)	4 (11%)	2 (13%)	2 (3%)	8 (13%)	3 (16%)
High risk/ Borderline lesion	3 (12%)	4 (14%)	12 (33%)	1 (7%)	11 (15%)	8 (13%)	3 (16%)
Proliferative changes	25 (80%)	17 (58%)	20 (66%)	12 (80%)	61 (82%)	46 (74%)	13 (68%)

Figure 1. Cross-tabulation of risk factors considered part of high risk screening and final histopathology.

Figure 2 - 227

Histology	Risk factors for high risk screening						
	Germline mutation (n = 30)	History of breast cancer (n = 29)	History of atypia (n = 36)	Nipple discharge (n = 15)	> 1 risk factor (n = 74)	Family history (n = 62)	Others (n = 19)
Malignancy	2 (7%)	8 (28%)	4 (11%)	2 (13%)	2 (3%)	8 (13%)	3 (16%)
High risk/ Borderline lesion	3 (10%)	4 (14%)	12 (33%)	1 (7%)	11 (15%)	8 (13%)	3 (16%)
Proliferative changes	25 (83%)	17 (58%)	20 (56%)	12 (80%)	61 (82%)	46 (74%)	13 (68%)

Figure 2. Cross-tabulation of risk factors considered part of high risk screening and final histopathology.

Conclusions: Benign proliferative changes are the most common finding in MRI-guided breast biopsies. Malignancy and high risk/ atypical histology are noted in up to 21% and 16% of biopsies, respectively. The malignant diagnosis in MRI biopsies is significantly higher in a setting of concurrent breast cancer and is independent of specific MRI features.

228 Upgrade Rate of Atypical Papillary Neoplasm Diagnosed on Breast Core Needle Biopsy

Paula Toro Castano¹, Andrew Sciallis¹, Xiaoyan Cui¹, Gloria Lewis¹

¹Cleveland Clinic, Cleveland, OH

Disclosures: Paula Toro Castano: None; Andrew Sciallis: None; Xiaoyan Cui: None; Gloria Lewis: None

Background: Papillary neoplasms of the breast are diagnostically challenging due to morphological overlap among entities. When definitive classification is not possible on core needle biopsy (CNB), we use the term "atypical papillary neoplasm" (APN), defined as cytologic and/or architectural atypia occurring in papillary lesions. The upgrade rate of atypical ductal hyperplasia (ADH) has been reported as 30%. The aim of this study is to evaluate the clinical significance of APN on CNB by determining upgrade rate on excisional biopsy.

Design: We collected CNB diagnosed as APN in a single institution between January 2000 and January 2022. Demographics and excisional biopsy reports were correlated.

Results: 55,669 CNB were performed. Of these, we found 116 CNB with the diagnosis of APN in 113 patients. Excisional biopsy findings are summarized in table 1.

Excisional biopsy diagnosis	Number of cases (%)	Age in years
No residual tumor	1 (0.8)	85
Intraductal papilloma without atypia	2 (1.8)	65 and 73
ADH arising in an intraductal papilloma	11 (9.7)	61-85 (mean: 67)
Ductal carcinoma in situ (DCIS) or encapsulated papillary carcinoma (EPC)	57 (50.4)	38-91 (mean: 68)
Invasive ductal carcinoma (IDC), including microinvasive	42 (37.2)	43-85 (mean: 67)
	2 microinvasive (1.7% of the total)	

Conclusions: APN is used sparingly in our institution accounting for 0.2% of CNB. 88% of patients diagnosed with APN were upgraded to DCIS, EPC, or IDC on excisional biopsy. Age was not a factor in upgrade risk ($p=0.73$). Because the upgrade rate of APN is higher than for ADH (30%), complete excision with negative margins should be considered.

229 Interobserver Agreement in Scoring HER2 Negative and HER2 Low Immunohistochemistry (IHC) in Breast Cancer: Reasons for discordance and efficacy of single training session

Yun-An Tseng¹, Steffanie Charlyne Tamayo¹, C. James Sung², M. Ruhul Quddus², Katrine Hansen³, L.C. Hanley¹, Shivali Marketkar⁴, Evi Abada², Kamaljeet Singh¹

¹Women and Infants Hospital, Providence, RI, ²Women & Infants Hospital/Alpert Medical School of Brown University, Providence, RI, ³Brown University Pathology, Providence, RI, ⁴Framingham Union Hospital, Framingham, MA

Disclosures: Yun-An Tseng: None; Steffanie Charlyne Tamayo: None; C. James Sung: None; M. Ruhul Quddus: None; Katrine Hansen: None; L.C. Hanley: None; Shivali Marketkar: None; Evi Abada: None; Kamaljeet Singh: None

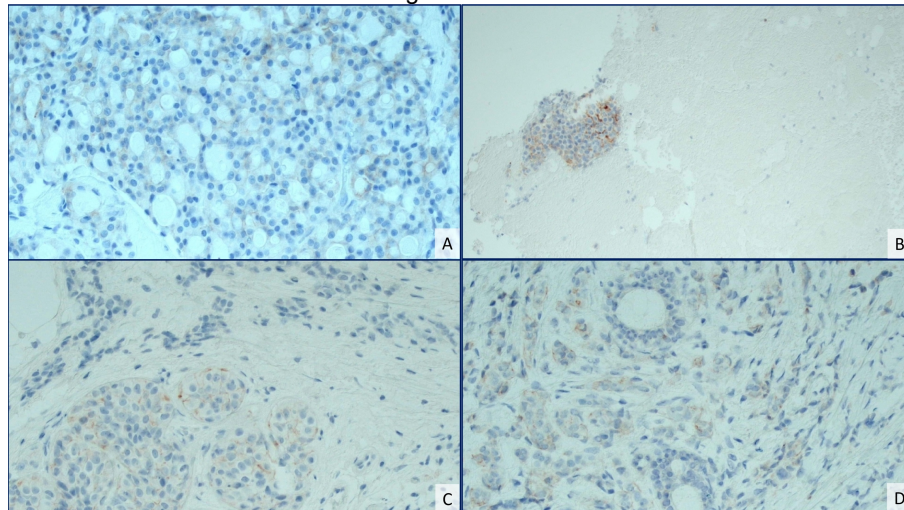
Background: The recent DESTINY-Breast04 clinical trial reported survival benefits of using Trastuzumab Deruxtecan in patients whose metastatic breast carcinoma showed low HER2 IHC expression (HER2-L). HER2-L is defined as a IHC score of 1+ or 2+ with negative FISH. These new findings may cause challenges for pathologists as the HER2 testing and reporting guidelines were designed with an emphasis on identifying HER2 positive tumors. Only limited data has reported poor agreement in scoring HER2-0 vs. 1+ on glass and scanned IHC slides. The aim of this project is to investigate the HER2 IHC concordance rate, with a particular focus on HER2-0 vs. HER2-L, among pathologists who practice in the same institution, and to evaluate impact of a training session on concordance improvement.

Design: Total 60 HER2 IHC and H&E stains from breast biopsies with invasive carcinoma were retrieved. The cases were reviewed by 9 breast pathologists (7 experienced attendings and 2 fellows) individually in 2 rounds of 30 cases each. An educational slide review session was provided between the 2 rounds addressing cases from 1st round that showed low concordance rate. SPSS (ver 27) was used to analyze the data and compute Cohen's kappa (κ) values.

Results: The overall complete agreement for HER2 was noted in 37/60 (62%) cases, with similar agreement in the 1st [19/30 (63%)] and 2nd round [18/30 (60%)]. For all 60 cases κ values ranged from .517 to .895 with 92% κ values in substantial agreement range or better ($\geq .61$). The agreement in diagnosing HER2-0 & HER2-L was 59%: 14/25 (56%) in the 1st round and 62% (16/26) in the 2nd round. For HER2-0 and HER2-L κ values ranged from .298 to .826, with only 45% of the κ values in substantial agreement or better range. Two or more scorers classified 5 HER2-0 as HER2-L & 3 HER2-L as HER2-0. In HER2-L group 50% of the scorer pairs κ values were ≤ 0 (no agreement) and only 14% of pairs showed substantial or better agreement (Table 1). Cytoplasmic blush (A), dislodged tumor cells in fibrin (B), staining of in-situ component (C) and lobular features (D [Figure1]) were considered potential reasons for difficulty in distinguishing HER2-0 vs. HER2-L staining.

Cohen's kappa range	(≤0) No agreement	.01-.20 (slight)	.21-.40 (fair)	.41-.60 (moderate)	.61-.80 (substantial)	.81-1 (almost perfect)
Overall concordance (n=60)	0	0	0	3 (8%)	23 (64%)	10 (28%)
HER2-0 vs. HER2-L concordance (n=52)	0	0	4 (11%)	16 (44%)	13 (36%)	3 (8%)
HER2-L only concordance (n=41)	18 (50%)	4 (11%)	5 (14%)	4 (11%)	4 (11%)	1 (3%)

Figure 1 - 229



Conclusions: Breast pathologists show poor agreement in distinguishing HER2-0 and HER2-L IHC scores in breast carcinomas. This disagreement may be related to pitfalls of the IHC staining assessment. Scoring HER2-L may require continuous education and calibration to increase awareness of these pitfalls and to improve concordance rate.

230 Comprehensive Clinical-Pathologic Assessment of Malignant Phyllodes Tumors: Proposing Refined Diagnostic Criteria

Gulisa Turashvili¹, Qingqing Ding², Yi Liu¹, Limin Peng¹, Miralem Mrkonjic³, Haider Mejbel¹, Yihong Wang⁴, Huina Zhang⁵, Gloria Zhang⁶, Jigang Wang⁷, Shi Wei⁸, Xiaoxian Li¹

¹Emory University, Atlanta, GA, ²The University of Texas MD Anderson Cancer Center, Houston, TX, ³Mount Sinai Hospital, University of Toronto, Toronto, ON, ⁴Brown University, Rhode Island Hospital, Providence, RI, ⁵University of Rochester Medical Center, Rochester, NY, ⁶Cleveland Clinic, Cleveland, OH, ⁷The Affiliated Hospital of Qingdao University, Qingdao, China, ⁸The University of Kansas School of Medicine, Kansas City, KS

Disclosures: Gulisa Turashvili: None; Qingqing Ding: None; Yi Liu: None; Limin Peng: None; Miralem Mrkonjic: None; Haider Mejbel: None; Yihong Wang: None; Huina Zhang: None; Gloria Zhang: None; Jigang Wang: None; Shi Wei: None; Xiaoxian Li: None

Background: The 5th edition of the World Health Organization (WHO) classification of breast tumors recommends diagnosing malignant phyllodes tumors (MPTs) when all of the following 5 morphologic features are present: permeative tumor borders, stromal overgrowth, marked stromal cellularity, marked stromal cytologic atypia and ≥ 10 mitoses per 10 high-power fields (HPF). We aimed to assess the performance characteristics of the WHO recommendation to capture MPTs and morphologic features predictive of distant metastasis in this multi-institutional retrospective study.

Design: MPTs diagnosed at participating institutions between 2000 and 2021 were identified. Selection criteria included excisions or mastectomies with available slides and clinical outcome. Clinical-pathologic data were collected. Statistical analyses were performed using R software and included univariate (Kaplan-Meier curves, log rank test) and multivariate models.

Results: A total of 65 MPTs were identified with median follow-up of 24.5 months (1-204). The median patient age was 49 years (22-89). The median tumor size was 8 cm (2-33). Stromal overgrowth was present in 56 cases (86%), marked stromal cellularity in 40 (61.5%), marked stromal atypia in 38 (58.5%), ≥ 10 mitoses per 10 HPF in 50 (77%), and at least focally permeative borders in 58 (89.5%). A subset of tumors (17, 26%) had heterologous elements, the most common being liposarcomatous differentiation (8, 47%). Distant metastases were observed in 20 (31%) patients (Table 1). All 5 morphologic features were identified in only 13 (20%) of the 65 cases and 7 (35%) of the 20 cases with distant metastases. In univariate analysis, only marked stromal atypia ($p=0.004$) and marked stromal cellularity ($p=0.017$) were associated with distant recurrence free survival (DRFS). Best subset selection procured in a multivariate Cox regression model showing association of stromal overgrowth, stromal atypia and stromal cellularity with DRFS (C-index 0.721, 95% CI 0.578, 0.863).

Table 1. Morphologic features of the 20 MPTs with distant metastases

Case	Tumor borders	Stromal Cellularity	Stromal atypia	Mitoses per 10 HPF	Stromal overgrowth
1	Permeative	Marked	Marked	≥ 10	Present
2	Permeative	Marked	Marked	≥ 10	Present
3	Permeative	Marked	Marked	≥ 10	Present
4	Permeative	Marked	Marked	≥ 10	Present
5	Permeative	Marked	Marked	≥ 10	Present
6	Permeative	Marked	Marked	≥ 10	Present
7	Permeative	Marked	Marked	≥ 10	Present
8	Focally permeative	Marked	Marked	≥ 10	Present
9	Focally permeative	Marked	Marked	≥ 10	Present
10	Focally permeative	Marked	Marked	≥ 10	Present
11	Well-defined	Marked	Marked	≥ 10	Present
12	Well-defined	Marked	Marked	≥ 10	Present
13	Permeative	Moderate	Marked	≥ 10	Present
14	Permeative	Moderate	Moderate	5-9	Present
15	Focally permeative	Moderate	Moderate	≥ 10	Present
16	Focally permeative	Moderate	Marked	≥ 10	Present
17	Focally permeative	Marked	Marked	5-9	Present
18	Permeative	Marked	Moderate	≥ 10	Absent
19	Focally permeative	Marked	Marked	5-9	Absent
20	Well-defined	Marked	Moderate	≥ 10	Absent

Conclusions: Our findings suggest that the current WHO recommendation will miss a significant number of MPTs with distant metastases. We propose refined diagnostic criteria for MPTs without requiring all 5 morphologic features: 1) a combination of stromal overgrowth with ≥ 1 of the features (marked stromal atypia, marked stromal cellularity, ≥ 10 mitoses per 10 HPF), or 2) in the

absence of stromal overgrowth, a combination of marked stromal cellularity with either marked stromal atypia or ≥10 mitoses per 10 HPF.

231 Correlation of HER2 Immunohistochemical Scores and HER2 mRNA, Oncotype Recurrence Score and Magee Scores on ER Positive, HER2 Negative Breast Cancers

Haley Tyburski¹, Cansu Karakas², Huina Zhang², Elena Liu², Bradley Turner², David Hicks²

¹University of Rochester, Rochester, NY, ²University of Rochester Medical Center, Rochester, NY

Disclosures: Haley Tyburski: None; Cansu Karakas: None; Huina Zhang: None; Elena Liu: None; Bradley Turner: None; David Hicks: Advisory Board Member: AstraZeneca

Background: The approval of trastuzumab deruxtecan in advanced HER2-low (IHC 1+ or 2+/ish-) breast cancers has led to a paradigm shift in the evaluation of HER2. Meanwhile, it raised a number of important questions related to the biologic significance of HER2-low expression as well as the best methodology that can be used to identify which patients with "HER2-negative" breast cancers will be the most likely to derive clinical benefit from this new targeted therapeutic approach. We herein retrospectively examined a large series of ER-positive breast cancer sent for Oncotype (ODX) testing, looking for correlates between the reported HER2 mRNA results, recurrence scores, Magee scores, Ki67 results, and HER2 IHC categories (0+, 1+ and 2+/ish-).

Design: A total of 750 ER positive, HER2 negative breast cancer samples from 2008 to 2018 that had been sent for ODX testing were included. HER2 mRNA levels, ODX recurrence score (RS), Magee score and Ki67 index were collected and analyzed by Welch's *t*-test. P<0.05 was considered statistically significant.

Results: Among HER2 IHC categories, there was a significant difference in HER2 mRNA values between IHC 0+ and IHC 1+ (8.80 vs 9.18, p<0.01), as well as between IHC 1+ and 2+/ish- (9.18 vs 9.35, p<0.05) (Table 1). Ki-67 index, recurrence scores by both ODX and Magee equation showed statistically significant differences between IHC 1+ and 2+/ish- cases, but not between HER2 0 and HER2 1+ cases (Fig 1). Further analysis between HER2 0 and HER2 low cases showed that only difference in HER2 mRNA levels reached statistical significance; while, the differences in RS, Magee scores and Ki-67 index between HER2 0 and HER2 low groups failed to reach statistical significance (Fig 2).

Table 1: Summary Statistics of Testing Methodologies Across HER2 IHC Categories

	Count (%)	Mean	SD	95% Confidence Interval	
				Lower Bound	Upper Bound
HER2 mRNA					
0+	261 (47%)	8.796	0.671	8.714	8.878
1+	196 (35%)	9.181	0.639	9.091	9.271
2+/Nonamplified	102 (18%)	9.348	0.622	9.226	9.470
Total	559				
Recurrence Score					
0+	334 (45%)	16.778	9.076	15.802	17.755
1+	269 (36%)	16.885	8.266	15.892	17.877
2+/Nonamplified	147 (20%)	19.102	11.033	17.304	20.900
Total	750				
Magee Score					
0+	334 (45%)	17.375	5.540	16.779	17.972
1+	269 (36%)	17.347	5.260	16.715	17.978
2+/Nonamplified	147 (20%)	19.521	5.839	18.569	20.473
Total	750				
Ki67					
0+	304 (43%)	14.95	14.10	13.36	16.54
1+	256 (36%)	14.54	12.65	12.99	16.10
2+/Nonamplified	145 (21%)	19.20	15.63	16.63	21.77
Total	705				

Figure 1 - 231

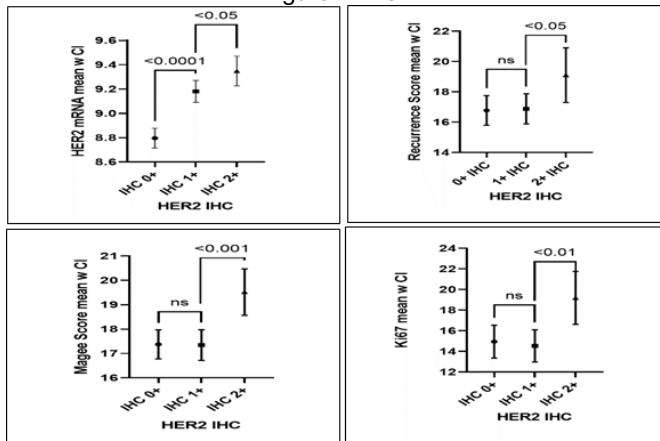
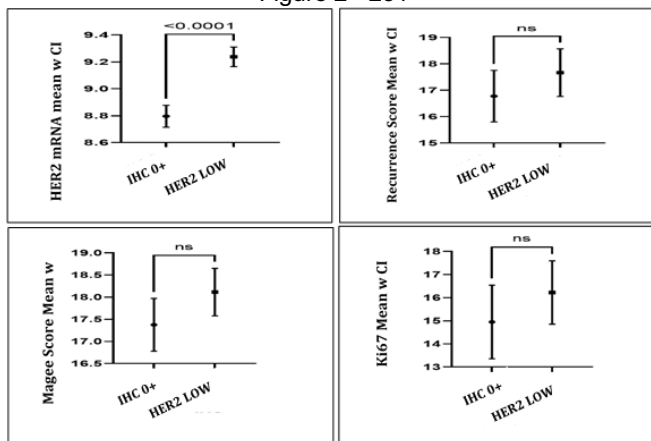


Figure 2 - 231



Conclusions: From this large cohort, IHC 0+, 1+, and 2+/ISH- appeared to be able to distinguish between quantitative levels of HER2 mRNA in these HER2-low expressing tumors. Given IHC 0+ and 1+ were indistinguishable in RS, Magee Scores, and Ki67 levels, IHC testing is not the most efficient when predicting the risk of recurrence between HER2-0 and HER2-low breast cancers. On the contrary, IHC 2+/ish- was significantly distinguished across each quantitative variable and expected to have a higher chance of recurrence as suggested by RS/Magee Score. Correlation with HER2 mRNA, RS, Magee scores need to be further evaluated as a methodology for identifying HER2-low breast cancers to determine who will gain the greatest benefit from new treatment.

232 Streptavidin-coated Phosphor Integrated Dot Fluorescent Nanoparticles (PID) Method could be a more Reliable Method on Detecting Low Levels of HER2 Expression in Breast Cancers

Haley Tyburski¹, Cansu Karakas², Elena Liu², Huina Zhang², David Hicks²

¹University of Rochester, Rochester, NY, ²University of Rochester Medical Center, Rochester, NY

Disclosures: Haley Tyburski: None; Cansu Karakas: None; Elena Liu: None; Huina Zhang: None; David Hicks: None

Background: Immunohistochemistry (IHC) for HER2 protein evaluation is a semi-quantitative method with relatively limited dynamic ranges and is not an ideal method for detecting low levels of HER2 expression. With the inclusion of HER2-low category in the HER2 evaluation, it is urgently needed to develop alternative methods for accurate and reliable evaluation of HER2 expression for selecting patient who would derive clinical benefit from the newly-approved anti-HER2 agent. Streptavidin-coated phosphor integrated dot fluorescent nanoparticles (PID) has been reported to be a valuable quantitative methodology for HER2 testing in breast cancers. In this study, we evaluated whether there was significant difference in the level of HER2 protein expression by PID across the different HER2 IHC subgroups.

Design: A total of 105 samples which were previously tested by PID assay were included. The corresponding HER2 IHC was performed by HercepTest and was scored according to ASCO/CAP HER2 testing guidelines. The average number of PID nanoparticles per cell (PID score/cell) and the average number of PID nanoparticles per unit area (PID score/ROI100um²) were collected and analyzed by descriptive statistics to produce a mean and confidence interval for each HER2 IHC category. P<0.05 was considered statistical significance.

Results: Both PID score/cell and PID score/unit had a broad dynamic range (2.25-294.26 and 1.53-140.65) across the different HER2 IHC subgroups, and increased with the IHC scores (Table 1). Statistical analysis revealed that there were significant differences in average PID score/cell between IHC 1+ vs. 2+/ish- groups ($p<0.05$), 2+/ish- vs. 2+/ish+ groups ($p<0.01$) and 2+/ish+ vs. 3+ groups ($P<0.01$), while no significant difference was achieved between HER2 0 and HER2 1+ groups. The average PID score/unit showed similar trend, although there was no significant difference between HER2 1+ and HER2 2+/ISH- groups (Fig 1). When comparing between HER2-0, HER2-low and HER2-positive categories, the significant differences on both PID score/cell and PID score/unit were achieved between HER2-0 and HER2-low, as well as between HER2-low and HER2-positive cases (Fig 2).

Table 1: Summary Statistics of PID Scores Across HER2 IHC Categories

PID Score@cell	Count (%)	Mean	SD	95% Confidence Interval	
				Lower Bound	Upper Bound
0+	12 (11%)	3.317	1.672	2.254	4.379
1+	15 (14%)	5.247	3.602	3.252	7.241
2+/Nonamplified	24 (23%)	9.288	6.641	6.483	12.092
2+/Amplified	32 (30%)	48.931	71.038	23.319	74.543
3+	22 (21%)	229.86	145.24	165.46	294.26
Total	105				
PID Score@ROI100 um ²	Count (%)	Mean	SD	Lower Bound	Upper Bound
0+	12 (24%)	2.167	1.008	1.526	2.807
1+	15 (29%)	3.873	3.797	1.771	5.976
2+/Nonamplified	24 (47%)	6.525	5.223	4.320	8.730
2+/Amplified	32 (30%)	23.597	29.936	12.804	34.390
3+	22 (21%)	114.35	59.314	88.052	140.65
Total	105				

Figure 1 - 232

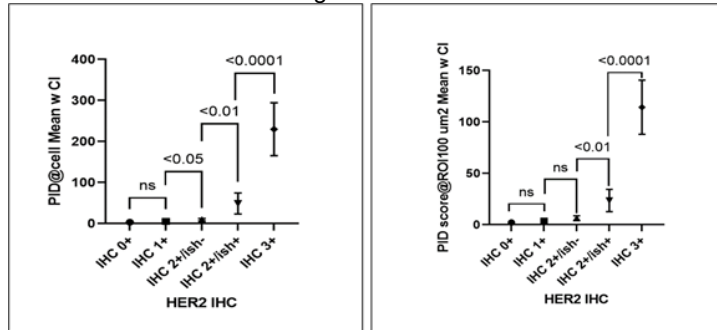
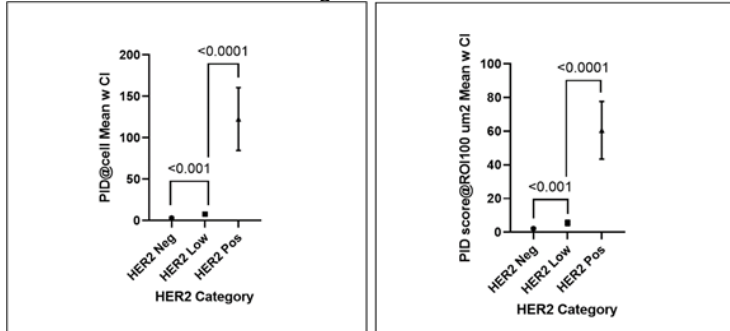


Figure 2 - 232



Conclusions: The preliminary results demonstrated quantitative PID method has a broad dynamic ranges (~133 folds) and could provide more reliable evaluation on HER2-low expressing breast cancers. Further evaluation of PID in the large case cohort and extensive clinical validation are needed.

233 Mammographic Architectural Distortion of the Breast on Core Needle Biopsy: Outcomes, Frequency of Malignancy and Radiologic-Pathologic Correlation

Elmira Vaziri Fard¹, Dena Khaefpanah², Zahra Alhusain², Oluwole Fadare³, Farnaz Hasteh⁴, Somaye Zare⁴

¹UC San Diego Health, San Diego, CA, ²UC San Diego Medical Center, San Diego, CA, ³UC San Diego School of Medicine, La Jolla, CA, ⁴University of California, San Diego, La Jolla, CA

Disclosures: Elmira Vaziri Fard: None; Dena Khaefpanah: None; Zahra Alhusain: None; Oluwole Fadare: None; Farnaz Hasteh: None; Somaye Zare: None

Background: Mammographic architectural distortion (MAD) is defined as distorted normal breast architecture without definitely visible mass in the Breast Imaging Reporting and Data System (BI-RADS) lexicon. MAD have been associated with a wide variety

of benign or malignant lesions. In this study, we evaluated the outcomes of this radiological finding at our institution, including the frequency with which malignancy is identified in the associated biopsy.

Design: Our pathology data base was searched for all breast core needle biopsies (CNB) performed for a radiologic indication of MAD between 1/2011 and 6/2022. Radiologic and pathology findings were reviewed.

Results: A total of 242 cases were identified, comprising approximately 1.8% of all CNBs. The age of patients ranged from 22 to 86 (mean: 58). The pathologic diagnoses were classified as malignant (40.5%), atypical (4.5%), and benign (55%). Of 99 malignant cases, 74 (74.8%) were invasive carcinomas, 22 (22.2%) were ductal carcinoma in situ (DCIS), and 2 (2%) showed metastatic carcinoma. Of the invasive cancers, 53 (71.6%) were invasive ductal carcinoma (IDC), 15 (20.2%) were invasive lobular carcinoma (ILC), and 6 (8.1%) were mixed type carcinomas. Among the cases with metastatic carcinomas, one was high grade serous carcinoma of gynecologic origin and one lung adenocarcinoma. Among the 11 atypical lesions, there were 6 (54%) atypical ductal hyperplasia and flat epithelial atypias, and 5 (46%) lobular carcinoma in situ. Benign lesions (133, 55%) included 29 complex sclerosing lesion/radial scar, 3 intraductal papillomas, 3 fibroadenomas, and 96 cases that encompass a variety of benign findings such as fibrocystic changes, fibrotic stromal changes, mastitis, and fibroadenomatous alterations. Malignant outcomes were associated with older age (mean 65.2 vs 55.1 years, p < 0.001).

Conclusions: At our institution, approximately 1.8% of breast core needle biopsies were performed for MAD, and up to 40.5% of these biopsies showed a malignant histologic finding. The majority of malignant cases (74.8%) were invasive carcinomas, most of which were invasive ductal carcinomas. Malignant outcomes were associated with older age. These findings support that a needle biopsy should be performed in MAD cases given the high number of malignant cases.

234 Radial Scar without Atypia on Biopsy- Excision or Not?

Jayalakshmi Venkateswaran¹, Ramapriya Vidhun², Madhavi Raghu¹

¹Danbury Hospital, Danbury, CT, ²Western Connecticut Health Network, Danbury Hospital, Danbury, CT

Disclosures: Jayalakshmi Venkateswaran: None; Ramapriya Vidhun: None; Madhavi Raghu: None

Background: The management of radial scar/s (RS) is controversial due to the questionable intrinsic malignant potential of RS and coexistence of other high risk proliferative lesions requiring excision. In the past, all RS diagnosed on biopsy were excised. Upgrade to a carcinoma on excision was observed in less than 2.0%. Excising RS without atypia is debatable. RS can coexist with other proliferative high-risk lesions, including atypia, contributing to the overall upgrade rate to malignancy at excision. Rates of upgrade of RS to cancer at excision varies from 0-43%. Upgrade risk factors include- older age (>50 years), postmenopausal status, larger size on imaging, and presence of atypical hyperplasia. The most important reason for this variation is attributable to the coexistence of higher risk proliferative lesions. Other factors include biopsy needle size, and the number of cores obtained. The purpose of this study was to evaluate the upgrade rate of radial scars without atypia at excision.

Design: An IRB approved retrospective review of the pathology database was conducted for breast biopsies diagnosed as RS without atypia diagnosed at stereotactic and ultrasound biopsy between Jan 1, 2015, and May 31, 2022, at Danbury Hospital. Informed consent was waived. Upgrade rate to malignancy at excision was documented.

Results: During the study period, there were 234 biopsies with diagnoses of RS along with other lesions (benign and/or malignant). Eighty-three of these were identified as RS without atypia or malignancy. A total of 49.4% (41 of 83) of RS without atypia or malignancy diagnosed on core biopsies were surgically excised. A majority of cases (40/41 (97.6%) were benign. One case was upgraded to ductal carcinoma in-situ (DCIS) on excision (2.4%). There were no upgrades to invasive carcinoma. The biopsy needle size and the number of biopsies did not provide conclusive information in our study sample.

Table no. 1 Diagnosis of the RS on excision

Diagnosis on excision	No. of cases
Benign (not malignant)	40/41 (97.6%)
Ductal Carcinoma In Situ (DCIS) (malignant)	1/41 (2.4%)

Table no. 2 Diagnoses on excision of the biopsy proven RS

Diagnoses on excision	No. of cases	9G needle	No. of cores obtained
Usual Ductal Hyperplasia (UDH)	5/41 (12.2%)	3/41(7.3%)	4 to multiple
Atypical Ductal Hyperplasia (ADH)	9/41 (22.0%)	5/41 (12.2%)	4 to multiple
Lobular Carcinoma In Situ (LCIS)	3/41 (7.3%)	2/41 (4.9%)	4-6
Ductal Carcinoma In Situ (DCIS)	1/41 (2.4%)	1/41 (2.4%)	6

Conclusions: In this study, RS without atypia diagnosed at core needle biopsy showed an upgrade rate of 2.4% (DCIS). Excision of RS without atypia may not be necessary in every case. Imaging follow-up of these lesions with may be a reasonable management plan.

235 Interest of Artificial Intelligence Algorithms to Determine a HER2 Low Status in Breast Cancer

Kim Vianey¹, Cécile Maisin², Cécile Hayem³, Gilles Benaim², Emilie Courcet⁴, Olivier Deroo⁵, Nicolas Hamant⁶, Anne Le Hemon-Lepaul⁵, Anthony Jacquier⁴, Jean-Pierre Machayekhi⁵, Nelly Youssef-Provençal, Pierre Serra, Charlène Vigouroux⁶, Ossama Yacoub⁶, Magali Lacroix-Triki⁷, Marie Brevet

¹CYPATH-RB, Villeurbanne, France, ²CYPATH, Villeurbanne, France, ³Versailles, France, ⁴CYPATH, Dijon, France, ⁵CYPATH, Valence, France, ⁶CYPATH, Metz, France, ⁷Gustave Roussy, Cancer Campus, Grand Paris, Villejuif, France

Disclosures: Kim Vianey: None; Cécile Maisin: None; Cécile Hayem: None; Gilles Benaim: None; Emilie Courcet: None; Olivier Deroo: None; Nicolas Hamant: None; Anne Le Hemon-Lepaul: None; Anthony Jacquier: None; Jean-Pierre Machayekhi: None; Nelly Youssef-Provençal: None; Pierre Serra: None; Charlène Vigouroux: None; Ossama Yacoub: None; Magali Lacroix-Triki: None; Marie Brevet: None

Background: Novel anti-HER2 antibody drug conjugates (ADCs) have shown efficacy in invasive breast cancers (BCs) expressing low levels of HER2 (1+ by immunohistochemistry (IHC) and 2+ non-amplified). However, differentiating scores 0 from 1+ is challenging even for experienced pathologists. In private practice, pathologists diagnose frequently BCs and must be able to establish the HER2 low status with reliability and reproducibility. Artificial intelligence (AI) algorithms based on deep learning could help in the assessment of HER2 low score. The objectives of this work were 1) to assess the concordance of the diagnosis of HER2 low among pathologists practicing in a liberal structure and 2) to study the performance of AI algorithms in this indication.

Design: 200 whole slide images (WSI) centrally stained by IHC HER2 from primary BCs expressing low levels of HER2 were selected based on pathology reports. The slides were digitized and then subjected to an inter-observer study including 12 pathologists from a private laboratory. The same 200 slides were analyzed by a pathologist expert in breast pathology and then subjected to four AI tools designed for HER2 scoring. To study the performance of the algorithms, AI tests were performed on regions of interest (ROI) representative of HER2 labeling. In parallel, the ease of use of each software and algorithm was evaluated.

Results: After proofreading by the expert pathologist, the cohort included 41 "0" cases, 120 "1+" cases and 36 "2+" cases by IHC. With the expert pathologist as reference, the inter-observer studies showed an average concordance of 68% (range: 57-87%) with 10.6% of the cases (n=21) for which the concordance between pathologists was 100%. AI testing is ongoing. The first results show variable performances from 43 to 71% concordance with the reference.

Figure 1 - 235



Conclusions: Inter-observer agreement for HER2 scoring within a liberal group is similar to that observed in the literature. Ongoing training for establishing low HER2 status should increase concordance between observers. The guidelines used to configure the HER2 scoring and their ability to recognize artefacts partly explain the differences in performance observed between the AI algorithms. The use of these AI tools in routine practice will require prospective validations but also perfect integration and interoperability with the image management systems currently deployed in pathology laboratories.

236 Epigenetic Methylation Profiles of 5-hydroxymethylcytosine (5hmC) Modified Loci in Breast Phyllodes Tumors

Jasmine Vickery¹, Lu Gao¹, Ryan Owyang², Chuan He², Anna Biernacka²

¹University of Chicago Medical Center, Chicago, IL, ²University of Chicago, Chicago, IL

Disclosures: Jasmine Vickery: None; Lu Gao: None; Ryan Owyang: None; Chuan He: None; Anna Biernacka: None

Background: The molecular pathogenesis of breast phyllodes tumors (PTs) is not fully understood. Most studies have concentrated on genetic alterations, e.g., chromosomal imbalances or somatic mutations (e.g., MED12 and TERT genes), while little is known about epigenetic changes. 5-Hydroxymethylcytosine (5hmC) has been recognized as a stable epigenetic mark showing global loss and/or specific redistribution patterns in various tumor types. Nano-hmC-Seal is a 5hmC enrichment next-

generation sequencing (NGS) assay capable of trapping covalently and isolating 5hmC-modified-loci of genomic DNA extracted from FFPE samples. Herein, we employ this technique for genome-wide 5hmC profiling of benign (BEN) and malignant (MALIG) PTs.

Design: Six BEN and six MALIG PTs from women with comparable age and race were selected to minimize confounding variables. Following extraction, genomic DNA fragments were ligated with standard adaptors, selectively labeled with an azide tag at 5hmC sites, biotinylated, streptavidin-bead-captured, and then underwent NGS. Data analysis was carried out using NGS analysis tools such as bowtie2 and DESeq2.

Results: Of the 31781 distinguishable 5hmC-enriched regions identified, 320 were statistically different between BEN and MALIG PTs ($p<0.005$). Principal component analysis and heat-mapping successfully separated BEN from MALIG samples (Fig 1). We further identified 168 differentially 5hmC-modified genes ($p<0.005$), including 8 genes with FDR<0.05 (AJAP1, ARHGEF39, KCNH2, HS3ST6, PLEKHO1, NFAM1, IRF2BP2, and EPOR). The 5hmC-seal sequencing reads showed a distinct genomic distribution, enriched most in the promoter/enhancer regions, depleted at the transcription start site (TSS), and modestly enriched in gene bodies. Whereas the level of promoter enrichment was similar between BEN and MALIG PTs, on the gene bodies and after the transcription end site (TES), BEN PTs had much higher 5hmC levels of mapped reads, indicating a greater global amount of 5hmC in BEN vs. MALIG PTs (Fig 2). The selected differentially 5hmC-modified genes ($|fc|>20\%$, $p<0.01$) involved several top canonical pathways, including WNT/ β -catenin signaling and G1/S checkpoint regulation.

Figure 1 - 236

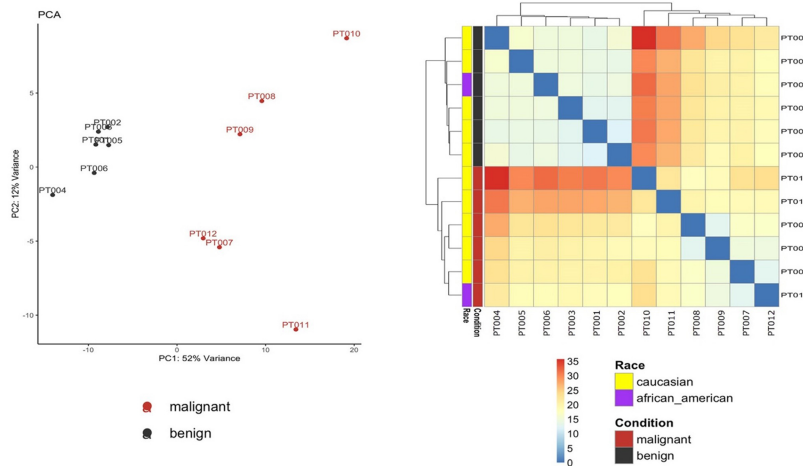


Figure 1. Differentially 5hmC-modified regions (DhMRs) can successfully separate BEN from MALIG phyllodes tumors through principal component analysis (PCA) and heatmap.

Figure 2 - 236

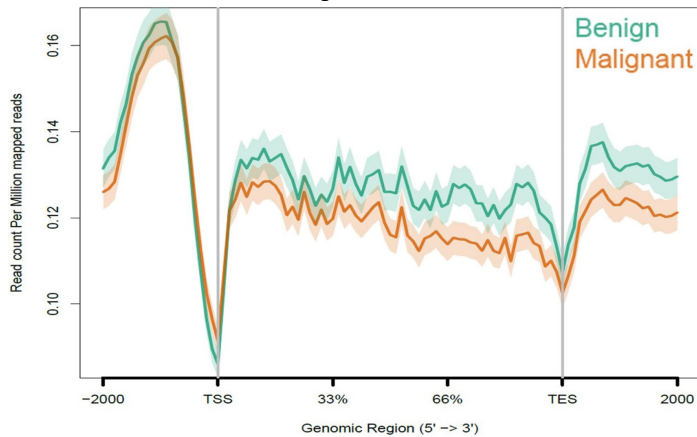


Figure 2. The distribution of 5hmC between BEN and MALIG samples is similar in the promoter regions (from -2000 to TSS) but has a much higher 5hmC level in BEN compared to MALIG at Gene Bodies (from TSS to TES) and regions after TES.

Conclusions: BEN and MALIG PTs show distinct methylation signatures by genome-wide 5hmC profiling. While we are currently investigating the borderline category and adjacent normal breast tissue, this pilot report suggests a potential use of 5hmC profiling in the categorization of PTs, in addition to uncovering the underlying PTs biology.

237 Hematolymphoid Neoplasms Involving the Breast: A Single Institution Clinicopathologic Study of 59 patients

Jasmine Vickery¹, Swetha S², Jeeva Alphonsa Joy³, Faiza Siddiqui¹, Daniel Arber⁴, Sandeep Gurbuxani⁴, Anna Biernacka⁴, Girish Venkataraman¹

¹University of Chicago Medical Center, Chicago, IL, ²Chennai, India, ³Government Medical College, Ernakulam, India, ⁴University of Chicago, Chicago, IL

Disclosures: Jasmine Vickery: None; Swetha S: None; Jeeva Alphonsa Joy: None; Faiza Siddiqui: None; Daniel Arber: None; Sandeep Gurbuxani: None; Anna Biernacka: None; Girish Venkataraman: None

Background: Hematopoietic neoplasms (HN) involving the breast are rare, mostly comprising lymphomas. Knowledge of presentation (primary [PBHN] vs. secondary [SBHN]), radiologic aspects, and their outcomes are critical to a breast pathologist for seeking appropriate hematopathology consultation. Herein, we present our experience of breast HN in the past 20 years.

Design: We identified 59 patients (pts) diagnosed at the University of Chicago Medical Center between 2002-2021. Demographic, pathologic, radiologic, therapy, relapse data, and vital status were abstracted. Data were examined using univariable statistics with event-free and overall survival (EFS, OS) as primary outcomes examined with the lymphoma subgroup using Cox PH regression adjusted for age.

Results: The cases included 27 (46%) PBHN and 32 (54%) SBHN comprising 93% females, mostly Caucasian (79%). The mean age at diagnosis was 58.8 yrs. 5 of 59 pts presented with concurrent breast carcinoma (BC: 4 IDC SBR gr II/III, 1 HG DCIS); 3 of 5 with BC preceding; 1 synchronous; and 1 BHN preceding. Lymphomas were the most frequent hematopoietic neoplasm (Figure 1), but unusual HN types were also identified and included ALCL, histiocytic sarcoma, and AML. Examining the lymphoma cohort (86.4% of all cases), pts with PBL were significantly older than SBL (61.2 vs. 49.8 yrs, p<0.02). There was no tumor size difference between PBL vs. SBL (median 2.1 cm). The most frequent lymphomas were MZL (32.2%) and DLBCL/HGBCL, NOS (33.9%), followed by FL (15%) (Fig. 1) including two DLBCLs that were transformed-FL. Over half of MZL and DLBCLs were primary in the breast with two MZL pts with underlying autoimmune disease. Although 2 patients had breast implants, no cases of implant-associated ALCL were diagnosed. Within B-cell lymphomas, 20 (37%) were high grade with inferior 10-yr OS (age-adjusted HR 5.47, 95% CI 1.38, 21.64) compared to low-grade without any impact on EFS (Figure 2)

Figure 1 - 237

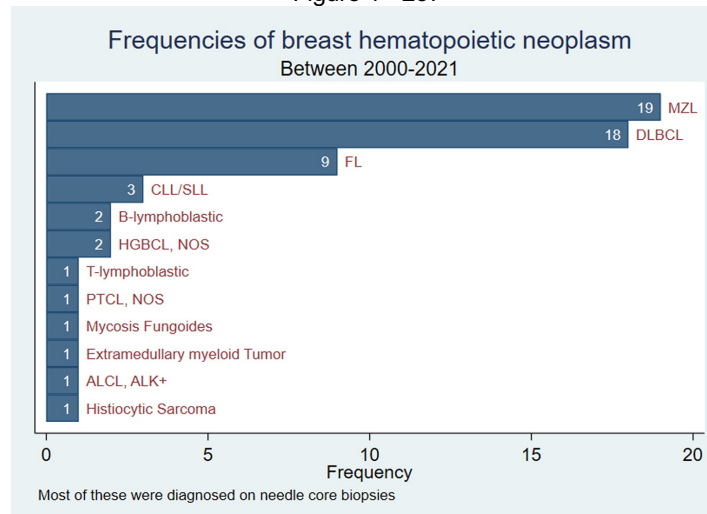


Figure 1. Marginal zone lymphoma (MZL), Diffuse large B-cell lymphoma (DLBCL), Follicular lymphoma (FL), Chronic lymphocytic/Small lymphocytic leukemia/lymphoma (CLL/SLL), High-grade B-cell Lymphoma, Not Otherwise Specified (HGBCL, NOS), Peripheral T-cell lymphoma (PTCL), Extramedullary myeloid Tumor/Acute myeloid Lymphoma (AML), Anaplastic Large Cell Lymphoma ALK+, (ALCL, ALK+).

Figure 2 - 237

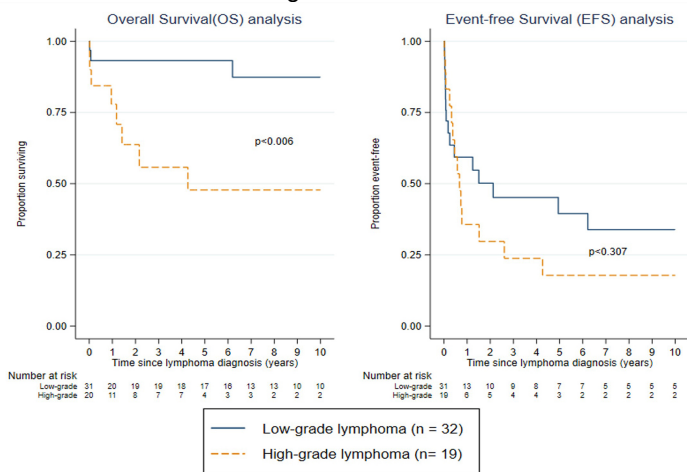


Figure 2. Kaplan-Meier curves of overall and event-free survival for low and high-grade breast lymphomas.

Conclusions: This is one of the largest cohorts by far describing HN in the breast. Patients with PBL were significantly older while DLBCL and MZL remain the most common lymphomas involving this site. Radiographically, the presentation might sometimes mimic breast cancer and unusual HN may also be identified at this site (myeloid sarcoma, histiocytic sarcoma, PTCL).

238 INSM1 Expression Is superior to Traditional Markers of Neuroendocrine Differentiation in Breast Neoplasms with Neuroendocrine Feature

Roxanne Wadia¹, Reza Golestani², Peter Podany², Jennifer Moreira-Dinzez², Tong Sun³, Uma Krishnamurti², Malini Harigopal³

¹Yale New Haven Hospital, New Haven, CT, ²Yale School of Medicine, Yale New Haven Hospital, New Haven, CT, ³Yale School of Medicine, New Haven, CT

Disclosures: Roxanne Wadia: None; Reza Golestani: None; Peter Podany: None; Jennifer Moreira-Dinzez: None; Tong Sun: None; Uma Krishnamurti: None; Malini Harigopal: None

Background: In breast tumors, neuroendocrine (NE) differentiation is seen in neuroendocrine tumors (NET), neuroendocrine carcinomas (NEC), solid papillary carcinomas, mucinous carcinomas, and invasive ductal carcinomas (IDCs) with NE differentiation. Diagnosis of NE differentiation relies on immunohistochemistry for synaptophysin (SYN) and chromogranin-A (CHR). INSM1 is a sensitive and specific NE marker and has been shown to be a reliable marker for NE differentiation in NET and NECs of GI and lung origins. Few studies have shown similar results in INSM1 in breast carcinomas with NE differentiation. In this study we investigated the value of INSM1 expression as a marker of NE differentiation in tumors with NE morphology by comparing INSM1 expression with traditional markers of NE differentiation.

Design: Core needle biopsies or excisional biopsies between 2017 and 2022 were assessed for NE differentiation in tumors with NE morphology on histology based on cytological and/or architectural features. INSM1, SYN, and CHR stains were performed. Positive staining was defined as any cytoplasmic staining for SYN and CHR and moderate to strong nuclear staining for INSM1 in >5% of cells. Percentage of positive cells were calculated using 500 cell count.

Results: Thirty-three cases with NE morphology were evaluated in this study. SYN was positive in 23 (sensitivity of 70%), chromogranin in 18 (sensitivity of 55%) and INSM1 in 25 (sensitivity of 76%). INSM1 expression was concordant with SYN in 31 (94%) and chromogranin in 24 (73%) of cases. Twenty-five of 33 cases (76%) expressed SYN or CHR. This included 4 NETs, 4 mucinous carcinomas, 2 NE carcinomas, 1 solid papillary carcinoma and 14 IDCs with NE differentiation. There was one case out of 33 (3%) that was positive for INSM1 and negative for SYN and CHR. Seven cases out of 33 (21%) were negative for all NE markers, despite displaying concerning features on H&E. Additionally INSM1 expression in breast carcinoma without NE differentiation was evaluated in a tissue microarray consisting of 203 IDCs without NE differentiation. INSM1 was positive in 3 cores (specificity 98.5%).

Count	Synaptophysin	Chromogranin	INSM1
15	Positive	Positive	Positive
8	Positive	Negative	Positive
1	Negative	Positive	Positive
1	Negative	Positive	Negative
1	Negative	Negative	Positive
7	Negative	Negative	Negative

Figure 1 - 238

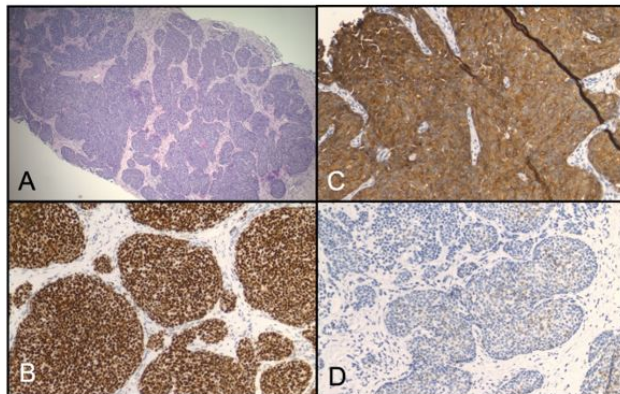


Figure 1. Neuroendocrine tumor of the breast. A) H&E stain shows nests of invasive carcinoma infiltrating into stroma. B) Synaptophysin immunostain shows diffuse cytoplasmic stain in >95% of cells. C) INSM1 immunostain shows diffuse strong nuclear staining pattern in >95% of cells. D) Chromogranin immunostain shows cytoplasmic staining pattern in 50% of cells.

Figure 2 - 238

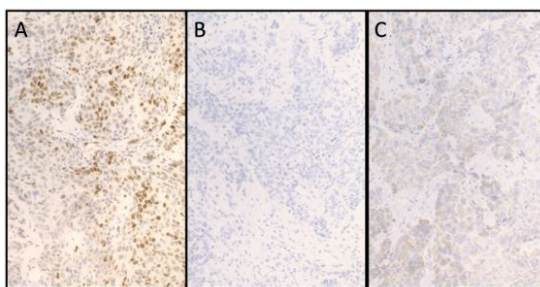


Figure 2. Immunostaining in an invasive ductal carcinoma shows focal moderate expression of INSM1 (A). Tumor cells are negative for synaptophysin (B), but weakly express chromogranin (C)

Conclusions: Our findings suggest that INSM1 is a highly sensitive and specific marker for breast tumors with neuroendocrine features and can be considered as a reliable diagnostic tool in conjunction with SYN and or CHR. However, molecular profile and clinical implications of INSM1 expression in breast tumors needs to be further investigated.

239 Comparative Analysis of Polyclonal TRPS1 and Monoclonal TRPS1 in Multiple Organs: Do Only Mammary Epithelium Express TRPS1?

Chenglong Wang¹, Jin Zhu², Li Peng², Yonggang Liu², Yong Zhao², Youde Cao², Shanshan Yu²

¹Chongqing Hospital of Traditional Chinese Medicine, Chongqing, China, ²College of Basic Medicine, Chongqing Medical University, Chongqing, China

Disclosures: Chenglong Wang: None; Jin Zhu: None; Li Peng: None; Yonggang Liu: None; Yong Zhao: None; Youde Cao: None; Shanshan Yu: None

Background: TRPS1 has been identified as a specific and sensitive biomarker for breast cancer. However, a few tumors of non-mammary origin also express TRPS1, which can cause a diagnostic challenge. To date, whether TRPS1 is also a lineage-restricted transcription factor for non-mammary tumors remains unknown, and the details of its expression in the normal counterparts are not even known. We aimed to assess the expression of TRPS1 in different types of relatively normal organs using polyclonal TRPS1 (pTRPS1) and monoclonal TRPS1 (mTRPS1).

Design: We collected 135 samples from 27 different organs (n= 5 for each). Whole tissue sections were stained with pTRPS1 and mTPRS1 using Leica Bond Max autostainer system following standard automated protocols. Only nuclear staining was considered as pos and their immunoreactive scores were calculated by multiplying a number representing the percentage of immunoreactive cells (0, <1%; 1, 1%-10%; 2, 11%-50%; and 3, 51%-100%) by the staining intensity (0, no nuclear staining at 40x power; 1, visible at 40x power; 2, visible at 20x power; and 3, visible at 4-10x power). The scores were defined as neg (0 or 1), low pos (2), intermediate pos (3 or 4), or high pos (6 or 9).

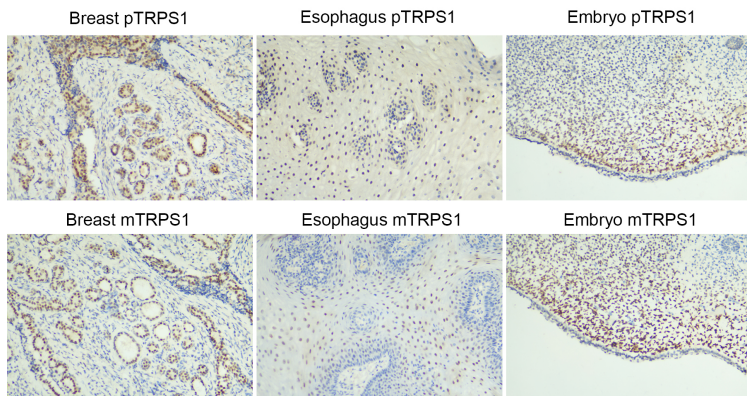
Results: pTRPS1 and mTPRS1 were both high pos in breast epithelium (5, 100%), embryonic mesenchymal cells (5, 100%), and squamous epithelium of uterine cervix (5, 100%), tonsil (5, 100%) and esophagus (5, 100%). In the skin, mTPRS1 was low pos in

ABSTRACTS | BREAST PATHOLOGY

epidermis (2, 40%), and pos in appendages (5, 100%), with high, intermediate and low pos in sebaceous glands, eccrine and hair follicles, respectively, but neg in apocrine; otherwise, pTRPS1 was low pos only in eccrine (3, 60%). In the brain, mTPRS1 was low-intermediate pos in ependyma (5, 100%, with 2 intermediate pos and 3 low pos), and intermediate pos in glial cells (5, 100%). Moreover, mTRPS1 was high pos in endometrial glands (5, 100%), intermediate pos in endocervical glands (5, 100%) and low pos in bladder urothelium (2, 40%).

Type of organs	Type of tissue/cells	mTRPS1			pTRPS1	
		Negative, n (%)	Positive, n (%)		Negative, n (%)	Positive, n (%)
			Low	Intermediate		High
Breast	Epithelium			5 (100%)		5 (100%)
Esophagus	Squamous epithelium			5 (100%)		5 (100%)
Tonsil	Squamous epithelium			5 (100%)		5 (100%)
Embryo (spontaneous abortion)	Mesenchymal cells			5 (100%)		5 (100%)
Uterine cervix	Squamous epithelium			5 (100%)		5 (100%)
	Endocervical glands		5 (100%)		5 (100%)	
Endometrium	Glands			5 (100%)	5 (100%)	
Skin	Sebaceous glands			5 (100%)	5 (100%)	
	Eccrine		5 (100%)		2/5 (40%)	3/5 (60%)
	Hair follicles	5 (100%)			5 (100%)	
	Apocrine	5 (100%)			5 (100%)	
	Epidermis	3/5 (60%)	2/5 (40%)		5 (100%)	
Bladder	Urothelium	3/5 (60%)	2/5 (40%)		5 (100%)	
Brain	Meninges	5 (100%)			5 (100%)	
	Choroid plexus	5 (100%)			5 (100%)	
	Ependyma		3/5 (60%)	2/5 (40%)	5 (100%)	
	Glial cells			5 (100%)	5 (100%)	
Pituitary		5 (100%)			5 (100%)	
Pancreas		5 (100%)			5 (100%)	
Adrenal gland		5 (100%)			5 (100%)	
Lung		5 (100%)			5 (100%)	
Salivary		5 (100%)			5 (100%)	
Kidney		5 (100%)			5 (100%)	
Prostate		5 (100%)			5 (100%)	
Seminal vesicle		5 (100%)			5 (100%)	
Thyroid		5 (100%)			5 (100%)	
Spleen		5 (100%)			5 (100%)	
Stomach		5 (100%)			5 (100%)	
Small intestine		5 (100%)			5 (100%)	
Colon		5 (100%)			5 (100%)	
Liver		5 (100%)			5 (100%)	
Fallopian tube		5 (100%)			5 (100%)	
Ovary		5 (100%)			5 (100%)	
Placenta		5 (100%)			5 (100%)	
Testis		5 (100%)			5 (100%)	

Figure 1 - 239



Conclusions: TRPS1 is a sensitive marker for breast epithelium, non-skin origin squamous epithelium and mesenchymal cells. Moreover, pTRPS1 is more specific for these cells than mTRPS1, with the pTRPS1 being high pos only in these cells.

240 Significance of HER2 Status in Neoadjuvant Chemotherapy for Breast Cancer Patients

Chengqin Wang¹, Xiaoming Xing¹, Zhaoxu Chen¹, Zhimin Wei¹, Yujun Li¹

¹The Affiliated Hospital of Qingdao University, Qingdao, China

Disclosures: Chengqin Wang: None; Xiaoming Xing: None; Zhaoxu Chen: None; Zhimin Wei: None; Yujun Li: None

Background: Recently, HER2-low has received much attention as a new breast cancer subtype, however, its significance in adjuvant chemotherapy (NAC) patients is unclear. This study aims to evaluate the correlation between HER2 status and clinicopathological features in NAC breast cancer patients and to analyze the prognostic significance of HER2 status.

Design: The clinicopathological data of 166 female patients with primary invasive breast cancer who received NAC in our institution (from January 2017 to June 2019) were collected. All patients underwent mastectomy and axillary lymph node dissection after NAC. Preoperative HER2 status was stratified into HER2-zero (IHC 0), HER2-low (IHC 1+ or IHC2+/FISH negative) and HER2-high (IHC 2+/FISH positive or IHC3+). Median follow-up was 46 months with disease-free survival (DFS) as study endpoint.

Results: Of the 166 patients, the proportion of HER2-high tumors (75, 45.2%) was higher than that of HER2-low(70, 42.2%) and HER2-zero(21, 12.6%). Hormone receptor (HR)+ was more common in the HER2-low tumors than in the HER2-zero ($p=0.036$) and HER2-high ($p<0.001$) (Fig. 1). There was no significant difference in postoperative pathological complete response (pCR) rates among the three groups (Fig.1). In addition, no difference was found in postoperative Miller-Payne grading system($p=0.140$) and Sataloff lymph node grade ($p=0.502$) between HER2-low and HER2-zero tumors(Table 1). In the HR+ tumors, the HER2-low accounted for 58.0%. Compared with HER2-zero ,ER levels were higher in the HER2-low tumors, but not statistically significant ($n=0.738$).However, compared to HER2-high, HER2-low tumors had higher ER level ($p=0.030$), lower Ki-67 proliferation index($p=0.014$) and differences in Miller-Payne grading system ($p=0.047$).In the HR-tumors, the proportion of HER2-high was 62.3% and there was no significant difference in clinicopathological features among the three groups (all $p>0.05$).Kaplan-Meier survival analysis found that HER2 status had no effect on DFS of the overall, HR+ and HR- patients (log-rank, all $p>0.05$). Furthermore, pCR status (log-rank, $p=0.914$) also had no effect on patient DFS (Fig. 2). Univariate analysis showed that HER2 status ($HR=0.757$, 95% CI,0.164-3.505, $p=0.722$), HR status ($HR=1.053$, 95% CI,0.655-1.691, $p=0.831$) and pCR status ($HR=2.968$, 95% CI,0.379-23.215, $p=0.300$) had no significance for the prognosis of NAC patients. Only age was an independent prognostic factor affecting DFS of NAC patients in univariate ($HR=0.955$, 95% CI,0.913-0.995, $p=0.041$.)and multivariate($HR=0.943$, 95% CI,0.893-0.996, $p=0.035$) analyses.

Table1: Baseline clinicopathological characteristics according to HER2 status of 166 NAC patients.

Clinicopathological characteristics	Overall (N=166, %)	HER2-zero (N=21, 12.6%)	HER2-low (N=70, 42.2%)	HER2-high (N=75, 45.2%)	P-HER2 (zero vs low)	P-HER2 (low vs high)
Age/years						
Median/range	50/22-72	50/22-67	52/29-70	50/24-72	0.627	0.456
Mean±SD	49.2±10.3	48.0±12.3	50.0±10.4	48.7±9.8		
Menopausal status						
Pre/peri-menopausal	106 (63.9)	13 (61.9)	41 (58.6)	52 (69.3)	0.785	0.177
Postmenopausal	60 (36.1)	8 (38.1)	29 (41.4)	23 (30.7)		
Histotype						
Ductal	153 (92.2)	16 (76.2)	65 (92.9)	72 (96.0)	0.053	0.633
Lobular	4 (2.4)	1 (4.8)	2 (2.9)	1 (1.3)		
Other	9 (5.4)	4 (19.0)	3 (4.2)	2 (2.7)		
Grade						
1	3 (1.8)	0 (0.0)	2 (2.9)	1 (1.3)	0.121	0.087
2	83 (50.0)	9 (42.9)	42 (60.0)	32 (42.7)		
3	57 (34.3)	9 (42.9)	20 (28.6)	28 (37.3)		
Unknown	23 (13.9)	3 (14.2)	6 (8.5)	14 (18.7)		
pT						
0/is	16 (9.6)	2 (9.5)	4 (5.7)	10 (13.3)	0.984	0.341
1	84 (50.6)	10 (47.6)	35 (50.0)	39 (52.0)		
2	48 (28.9)	7 (33.4)	20 (28.6)	21 (28.0)		
3	18 (10.9)	2 (9.5)	11 (15.7)	5 (6.7)		
pN						
0	57 (34.3)	8 (38.1)	21 (30.0)	28 (37.3)	0.989	0.931
1	54 (32.5)	5 (23.8)	23 (32.9)	26 (34.7)		
2	31 (18.7)	5 (23.8)	11 (15.7)	15 (20.0)		
3	24 (14.5)	3 (14.3)	15 (21.4)	6 (8.0)		
Ki67						
≤20%	78 (47.0)	8 (38.1)	41 (58.6)	29 (38.7)	0.120	0.055
>20%	71 (42.8)	11 (52.4)	25 (35.7)	35 (46.7)		
Unknown	17 (10.2)	2 (9.5)	4 (5.7)	11 (14.6)		
Miller-Payne						
G1	22 (13.2)	2 (9.5)	15 (21.4)	5 (6.7)	0.140	0.015
G2	33 (19.9)	2 (9.5)	14 (20.0)	17 (22.7)		
G3	71 (42.8)	13 (62.0)	29 (41.5)	29 (38.7)		
G4	22 (13.3)	2 (9.5)	7 (10.0)	13 (17.3)		
G5	18 (10.8)	2 (9.5)	5 (7.1)	11 (14.6)		
Sataloff lymph node Grade						
N-A	7 (4.2)	4 (19.0)	1 (1.4)	2 (2.7)	0.502	0.307
N-B	50 (30.1)	4 (19.0)	20 (28.6)	26 (34.6)		
N-C	20 (12.1)	1 (4.8)	9 (12.9)	10 (13.3)		
N-D	89 (53.6)	12 (57.2)	40 (57.1)	37 (49.4)		
Recurrence or metastasis						
Yes	18 (10.8)	2 (9.5)	9 (12.9)	7 (9.3)	0.977	0.499
No	148 (89.2)	19 (90.5)	61 (87.1)	68 (90.7)		

Figure 1 - 240

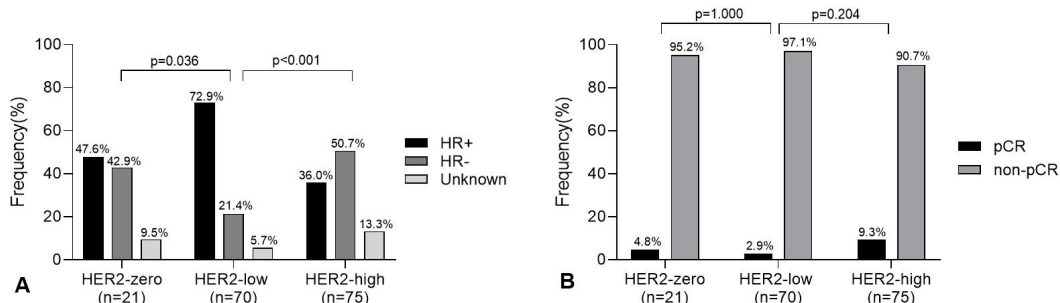


Figure 1:Differences in HR status (A) and pCR status (B) in HER2-zero, HER2-low and HER2-high groups.

Figure 2 - 240

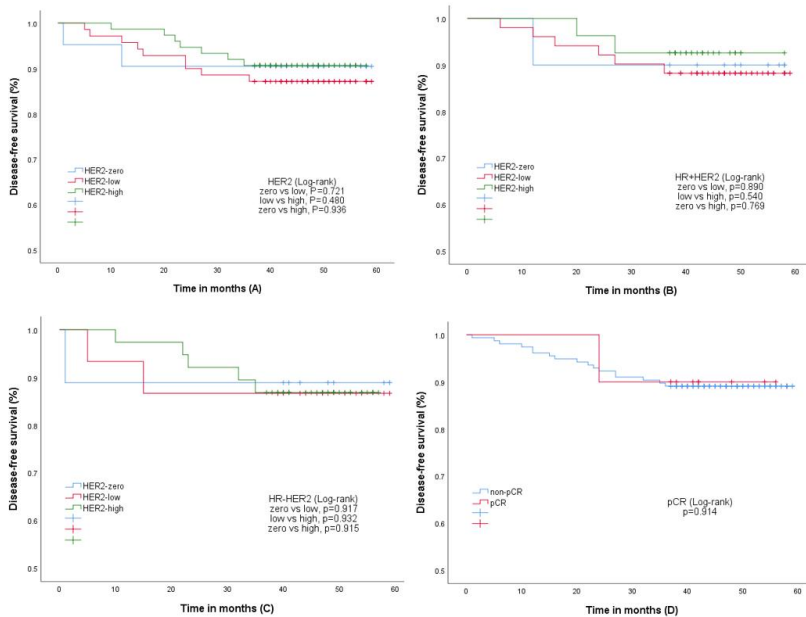


Figure 2: Kaplan-Meier curves of DFS according to HER2 status in overall patients (A), HR+ patients (B) and HR- patients (C); Kaplan-Meier curves of DFS according to pCR in overall patients (D).

Conclusions: HER2-low tumors were strongly associated with HR status, however, no evidence was found that HER2 status was associated with chemotherapy response and prognosis in NAC patients.

241 Concordance between Pathologists and between Specimen Types in Detection of Low HER2 Protein Expression in Invasive Breast Carcinoma by Immunohistochemistry

Jing Wang¹, Esther Yoon², Savitri Krishnamurthy³

¹Baylor College of Medicine, Houston, TX, ²Cleveland Clinic Florida, Weston, FL, ³The University of Texas MD Anderson Cancer Center, Houston, TX

Disclosures: Jing Wang: None; Esther Yoon: None; Savitri Krishnamurthy: None

Background: HER2-targeted therapy for invasive breast cancer was until now available only for patients with a HER2 immunohistochemistry (IHC) score of 3+ or a score of 2+ with gene amplification. Recent clinical trials suggest that HER2-targeted therapy may also benefit patients with HER2-low breast cancer, defined as an HER2 score of 1+ or 2+ and no gene amplification. We evaluated concordance between pathologists and between core biopsy and surgical excision in establishing HER2-low status by light microscopic examination of HER2 IHC.

Design: The study included 61 patients with early-stage invasive breast cancer classified as HER2 negative (0, 1+, or 2+ and no gene amplification by fluorescence in situ hybridization) by standard-of-care core biopsy evaluation. Representative tumor from surgical excision was immunostained for HER2. Three pathologists independently interpreted HER2 IHC staining on core biopsy and surgical excision specimens. Consensus diagnosis was obtained in discordant cases. Kappa statistic evaluated agreement of HER2 scores between the study pathologists, agreement between the study pathologists and the pathologists who initially reported the core biopsy's HER2 score, and agreement between the HER2 consensus scores for the core biopsy and surgical excision specimens.

Results: HER2 IHC scores were concordant between the study pathologists in 50 (82%) core biopsy and 53 (87%) surgical resection specimens. HER2 consensus scores were concordant between the core biopsy and surgical excision specimens in 37 (61%) cases; low (1+ or 2+) HER2 expression was identified in 29 (48%) core biopsy and 26 (43%) surgical excision specimens. Kappa statistics were 0.79 and 0.84, respectively, for interpathologist agreement on core biopsy and surgical resection specimens; 0.52 for agreement between the study pathologists and initial pathologists; and 0.32 for agreement in HER2 consensus scores between the core biopsy and surgical excision specimens.

Conclusions: Interobserver agreement among study pathologists was good for both core biopsy and surgical excision specimens. Agreement was poor between the core biopsy and surgical excision specimens, suggesting intratumoral heterogeneity in HER2 protein expression at the lower end of the spectrum. Testing of both core biopsy and surgical excision specimens may increase the rates of identification of HER2-low status in selecting patients for targeted therapy.

242 Circulating Tumour Cells Correlate With Markers of Inflammatory Response in Metastatic Breast Cancer

Mark Ward¹, Tanya Kelly², Sarah Lochrin¹, Roisin O'Connor², Joanne Felce³, Elaine Kilgour³, Robert Brooks⁴, Doug Brooks⁴, Stavros Selemidis⁵, Waseem Kamran⁶, James Beirne⁶, Feras Saadeh⁶, John Kennedy², Lucy Norris², Cara Martin¹, Sharon O'Toole¹, John O'Leary²

¹Trinity St. James's Cancer Institute, Dublin, Ireland, ²Trinity College Dublin, Dublin, Ireland, ³Manchester Cancer Research Centre, Manchester, United Kingdom, ⁴University of South Australia, Adelaide, Australia, ⁵RMIT, Melbourne, Australia, ⁶St. James's Hospital, Dublin, Ireland

Disclosures: Mark Ward: None; Tanya Kelly: None; Sarah Lochrin: None; Roisin O'Connor: None; Joanne Felce: None; Elaine Kilgour: None; Robert Brooks: None; Doug Brooks: None; Stavros Selemidis: None; Waseem Kamran: None; James Beirne: None; Feras Saadeh: None; John Kennedy: None; Lucy Norris: None; Cara Martin: None; Sharon O'Toole: None; John O'Leary: None

Background: Cancer cells that transit from primary tumours into the circulatory system are known as circulating tumour cells (CTCs). Classical CTC detection forms part of the liquid biopsy and relies on EpCAM affinity-based technologies such as CellSearch. The FDA has recently approved the Parsortix® for metastatic breast cancer (MBC) CTC enrichment. Breast cancer patients commonly present with local and systemic changes in the immune-inflammation index and recent studies report that CTCs associated with peripheral immune cells may have a higher metastatic potential.

Design: Peripheral blood specimens were prospectively collected from MBC patients (n=20) and processed for CTC isolation within 4 h of blood draw using Parsortix®. Isolated cells were immunophenotyped (CTC-ID; DAPI, CD45, CK19/panCK/EpCAM and HER2) by immunofluorescence microscopy. A subset of patients (n=10) had CTC enumeration performed on both Parsortix and CellSearch (CRUK Manchester). Patients were stratified as <5 CTC/7.5ml or ≥5 CTC/7.5 and tested for correlation with clinical markers of inflammation and survival.

Results: 85% of MBC patients had ≥1 CTC (1-220 cells/7.5ml) detected. Concordance was found between CellSearch and Parsortix CTC counts. 50% of patients were found to have at least 1 HER2+ CTC. Presence of ≥5 CTCs or CTC clusters was associated with shorter survival time in MBC. Patients with ≥5 CTCs had an increase in platelet to lymphocyte ratio (PLR). CTC positivity was also associated with higher plasma levels of plasminogen activator inhibitor 1 (PAI-1). High CTC count did not correlate with CA15.3 levels.

Conclusions: We report that the use of expanded CTC-ID markers for CTC enumeration on cells isolated using Parsortix correlate with markers of inflammation in metastatic breast cancer. The presence of CTCs and CTC clusters is a marker of aggressive disease in MBC. HER2+ CTCs were also detected in HER2- patients. High CTC counts were associated with an increase in PLR and PAI-1 levels indicating that high CTC trafficking is associated with an altered inflammatory response which may aid in metastatic dissemination.

243 Nipple Adenoma - A Clinicopathologic Study of 42 Cases

Maximillian Weigelt¹, Andrew Sciallis², Patrick McIntire², Jennifer Ko², Steven Billings³, Shira Ronen²

¹Cleveland Clinic Foundation, Cleveland, OH, ²Cleveland Clinic, Cleveland, OH, ³Cleveland Clinic, Lerner College of Medicine, Cleveland, OH

Disclosures: Maximillian Weigelt: None; Andrew Sciallis: None; Patrick McIntire: None; Jennifer Ko: None; Steven Billings: None; Shira Ronen: None

Background: Nipple adenoma (NA) is a rare, benign proliferation of the lactiferous nipple ducts. It presents as a skin growth, rash, erosive lesion, and/or with nipple discharge. It may be clinically mistaken for Paget disease or squamous cell carcinoma. No large case series of nipple adenoma has been undertaken since the 1980s. Herein, we report a series of 42 cases of nipple adenoma to broaden our understanding of its clinicopathologic characteristics.

Design: After IRB approval, cases of NA were retrieved from the in-house and consultation archives from 2003-2022. For inclusion, cases had to have a dense ductal proliferation in breast tissue with close proximity to the nipple epidermis. Medical records were reviewed. Referring physicians were contacted when necessary.

Results: 42 cases met criteria. 36 had follow-up data. All were female, with a mean age of 57 years (26-78 years). The left breast (62%) was more common than the right breast (38%). Tumor size averaged 0.9 cm (0.2 – 1.5 cm). 25 patients (68%) were symptomatic. Common symptoms included bloody nipple discharge and itching/irritation (24% each). A skin growth was present in 59%. 67% were excised: primarily (33%) or via re-excision after biopsy (33%). In a median follow-up time of 66 months (0.5-227 months), 94% were alive with no evidence of disease, and 6% were dead from other causes. One patient developed invasive ductal carcinoma (IDC) adjacent to the excision site at 98 months. Four histologic patterns were noted: adenosis-like (dense proliferation of small-to-medium ducts) (Fig. 1); large duct (medium-to-large caliber ducts); papillary-like (frond-like architecture with

branching, slit-like lumens); and pseudo-infiltrative (ducts distorted by dense stromal fibrosis) (Fig. 2). All cases demonstrated bi-layered epithelium visible on H&E. Histopathologic characteristics are summarized in Table 1.

Histopathologic Feature	N = 42 (%)
Major Architectural Pattern	
Adenosis-like	17 (40)
Large-Duct	12 (29)
Papillary-like	12 (29)
Pseudooinfiltrative	1 (2)
Bi-layered Epithelium on H&E	42(100)
Stroma	
Fibrotic	36 (86)
Fibrotic and Sclerotic*	6 (14)
Usual Ductal Hyperplasia	32 (76)
Warty-like Growth	27/38 (71)
Smooth Muscle	
Periphery	21 (50)
Central	9 (21)
Apocrine Differentiation	20 (48)
Papillary-like Forms	19 (45)
Symmetry	18/23 (78)
Open to Skin Surface	18/35 (41)
Ulceration	8/39 (21)
Erosion	5/39 (13)
Pseudooinfiltration (Focal)	7 (17)
Keratin Cyst Formation	7 (17)
Squamous Differentiation	5 (12)
Prominent Inflammation	
Lymphoplasmacytic	4 (10)
Lymphocytic with Rare Eos	1 (2)
Connection to Hair Follicle	3 (7)
Mitotic Figures (rare)	3 (7)
Wedge-Shaped Growth	1 (2)
Solid Growth	1 (2)
Necrosis	0 (0)
Desmoplasia	0 (0)
Perineural Invasion	0 (0)

Figure 1 - 243

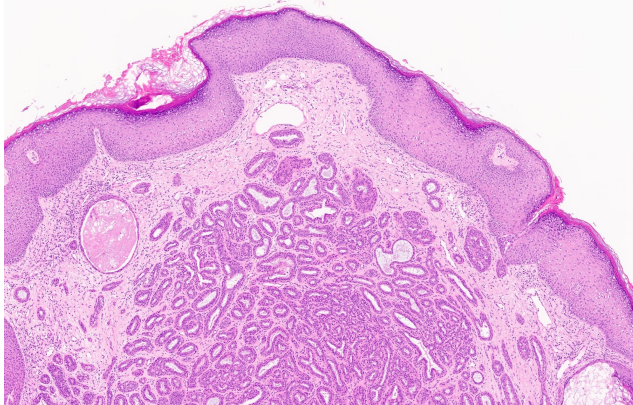
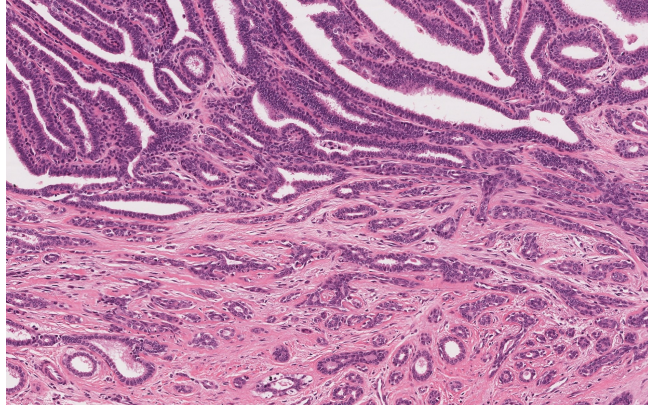


Figure 2 - 243



Conclusions: We report a large series of NA with four principle architectural patterns, which are often intermixed with one predominating. The most pertinent differential diagnosis is IDC, especially when the pseudo-infiltrative pattern is present. Overall symmetry, lack of cytologic atypia, and bi-layered epithelium (typically visible on H&E) support a diagnosis of NA. Syringocystadenoma papilliferum may also be confused for NA; NA is often lacking the prominent cystic invagination with papillary formation and abundant plasma cells in the stroma. Simple excision is curative, and recurrence is rare.

244 Invasive Breast Carcinoma with Micropapillary Features: HER2 status Following 2018 American Society of Clinical Oncology/College of American Pathologists (ASCO/CAP) Guidelines and Clinicopathologic Features

Diane Wilcock¹, Deepika Sirohi¹, Lesley Lomo², Daniel Albertson³, Jolanta Jedrzkiewicz³, Jonathon Mahlow¹, Ana Ruano¹, Allison Cleary¹, Michael Balatico³, H. Evin Gulbahce³

¹The University of Utah/ARUP Laboratories, Salt Lake City, UT, ²University of Utah Health Sciences Center/Huntsman Cancer Institute, Salt Lake City, UT, ³The University of Utah, Salt Lake City, UT

Disclosures: Diane Wilcock: None; Deepika Sirohi: None; Lesley Lomo: None; Daniel Albertson: None; Jolanta Jedrzkiewicz: None; Jonathon Mahlow: None; Ana Ruano: None; Allison Cleary: None; Michael Balatico: None; H. Evin Gulbahce: None

Background: Breast carcinomas with micropapillary features (BrCaMP) may be HER2-amplified despite negative HER2 immunohistochemistry (IHC). ASCO/CAP guidelines recommend basolateral staining in BrCaMP should be reported as equivocal expression (2+) and reflexed to Fluorescence In Situ Hybridization (FISH) testing. Amplification rates over 40% were reported following 2013 ASCO/CAP guidelines with alternate probes in FISH equivocal cases. In this study we assessed the amplification rates, clinicopathologic features and treatment of patients with BrCaMP following updated 2018 ASCO/CAP guidelines.

Design: Breast cancer cases with “micropapillary” in the diagnoses between 1/2019-2/2022 were retrospectively identified. All available clinicopathologic information was recorded including treatment and follow-up. Slides were reviewed to determine the extent of micropapillary histology.

Results: 48 cases were identified with average age of 61.4 (range:35-97). 7(14.6%) were biopsy, 41(85.4%) excision. Micropapillary histology varied from 5-100%, (5-≤10% in 8; 10-50% in 13; ≥50% in 27). 12(25%) had mucinous features. 4(8.3%) was grade 1, 32(66.7%) grade 2, 12(25%) grade 3. 44(91.7%) were Estrogen Receptor (ER) positive, 3(6.3%) ER&PR negative. 23(47.9%) were T1 stage, 14(29.2%) lymph node negative (N0). 12(25%) were HER2 positive by IHC or FISH (Table). 6/30 (25%) of IHC 1+/2+ were FISH amplified. 11/12 (91.7%) of HER2 positive patients got targeted therapy. 8 patients got neoadjuvant therapy (NAT) (4 HER2 positive, 4 HER2 negative), 1/8 NAT had complete pathologic response (HER2 3+ case). After an average follow up of 22.7 months (range=3-125; median=18), 37 patients were alive with no evidence of disease, 8 alive with recurrent/metastatic disease, 3 dead from breast cancer.

HER2 FISH GROUP*	HER2 IMMUNOHISTOCHEMISTRY					Total
	0	1+	2+	3+	Not Done	
Group 1 <i>HER2/CEP17≥2.0 HER2 copy ≥4.0/cell</i>	0	2	4	0	3	9
Group 4 <i>HER2/CEP17<2.0 HER2 copy ≥4.0 AND <6.0/cell</i>	0	10	3	0	0	13
Group 5 <i>HER2/CEP17<2.0 HER2 copy <4.0/cell</i>	4	6	5	0	8	23
FISH Not Done	0	0	0	3	0	3
Total	4	18	12	3	11	48

*There were no FISH Group 2 &3 cases.

Conclusions: Following 2018 ASCO/CAP guidelines 25% of BrCaMP were HER2 positive, higher than what is expected for all breast cancers but lower than expected following 2013 recommendations for BrCaMP. 11.1% of IHC 1+/negative, and 33.3% of IHC 2+/equivocal cases were FISH amplified emphasizing FISH should be part of HER2 testing for these tumors. Both the lymph node negativity (pN0) and (in those receiving NAT) the rate of complete pathologic response was low, suggesting these are biologically aggressive tumors.

245 Hierarchical Clustering of Immune Checkpoint Genes Reveal Signatures Associated to Clinical, Molecular, and Histological Features that are Shared Between Molecular Subtypes

Jahg Wong¹, Alexandre Archambault-Marsan², Ayman Al Shoukari³, Maëlle Batardière⁴, Leonardo Lando⁵, Vincent Quoc-Huy Trinh⁶, Philippe Echelard⁷

¹Centre Hospitalier de l'Université de Montréal (CHUM), Montreal, QC, ²Université de Montréal, Montreal, QC, ³American University of Beirut, Beirut, Lebanon, ⁴Institute for Research in Immunology and Cancer, Montréal, QC, ⁵University of Toronto, Toronto, ON, ⁶Institute for Research in Immunology and Cancer, Montreal, QC, ⁷Université de Sherbrooke, Sherbrooke, QC

Disclosures: Jahg Wong: None; Alexandre Archambault-Marsan: None; Ayman Al Shoukari: None; Maëlle Batardière: None; Leonardo Lando: None; Vincent Quoc-Huy Trinh: None; Philippe Echelard: None

Background: Immune checkpoint gene expression clusters into specific patterns, which have been shown to have significant impact on disease progression. However, they were often studied within the confines of a specific molecular disease and with a

ABSTRACTS | BREAST PATHOLOGY

limited set of genes in breast cancer. We aim to study the molecular, histological, and clinical correlates of immune checkpoint genes signatures by incorporating a complete set of genes with immune checkpoint features.

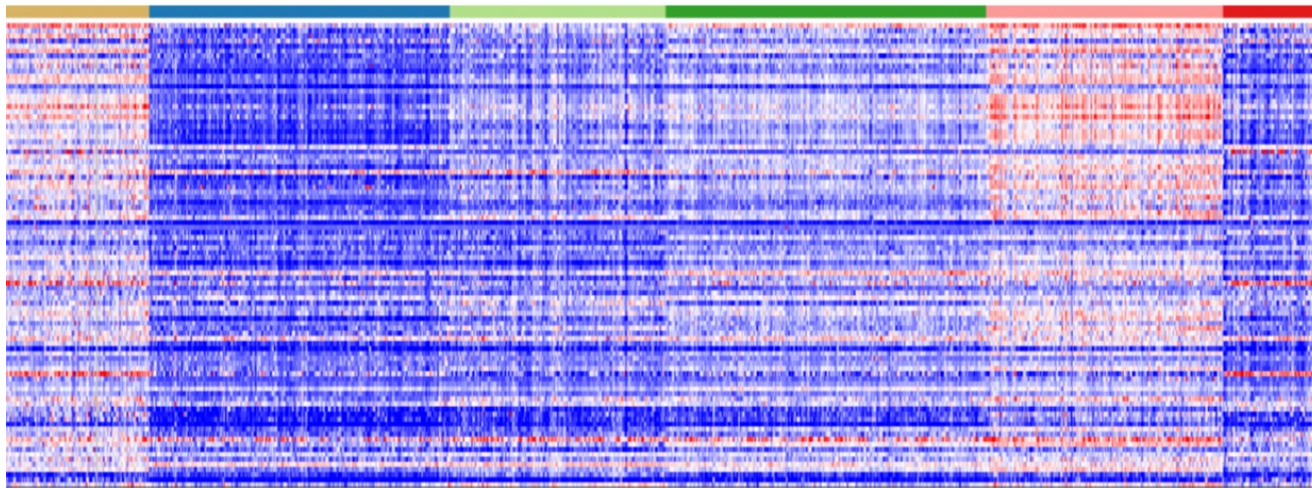
Design: We used the Cancer Genome Atlas (TCGA) Pan-Cancer dataset. We extracted clinical, pathology reports, histological slides and RNA-seq data using the GDC Data Transfer Tool. We selected 108 immune checkpoint genes based on a review of the literature. We performed K-means clustering in STATA. A screeplot was used to determine the optimal number of groups. Each IC group was then correlated to clinical, pathology, and histological parameters in SPSS.

Results: There were 1081 breast cancers in the TCGA. The screeplot highlights the optimal 6 groups for K-means clustering (figure 1). Group 1 is defined by NECTIN2, COL2A1, TNFSRF18 overexpression and CD96, CD247 under expression. Group 2 is inverted, with CD96 and CD247 overexpression, and NECTIN2, COL2A1, and FGL1 underexpression. Group 3 is defined by CCL19 and ADORA2A overexpression, while PVR and ILBP2 are underexpressed. Group 4 is TNFRSF18, COL2A1 overexpressed, but CD3E and CD2 underexpressed. Group 5 is PVR and ULBP2 overexpressed, and CCL19, PVRIG, KRLK1 underexpressed. Finally, Group 6 is defined by CD96, CD247 overexpression, and NECT2 and CD276 underexpression. These groups were associated with AJCC Stage ($p=0.004$), fraction of genome altered ($p<0.0001$), SBR grade ($p<0.0001$), cribriform features ($p<0.0001$), tumor necrosis ($p<0.0001$), stromal tumor infiltrating lymphocytes, intratumoral lymphocytes, peritumoral lymphocytes ($p<0.0001$ for all inflammatory features). Fraction of genome altered and hotspot counting of TILs were also significant ($p<0.0001$). Most notably, even though significant trends of immune checkpoint groups are noted within each subtype (table 2), these patterns are shared between molecular subgroups.

Table 1. Immune checkpoint groups according to breast cancer subtypes.

	Luminal A	Luminal B	HER2-Enriched	TNBC	P
Group 1	107 (21%)	41 (21%)	7 (9%)	12 (7%)	P<0.0001
Group 2	95 (19%)	47 (24%)	24 (31%)	51 (30%)	
Group 3	163 (33%)	41 (21%)	16 (21%)	19 (11%)	
Group 4	30 (6%)	20 (10%)	3 (4%)	10 (6%)	
Group 5	48 (10%)	27 (14%)	12 (15%)	41 (24%)	
Group 6	56 (11%)	20 (10%)	16 (21%)	38 (22%)	

Figure 1 - 245



Conclusions: By approaching all immune checkpoints genes comprehensively, we identify 6 immune checkpoint classes with defining clinical, molecular, and histological features. These patterns are significantly associated with specific subtypes, but are still shared between all breast cancers regardless of subtype.

246 Evaluation of Factors Affecting Neoadjuvant Treatment Response in Breast Cancer Metastatic to Local Lymph Nodes

Ariel Wu¹, Lulu Sun², Ling Chen¹

¹Barnes-Jewish Hospital/Washington University, St. Louis, MO, ²Washington University School of Medicine in St. Louis, St. Louis, MO

Disclosures: Ariel Wu: None; Lulu Sun: None; Ling Chen: None

Background: Treatment options for breast cancer include the use of neoadjuvant systemic therapy, which can reduce tumor volume and potentially limit the extent of surgery. After surgery, pathologists evaluate the tumor response to therapy, which

correlates with survival outcomes and can guide further treatment. Methods of measuring tumor response within the breast are well defined. However, there is scant literature regarding characterization of metastatic tumor in local lymph nodes (LN) and the factors that influence LN tumor response. The objectives of this study are: i) to describe post-neoadjuvant histology of LNs from patients with node-positive disease at diagnosis, and ii) to determine the clinicopathologic features that correlate with or predict LN tumor response.

Design: With IRB approval, all post-treatment mastectomy specimens at our institution from Jan 2020 to July 2022 were identified. Only cases with LN metastasis at diagnosis confirmed by biopsy or fine needle aspiration were included. H&E slides were reviewed to identify histologic findings in LNs. Clinicopathologic features were recorded from the electronic medical record. Statistical analysis was performed using the chi-square test and logistic regression analysis.

Results: Thus far, 33 cases have been evaluated (anticipated ~100 cases). Eleven cases showed a CR in both the LN and the breast, with 3 cases with LN CR but residual tumor in the breast. Notably, 3 cases (9%) had a breast CR but residual LN tumor, and 8 cases (24%) had greater tumor burden in the LN compared to the breast. Recurrent histologic features of partial or complete LN response included pale or dense fibrosis, hemosiderin deposition, capsular thickening, and histiocytic reaction. Three cases (9%) showed no definitive histologic evidence of prior metastasis, despite the presence of biopsy site or clip. Breast CR both significantly correlated with ($p=0.0003$) as well as predicted ($p=0.001$) CR in the LN. Histologic type and grade, hormone receptor and HER2 status, type of therapy, and completion of therapy did not significantly correlate with or predict LN CR.

Conclusions: We found that breast CR correlated with and predicted LN CR. Interestingly, some tumors had a better response in the breast than in the LN, raising the possibility of the local environment or genetic changes in the metastasis modifying treatment effect. The results of this study will improve pathology practice and deepen our understanding of metastatic tumor response to therapy.

247 Computational Analysis of Whole Slide Image Stromal Signatures Identifies Unique Features Associated with Breast Cancer PTEN Mutational Status

Dongling Wu¹, Yihong Wang², Saroja Devi Geetha¹, Swachi Jain³, Sean Hacking⁴

¹Long Island Jewish Medical Center/Northwell Health, Manhasset, NY, ²Brown University, Rhode Island Hospital, Providence, RI, ³Donald and Barbara Zucker School of Medicine at Hofstra/Northwell, New York, NY, ⁴Laboratory Medicine Program, Departments of Anatomical Pathology, University Health Network and University of Toronto, Toronto, ON

Disclosures: Dongling Wu: None; Yihong Wang: None; Saroja Devi Geetha: None; Swachi Jain: None; Sean Hacking: None

Background: The trajectory of breast cancer studies has broadened from solely tumor cell based to being more holistic, inclusive of tumor-associated desmoplastic stromata and tumor infiltrating lymphocytes (TILs). Today we understand the components of desmoplastic stroma, cancer-associated fibroblasts (CAFs) and TILs are of clinical significance. Phosphatase and Tensin homolog deleted on chromosome ten (PTEN) constitutes a negative regulator of the proto-oncogenic phosphatidylinositol-3-kinase (PI3K)/protein kinase B (Akt) pathway. Genetic mutations involving PTEN in stromal fibroblasts have been found to accelerate extracellular matrix (ECM) remodeling, innate immune cell infiltration, and promote angiogenesis in breast cancer.

Design: We compared PTEN mutational status and RNA expression using a TCGA PTEN data cohort. We then analyzed the heterogeneity of tumoral microenvironment (TME) in PTEN mutated breast cancer using whole slide images (WSIs) to demonstrate the significance of stromal computational signatures using Qupath and our previously developed supervised machine learning (ML) methods: proportionated stroma area (PSA), myxoid stromal ratio (MSR) and immune stroma proportion (ISP). Computational signatures can be seen in Figure 1.

Results: Our study included 176 breast cancers with a PTEN mutational frequency of 53%. PTEN mutated breast cancers were associated with higher MSR($p<0.001$). In total cohort, high PSA, high MSR and low ISP were associated with high pathologic stage($p<0.05$), lymph node metastasis($p=0.018$). Worse disease specific survival was associated with higher PSA($p<0.001$) and MSR($p<0.001$), regardless of PTEN mutational status. In PTEN mutated cohort, high PSA and MSR were associated with high pathologic stage($p<0.05$). In wild type cohort, PSA showed similar prognostic trend to the PTEN mutated cohort($p=0.001$), whereas MSR did not show prognostic value($p=0.287$) (Table 1). Based on PTEN RNA expressions, tumors which had low PTEN expression had higher stage($p=0.03$), and amongst all the subtypes, triple negative breast cancers were most commonly seen (Figure 2).

T-Test	PSA	P-value	MSR	P-Value	ISP	P-Value
PTEN mutation		0.987		<0.001		0.213
Mutated	47.837		24.103		8.927	
Non-mutated	47.809		15.147		10.295	
pT stage						
pT1	41.667		16.656		11.87	
pT2	47.76	0.003	18.668	0.251	9.87	0.087
pT3	53.96	<0.001	18.928	0.011	6.28	<0.001
pT4	54.3	0.035	30	0.032	7.2	0.106
PTEN mutated						
pT1	43.60		19.78		11.49	
pT2	49.851	0.153	22.49	0.257	8.95	0.115
pT3	56.43	0.002	34.93	0.013	5.23	0.005
pT4	59.67	0.035	32.40	0.125	8.7	0.281
Wild type						
pT1	38.96		12.19		12.42	
pT2	49.05	0.001	14.47	0.287	10.9	0.226
pT3	51.79	0.005	18.57	0.087	7.2	0.026
pT4	46.4	0.262	18.57	0.054	4.95	0.123
pN stage						
N0	45.961	0.018	16.849	0.009	10.592	0.042
N1-N3	49.645		22.645		8.643	
DS survival		<0.001		<0.001		0.161
Alive	46.131		18.381		9.595	
Death	57.924		31.529		7.881	

Figure 1 – 247

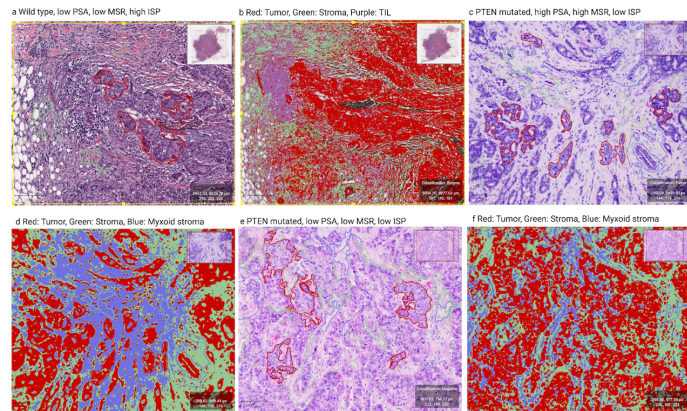
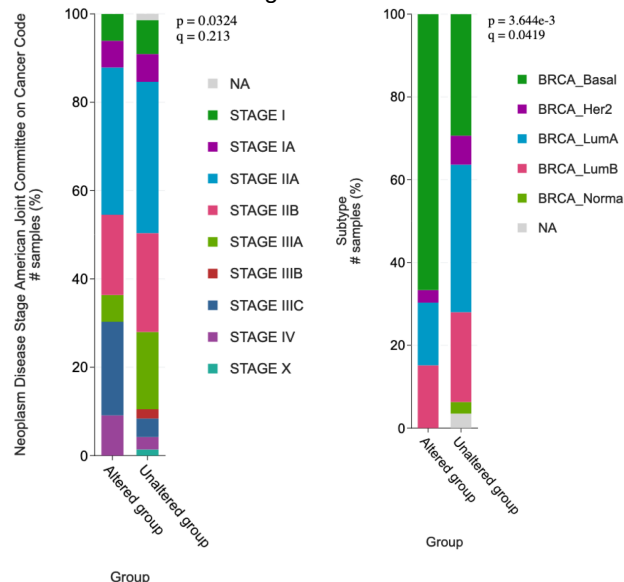


Figure 2 - 247



Conclusions: The stromal features of PTEN mutated breast cancer is different than that of the wild type. PTEN mutated breast cancer is associated with increased MSR. While PSA is quantitatively associated with disease specific survival in wild type and mutant breast tumors, MSR acts as a prognostic signature unique to PTEN mutated breast tumors. Our findings must be validated in other independent data sets.

248 Ki-67 Evaluation in HR+/HER2- Node-Positive High Risk Early Breast Cancer on Patients

Eligible for Abemaciclib Using Artificial Intelligence

Sayeeda Yasmeen¹, Al Amin², Wiam Bshara¹, Mohamed Desouki¹, Thaer Khoury¹

¹Roswell Park Comprehensive Cancer Center, Buffalo, NY, ²University at Buffalo, SUNY, Buffalo, NY

Disclosures: Sayeeda Yasmeen: None; Al Amin: None; Wiam Bshara: None; Mohamed Desouki: None; Thaer Khoury: None

Background: Abemaciclib combined with endocrine therapy have shown benefit for patients with early-stage breast cancer (BC) that are hormonal receptor (HR)+/HER2-, node-positive, and high-risk. One of the inclusion criteria is Ki-67 \geq 20% using specific clone (PharmDX, Agilent). However, the cost of this antibody is high. The aim of the study is to compare MIB-1 vs. PharmDX clone using artificial intelligence.

Design: Tumors from eligible patients for the treatment are prospectively stained with MIB1 and PharmDx clones as part of our internal quality control process. The slides were scanned in Aperio scanning system. The tumor was manually annotated on both stains for each case using copy and paste function. A nuclear algorithm was developed and the annotated areas were scored. The percentage of each of the staining intensities were recorded. The following pathological datapoints were recorded: histologic type, Nottingham grade, ER, PR, HER-2, T stage, N-stage, and treatment (Abemaciclib). Data were analysed including all intensities (0+, 1+, 2+, and 3+), then the percentage of 1+ was subtracted from the final score. Correlation between the two clones was calculated, as a continuous variable as well as using 20% cutoff.

Results: A total of 31 cases were included (28 ductal, 3 lobular). AJCC TN stage was II in 27 (87.1%) and III in 4 (12.9%). 11 (35%) patients were eligible for Abemaciclib (Ki-67 \geq 20%) based on PharmDx results and 10 (32%) patients based on MIB1 results. Three patients received Abemaciclib. The average for PharmDx and MIB1 were 17% \pm 12 and 15% \pm 11, respectively with correlation coefficient (*r*) of 0.92, *p*=0.23. When the percentage of 1+ staining was omitted from the final analysis, the average for the PharmDx and MIB1 were 14% \pm 12 and 11% \pm 9, respectively (*r* = 0.91, *p*=0.23). However, the number of patients eligible for Abemaciclib dropped to 8 (25%) when adopting either PharmDx or MIB1 results. No statistically significant difference found between stage II and III, or grade 1 or 2 and 3 when Ki67 cutoff of 20% was adopted (*p*=0.447 and *p*=0.404).

Conclusions: In our cohort, PharmDx clone is not superior to MIB1 stain and either of the clones can be used in the clinical laboratory to direct therapy with Abemaciclib. Considering the weak staining of Ki-67 (1+) increases the final score and consequently the number of eligible patients for Abemaciclib, the benefit from treatment is unclear. Validation of different clones in the clinical laboratories is warranted.

249 Pitfalls of Keratin and P63 Expression and Utility of Targeted DNA Sequencing and HMGA2 in Malignant Phyllodes Tumors of the Breast

Julia Ye¹, Talent Theparee², Gregory Bean³, Christopher Schwartz¹, Poonam Vohra¹, Guofeng (George) Gao⁴, Grace Allard⁵, Megan Troxell⁶, Yunn-Yi Chen¹, Gregor Krings¹

¹University of California, San Francisco, San Francisco, CA, ²UCSF Medical Center, San Francisco, CA, ³Stanford Medicine/Stanford University, Stanford, CA, ⁴Stanford University School of Medicine, Stanford, CA, ⁵Feinberg School of Medicine/Northwestern University, Chicago, IL, ⁶Stanford University Medical Center, Stanford, CA

Disclosures: Julia Ye: None; Talent Theparee: None; Gregory Bean: None; Christopher Schwartz: None; Poonam Vohra: None; Guofeng (George) Gao: None; Grace Allard: None; Megan Troxell: None; Yunn-Yi Chen: None; Gregor Krings: None

Background: Malignant phyllodes tumors (MPT) are aggressive fibroepithelial tumors with high risk for recurrence, metastasis and mortality. Distinguishing MPT from metaplastic carcinoma (MBC) or sarcoma can be challenging in cases with malignant stromal overgrowth, yet diagnosis of MPT versus MBC has important management and treatment implications. Keratin and P63 expression is typical of MBC but has been described in a subset of MPT, although data remains limited. Additional ancillary tools to distinguish MPT from MBC are needed.

Design: Immunohistochemistry (IHC) was performed on whole sections or tissue microarrays of 58 MPT for one or more keratins (CK) (cocktail, Cam5.2, CK14, CK5/6, CK7, MNF116 and/or CK34βE12), P63, TRPS1, GATA3, CD34, β-catenin (BCAT) and HMGA2 and scored in stroma (<20% focal [F], 21-80% patchy [P], ≥80% diffuse [D]). Results were compared to MBC. For a subset of MPT (n=23), next generation DNA sequencing (NGS) was performed using an assay targeting exons of 480 cancer genes.

Results: TRPS1 was positive in 68% (21/31) MPT (42% F, 53% P, 5% D), which was similar to MBC (57%, 20/35) ($p=.45$). 3/3 MPT with heterologous chondrosarcoma, 4/4 osteosarcoma and 3/4 liposarcoma were TRPS1+. GATA3 was positive in 16% (5/31) MPT, each with 1-2+ staining in <5% cells, compared to 54% (25/46) of MBC ($p=.001$). BCAT was nuclear in 58% (22/38) MPT (67% F, 19% P, 14% D) and 53% (20/38) MBC ($p=.82$). BCAT and GATA3 were also usually F in MBC. CK was expressed in 38% (21/56) MPT and was F in all cases. P63 was positive in 67% (32/48) MPT (85% F, 15% P). Of MPT with CK and P63 IHC, 38% (18/47) were CK+/P63+, compared to 96% (44/46) MBC ($p<.001$). The remaining MPT were CK-/P63+ (30%), CK+/P63- (6%), or CK-/P63- (26%). CD34 was expressed in 60% (29/48) MPT but was negative in 45% CK+ and/or P63+ tumors. Of 17 MPT with CK and/or P63 expression that were sequenced, 7 (41%) had pathognomonic MED12 mutations, including 6 of 7 CK+/P63+ and 3 CD34- tumors. Nuclear HMGA2 was expressed in 77% (24/31) MPT (17% F, 29% P, 54% D). Of CD34- tumors, HMGA2 was positive in ≥10% cells in 85% MPT vs 8% (3/40) MBC ($p<.001$) and in ≥50% cells of 62% (8/13) MPT vs 3% (1/40) MBC ($p<.001$).

Conclusions: MPT often express CK and/or P63, although staining is usually focal and co-expression is less common than in MBC. NGS can be very useful to confirm the MPT diagnosis in these cases. HMGA2 is a promising marker to distinguish MPT from MBC, especially in CD34- cases. TRPS1 and BCAT are less useful.

250 Nuclear Staining for Pan-Trk by Immunohistochemistry Is Highly Specific for Secretory Carcinoma: Pan-Trk in Various Subtypes of Breast Carcinoma

Qiqi Ye¹, Cody Han¹, Hui Chen¹, Aysegul Sahin¹, Lei Huo¹, Qingqing Ding¹

¹The University of Texas MD Anderson Cancer Center, Houston, TX

Disclosures: Qiqi Ye: None; Cody Han: None; Hui Chen: None; Aysegul Sahin: None; Lei Huo: None; Qingqing Ding: None

Background: Secretory carcinoma typically harbors a pathognomonic t(12;15)(p13;q25) balanced translocation, resulting in ETV6-NTRK3 gene fusion. Pan-Trk immunohistochemistry (IHC) has been demonstrated as a sensitive assay (>95%) to detect the ETV6-NTRK3 fusion product. A previous study showed focal weak pan-Trk nuclear staining in 10% non-secretory breast carcinomas. To further examine the specificity of pan-Trk IHC, we evaluated pan-Trk staining in various subtypes of breast carcinoma.

Design: The study cohort consists of 343 patients with invasive breast carcinoma (IBC) diagnosed between 2011 and 2021, including 154 TNBCs (7 secretory carcinomas, 36 metaplastic carcinomas including 12 matrix-producing carcinomas, 5 adenoid cystic carcinomas, 5 with apocrine differentiation, and 101 IBCs of no special type), 101 ER-positive/HER2-negative IBCs, and 88 HER2-positive IBCs. In addition, 6 secretory carcinomas of salivary gland origin were included as positive controls. Pan-Trk IHC was performed on whole slide sections of the 13 secretory carcinomas, 5 adenoid cystic carcinomas and 5 apocrine carcinomas, and on tissue microarrays of the remaining tumors, using a rabbit monoclonal antibody (clone EPR17341, Abcam) on a Leica Bond-Max autostainer. Nuclear staining of any intensity in the invasive carcinoma cells was considered positive.

Results: All 13 secretory carcinomas of the breast and salivary gland origins exhibited moderate to strong pan-Trk nuclear staining. In contrast, no nuclear staining was identified in any of the 336 non-secretory IBCs including 147 cases of different subtypes of TNBC, 101 ER positive and 88 HER2 positive IBCs (Table 1). Focal cytoplasmic pan-Trk staining was observed in 9 non-secretory IBCs (2.7%), which was considered as nonspecific and negative.

Table 1 Pan-Trk expression in breast carcinoma subtypes (n=343)

Tumor type		pan-TRK No. (%)		Total
		Positive (nuclear)	Negative	
TNBC	Secretory carcinoma	6 (100%)	0 (0%)	6
	Secretory carcinoma	7 (100%)	0 (0%)	7
	MBC	0 (0%)	36 (100%)	36
	AdCC	0 (0%)	5 (100%)	5
	Apocrine carcinoma	0 (0%)	5 (100%)	5
	NST	0 (0%)	101 (100%)	101
ER positive IBC		0 (0%)	101 (100%)	101
HER2 positive IBC		0 (0%)	88 (100%)	88

Abbreviations: AdCC-adenoid cystic carcinoma; IBC-invasive breast carcinoma; NST-no special type; MBC-metaplastic carcinoma; TNBC-triple negative breast carcinoma.

Conclusions: Our results indicate that positive nuclear staining for pan-Trk is highly specific for secretory carcinoma. In low to intermediate grade invasive breast carcinomas that share histologic features with secretory carcinomas, the addition of pan-Trk to a routing panel of ER/PR/HER2 is highly diagnostic. Our results also support that pan-Trk can differentiate secretory carcinoma from its triple-negative histological mimics such as adenoid cystic carcinoma, matrix-producing carcinoma and apocrine carcinoma, although this finding needs to be validated in larger studies.

251 TRPS1 Expression in Neuroendocrine Neoplasms of Breast and Other Organs

Qiqi Ye¹, Audrey Liu¹, Jeannelyn Estrella¹, Neda Kalhor¹, Constance Albarracin¹, Qingqing Ding¹, Yun Wu¹

¹The University of Texas MD Anderson Cancer Center, Houston, TX

Disclosures: Qiqi Ye: None; Audrey Liu: None; Jeannelyn Estrella: None; Neda Kalhor: None; Constance Albarracin: None; Qingqing Ding: None; Yun Wu: None

Background: Primary neuroendocrine (NE) neoplasms are rare in the breast. In the absence of in situ carcinoma, metastasis from other organ systems need to be ruled out first. In addition to widely used GATA3, TRPS1 is a recently identified marker for breast origin. It is significantly more sensitive than GATA3, particularly in triple-negative breast carcinomas. In current study, we investigated TRPS1 expression in breast neuroendocrine neoplasms, including well differentiated neuroendocrine tumor (NET) and poorly differentiated neuroendocrine carcinoma (NEC) and compared its expression in neuroendocrine neoplasms in lung, gastrointestinal tract and pancreas.

Design: A total of 81 cases of NE neoplasms were included in our study cohort, including 38 breast cases (29 ER positive NET, 9 triple negative NEC), 18 lung cases (5 typical carcinoid, 7 atypical carcinoid, and 6 NEC), 13 gastrointestinal cases (10 NET, 3 NEC), and 12 pancreatic cases (9 NET, 3 NEC). Slides were subjected to immunohistochemical staining using rabbit monoclonal TRPS1 antibody (1:2000, clone EPR16171, Abcam, Cambridge, UK), and mouse monoclonal GATA3 antibody (1:600, clone L50-823, Cell Marque, Rocklin, CA). Only nuclear staining was considered as positive. The immunoreactivity scores were calculated semi-quantitatively and categorized as negative (<1%), low positive (1-10%), intermediate positive (11-50%), and high positive (>50%).

Results: TRPS1 exhibited moderate to strong expression in all 29 breast NETs (100%) (Table 1). Two of 9 (22%) breast NECs showed weak (1 case) to moderate (1 case) staining. All 29 breast NETs were also strongly positive for GATA3 (100%), but none of the 9 NECs expressed GATA3. Not surprisingly, no TRPS1 staining was found in all 18 lung and 12 pancreatic NE neoplasms. Among 13 gastrointestinal NE neoplasms, only 1 NEC showed scattered low positivity (<10%) for TRPS1.

Table 1 TRPS1 expression in neuroendocrine neoplasms of breast and other organs (n=81).

Organ	Tumor type	TRPS1 No. (%)			Total
		Positive (nuclear)	Intermediate	High	
		Low		Negative	
Breast	NET	0	5 (17%)	24 (83%)	29
	NEC	1 (11%)	1 (11%)	0	7 (78%)
Lung	Typical/atypical carcinoid	0	0	0	12 (100%)
	NEC	0	0	0	6 (100%)
Gastrointestinal	NET	0	0	0	10 (100%)
	NEC	1 (33%)	0	0	2 (67%)
Pancreas	NET	0	0	0	9 (100%)
	NEC	0	0	0	3 (100%)

Conclusions: Our study demonstrated that TRPS1 is universally expressed in mammary NET, and it is a good marker to differentiate primary mammary NET from metastatic NET of other organs, including lung, gastrointestinal and pancreas. There is a limited utility of TRPS1 in differentiating mammary NEC from NEC of other organ systems. Clinical radiographic correlation is paramount in diagnosing primary NEC of the breast.

252 Quantitative Image Analysis of Low HER-2/NEU Protein Expression in Breast Cancer by Immunohistochemistry: An Intralaboratory Study to Evaluate the Reproducibility of Low HER-2/NEU Testing

Mustafa Yousif¹, Sundis Mahmood², Alexander Taylor², Ellen Chapel¹, Celina Kleer², Liron Pantanowitz², Sara Abbott¹

¹Michigan Medicine, University of Michigan, Ann Arbor, MI, ²University of Michigan, Ann Arbor, MI

Disclosures: Mustafa Yousif: None; Sundis Mahmood: None; Alexander Taylor: None; Ellen Chapel: None; Celina Kleer: None; Liron Pantanowitz: None; Sara Abbott: None

Background: Evaluation of human epidermal growth factor receptor 2 (HER2) expression is an essential prognostic and predictive parameter in breast cancer. HER2 assessment by immunohistochemistry (IHC) is reported as negative (0 or 1+), equivocal (2+), or positive (3+). HER2 low breast cancers account for approximately 50% of all breast cancers, including those with an IHC score of 1+ and those with an IHC score of 2+ and negative amplification by FISH. Recent approval of fam-trastuzumab-deruxtecan-nxki for use in a subset of HER2 low breast cancers has increased the diagnostic importance of distinguishing IHC 0 from IHC 1+ cases, as

this distinction now carries an actionable clinical difference. This study aims to determine whether quantitative image analysis (QIA) of low HER2 IHC score is more accurate than manual pathologist scoring.

Design: A retrospective review identified 157 invasive breast carcinomas (167 HER2 slide assessments) where QIA scored HER2 IHC slides as HER2 negative (0 or 1+). All IHC slides were blindly reviewed by two fellowship-trained breast pathologists who reached a consensus on "true" HER2 IHC status. "True" HER2 IHC score was compared to QIA-assigned HER2 IHC score and both pathologists with and without access to QIA-assigned HER2 IHC score. When available, HER2 FISH results were included for comparison.

Results: QIA-assigned HER2 IHC score as well as pathologist-assigned HER2 IHC score, with QIA access, agreed with the final "true" designation of HER2 negative versus HER2 low positive score in 92% of cases (153/167), whereas pathologist-assigned HER2 IHC score, with no QIA access, agreed with the "true" designation in 84% of cases (141/167). Disagreements with the "true" interpretations were considered false positive (FP) reads by both the QIA (7%) and the pathologist with no QIA access (11%), whereas the pathologist-assigned HER2 IHC score with QIA access has the least FP reads (5%). In discordant cases where the "true" IHC interpretation was considered 2+, additional HER2 FISH was negative in 86% of cases(6 of 7). Rereview demonstrated that a common cause of FP QIA-reads was the inadvertent inclusion of DCIS in the analysis.

Comparison of "True" HER2 IHC score with QIA HER2 IHC score assessment and pathologist manual score assessment					
"True" HER2 IHC score					
	HER2 negative (score = 0) (n=105)	HER2 low positive (score =1+) (n=55)	HER2 low positive (score = 2+, FISH negative) (n=6)	HER2 positive (score = 2+, FISH positive) (n= 1)	
QIA-assigned HER2 score	0 (n=94)	93 (56%)	1 (1%)	0	0
	1+ (n=73)	12 (7%)	54 (32%)	6 (4%)	1 (1%)
	2+ (n=0)	0	0	0	0
Pathologist-assigned HER2 score with no access to the QIA-assigned HER2 IHC score	0 (n=90)	87 (52%)	3 (2%)	0	
	1+ (n=65)	17 (10%)	47 (28%)	1 (1%)	
	2+ (n=12)	1 (1%)	5 (3%)	5 (3%)	1 (1%)
Pathologist-assigned HER2 score with access to the QIA-assigned HER2 IHC score	0 (n=98)	97 (58%)	1 (1%)	0	0
	1+ (n=57)	8 (5%)	49 (29%)	0	0
	2+ (n=12)	0	5 (3%)	6 (4%)	1 (1%)

Shaded squares represent agreement between "True" HER2 score and QIA-assigned or pathologist-assigned HER2 score (with and without QIA access) regarding HER2 negative versus HER2 low positive case status.

Conclusions: Quantitative image analysis is a helpful diagnostic support tool for pathologists that improves standardization of low positive HER2 IHC scoring. QIA assessment of HER2 IHC demonstrated excellent concordance with consensus pathologist opinion and reliably discriminated between HER2 low positive and negative cases.

253 Clinicopathologic and Genomic Features of Lobular-Like Invasive Ductal Carcinoma: A Distinct Entity?

Jing Yu¹, Edaise M. da Silva², Hae-Sun La³, Beth Clark¹, Jeffrey Fine⁴, Gloria Carter¹, Tatiana Villatoro³, Thing Rinda Soong⁴, Thais Basili², Juan Blanco-Heredia², Pier Selenica², Qiqi Ye⁵, Arnaud Da Cruz Paula², Higinio Dopeso², Adrian Lee⁴, Steffi Oesterreich⁴, Jorge Reis-Filho², Rohit Bhargava¹

¹UPMC Magee-Womens Hospital, Pittsburgh, PA, ²Memorial Sloan Kettering Cancer Center, New York, NY, ³University of Pittsburgh Medical Center, Pittsburgh, PA, ⁴University of Pittsburgh, Pittsburgh, PA, ⁵The University of Texas MD Anderson Cancer Center, Houston, TX

Disclosures: Jing Yu: None; Edaise M. da Silva: None; Hae-Sun La: None; Beth Clark: None; Jeffrey Fine: None; Gloria Carter: None; Tatiana Villatoro: None; Thing Rinda Soong: None; Thais Basili: None; Juan Blanco-Heredia: None; Pier Selenica: None; Qiqi Ye: None; Arnaud Da Cruz Paula: None; Higinio Dopeso: None; Adrian Lee: None; Steffi Oesterreich: None; Jorge Reis-Filho: None; Rohit Bhargava: None

Background: Invasive lobular carcinomas (ILCs) are typically characterized by loss of E-cadherin expression due to bi-allelic inactivation of the *CDH1* gene. A subset of breast cancers displays a single cell infiltrative growth pattern similar to classical ILCs and yet, in contrast to classical ILCs, they retain diffuse strong membranous E-cadherin reactivity and membranous p120 expression (Figure 1). We refer to such cases as "lobular-like invasive ductal carcinoma" (LLIDC). The study aims to explore (1) if such cases show biallelic inactivation of *CDH1* similar to classical ILCs; (2) whether they exhibit clinical-pathological features comparable to classical ILCs or invasive ductal carcinoma of no special type (IDC).

Design: LLIDC cases (n=166) were analyzed and compared with classical ILC (n=104) and grade-matched IDC (n=100) regarding clinical-pathologic and radiological characteristics, survival outcomes, and prognostic/predictive factors. An exploratory, hypothesis generating analysis of the genomic features of 14 randomly selected LLIDCs and classical ILCs (7 from each category) was performed utilizing an FDA-authorized targeted capture assay.

Results: LLIDC displayed an underestimation of tumor size on imaging and frequent positive margins on first resection similar to ILC; however, revealed a higher rate of lymphovascular invasion similar to IDC and an intermediate pathologic tumor size between ILC and IDC. Survival outcomes of all groups were similarly influenced by traditional prognostic factors and the multivariable prognostic score of Magee Equation 2 (ME2). Sequencing analysis revealed that all classical ILCs harbored 16q loss-of-heterozygosity (LOH) and *CDH1* mutations (7/7); however, 5 of the 7 LLIDCs did not harbor *CDH1* mutations or genomic rearrangements (Figure 2). *CDH1* mutations were identified in the other 2 LLIDCs: one with a subclonal *CDH1* in-frame indel mutation coupled with LOH (this case showed focal areas of E-cadherin membranous loss on re-review), and the other harboring a complex in-frame indel with subclonal LOH that had a negligible impact on protein structure.

Figure 1 - 253

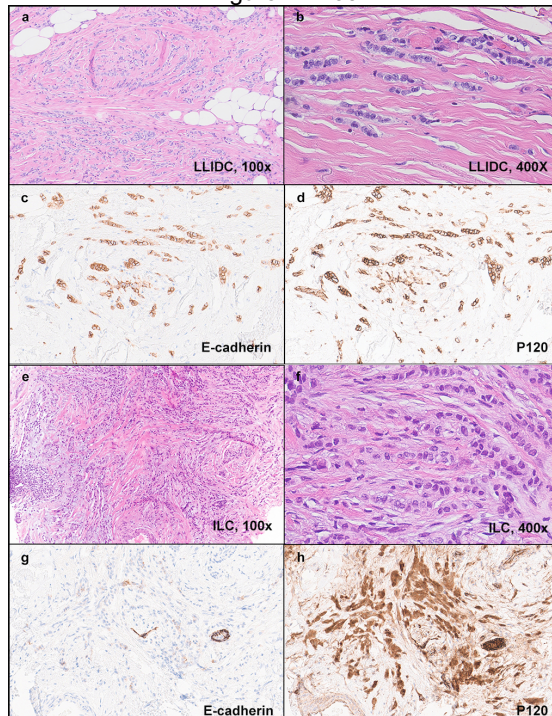
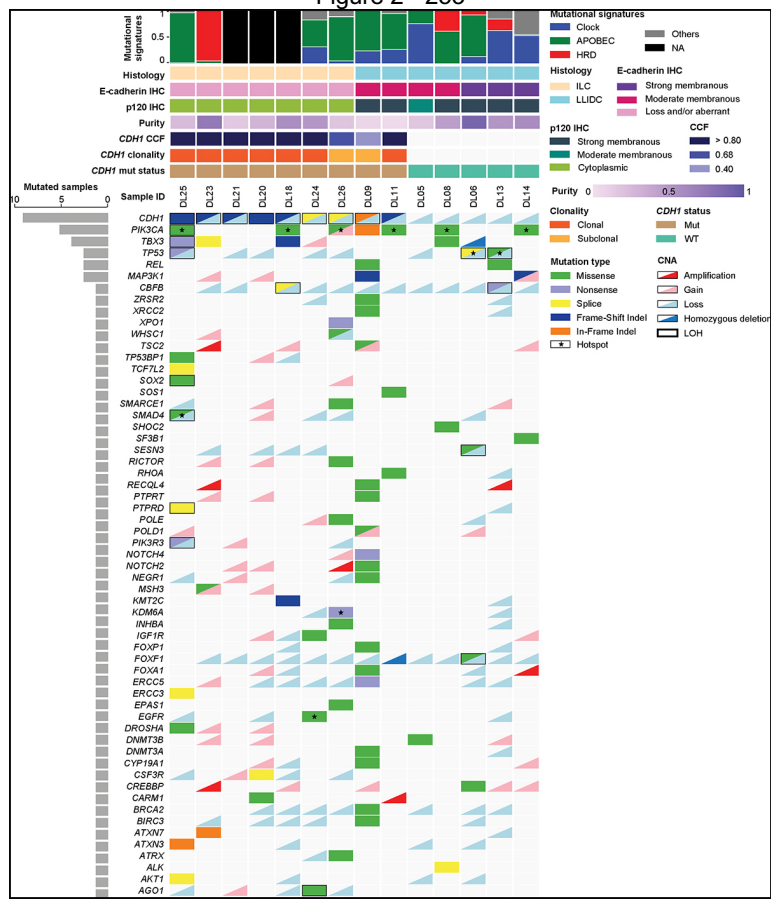


Figure 2 - 253



Conclusions: Despite the histologic similarities, LLIDCs differ from classic ILCs based on the lack of *CDH1* bi-allelic inactivation and the retained membranous E-cadherin/p120 catenin expression. LLIDCs have clinical-pathologic features intermediate between classical ILC and IDC. Further studies are required to ascertain the cause of the discohesiveness of LLIDC cells.

254 Loss of H3K27me3 Immunohistochemistry in Primary Breast Neoplasms

Qiqi Yu¹, Ashley Cimino-Mathews¹, John Gross², Andres Matoso³, Pedram Argani⁴, Marissa White¹, Lysandra Voltaggio⁴

¹Johns Hopkins University School of Medicine, Baltimore, MD, ²The Johns Hopkins Medical Institutions, Baltimore, MD, ³Johns Hopkins Medical Institutions, Baltimore, MD, ⁴Johns Hopkins Hospital, Baltimore, MD

Disclosures: Qiqi Yu: None; Ashley Cimino-Mathews: None; John Gross: None; Andres Matoso: None; Pedram Argani: None; Marissa White: None; Lysandra Voltaggio: None

Background: H3K27me³ is a histone trimethylation modification observed on the transcriptional suppressor, polycomb repressive complex 2 (PRC2). H3K27me³ loss occurs in the setting of PRC2 inactivation, which results in activated transcription and tumor progression. H3K27me³ loss by immunohistochemistry may be a diagnostic adjunct for malignant peripheral nerve sheath tumor (MPNST) among spindle cell neoplasm, but loss is seen in other tumors including melanoma. MPNST is among the differential diagnosis of spindle cell tumors in the axilla, but to our knowledge, H3K27me³ labeling has not previously been evaluated in primary breast tumors.

Design: H3K27me³ immunohistochemistry was performed on previously constructed tissue microarrays of invasive breast carcinomas and fibroepithelial lesions. Labeling was scored as positive (retained), variably positive (retained), and negative (lost; 0% labeling). Non-neoplastic cells including epithelium and lymphocytes served as positive internal controls. 91 evaluable primary breast carcinomas consisted of 28 basal-like triple negative breast carcinomas (TNBC), 11 non-basal TNBC, 19 ER+/HER2-, 6 ER+/HER2+, and 13 ER-/HER2+ carcinomas and 15 metaplastic carcinomas. 41 evaluable fibroepithelial lesions consisted of 31 phyllodes tumors (14 malignant, 9 borderline, 8 benign) and 10 fibroadenomas. H3K27me³ labeling was compared to Sox10 labeling, previously reported for all tumors (Human Pathol. 2013;44:959-65).

Results: Complete H3K27me³ loss was observed in 8 (9%) of invasive carcinomas, including 5 (18%) basal-like TNBC, 1 (7%) metaplastic carcinoma, 1 (5%) ER+/HER2- carcinoma, and 1 (8%) ER-/HER2+ carcinoma. H3K27me³ loss was more frequent in phyllodes tumors (29%, p=0.0128), with loss in 5 (36%) malignant, 3 (33%) borderline, and 1 (13%) benign phyllodes tumors.

H3K27me³ loss was not observed in non-basal TNBC, ER+/HER2+ carcinomas, or fibroadenomas. The majority (80%) of invasive carcinomas with H3K27me³ loss also displayed Sox10 labeling, compared to none of the phyllodes tumors ($p=0.0294$).

Conclusions: H3K27me³ loss occurs in malignant spindle cell lesions of the breast, including metaplastic carcinoma and phyllodes tumors. Half of breast carcinomas with H3K27me³ loss also display Sox10 positivity, which further overlaps with the immunophenotype of MPNST. H3K27me³ loss alone cannot be used to support the diagnosis of MPNST in the breast or axilla, and labeling should be interpreted in the context of a targeted immunopanel, tumor morphology and clinical history.

255 Pan-TRK Expression in Non-Secretory Breast Carcinoma

Sara Zadeh¹, Jinbo Fan¹, Robin LeGallo¹, Eli Williams¹, Anne Mills²

¹The University of Virginia Health System, Charlottesville, VA, ²University of Virginia, Charlottesville, VA

Disclosures: Sara Zadeh: None; Jinbo Fan: None; Robin LeGallo: None; Eli Williams: None; Anne Mills: None

Background: While *ETV6-NTRK3* translocations are well-established in secretory breast carcinoma, recent studies have shown other *NTRK* gene rearrangements in rare (<0.2%) non-secretory breast carcinomas. This molecular abnormality is of considerable clinical interest due to the potential vulnerability of these tumors to targeted tyrosine kinase inhibition, with response rates of >50% described in studies of solid tumors bearing this molecular signature. Pan-TRK immunohistochemistry is increasingly enlisted to as a screen for translocations involving *NTRK1*, *NTRK2*, and *NTRK3*, however expression rates have not been well-studied in non-secretory breast carcinoma.

Design: Tissue microarrays containing 285 non-secretory breast carcinomas were stained with pan-TRK immunohistochemistry. Immunoexpression was evaluated as positive or negative based on the presence of any staining. Positive cases were scored by intensity (1+, 2+, 3+) and extent (% tumor cells staining), and the cellular compartment staining was recorded (membranous, cytoplasmic, or nuclear).

Results: Six (2%) of breast carcinomas expressed pan-TRK. The average patient age was 57 (range: 44-77) (See Table). All were HER2-negative invasive ductal carcinomas; five were ER-positive, one was triple-negative. All positive cases showed membranous pan-Trk expression with one case also showing cytoplasmic staining; no nuclear staining was appreciated. Pan-Trk positivity extent ranged from 5-80%, with intensity from 1-2+; no cases showed strong (3+) expression. In the three cases with an associated intraepithelial component, pan-TRK expression was present in both the *in situ* and invasive tumor.

Characteristics of Pan-Trk+ Non-Secretory Breast Carcinoma

Patient Age	Stage	Histology	Grade	ER/PR/HER2 Status	Pan-TRK Expression
44	pT1bN1mic	Ductal	1	ER+/PR-/HER2-	1+, 25%; membranous and cytoplasmic
54	pT1bN0	Ductal	2	ER+/PR+/HER2-	1+, 25%, membranous
77	pT1bN0	Ductal	2	ER+/PR+/HER2-	1-2+, 70%; membranous
58	pT4dN3c	Ductal	3	ER-/PR-/HER2-	2+, 30%; membranous
52	pT1cN0	Ductal	1	ER+/PR+/HER2-	1+, 5%; membranous
58	pt2NX	Ductal	2	ER+/PR+/HER2-	1-2+; 80%; membranous

Conclusions: Pan-Trk immunohistochemical expression is uncommon in non-secretory breast cancer and may represent a useful screen for underlying *NTRK* gene rearrangements. The overall low rate of positivity suggests that enlisting this immunostain will not result in unnecessarily triaging large numbers of cases to molecular testing. Future studies correlating pan-TRK expression patterns with *NTRK* status are needed.

256 Her2-Low Breast Cancer: Incidence, Clinical, Pathological Characteristics, and Oncotype Dx Scores

Gloria Zhang¹, John Van Arnam², Xiaoyan Cui¹, Gloria Lewis¹, Patrick McIntire¹, Raza Hoda¹, Nancy Fong¹, Christine Booth¹, J. Jordi Rowe¹, Sherin Hashem¹, Andrew Sciallis¹, Megan Kruse¹

¹Cleveland Clinic, Cleveland, OH, ²Cleveland Clinic Foundation, Cleveland, OH

Disclosures: Gloria Zhang: None; John Van Arnam: None; Xiaoyan Cui: None; Gloria Lewis: None; Patrick McIntire: None; Raza Hoda: None; Nancy Fong: None; Christine Booth: None; J. Jordi Rowe: None; Sherin Hashem: None; Andrew Sciallis: None; Megan Kruse: None

Background: Recent clinical trials have demonstrated significantly improved survival from novel therapeutic compounds, particularly the new HER2-targeting antibody-drug conjugates (ADCs), in a subset of patients with "HER2-low" breast cancer. The

FDA recently approved the first targeted therapy for unresectable and metastatic HER2-low breast cancers, defined as HER2 IHC scores of 1+ or 2+ with negative ISH results. HER2-low breast cancers are not well characterized, and further studies are needed.

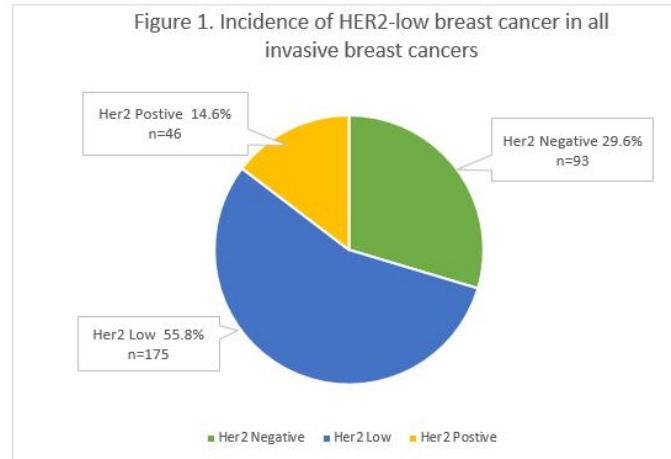
Design: We identified 314 consecutive cases of invasive breast cancers with complete clinical and pathological data from 1/1/2019 to 4/31/2019 by retrospective search of the pathology information system at the Cleveland Clinic. We studied the incidence, clinical and pathological characteristics in the HER2-low group and HER2-negative group (IHC score of 0). HER2 incidence also was studied in another 150 patients sent for Oncotype Dx.

Results: All 314 patients with invasive breast cancer in the study were female. The median patient age was 62 years for both Her2-low and Her2-negative groups. According to the HER2 scores by immunochemistry, 29.6% were 0 (93/314), 34.1% were 1+, 21.7% (68/314) were 2+ with negative FISH, and 14.6% (46/314) were 3+. The HER2-low cases accounted for 55.8% (175/314) of all patients. HER2 status in different clinical stages is summarized in table 1. HER2-low breast cancers were predominantly: ductal type (70.9%), Nottingham grade 2 (48.6%), ER-positive (89.7%), no LVI (54.9%), clinical stage I (69.7%), underwent partial mastectomy (59.4%), and not received adjuvant chemotherapy (61.6%). Compared to the HER2-low group, the HER2-negative group had more triple-negative cases (21.5% vs. 10.3%), more clinical stage IV cases (8.6% vs. 4.6%), and more deceased patients (10.8% vs. 6.9%). However, when adjusted for ER status, there was no significant difference in the examined variables between HER2-low and HER2-negative groups. Among the 150 cases sent for OncotypeDx, 59.3% were HER2-low (89/150), and 40.7% were HER2-negative (61/150). There is no significant difference between HER2-negative and HER2-low groups; both showed similar percentages for cases with scores of 0-10, 11-25, and >25.

Table 1. HER2 status in patients with different clinical stages

Clinical Stage	Patient #	Her2 0		HER2 low		HER2 positive	
		n	Percentage	n	Percentage	n	Percentage
I	211	60	28.4%	122	57.8%	29	13.7%
II	61	19	31.1%	33	54.1%	9	14.8%
III	18	6	33.3%	7	38.9%	5	27.8%
IV	18	8	44.4%	8	44.4%	2	11.1%
Unknown	6						
Total	314						

Figure 1 - 256



Conclusions: HER2-low breast cancers account for a significant part of invasive breast cancer (55.8% in this study). Our study provides valuable characteristics from consecutive, real-world patients and helps better understand this newly defined subset of breast cancer.

257 The Local Recurrence of DCIS, The Experience from A Single Institution for The Last 20 Years

Hui Zhang¹, Khin Su Mon¹, Alessa Aragao², Ping Tang¹

¹Loyola University Medical Center, Maywood, IL, ²Mayo Clinic, Rochester, MN

Disclosures: Hui Zhang: None; Khin Su Mon: None; Alessa Aragao: None; Ping Tang: None

Background: Ductal carcinoma in situ (DCIS) consists of 20% of all breast cancer diagnosed annually in the US. The standard of care for DCIS is breast conserving therapy including lumpectomy and radiation therapy. Around 10-20% of DCIS will have local recurrence, and half of the recurrence will be invasive cancer. Thus, it is critical to identify subgroup of DCIS patients with features

of higher risk for local recurrence. Many studies have shown that positive or close resection margin (<2mm) is the most important factor associated with local recurrence. Other factors such as younger age, larger and higher grade tumors are also suggested to be associated with recurrence.

Design: We have identified 509 consecutive cases of DCIS diagnosed and treated in our institution for the last 20 years and studied clinical and pathologic features that are associated with local recurrence.

Results: Among the 509 cases of DCIS, 3.5% (18 cases) were with local recurrence (11 cases recurred as DCIS and 7 cases recurred as invasive carcinoma) (Table). The recurrence occurred between 1 and 20 years after the original diagnosis. In our cohort of DCIS, the local recurrence is significantly associated with close margin (<2mm), younger patients (<40 years old), and lumpectomy. The recurrence is not significantly associated with high grade ER/PR low (<10% weak staining) or negativity and tumor size, although larger tumors are seen more frequently in the recurrence group. Interestingly, we also noted that majority of recurrence with invasive carcinoma (6 out of 7 cases) were from DCIS with high nuclear grade.

	DCIS no recurrence	DCIS with recurrence	P value
Cases No.	491	18	
Age (Y)	29-87	38-76	0.0389
<41	22 (4.5%)	2 (11.1%)	
41-60	217 (44.2%)	12 (66.7%)	
>60	252 (51.3%)	4 (22.2%)	
Size (cm)			0.1206
<1.5	224 (*6) (47.0%)	6 (*2) (33.3%)	
1-5-4	162 (*7) (33.9%)	5 (*1) (27.8%)	
>4	92 (*5) (19.1%)	7 (66.7%)	
No data	14	0	
Nuclear grade			0.1673
1	88 (17.9%)	3 (16.7%)	
2	179 (36.5%)	3 (16.7%)	
3	224 (45.6%)	12 (66.6%)	
Tumor markers			0.6459
ER/PR negative	76 (16.3%)	2 (11.1%)	
ER/PR low **	12 (2.6%)	1 (5.6%)	
ER/PR positive	378 (81.1%)	15 (83.3%)	
No data ***	25	0	
Type of surgery			0.0314
Mastectomy	141 (28.7%)	1 (5.6%)	
Lumpectomy	350 (71.3%)	17 (94.4%)	
Margin status			0.0369
Positive	5 (1.0%)	0 (0%)	
<2mm	88 (18.0%)	7 (38.9%)	
>2mm	397 (81.0%)	11 (61.1%)	
No data ***	1	0	

*No of cases that are multifocal

** ER/PR low defined as either ER or PR with an Allred Score of 3, while the other marker is either 3 or negative

*** For statistical purpose, cases with no data were excluded from the analysis

Conclusions: With proper treatment, the local recurrence from DCIS is low, supporting the recent trend of de-escalating treatment for DCIS. Margin status is still the most important factor for local recurrence, while younger patients and lumpectomy are at higher risk for it.

258 Genetic Landscape and Clinicopathological features of Squamous Cell Carcinomas of the Breast

Shuling Zhou¹, Yimin Li², Siyuan Zhong³, Ming Li¹, Hong Lv¹, Mengyuan Cai¹, Chengjia Shen⁴, Xiaoli Xu¹, Yufan Cheng¹, Rui Bi⁴, Bao-Hua Yu¹, Xiaoyu Tu¹, Ruohong Shui¹, Xiaoyan Zhou⁴, Wentao Yang¹

¹Fudan University Shanghai Cancer Center, Shanghai, China, ²Fudan University Shanghai Cancer Center, Fudan University Shanghai Medical College, Shanghai, China, ³Shanghai First Maternity and Infant Hospital, Shanghai, China, ⁴Fudan University Shanghai Cancer Center, Shanghai Medical College, Fudan University, Shanghai, China

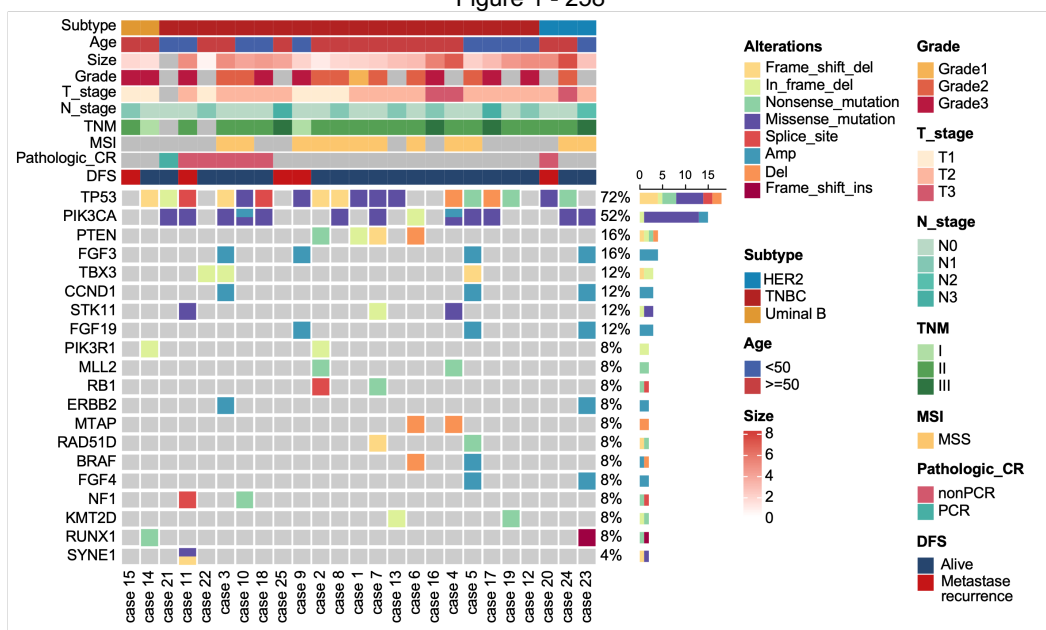
Disclosures: Shuling Zhou: None; Yimin Li: None; Siyuan Zhong: None; Ming Li: None; Hong Lv: None; Mengyuan Cai: None; Chengjia Shen: None; Xiaoli Xu: None; Yufan Cheng: None; Rui Bi: None; Bao-Hua Yu: None; Xiaoyu Tu: None; Ruohong Shui: None; Xiaoyan Zhou: None; Wentao Yang: None

Background: Squamous cell carcinoma of breast (SCC) is a subtype of metaplastic breast carcinoma (MBC). Its clinicopathological and molecular features are not well recognized due to its rarity. A better understanding of molecular features may lead to better treatment approaches for this type of aggressive tumor.

Design: 70 pure SCCs (69.3%, 70/101) and 31 mixed SCCs (30.7%, 31/101) from 2007–2022 in our center were analyzed. In mixed cases, the proportion of SCCs was more than 50% in each case. Twelve patients received neoadjuvant chemotherapy and the histological response was assessed according to the Miller-Payne (MP) grading system. Seventeen pure cases and three mixed cases were sequenced by DIAN (Hangzhou Lab) using a 324-gene platform or in our center by a 520-gene platform with licensed technologies.

Results: All cases were female ranging from 26 to 80 years (median 52 years). The mean diameter of the tumor was 19 (5-140) mm and the median disease-free survival (DFS) was 15 (2-116) months. Of the 89 early breast cancer patients, more than two-thirds (76.1%, 67/88) were stage II or Stage III at the initial diagnosis and ten patients (23.9%, 21/88) had lymph node metastasis. Recurrence and/or distant metastasis occurred in 24 patients (27%, 24/90) after 1-49 months' (median 15 months) follow-up. One patient achieved pathological complete remission (pCR) (8%, 1/12) with MP grade 5 and no lymph node metastasis after neoadjuvant chemotherapy. MP grade of the remaining 11 patients was grade 1 in 3, grade 2 in 6, grade 3 in 1 and grade 4 in 1, all of which were non-pCR (92%, 11/12) even though two of them received HER2-targeted therapy. And one of the 2 patients occurred bone metastasis during neoadjuvant chemotherapy. The most frequently identified pathogenic aberrations were in TP53(75%, 15/20) and PI-3 kinase pathway(60%, 12/20). TERT promoter mutations were identified in 10% (2/20). Other gene alterations corelated to chromatin remodeling, DNA repair, cell cycle, metabolism could also be seen in our cohort.

Figure 1 - 258



Conclusions: Squamous cell carcinoma of the breast is extremely rare and the tumor is usually resistant to conventional chemotherapy. Although most of the tumors are triple negative, neoadjuvant therapy should not be given priority in initial treatment decisions. Genomic profile using next-generation sequencing can identify clinically meaningful alterations that have the potential to guide targeted treatment decisions in patients with primary or metastatic SCC.

259 The Clinicopathological Characteristics Associated with the Efficacy of Neoadjuvant Targeted Therapy for HER2-positive Breast Cancer: A multivariable analysis

Ping Zhu¹, Hong Lv², Qianming Bai², Ruohong Shui², Xiaoli Xu², Wentao Yang²

¹Fudan University Shanghai Cancer Center, Fudan University, Shanghai, China, ²Fudan University Shanghai Cancer Center, Shanghai, China

Disclosures: Ping Zhu: None; Hong Lv: None; Qianming Bai: None; Ruohong Shui: None; Xiaoli Xu: None; Wentao Yang: None

Background: To investigate the clinicopathological features associated with the efficacy of neoadjuvant therapy for HER2-positive breast cancer.

Design: A total of 480 cases of HER2-positive breast cancer who received neoadjuvant therapy, diagnosed at the Department of Pathology of Fudan University Shanghai Cancer Center from 2015 to 2020, were retrospectively collected. Clinicopathological parameters such as age, tumor size, molecular subtype, type of targeted therapy, Ki-67 proliferation index, ER expression level,

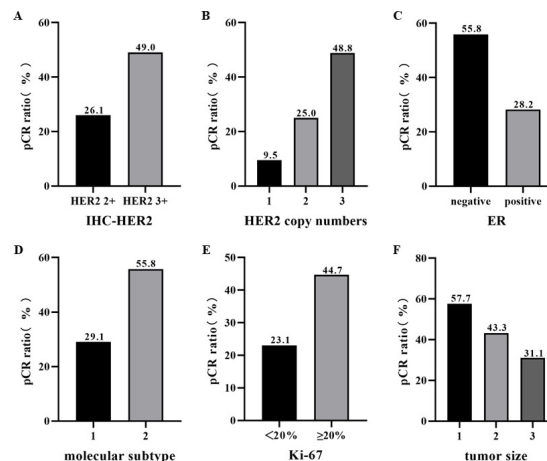
HER2 immunohistochemical (IHC) expression level, and HER2 amplification status were analyzed to correlate with the efficacy of neoadjuvant therapy.

Results: Among 480 patients with HER2-positive breast cancer, 209 achieved pathology complete response (pCR) after neoadjuvant therapy, with a pCR rate of 43.5%. 457 patients received chemotherapy plus trastuzumab and 23 patients received chemotherapy with trastuzumab and pertuzumab. A total of 198 cases (43.3%) achieved pCR in patients with chemotherapy plus trastuzumab, and 11 patients (47.8%) with chemotherapy plus trastuzumab and pertuzumab achieved pCR. The pCR rate in the latter group was higher, but there was no statistical significance. The results showed that the pCR rate of IHC-HER2 3+ patients (49%) was significantly higher than that of IHC-HER2 2+ patients (26.1%) ($p < 0.001$). The higher the mean HER2 copy number in the FISH assay, the higher the pCR rate was achieved. The expression level of ER was inversely correlated with the efficacy of neoadjuvant therapy, and the pCR rate in the ER-positive group (28.2%) was significantly lower than that in the ER-negative group (55.8%) ($p < 0.001$). The pCR rate (29.1%) of patients with luminal B type was lower than that of HER2 overexpression type (55.8%) ($p < 0.001$). In addition, higher Ki-67 proliferation index was associated with higher pCR rate ($p < 0.001$). The pCR rate was the highest in the tumor size ≤ 2 cm group (57.7%), while the pCR rate in the tumor size > 5 cm group was the lowest (31.1%). The difference between the groups was significant ($p = 0.005$).

Table 1. Correlation between clinicopathological features related to the efficacy of neoadjuvant therapy and pCR in HER2 positive breast cancer

Parameter	Group	pCR ratio (%)	95%CI (%)	Pvalue
Total specimen	--	(209/480)	43.5	39.1-48.0
Age	≤ 50	(102/246)	41.5	35.3-47.7
	> 50	(107/234)	45.7	39.3-52.2
Tumor size	≤ 2 cm (1)	(41/71)	57.7	46.0-69.5
	2cm-5cm (2)	(145/335)	43.3	38.0-48.6
	> 5 cm (3)	(23/74)	31.1	20.3-41.9
Targeted therapy	trastuzumab	(198/457)	43.3	38.8-47.9
	trastuzumab and pertuzumab	(11/23)	47.8	25.7-69.9
Molecular subtype	Luminal B (1)	(64/220)	29.1	23.0-35.1
	HER2 positive (2)	(145/260)	55.8	49.7-61.8
Ki-67	$< 20\%$	(6/26)	23.1	5.7-40.4
	$\geq 20\%$	(203/454)	44.7	40.1-49.3
ER	negative (0)	(149/267)	55.8	49.8-61.8
	positive (1-100%)	(60/213)	28.2	22.1-34.3
IHC-HER2	2+	(30/115)	26.1	17.9-34.2
	3+	(179/365)	49.0	43.9-54.2
HER2/CEP17	< 2.0	(4/9)	44.4	3.9-85.0
	≥ 2.0 and < 3.0	(12/42)	28.6	14.3-42.8
	≥ 3.0 and < 10.0	(26/78)	33.3	22.6-44.0
HER2 copy numbers	≥ 10.0	(167/351)	47.6	42.3-52.8
	≥ 4.0 and < 6.0 (1)	(2/21)	9.5	(-) 4.2-23.2
	≥ 6.0 and < 10.0 (2)	(18/72)	25.0	14.8-35.2
FISH positive group	≥ 10.0 (3)	(189/387)	48.8	43.8-53.8
	HER2/CEP17-2.0 and HER2 copy numbers ≥ 6.0	(4/9)	44.4	3.9-85.0
	HER2/CEP17 ≥ 2.0 and HER2 copy number 4.0-6.0	(2/21)	9.5	(-) 4.2-23.2
	HER2/CEP17 ≥ 2.0 and HER2 copy numbers ≥ 6.0	(203/450)	45.1	40.5-49.7

Figure 1 - 259



Conclusions: Multiple clinicopathological features were significantly associated with the efficacy of neoadjuvant therapy for HER2-positive breast cancer. In-depth exploration of the relationship between these clinicopathological features and the efficacy of neoadjuvant therapy for HER2-positive breast cancer is of great significance for treatment decision-making and efficacy prediction.

260 TRPS1 and GATA3 Immunohistochemistry in Secretory Carcinomas of Breast Compared to Secretory Carcinomas of Salivary Gland

Patricija Zot¹, Muhammad Ahmad², Malvika Solanki¹, Gloria Zhang³, Tolgay Öcal⁴, Miglena Komforti⁵, Justin Koeplin¹, Jenna Capelle¹, Charles Sturgis¹

¹Mayo Clinic, Rochester, MN, ²New York-Presbyterian/Weill Cornell Medicine, New York, NY, ³Cleveland Clinic, Cleveland, OH, ⁴Mayo Clinic, Scottsdale, AZ, ⁵Mayo Clinic, Jacksonville, FL

Disclosures: Patricija Zot: None; Muhammad Ahmad: None; Malvika Solanki: None; Gloria Zhang: None; Tolgay Öcal: None; Miglena Komforti: None; Justin Koeplin: None; Jenna Capelle: None; Charles Sturgis: None

Background: Secretory carcinoma (SC) of the breast is a rare type of triple-negative breast carcinoma that generally confers a good prognosis. It histologically resembles SC of the salivary gland and harbors the same genetic mutation, *ETV6-NTRK3* gene fusion. Recent studies have shown TRPS1 immunohistochemistry (IHC) to be a sensitive and specific marker for triple negative breast carcinomas. This study compares results of TRPS1 and the historical marker GATA3 in SC of the breast and salivary gland.

Design: A total of 11 archival cases of SC were identified at multiple institutions. Of those, 5 were of breast origin and 6 were of salivary origin. Each case was studied by both TRPS1 and GATA3 IHC and was evaluated independently by two breast pathologists. The IHC slides were scored for percentage of immunoreactive cells as well as the intensity of staining (Table 1). For TRPS1 and GATA3, only nuclear staining was counted as positive (Figure 1).

Results: The patients with a diagnosis of SC of the breast were female (100%) ranging in age from 22 to 78 years. The primary site of SC of salivary gland was right parotid gland (50%), left soft palate (16.6%), left submandibular gland (16.6%), and left sublingual gland (16.6%). SC of salivary origin patients ranged from 30 to 64 years and were predominantly male (83%). All patients with SC of breast showed diffuse and moderate to strong intensity IHC positivity with TRPS1. While immunoreactivity with TRPS1 was present in patients with SC of salivary origin, this was less often diffuse and always of low intensity. GATA3 IHC on the other hand showed highly variable results in SC of the breast. GATA3 in SC of salivary origin was consistently diffusely and strongly positive (Table 1 and Figure 1). The scoring agreement between pathologists was 90% initially and 100% at consensus.

Table 1: Percentage of immunoreactive cells and intensity of staining in SC of the breast and salivary gland.				
IHC Percentage:	0, <1%	1, 1-10%	2, 11-50%	3, 51-100%
IHC Intensity:	0, Negative	1, Weak	2, Moderate	3, Strong
IHC Total score:	0-1, NEG	2, Low POS	3-4, Intermediate POS	6-9, High POS
Breast		Percentage	Intensity	Total score
TRPS1	Range	3	2-3	6-9
	Average	3	2.8	8.4
GATA3	Range	0-3	0-3	0-9
	Average	1.8	1.6	4.8
Salivary gland		Percentage	Intensity	Total score
TRPS1	Range	2-3	1	2-3
	Average	2.7	1	2.7
GATA3	Range	3	3	9
	Average	3	3	9

Figure 1 - 260

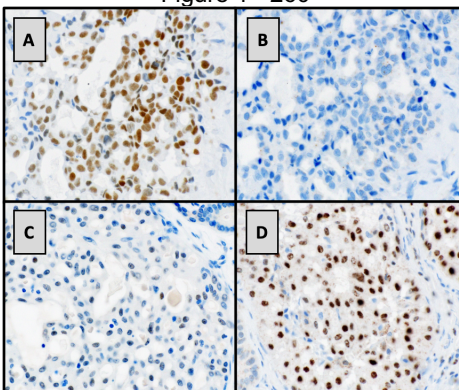


Figure 1. (A) SC breast, TRPS1, 60X. (B) SC breast GATA3, 60X. (C) SC salivary gland, TRPS1, 60X. (D) SC salivary gland, GATA3, 60X.

Conclusions: In our cohort, all cases of SC of breast showed diffuse and moderate to strong TRPS1 positivity, while no cases of SC of salivary origin showed this pattern. SC of salivary gland was more likely to be diffusely and strongly GATA3 positive. TRPS1 may be a valuable adjunctive study at confirming SC of breast versus salivary gland primary, and combination of this marker with GATA3 may prove helpful.

261 Clinicopathological Characteristics of 22 Cases of Apocrine Encapsulated Papillary Carcinoma

Ke Zuo¹, Xiaoli Xu¹, Rui Bi², Ruohong Shui¹, Wentao Yang¹

¹Fudan University Shanghai Cancer Center, Shanghai, China, ²Fudan University Shanghai Cancer Center, Shanghai Medical College, Fudan University, Shanghai, China

Disclosures: Ke Zuo: None; Xiaoli Xu: None; Rui Bi: None; Ruohong Shui: None; Wentao Yang: None

Background: Apocrine encapsulated papillary carcinoma (AEPC) is rare, and no more than 10 cases have been reported in previous literature. Although it has high level expression of AR and GCFP15 protein, tumor cells show triple-negative (ER-PR-HER2-) phenotype. Our study is aimed to explore whether the clinicopathological characteristics of AEPC are different from those of classical EPC.

Design: 22 cases of AEPC were identified in our department since 2014. Clinicopathologic data were reviewed and relevant prognosis information was analyzed.

Results: All of the 22 patients were female, the median age at diagnosis was 61.5 (range: 49-82). Fifteen cases were consultation cases and seven cases were diagnosed and treated in our center. For consultation cases, the major concern of the original diagnosis was whether the tumor was malignant or not. Histologically, most of the AEPC were cystic with glandular and papillary growth pattern. The papillary structures were covered by cells with uniform apocrine differentiation. The degree of cellular atypia varied among cases, but no severe atypia was identified. Myoepithelial cells were absent along the papillary structure and the periphery of the lesion. Of the 22 AEPC, 13 cases had no stromal invasion, 6 cases had microinvasion (<1mm), and 3 cases had frank invasion (1-4mm). Tumor cells were negative for ER, PR and HER2 (0/1+/2+), while diffusely positive for AR and GCFP15. The median Ki-67 proliferation index was 10% (range: 5-20%). Fifteen patients had no postoperative adjuvant therapy, while seven patients received either adjuvant radiotherapy and/or chemotherapy. The follow-up information was available in 21 patients. In the median follow-up time of 35.5 months (range: 5.4-99.6m), none of the patients experienced recurrence and/or metastasis.

Figure 1 - 261

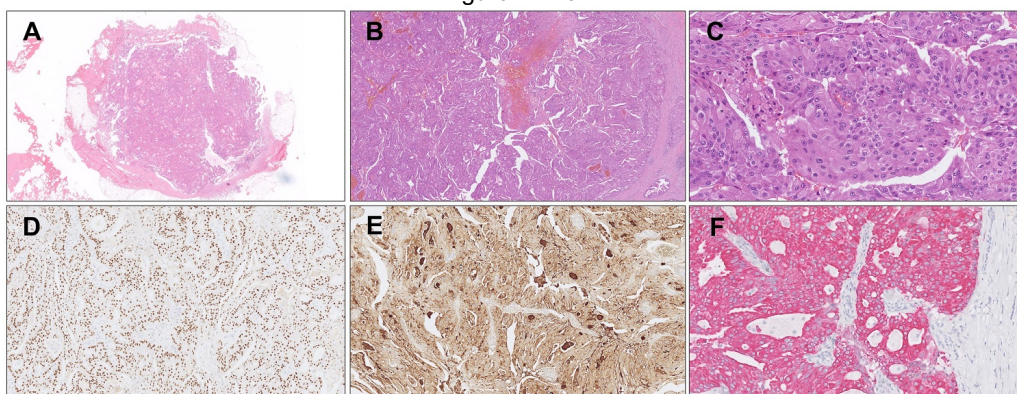


Figure 1. A. Typical AEPC presented with intracystic papillary component surrounded by a thick fibrous capsule at low power. B. Papillary structure of AEPC. C. Apocrine cytromorphology of AEPC. D. AEPC positive for AR. E. AEPC positive for GCFP15. F. AEPC positive for AE1/AE3 (red) but negative for myoepithelial marker p63

Conclusions: For classical EPC, patients generally have a good prognosis and are treated as ductal carcinoma in situ. In our study, no recurrence and/or metastasis were observed in all AEPC patients with or without postoperative adjuvant therapy. Although the tumor immunophenotype was triple-negative, there were significant differences between AEPC and triple-negative breast cancer (TNBC) of no special type. Therefore, the indolent biological behavior of AEPC is different from that of TNBC of no special type, but much closer to classical EPC. It might be more appropriate to treat patients with the same strategies for classical EPC.